57/1/2025
ISSN 1338-3523
ISSN 0369-2086

Mineralia Slovaca

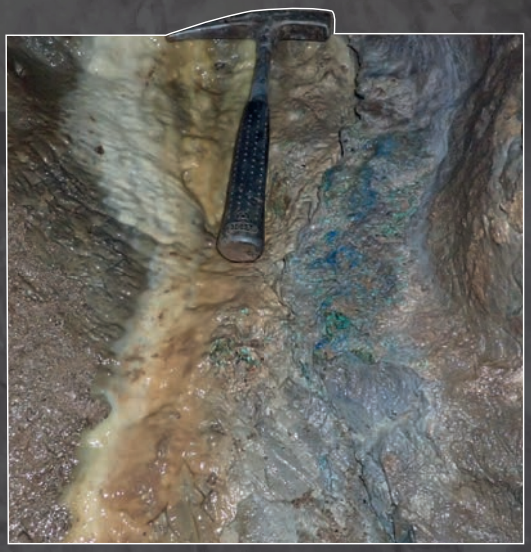

Štátny geologický ústav Dionýza Štúra Bratislava

Mineralia Slovaca

Časopis pre základné a aplikované vedy o Zemi

Journal of Basic and Applied Earth Sciences

Mineralia Slovaca (Web ISSN 1338-3523, ISSN 0369-2086), EV 3534/09, vychádza dvakrát ročne. Vydavateľ a tlač: Štátny geologický ústav Dionýza Štúra, Mlynská dolina 1, 817 04 Bratislava, IČO 31 753 604. Dátum vydania čísla 57/1/2025: október 2025.
Predplatné v roku 2025 vrátane DPH, poštovného a balného pre jednotlivcov 22,00 €, pre členov SGS a geologických asociácií 20,90 €, pre organizácie v SR 31,90 €, pre organizácie v ČR 55,00 €. Cena jednotlivého čísla pri nákupe cez e-shop alebo pri osobnom nákupe v predajni ŠGÚDŠ v RGS Košice je 6,05 € vrátane DPH. Časopis možno objednať v redakcii a v knižnici regionálnej geologickej služby v Košiciach.

Adresa redakcie:
Štátny geologický ústav D. Štúra, Mlynská dolina 1, 817 04 Bratislava. Telefón: 02/59 375 257; e-mail: mineralia.slovaca@geology.sk, e-mail knižnica: secretary.ke@geology.sk

Mineralia Slovaca (Web ISSN 1338-3523, ISSN 0369-2086) is published twice a year by the State Geological Institute of Dionýz Štúr Bratislava, Slovak Republic. The date of issuing of the number 57/1/2025: October, 2025.
Subscription for the whole 2025 calendar year (two numbers of the journal): 66.00 € (Europe), 77.00 € (besides Europe), including VAT, postage and packing cost. Claims for nonreceipt of any issue will be filled gratis.
Order of the Editorial Office: Štátny geologický ústav D. Štúra – RC Košice (Library), Jesenského 8, SK-040 01 Košice, Slovak Republic. Phone: +421/55/625 00 43; fax: +421/55/625 00 44, e-mail: mineralia.slovaca@geology.sk, library: secretary.ke@geology.sk

PÔVODNÉ ČLÁNKY – ORIGINAL PAPERS

FRONT COVER:

Photographs from the Blue Cave from the paper Littva et al. **Upper left side** – blue to green dripstones and flowstones in Sieň modrých šmolkov Hall (Photo: J. Littva).

Upper right side, upper photograph – close-up side view of the vein containing malachite, euhedral calcite crystals and rusty brown iron oxides, macroscopic iron oxide crystals can also be seen in the rock below the vein (Photo: J. Littva).

Upper right side lower photograph – blue to green speleothems in the passage leading from the cave entrance nr. 2 (Photo: J. Littva).

Middle row, left – stalactites in the Sieň modrých šmolkov Hall (Photo: J. Littva). **Middle row, right** – fractured bedrock mineralised by the malachite and azurite near the "blue spot" (Photo: L. Dušeková).

Bottom photograph – Fold-and-thrust structure in the Bociansky banícky dóm Chamber displaying top-to-the-west sense of motion (Photo: J. Littva).

BACK COVER

Rock wall in the Malužinský dómik Chamber exposing side view of the NE-SWstrike-slip fault that dismembers a low-angle thrust fault (Photo: P. Staník).

PREDNÁ OBÁLKA

Fotografie z Modrej jaskyne z článku Littva et al. **Vľavo hore** – modré až zelené kvaple a sintrové náteky v sieni Modrých šmolkov (foto: J. Littva).

Vpravo hore, horná fotografia – detailný bočný pohľad na žilu obsahujúcu malachit, idiomorfné kryštály kalcitu a hrdzavohnedé oxidy železa, makroskopické kryštály oxidov železa sú viditeľné aj v hornine pod žilou (foto: J. Littva).

Vpravo hore, dolná fotografia – modré až zelené speleotémy v chodbe vedúcej od jaskynného vchodu č. 2 (foto: J. Littva).

Stredný rad, vľavo – stalaktity v Sieni modrých šmolkov (foto: J. Littva). **Vpravo** – porušená hornina mineralizovaná malachitom a azuritom v blízkosti „modrého fľaku" (foto: L. Dušeková).

Spodná fotografia – vrásovo-násunová štruktúra v sále Bocianskeho baníckeho dómu so zmyslom pohybu „vrch na západ" (foto: P. Staník).

ZADNÁ OBÁLKA

Skalná stena v Malužinskom dómiku poskytujúca bočný pohľad na sv.-jz. smerne posuvný zlom rozdeľujúci mierne sklonený násun (foto: P. Staník).

Mineralia Slovaca, Web ISSN 1338-3523, ISSN 0369-2086, https://doi.org/10.56623/ms.2025.57.1.1
57, 1 (2025), 3 – 4,

In memory of **Zoltán Németh** (* 1962 – † 2025)

Zoltán Németh, our friend and colleague and long-standing scientific editor of *Mineralia Slovaca* tragically left us forever on May 4, 2025.

Zoltán was born in the family of a mining engineer. He received his engineering degree in the field of mining geology and geological prospecting at the Technical University in Košice, in 1986. During his studies, he chose structural geology as his main tool for understanding geological processes.

After completing his university studies, he worked in the company Geologický prieskum Spišská Nová Ves, š. p., and then in the company Geocomplex, a. s., Bratislava. In 1996 he joined the State Geological Institute of Dionýz Štúr (SGIDŠ) in the regional centre in Košice, where he worked until the end of his career.

He was engaged in regional-tectonic research and detailed field mapping. Initially, he worked mainly under the supervision of RNDr. P. Grecula, DrSc., in the Gemeric Unit, where Zoltán contributed significantly to the creation of the geological and tectonic map of the Spišsko-gemerské rudohorie Mts. at a scale of 1:25 000.

He participated in the preparation of 5 regional-geological maps at a scale of 1:50 000 and accompanying explanatory notes (Spišsko-gemerské rudohorie, Slovenský raj, Galmus and Hornádska kotlina Basin, Malé Karpaty Mts., Záhorská nížina Lowland and Strážovské vrchy Mts. – eastern part). He is also co-author of the General Geological Map of Slovak Republic at scale 1:200 000 (sheet Košice) and contributed to the compilation of Geological and educational maps of the Zemplínske vrchy Mts. and the Medzev–Jasov region.

In 1996–1998 he was principal investigator of the UNESCO/IUGS project IGCP 276 – *Paleozoic in the Tethys*. At this time, he successfully completed his doctoral studies in petrology with a focus on structural petrology and petrotectonics at the Faculty of Natural Sciences of Comenius University in Bratislava. He obtained his PhD. degree in 2001. He also completed specialised courses on geochronology at the University of Georgia, Athens, Georgia, U.S.A. (1994), and textural goniometry at the Karl-Franzens Universität Graz, Austria (1998).

In 2000–2004 he participated in research on the genesis of magnesite and talc in the framework of the UNESCO/IUGS IGCP 443 *Magnesite and Talc – Geological and Environmental Correlations* project, where he coordinated the activities of 40 countries as the Secretary and International Organizational Leader and co-authored a monograph on this topic.

From 2006 to 2010 he worked as the head of the Regional centre of SGIDŠ in Košice. Since 2021 he was the Head of the Department of International Relations of SGIDŠ and at the same time LEAR – Legal Entity Appointed Representative for SGIDŠ at the European Commission.

Zoltán devoted a large part of his active work to the tasks of geology of mineral deposits (deposits Dobšiná, Smolník, Košice I). He participated in metallogenesis and tasks on the environmental risk projects; potential sources of metallic magnesium; CO_2 sequestration by the carbonatization of ultramafic rocks; conversion of asbestos into an environmentally benign mixture of carbonates; sources of critical minerals; sources of silicon and raw materials for the renewable energy and electromobility industries. He served as an expert in the EC DG Growth – ERECON project on the supply of REE elements to the European industry in the crisis year 2010. In 2015–2018, as a commissioned staff member of the SGIDŠ, he participated in the international MINATURA 2020 project as a leader of the national research team in the harmonisation of European geological and mining legislation. He has also worked on applied projects, hydrogeological and engineering geological mapping, monitoring of environmental burdens and CO_2 capture and storage.

In recent years, as a member of the international team of the Coordination and Support Action Geological Service for Europe (CSA GSEU), he has been actively involved in the compilation of the *Lithotectonic Map of Europe* and related databases and dictionaries within the work package group. He fully applied his long year experience of research in the field of structural geology in this task. Based on the gradual formation of geosutures during orogenesis, he clearly understood the global geodynamics of polyorogenic zones in the Alpine-Carpathian-Himalayan belt and in his latest publication he explained the formation of geosutures and subduction zones as a consequence of the upwelling of the deep mantle into the upper mantle as the part of the rotation of the Earth in time. This mixing and upwelling of the mantle caused differential rotation between the lithosphere and the mantle, producing subductions and later geosutures. Unfortunately, tragic circumstances prevented him from finishing work on the project which he devoted a lot of time and energy.

His editorial and organizational activities are significant and cannot be overlooked. Since 1995, he has served in the editorial board of the journal *Mineralia Slovaca*, first as a translator and English language corrector and later, since 2006, as a scientific editor. He was a second long-standing scientific editor and shaped the journal into the present format. For many years he prepared the newsletter of the Slovak Geological Society (*Geovestník*) within the *Mineralia Slovaca*. With his great contribution, the *Mineralia Slovaca* was indexed by the Scopus database in 2017.

He was a long-standing and active member of the Slovak Geological Society (SGS), organizer and co-organizer of several dozen scientific events (congresses, conferences, and the "Pre-Christmas Seminars" of the SGS) and numerous other international events.

Despite the health problems that have affected him in recent years, he has always been full of life optimism and great outlook on life. It is necessary to emphasize that Zoltán was extremely hard-working, very responsible and internally disciplined. He was admirable in many ways as educated, professional and person with excellent communication and organizational skills. Zoltán left us unexpectedly after a tragic car accident near Plavnica. He will always live in our memories.

We sincerely thank You, Zoltán, for your friendship, your indispensable cooperation and for everything you have done for the geoscience in the Western Carpathians.

Martin Radvanec, Ľubomír Hraško & Ľubomír Gazdačko

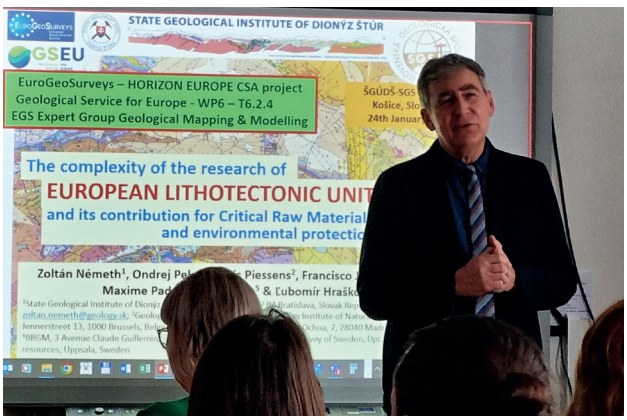

Mineralia Slovaca, Web ISSN 1338-3523, ISSN 0369-2086, https://doi.org/10.56623/ms.2025.57.1.2
57, 1 (2025), 5 – 38, © Authors 2025. CC BY 4.0

Geological setting and origin of Blue Cave with blue and green carbonate speleothems (Central Slovakia)

JURAJ LITTVA*[1], PAVEL BELLA[1, 2], ĽUDOVÍT GAÁL[1], and PAVEL HERICH[1, 3]

[1] State Nature Conservancy of the Slovak Republic, Slovak Caves Administration, Hodžova 11, 031 01 Liptovský Mikuláš, Slovak Republic
[2] Department of Geography, Faculty of Education, Catholic University in Ružomberok, Hrabovská cesta 1, 031 04 Ružomberok, Slovak Republic
[3] Department of Physical Geography and Geoecology, Faculty of Natural Sciences, Comenius University in Bratislava, Mlynská dolina, Ilkovičova 6, 842 15 Bratislava 4, Slovak Republic
*Corresponding author: juraj.littva@ssj.sk, https://orcid.org/0000-0002-5674-2447

Abstract: Blue to green carbonate speleothems are a principal feature of Blue Cave, located in the northeastern part of the Nízke Tatry Mountains. The copper, colouring the speleothems, was thought to originate from the Permian volcanics neighbouring the Middle Triassic carbonates hosting the cave. Tracing sparse mentions about the Pb-Zn-(Cu) ores in the carbonates, we identified previously overlooked studies, that studied of the mineralisation in surprising detail. Based on the data from these works, remapping of the area, and by examining the geology and geomorphology of the Blue Cave, we conclude the following. 1) The Hronic Unit near the Blue Cave forms two nappes, and the carbonates hosting the cave are involved in the structurally imbricated zone at the top of the lower nappe. 2) The imbricated thrusts predispose the Pb-Zn-(Cu) sulphide mineralisation in the carbonates, while secondary azurite and malachite follow younger NE-SW and NW-SE fractures. 3) This mineralisation, rather than the volcanics, provided copper for the coloured speleothems, formed along NW-SE fractures. 4) The dissolution of carbonates by the sulphide oxidation might have created the precursor porosity for later cave formation. 5) The Blue Cave formed in three stages. In Stage I – likely in the Middle Pleistocene – the cave formed below the water table, underneath the stream terrace levelled by the surface stream. During the later valley incision and formation of lower-lying stream terraces in Stage II, the cave was modified by episodic floodwaters. As they bear floodmarks, the coloured speleothems formed mostly during this stage. The bedded and fractured bedrock that predisposed the solution also contributed to the cave's remodelling by collapse during Stage III.

Key words: Hronic Unit, Pb-Zn ores, copper minerals, blue and green speleothems, speleogenesis, phreatic morphologies

Graphical abstract

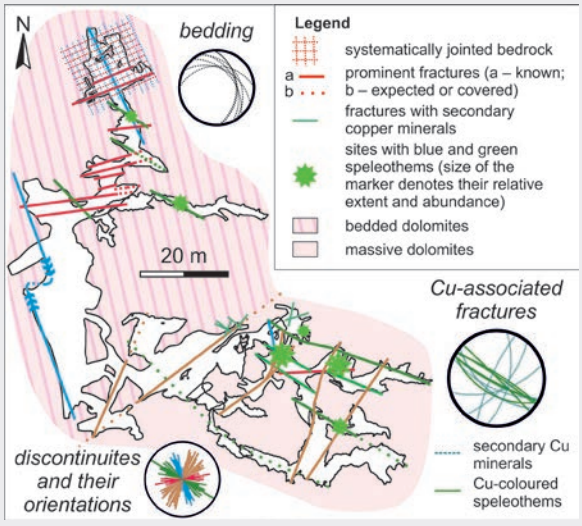

Highlights

- The Hronic Unit in the study area is formed by two nappes with the tectonically imbricated zone in the upper part of the lower nappe instead of three nappes originally interpreted by previous research.
- Copper, causing the colour of the cave's speleothems, is derived from the Pb-Zn-(Cu) ores in the carbonates that host the cave, not nearby basalts as previously thought.
- Malachite and azurite occurrences were discovered in the cave's host rock.
- The sulphuric acid from the oxidised sulphide ores did not form the cave, but it might have enhanced the porosity of the host rock, facilitating later karstification.
- The cave is genetically related to the levelling of the stream terrace above the cave, probably during the Middle Pleistocene, and subsequent periodical valley incision.

Introduction

The Blue Cave (Modrá jaskyňa in Slovak), discovered near the Malužiná village in 2016 (Šmoll, 2017), is so far the only cave in the territory of Slovakia with the reported extensive occurrence of blue and green speleothems. The cave is located in northern Slovakia on the northeastern slopes of the Nízke Tatry Mountains (Fig. 1A), on the left (western) side of the valley cut by the Boca Stream. The cave entrances lie at altitudes of 752 and 767 m a.s.l.

(Pristašová, 2024), near the confluence of Boca Stream with its right tributary, the Malužiná Stream. The cave was discovered by G. Majerníčková, J. Šmoll, and M. Šušeľ, and its currently known passages reach a length of 657 m and a vertical span of 25 m (Šmoll, 2017).

Orvošová et al. (2016) used geochemical and mineralogical methods to determine copper as a predominant chromophore colouring the speleothems, although elevated amounts of zinc, barium, and iron were also detected. These elements were associated with the weathering of the Cu-Zn-Fe mineralisation in the cave's proximity. The nearby Permian volcanics containing barite-sulphide ore veinlets were considered as a likely source (Orvošová et al., 2016). However, the evidence from other research works suggests the possibility of a different copper source.

Approximately 1.5 km to the northwest of the cave, in the so-called Olovienka (approximate translation – 'Leadeling') Ravine, abandoned mines have been excavated in the same carbonate rock formation that hosts the Blue Cave. Sparse mentions in literature (e.g. Chovan et al., 1996; Biely et al., 1997, p. 186) claimed that these works exploited lead-zinc sulphide mineralisation, interpreted as metasomatic-hydrothermal in origin. This prompted further research, during which we discovered several unpublished technical reports archived in the Archive of the State Geological Institute of Dionýz Štúr (Kantor, 1957; Hanáček, 1963; Biely, 1964; Ivanov et al., 1965) and one conference paper (Kantor, 1977). These reports present comprehensive results from mineralogical and geochemical investigations conducted not only near the mines but also in the wider area, including the rocks adjacent to the Blue Cave. The data from the reports provide new perspectives on potential copper sources, prompting the reassessment of the proposition of Orvošová et al. (2016) that copper is derived from the weathering of the Permian volcanics.

Besides the presence of the uniquely-coloured carbonate speleothems, the Blue Cave could be potentially significant from a geomorphological point of view. The carbonate-hosted lead and zinc sulphide ores are associated with caves that were formed by sulphuric acid and exhibit specific morphological and mineralogical features resulting from this process (see De Waele et al., 2024 and references within). Indeed, some of the rediscovered works (Hanáček, 1963; Biely, 1964; Ivanov et al., 1965) reported the presence of sulphide minerals very close to the cave. On the other hand, the cave's position immediately downstream from the non-karstic area suggests that the cave was formed primarily by waters from the surface stream. Therefore, a study of the cave's morphology is necessary to understand which processes formed the Blue Cave.

Additional geological research of the cave was done primarily to (1) understand the characteristics of the host rock and (2) find out how the presence of fractures predisposed the distribution of the cave passages and blue and green speleothems. In addition, the study of the geological structures in the cave could also contribute to the understanding of the geology in the regional context. The region near the Blue Cave is traditionally considered one of the 'key areas' for understanding the geology of the entire Western Carpathians (Zoubek, 1952). An important tectonic contact between three high-order geological units (Tatric, Veporic, and Hronic Units) is located to the south of the cave (Fig. 1B). Hence, we will provide a brief description of the geological setting.

Geological setting

The Čertovica thrust zone, separating the two Western Carpathian main thick-skinned geological units (Tatric and Veporic), is exposed southward from the Blue Cave (Fig. 1B). To the north, this thrust zone is overlain by a thin-skinned nappe stack of the Hronic Unit (Fig. 1B). The Hronic rocks are composed primarily of the Upper Paleozoic siliciclastic, volcaniclastic, and volcanic rocks, as well as the Mesozoic siliciclastic and carbonate formations (Biely et al., 1992; Appendix 1 in Tulis & Novotný, 1998). The Middle to Upper Triassic Hronic carbonates cropping out in the area can be assigned to two distinct facial sequences – Biely Váh Basin and Čierny Váh Platform sequence (*sensu* Havrila, 2011). The former one is a deep-water sequence occurring in the uppermost tectonic unit, while the latter one represents a shallow-water sequence present in the lower tectonic units (Fig. 1C; Biely et al., 1992, 1997; Havrila, 2011). The shallow-water Triassic carbonates that host the cave are poorly understood and lack a formal stratigraphic name; accordingly, we denote them as 'Čierny Váh carbonates'.

The tectonic structure of the Hronic Unit near the cave is complex, due to the tectonic disruption of its internal structure during multi-stage deformation. Thrusting with a general top-to-the-northwest sense of movement occurred during the Cretaceous nappe stacking (Biely, 1963; Kováč & Filo, 1992; Biely et al., 1997, p. 147–149; Kováč & Havrila, 1998). Subsequent post-Cretaceous deformation stages involved the rejuvenation and oversteepening of the thrust planes, including the dissection of the nappe stack by steep parallel and cross-cutting faults (Biely et al., 1997, p. 147–149; Tulis & Novotný, 1998, p. 70–71; Olšavský, 2008, p. 168–173). Two ore prospecting boreholes (Biely, 1964) named Ma-1 (165 m deep) and Ma-2 (145 m deep) were drilled near the cave (Figs. 1C, 2A–C, and 3). In both of them, tectonically perturbed rocks were observed underneath the fluvial sediments. In the borehole Ma-1, Biely (1964) described several repetitions of the Lower Triassic siliciclastics and Middle Triassic carbonates (Fig. 3), indicative of their intense tectonic reworking. In the

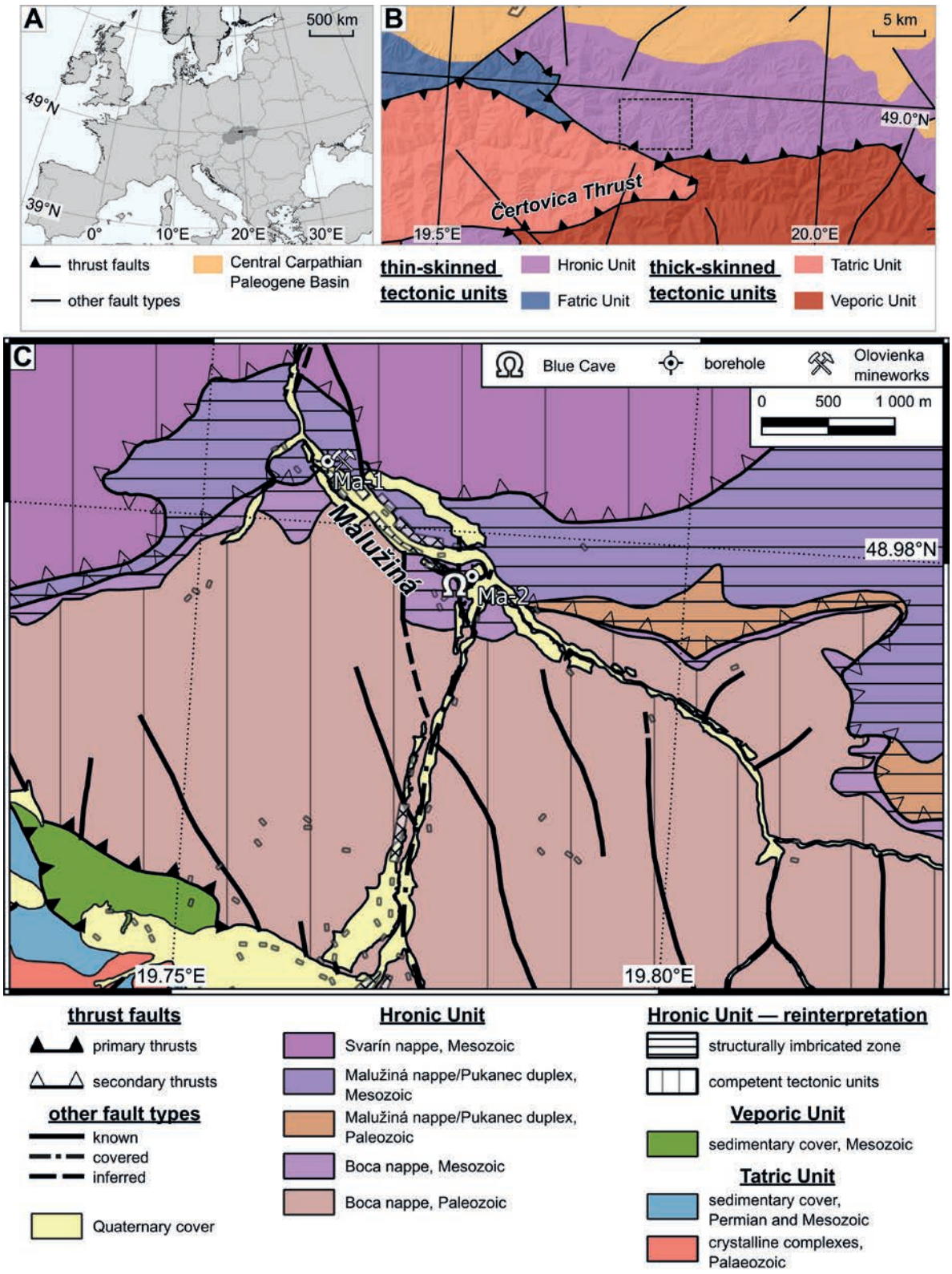

Fig. 1. Location and geological setting of the Blue Cave. **A** – Location of the study area shown on a map of Europe as a black rectangle. **B** – Structural sketch depicting the main tectonic units in the broader area near the Blue Cave (modified from Lexa et al., 2000), the dashed rectangle denotes the extent of figure C. **C** – Tectonic map (simplified from the original map of Biely et al., 1992) depicting main tectonic units in the vicinity of the Blue Cave according to the interpretation of Biely (1997) and our reinterpretation; the extent of Quaternary fluvial and slope sediments is based on the mapping results from this study.

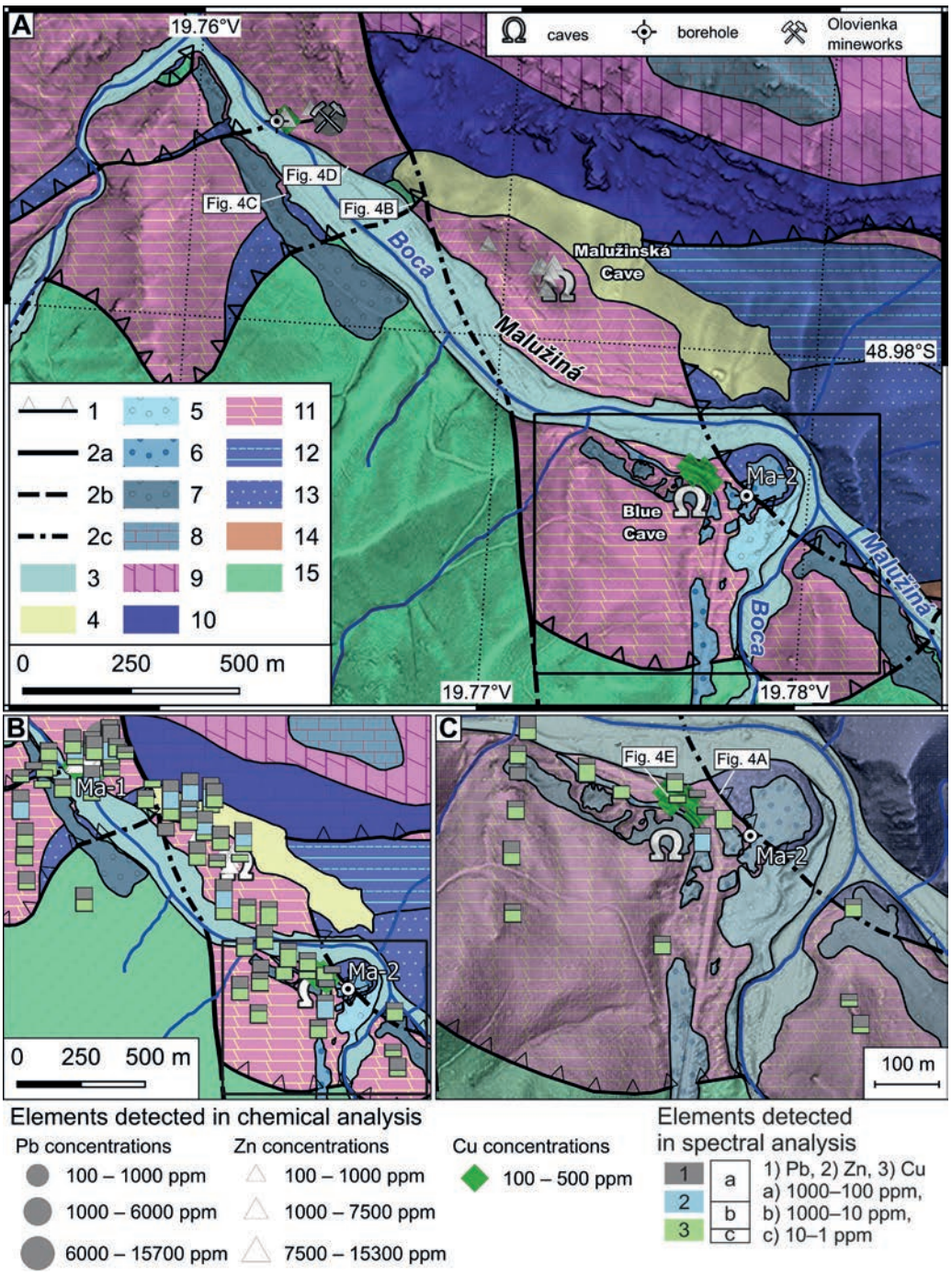

Fig. 2. Geology of the study area. **A** – Updated geological map of the study area (based on Biely et al., 1992; modified according to Tulis & Novotný, 1998, Appendix 1; Olšavský, 2008, Fig. 41, 79, 80, 81; and our mapping) overlain on the hillshade model from LiDAR data (source: ÚGKK SR), with marked-out sampling sites with concentrations of Pb, Zn, and Cu above 100 ppm based on chemical analysis (Kantor, 1957; Hanáček, 1963; Ivanov et al., 1965) and sites of photos from photos in Fig. 4, the black rectangle denotes the extent of figure C. **B** – Same geological map from Fig. 1A with added sampling sites for spectral analysis of Pb, Zn, and Cu concentrations above 1 ppm. **C** – Close-up view of the geological map in the vicinity of the Blue Cave. **Legend:** Faults: **1** – thrusts; **2** – other fault types, **a** – known, **b** – assumed, **c** – covered; Quaternary: **3** – alluvial plain deposits; **4** – slope deposits; **5** – lower fluvial terraces; **6** – middle fluvial terraces; **7** – upper fluvial terraces; Middle Triassic: **8** – Reifling Fm., basinal limestones with chert nodules; **9** – Ramsau Fm., dolomites; **10** – Gutenstein Fm., limestones and dolomites; **11** – 'Čierny Váh carbonates', dolomites with occasional limestones; Lower Triassic: **12** – Šuňava Fm., variegated sandstones, mudstones, shales, and limestones; **13** – Benkovo Fm., sandstones and shales; **14** – Malužiná Fm., variegated sandstones and shales; **15** – Malužiná Fm., volcanics of basaltic to andesitic composition. See appendices for the original geochemical data.

borehole Ma-2, Biely (1964) reported the presence of Middle Triassic carbonates and the underlying Permian volcanics separated by a thrust (Fig. 3).

The tectonic complexity of the Hronic Unit near the Blue Cave has given rise to a broad range of interpretations of the internal architecture of the unit. These include (1) two tectonic units separated by a broad deformed zone containing tectonic slices (e.g. Biela, 1960, p. 24–27; Biely, 1960, 1962); (2) three tectonic units (e.g. Biely, 1963, 1964, p. 28–29); (3) two subordinate units belonging to the lower tectonic unit, overridden by the upper tectonic element (e.g. Biely, 1976, p. 60–64); (4) or two tectonic units with the lower one arranged into an array of tectonic slices (e.g. Badár et al., 1965, p. 69–72; Vozár et al., 1983, p. 83–85; Tulis & Novotný, 1998, p. 70–71, Appendix 1). Currently, three subordinate Hronic nappes are recognised (Fig. 1C), but doubts about their validity are still present (Biely et al., 1992, 1997, p. 147–149; Havrila, 2011, p. 13, Fig. 1). Recent findings of additional internal tectonic complications cast further doubt on this interpretation, as these would necessitate recognition of four or more subordinate nappes (Olšavský, 2007a, 2007b, 2008, p. 168–173).

The complexity of the Hronic Unit in the area also led to conflicting depictions of the geology near the Blue Cave in two of the most recent geological maps (Biely et al., 1992; Appendix 1 in Tulis & Novotný, 1998). According to the map of Biely et al. (1992), the carbonate block that hosts the cave is bounded by steep N-S-striking faults. In contrast, the same carbonates are bounded by E-W-striking thrusts in the map of Tulis and Novotný (1998, Appendix 1). The structural data from the cave and its vicinity could assist in resolving the difficulties in the interpretation of the internal structure of the Hronic Unit.

The precise arrangement of fluvial terraces near the Blue Cave is unclear. The known maps showing the Quaternary terraces (Čechovič, 1942; Ilavský & Ilavská, 1949; Jeremenko, 1956; Kubáň, 1956; Hanáček, 1963; Vozár, 1970, 1974; Biely, 1976; Kantor & Ďurkovičová, 1977; Vozár et al., 1983; Biely et al., 1992) tend to display a different number of terrace levels and even a different spatial distribution of terraces. Therefore, further work was required to verify the extent of terrace deposits.

Methods

To resolve the uncertainties in the geological setting of the Blue Cave obvious from the different geological maps, additional geological mapping was employed. In the broader area, the main tool used for the remapping was the LiDAR-based Digital Elevation Model (DEM, source: ÚGKK SR). LiDAR-based mapping aimed to determine the extent and distribution of the Quaternary sediments, with a particular focus on the stream terraces. Field mapping was employed in a radius of approximately 500 m from the cave and additionally around the Boca Stream, approximately 1 km downstream from the cave. Field mapping was used to further verify the extent of the terraces and to ascertain the structural position of the Čierny Váh carbonates within the Hronic Unit. The surface observations were further supplemented by the maps from unpublished reports and subsurface data.

The unpublished works (Kantor, 1957; Hanáček, 1963; Biely, 1964; Ivanov et al., 1965) are written in Slovak and Czech, so we digitised the data most pertinent for this paper to improve their availability for the wider scientific community. The digitised data were used in the figures and interpretations, and are provided as appendices to this paper. The maps showing the sites of the collected samples were georeferenced, and the results of chemical and semiquantitative spectral analyses were attributed to each site as a set of attributes in the QGIS software version 3.34.11 (QGIS Development Team, 2024). The detected amounts of Pb, Zn, and Cu in the chemical analysis were displayed on the map as individual symbols, while stacked bar charts were used to display detected amounts of Pb, Zn, and Cu in semiquantitative spectral analysis (Figs. 2A–C). The locations of boreholes Ma-1 and Ma-2 were also marked on the map (Figs. 1C and 2A–C), and the borehole logs were re-drawn as best as possible, since some parts of them have faded out. The results of chemical and semiquantitative spectral analyses from the borehole cores were added to the appropriate depth intervals of the borehole logs (Fig. 3).

We studied the Čierny Váh carbonates directly in the cave, where six samples (MM-1 to MM-6) were collected for the study in thin sections, and of those, four samples were also processed for the whole-rock analysis of major rock components (Tab. 1). One surface sample (MM-7) from the brecciated layer above the cave entrance No. 1 was also collected for thin-section study and whole-rock analysis. Thin sections and whole-rock analyses were prepared in the Geoanalytic Laboratory of the State Geological Institute of Dionýz Štúr in Spišská Nová Ves. The thin sections were studied using an optical microscope for the microfacial characterisation. In the whole-rock analysis, loss on ignition was determined by using gravimetric analysis and chemistry of the major components was determined by x-ray fluorescence spectrometry.

The 3D model of the cave and the surface around the entrances was scanned by the SLAM-based scanner GeoSLAM Zeb Horizon. The scanner has a reach of 100 meters, a speed of 300,000 points per second. The resultant point cloud was composed of the five parts for the cave and a single part for the surface. Each cave section was referenced to at least four fixed survey stations of the centerline. The centerline in quality UISv2 6-0-BCEF and mean error on a loop of 0.49 % was obtained by a compass method utilising calibrated DistoX2 and PocketTopo software (Heeb, 2020), then processed in Therion software (Mudrák & Budaj, 2010). The cave entrances were surveyed by the GNSS method with RTK correction using Trimble Geo 7x H-Star.

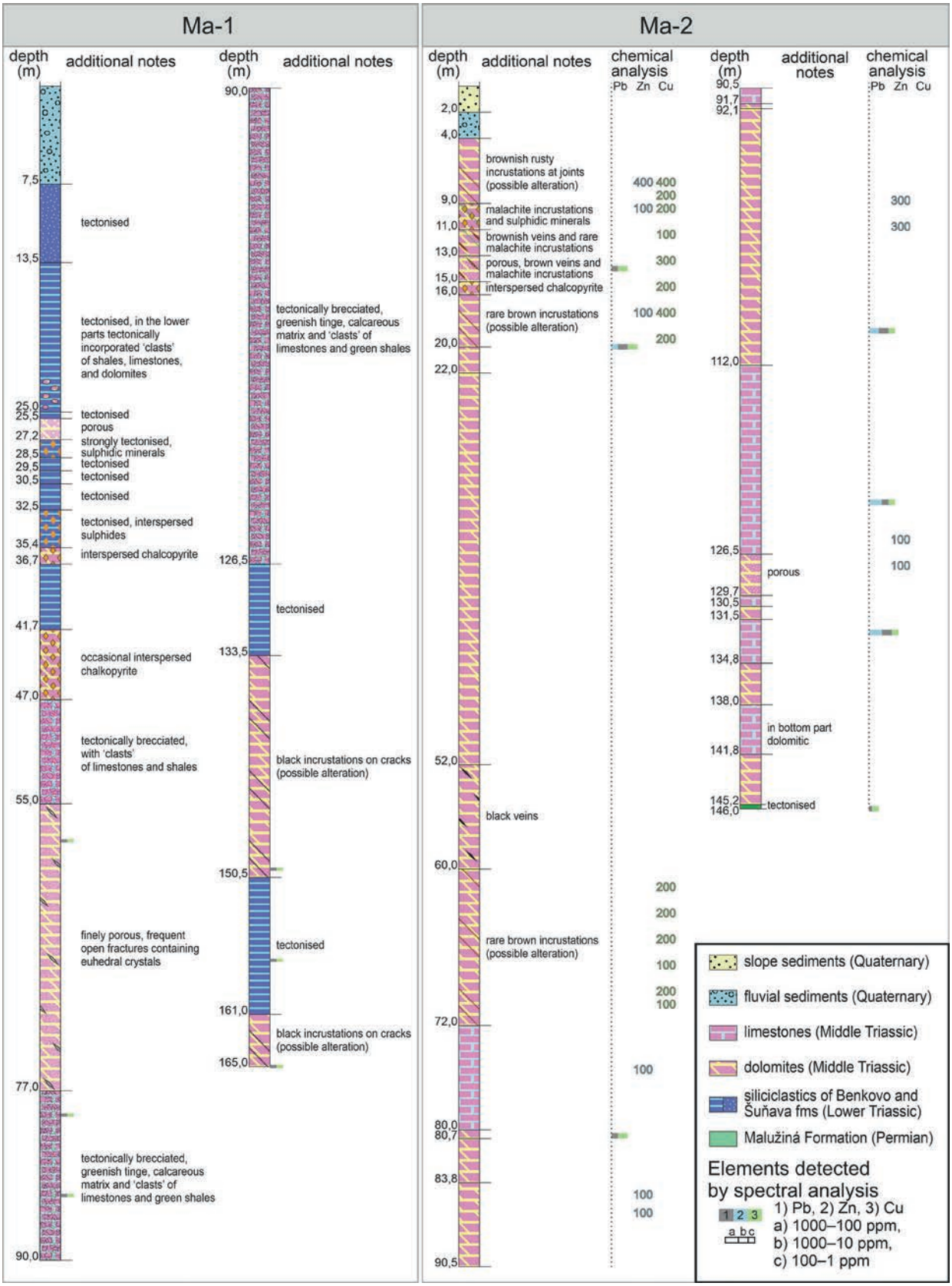

Fig. 3. Interpreted borehole logs from Biely (1964) with additional geochemical data from Ivanov et al. (1965). See the appendices for the original logs.

Tab. 1

Chemical composition of the samples from the host rock of the Blue Cave (LOI – loss on ignition).

[%]	MM-1	MM-3	MM-4	MM-6	MM-7
SiO_2	0.16	0.76	0.41	0.85	2.54
Al_2O_3	0.06	0.39	0.16	0.42	0.79
Fe_2O_3	0.52	0.23	0.14	0.15	0.58
CaO	29.8	30.5	30.4	29.8	32.3
MgO	21.6	20.6	21.3	21.5	18
TiO_2	< 0.01	0.02	< 0.01	0.02	0.06
MnO	0.10	0.02	0.04	0.02	0.06
K_2O	< 0.05	0.12	0.06	0.15	0.25
Na_2O	< 0.2	< 0.2	< 0.2	< 0.2	< 0.2
P_2O_5	0.02	0.01	0.01	0.02	0.02
LOI	47.6	47.3	47.3	46.9	45.3

Two approaches were used to measure structural discontinuities in the Blue Cave: measurements from the 3D model of the cave and field measurements directly in the cave. The measurements from the 3D model were done using the Compass plugin (Thiele et al., 2017) in CloudCompare ver. 2.13.1 (2023). Structural measurements of identified bedding planes, joints, fractures, faults, and slickensides in the cave were taken with an accuracy of ± 2° by the Freiberg Geological Structural Compass. The data were then processed in the software Stereo32 ver. 1.0.1 (Röller & Trepmann, 2003).

The inventory of solution cave morphologies and their spatial distribution, their relation to structural discontinuities, and the adjacent surface landforms, were used to reconstruct the processes of the origin and development of the cave. Also, lithological facies of preserved fluvial sediments contribute to clarifying the former hydrographical conditions during the cave formation. Using the cave map of P. Imrich, J. Szunyog, and others from 2016 (published in Šmoll, 2017), we studied the cave pattern. We determined the cave pattern and connectivity of cave passages based on the graph analysis applied to cave topology by Howard (1971). The period of formation of the cave was estimated based on a comparison of its relative height above the recent Boca Stream's streambed with the relative height and estimated age of stream terraces and cave levels in the nearby areas.

Results

Geological mapping

The geological mapping revealed that the Čierny Váh carbonates of the Blue Cave are not in a normal stratigraphic position, but are instead tectonically sandwiched between older non-karstic rocks. The Middle Triassic carbonates crop out as an isolated block on the left bank of the Boca Stream, flanked by the Upper Permian volcanics in the southwest and the Lower Triassic siliciclastics in the northeast. The tectonic position of the Čierny Váh carbonates between older rocks – subjacent volcanics and superjacent siliciclastics, can be deduced from their map expression (Figs. 2A and C). Additionally, the Upper Permian volcanics and the overlying Middle Triassic carbonates are in direct contact, without the stratigraphically intervening the Upper Permian to the Lower Triassic siliciclastics. The siliciclastics are also absent in the borehole Ma-2 (Biely, 1964), which penetrated through the Čierny Váh carbonates directly into the tectonic contact with underlying volcanics (Fig. 3). The absence of siliciclastics is particularly striking considering that the borehole is situated less than 15 m from the mapped contact of the siliciclastics and the Čierny Váh carbonates. Moreover, a small exposure of intensively deformed rocks was found at the contact between the Čierny Váh carbonates and siliciclastics, circa 100 m NE from the cave (Figs. 2C and 4A). Hence, we interpret the Middle Triassic Čierny Váh carbonates of the Blue Cave as a thrust sliver wedged between older rocks the underlying Permian volcanics and overlying Lower Triassic siliciclastics (Figs. 2A and C). Additional evidence of substantial thrusting can be found further from the cave and near the mines in the Olovienka Ravine.

Several tectonic slices of volcanic and siliciclastic rocks enclosed within dolomites were mapped near the Olovienka Ravine. On the left bank of the Boca Stream, approximately 150 m upstream from the ravine, Hanáček (1963) mapped siliciclastics within the dolomites, which do not appear in the subsequent geological maps. During our mapping, we found a de-vegetated slope that exposed not only the fragments of siliciclastics but also abundant fragments of volcanics (Figs. 2A and 4B). A small fan at the foot of a gully formed within carbonates also contained numerous clasts of volcanics, indicative of their upslope exposure. Abundant rauhwacken (cellular dolomites) occurring within the carbonates provide further evidence for the tectonic reworking of the rocks (Fig. 4D). Thanks to the subsurface data, the thrust fault mapped on the opposite bank can be traced to the mines in the Olovienka Ravine (Fig. 2A). On the left bank, the thrust is mappable due to the presence of the deformed siliciclastic rocks (Figs. 2A and 4C) older than the surrounding Čierny Váh carbonates. On the right bank, the siliciclastics were not

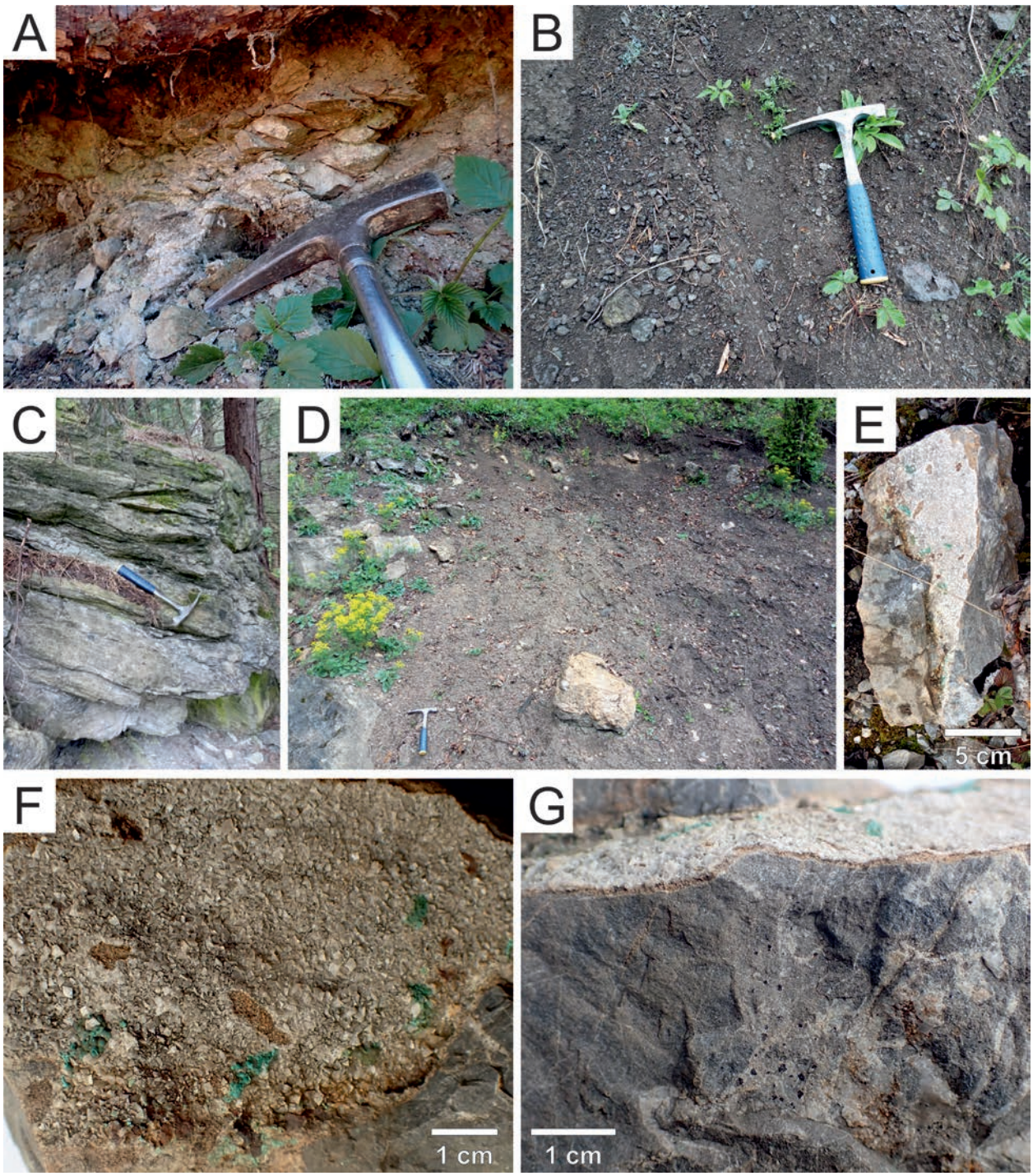

Fig. 4. Geological observations from the surface of the study area. **A** – Small exposure of tectonised rock at the contact between the underlying Middle Triassic carbonates and overlying Lower Triassic siliciclastics. **B** – Fragments of the Permian volcanic rocks exposed at the foot of a devegetated slope that occur between the Middle Triassic carbonates. **C** – Strongly tectonically stretched Lower Triassic siliciclastics that from a tectonic slice between the Middle Triassic carbonates. **D** – A zone containing yellowish fragments of tectonised carbonates (rauhwacken) within the grey, relatively undeformed carbonates exposed at the foot of a devegetated slope. **E** – Photograph of the malachite-bearing dolomite found in the talus below the outcrop near the Blue Cave. **F** – Close-up view of the vein in the dolomite containing malachite, euhedral calcite crystals, and rusty brown iron oxides. **G** – Close-up side view of the vein from figure F, macroscopic iron oxide crystals can also be seen in the rock below the vein. All photos by J. Littva.

mapped, but the borehole Ma-1 (Biely, 1964) penetrated several siliciclastic rock packages within the carbonates (Fig. 3). The siliciclastics were also observed in the walls of one of the mines in the Olovienka Ravine (Kantor, 1957), enabling us to interpolate the continuation of the thrust to this location. We interpret these observations as evidence of thrusting that disrupts the Čierny Váh carbonates and involves slices of older siliciclastics and volcanics.

Our mapping and the subsurface data from the unpublished reports have revealed a substantial tectonic reworking of the Čierny Váh carbonates. These rocks show distinctive internal deformation, with the Čierny Váh carbonates both incorporating and being incorporated into packages of the older siliciclastics and volcanics. Notably, these reworked rocks are positioned between the thick packages of less deformed rocks – the underlying Upper Permian volcanics and the Triassic carbonate suite of the overriding nappe (Figs. 1C and 2A).

Based on the observations from the DEM and field mapping, we mapped several terrace surfaces near the Blue Cave (Figs. 2A and C). The highest number of terrace risers seems to be preserved closer to the Blue Cave, at the confluence of the Boca Stream with its right tributary, the Malužiná Stream. Further from this point, the terrace preservation seems to be poorer (Figs. 2A and C). Unfortunately, this site is marked by extensive formation and collapse of karst features, which caused irregularities in the previously flat terrace surfaces, hampering the terrace mapping. Moreover, the area underwent considerable anthropogenic landscape modifications – the construction of roads, housing, and a recreational area. Resulting cut-and-fill earthworks resemble the terrace risers and benches, and thus complicate the determination of terrace levels. Therefore, instead of distinguishing individual terrace levels, we grouped the terraces into three categories: lower terraces, middle terraces, and upper terraces. Their relative heights above the recent streambed are 2–10 m, 10–20 m, and 20–30 m, respectively. Poor exposure of terrace risers prevented us from estimating the thickness of fluvial gravels on the terrace levels. A minimal gravel thickness of at least 2 meters can be assumed for one of the middle terraces, based on the presence of a two-meter-thick interval of fluvial gravels in borehole Ma-2 (Biely, 1964). The gravel thickness and the bedrock exposures in the terrace risers suggest that most of the terraces are strath-type terraces, possibly excepting some of the lower terraces.

Further from the cave, the terraces were mapped based on the DEM observations combined with data from previous geological maps (Jeremenko, 1956; Kubáň, 1956; Hanáček, 1963; Biely, 1976, p. 19; Vozár et al., 1983). Further verification was necessary for a flat surface at the left bank that extends from approximately 750 m downstream of the Blue Cave to approximately 200 m downstream of the Olovienka Ravine. The surface was mapped as a terrace only in the map of Hanáček (1963), but granitic pebbles were found in the geotechnical boreholes made at the same surface (Lošonská, 1984), corroborating the map. We mapped fluvial gravels at the flat surface, confirming Hanáček's (1963) map. Based on its relative height above the recent streambed (20–30 m), the terrace was assigned to the upper terraces.

The known parts of the Blue Cave are most closely associated with the upper and middle terraces. The elevation span of the documented cave spaces (between 742–767 m a.s.l.) predominantly corresponds to the position below the upper terraces, roughly at the level of the middle terraces. Some of the low-lying parts of the cave reach the level of the lower terraces as well. The association of the cave with the upper and middle terraces can also be observed in the map view (Figs. 2A and C).

Mineralogy and geochemistry of the area

In the studied area, the occurrences of the sulphide or malachite and azurite were noted at three localities: mines in the Olovienka Ravine, Malužinská Cave, and the Blue Cave. Sulphide minerals (galenite, sphalerite, pyrite, marcasite) were reported near mines (Kantor, 1957; Hanáček, 1963; Kantor, 1975) and in the nearby borehole Ma-1 (Figs. 2A, B, and 3). Cu sulphides (chalcopyrite and tetrahedrite), and also malachite and azurite occur in carbonates drilled by borehole Ma-2 at depths of 9–10 m and 15–16 m (Fig. 3). The dolomites covered by thin incrustations of malachite and azurite were observed in two surface outcrops (Hanáček, 1963; Ivanov et al., 1965), both associated with caves. The first one is located near the entrance of the Malužinská Cave (Figs. 2A and B), which presently lacks known spaces with coloured speleothems (Bella et al., 2014). The second outcrop, located less than a hundred meters from the Blue Cave, is presently completely covered by vegetation, preventing direct observation of the malachite or azurite. In a talus below the outcrop, we found a dolomite containing malachite (Figs. 4F and G) as well as small unidentified black minerals (Fig. 4G). Both mineral types are occasionally disseminated in the dolomitic rock mass. However, they are typically associated with veins in the dolomitic rock, along with the rusty-brown residue, possibly a weathering product of the sulphide minerals (Figs. 4F and G).

Following the distribution of minerals, the elevated trace quantities of Pb, Zn, and Cu also cluster approximately around mines in the Olovienka Ravine, the Malužinská Cave, and the Blue Cave (Figs. 2A–C). Hanáček (1963) and Ivanov et al. (1965) detected elevated amounts of copper utilising chemical analysis (up to 500 ppm) and semiquantitative spectral analysis (up to 1000 ppm) from both the outcrop and borehole samples. The trace amounts

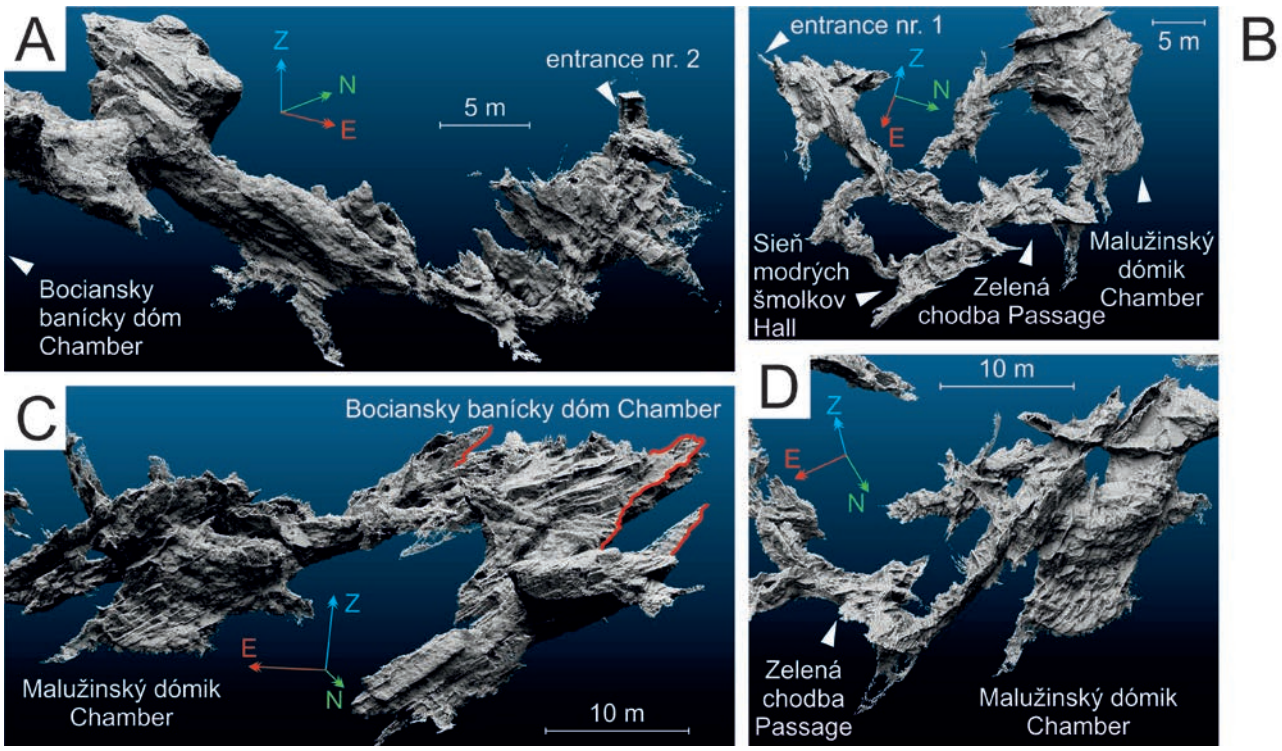

Fig. 5. Parts of the 3D model of the Blue Cave processed and viewed in CloudCompare (2023). **A** – The northwestern part of the Blue Cave formed in the bedded dolomites. Left side: Parts of the cave around the entrance nr. 2 controlled by the combination of joints and bedding. Right side: The bedding-controlled inclined passage leading to the Bociansky banícky dóm Chamber. **B** – The southeastern part of the Blue Cave, formed mostly in massive dolomites, with branching and intersecting passages that follow the bedrock fractures. **C** – A view of the Bociansky banícky dóm Chamber with thrust-and-fold structure (thrust outlined in red colour) and northwestern wall of the Malužinský dómik Chamber, exposing bedded dolomites. **D** – A view of the NE-SW fault that crosses the Malužinský dómik Chamber and separates the bedded and massive dolomites.

of lead are the highest near the mines. The same is true for trace amounts of zinc, although lower trace amounts of zinc were detected around the Malužinská Cave (Figs. 2A and B) and in the borehole Ma-2 (Fig. 3). Copper was detected around all three sites in trace amounts, but the rocks around the Blue Cave and in the borehole Ma-2 contain the highest concentration of copper. In the borehole, up to 400 ppm Cu and Zn, as well as < 100 ppm of Pb, were detected in dolomites at the depth interval of 6 to 20 m (Fig. 3), i.e. 746 to 734 m a.s.l. Thus, the Blue Cave is closely associated with the mineralised zone in the nearby borehole Ma-2, which contains Cu-sulphides, malachite, and trace amounts of Zn, Cu, and Pb.

Geological observations from the cave

The cave is hosted in grey and dark grey, sporadically brecciated dolomites, typically penetrated by a network of thin white calcite veins. The dolomites can be separated into two types based on the presence or absence of bedding. While the dolomites in the northwestern part of the cave are markedly bedded, in the southeastern part, the dolomites are massive-bedded (Figs. 5A–D and 7A). Both dolomite types markedly influence the character and morphology of the passages developed within them, as we will discuss later. The bed thickness in bedded dolomites generally ranges between 5–20 cm, with some thinner beds (2–3 cm) in between. Generally, the beds dip 25–45 degrees to the east, with some variations to the NE near the entrance and to the SE in the Malužinský dómik Chamber (Fig. 6). The dip and strike of the massive-bedded dolomites could not be observed. Both dolomite types are chemically similar, containing more than 20 % MgO (Tab. 1), and both are also microscopically similar. They comprise dolomicrosparite (samples MM-2, 3, and 6; Figs. 8A and C), breccia (samples MM-4 and MM-7; Fig. 8B), and dolosparite (samples MM-1 and 5; Fig. 8D), with sparry veins, dark brown stains after iron oxides, and microstylolites. The sample MM-5 was not completely recrystallised into dolosparite and contained patches of unrecrystallised dolosparite as well as fine pores (Fig. 8D). In the samples MM-3 and MM-6 from the bedded dolomites, dolomicrosparite has an occasional markedly directional texture, representing the bedding micrite (Fig. 8C). No fossils were found in the rocks and thin section, but based on the stratigraphic position above the Lower

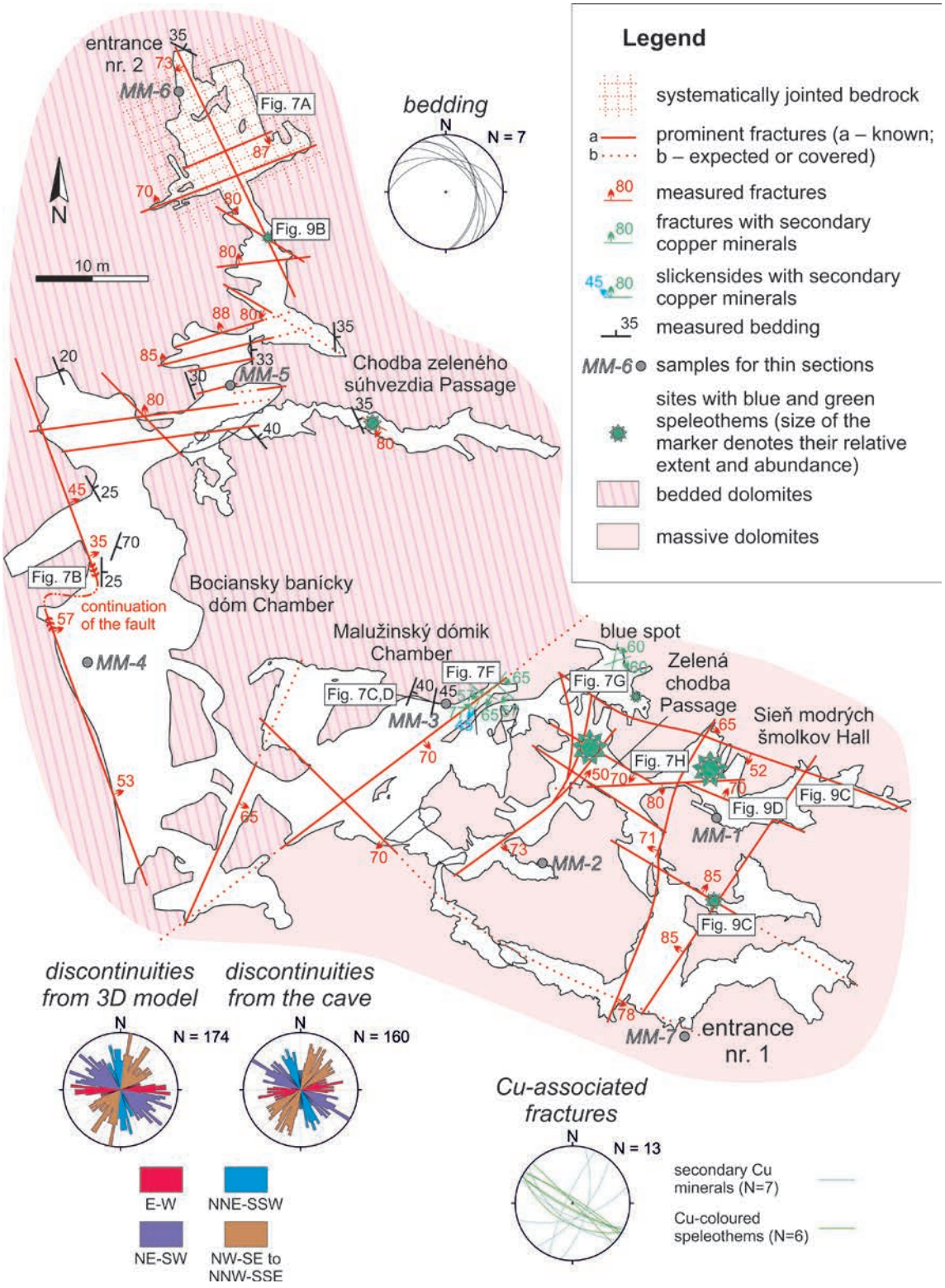

Fig. 6. Cave plan of the Blue Cave with marked-out geological features denoted in the legend and placement sites of photos from Figs. 7 and 9. The figure also includes two lower-hemisphere equal-angle stereographic projections and two rose diagrams with equal area-scaling generated in the Stereo32 software (Röller & Trepmann, 2003). The stereographic projections show great circles of fractures associated with the malachite and fractures associated with blue and green speleothems, and the bedding attitudes. The rose diagrams show strikes of the fractures measured from the 3D model and from the cave. The fracture sets are grouped into four colour-coded categories that are further discussed in the text.

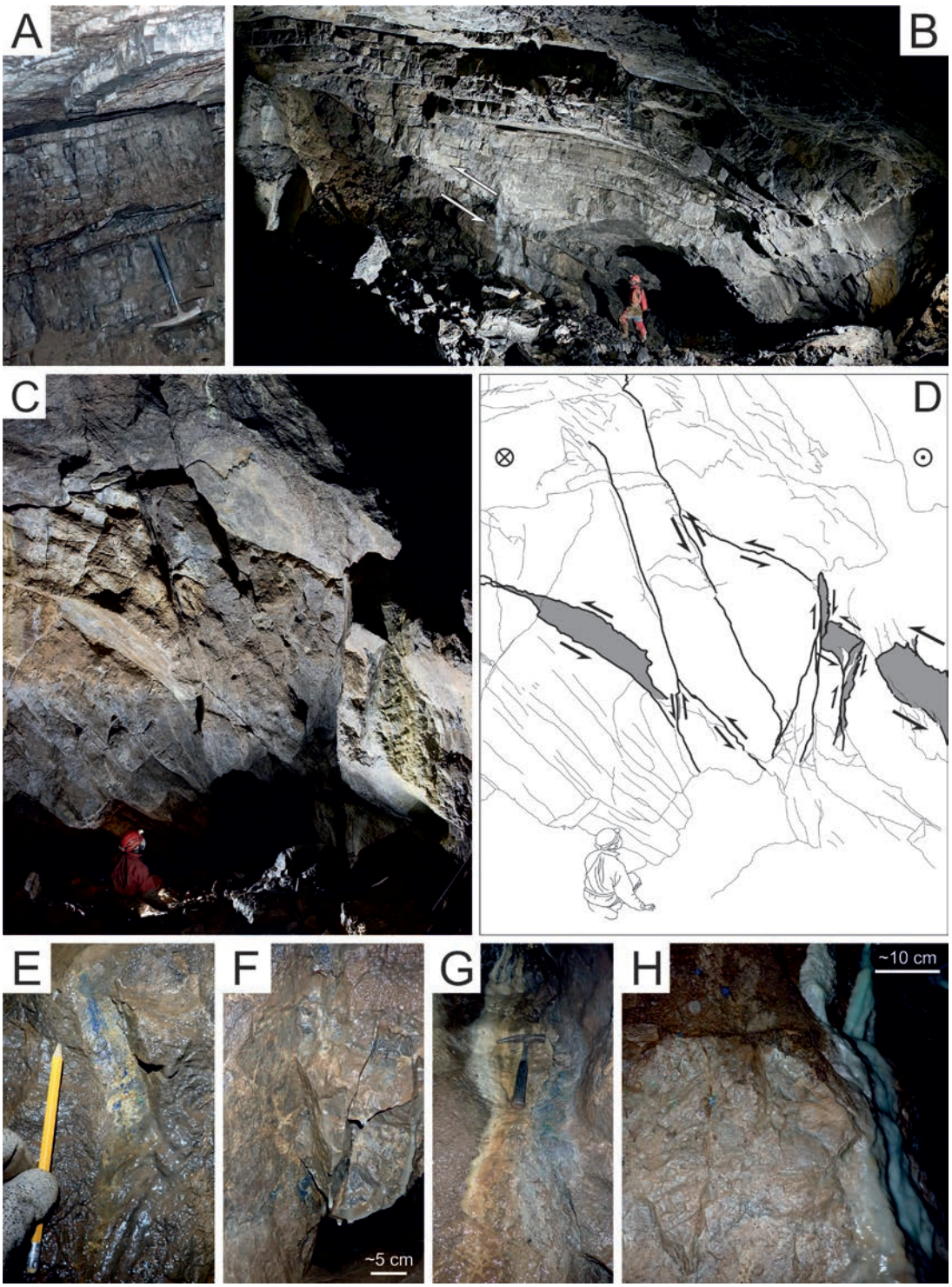

Fig 7. Lithological, structural, and mineralogical features observed in the Blue Cave. **A** – Bedded dolomites observed near the entrance nr. 2. **B** – Fold-and-thrust structure in the Bociansky banícky dóm Chamber, white half arrows denote movement sense. **C** – Rock wall in the Malužinský dómik Chamber exposing side view of the NE-SW-striking fault that dismembers a low-angle thrust fault. **D** – Interpreted sketch of figure C, with the dip slip component of movement denoted by half arrows and the strike slip component denoted by the circles (circled cross and circled dot – away from the viewer and towards the viewer, respectively). **E** – Slickenside of the fault shown in figures C and D, with calcite and possibly also azurite accretion steps indicating dextral movement sense. **F** – Azurite-bearing fractures in a crawlway concealed in the shadow in figure C. **G** – Fractured bedrock mineralised by the malachite and azurite near the 'blue spot'. **H** – Malachite and azurite occurring near the greenish speleothem in the Zelená chodba Passage. Photos: A, E, F, and H by J. Littva; B and C by P. Staník; G by L. Dušeková.

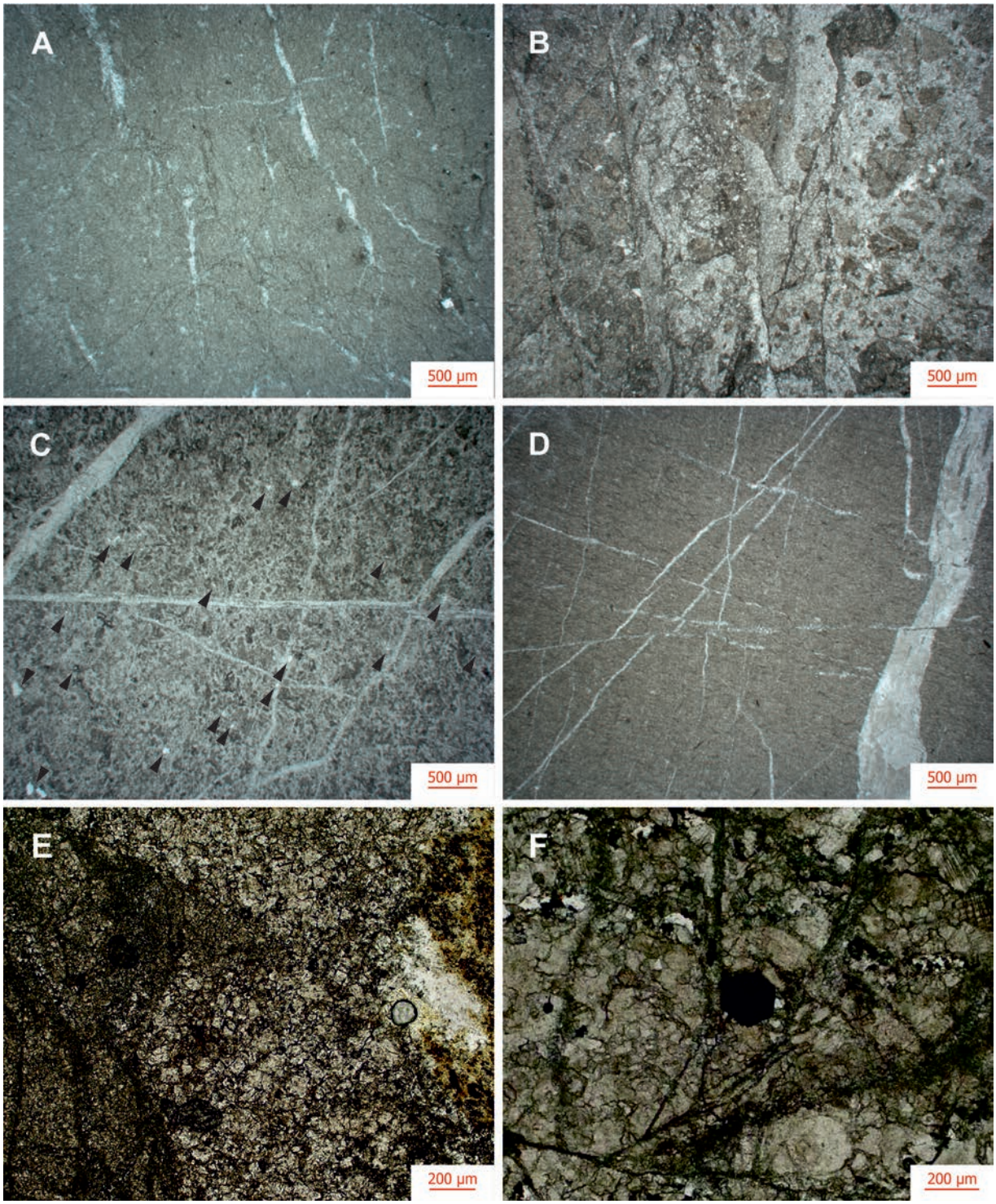

Fig. 8. Microphotographs of samples taken from the host rock of the Blue Cave, plane polarised light. **A** – Dolomicrosparite in the sample MM-3. **B** – Tectonically brecciated dolomicrite in the sample MM-4. **C** – Finely porous dolosparite with patches of unrecrystallised dolomicrite in the sample MM-5, pores marked by the black arrows. **D** – Bedding micrite in the sample MM-6. **E** – Euhedral dolomite crystals forming sparry matrix and iron oxides filling the intercrystalline pores, between the larger, less dolomitised clasts on the left and the right side of the picture. **F** – An euhedral iron oxide crystal that grew within the dolosparite of the sample MM-1. Photos: A–D by Ľ. Gaál; E and F by J. Littva.

Triassic rocks, we infer the Anisian age for the carbonates that host the Blue Cave.

In the thin section of the sample MM-7, we observed mineralisation that could be linked to the blue and green speleothems. Although the samples MM-4 and MM-7 are both breccias, they are markedly different. In the former, the dolomite clasts are compositionally uniform and have a brownish colour, and the crystals in the matrix are anhedral to subhedral and chiefly translucent (Fig. 8B). Based on the proximity to the thrust described below, the breccia in the sample MM-4 is likely tectonic. In the sample MM-7, the MgO concentration is slightly lower than in the sample MM-4, while concentrations of CaO and SiO_2 are slightly higher (Tab. 1). As the sample contains sparser, compositionally varied clasts, including the clasts of undolomitised limestone, it is likely of sedimentary origin. The matrix in the sample MM-7 is predominantly composed of euhedral crystals (Fig. 8E). The iron oxides filling the intercrystalline spaces among the matrix crystals lend the sample an overall rusty brown colour. Hence, the iron-oxides are not merely the primary constituent of the rock, but a result of secondary mineralisation, which exploited the intercrystalline porosity of the matrix.

In the sample MM-1, taken from the part of the cave most extensively decorated by blue and green speleothems, the mineralisation is even more intense. Instead of exploiting the porosity, up to 200 μm big (Fig. 8F) euhedral grains of the iron oxides developed directly among the grains. Despite the evidence of the mineralisation in the Čierny Váh carbonates, malachite and azurite were not directly observed in any of the thin sections from the collected samples.

In the cave, we encountered two major tectonic structures that have broader implications for the geology of the wider area. A conspicuous N-S-striking fold-and-thrust structure is observable both in the 3D scan and also directly in the Bociansky banícky dóm Chamber (Figs. 5C and 7B). It separates massive dolomites in the footwall from the brecciated dolomites in the hangingwall. In contrast to the thrusts observed on the surface, no older siliciclastic or volcanic rocks were incorporated into this structure. The second major structure is a steep NW-SE strike-slip fault zone guiding the Malužinský dómik Chamber. It separates the bedded dolomites prevalent to the northeast of the fault from the massive dolomites in the southeast (Fig. 5D). The faults of this zone dismember the thrust faults associated with the fold-and-thrust structure described above (Figs. 7C and D), constraining the post-thrusting age of the strike-slip fault. Although these two conspicuous structures predispose two of the three main chambers and halls of the Blue Cave, elsewhere, the cave spaces are guided by other tectonic structures.

The fractures that control the orientation of the cave spaces are oriented in four principal directions: NE-SW, NNW-SSE to NW-SE, NNE-SSW, and E-W (Fig. 6). In the passage leading from the entrance nr. 2 to the Bociansky banícky dóm Chamber, the E-W-striking sub-vertical (> 80°) fractures were the most frequently measured. The E-W fractures frequently predispose appearance of some salients of the main passage and also coincide with the passage's abrupt narrowings and widenings (Fig. 6). However, the main passage tends to follow the NW-SE to NNW-SSE fractures, which are most pronounced near the entrance nr. 2 in the form of the systematic joints (Fig. 6). Some of the blind branches and salients of both the main passage and Chodba zeleného súhvezdia Passage are also predisposed to this type of discontinuities (Fig. 6). From the Malužinský dómik Chamber to the entrance nr. 1, the fracture pattern changes, resulting in the different passage pattern of the cave. Although all fracture types were noted here, two fracture types are the most prominent: (1) steeply-dipping to subvertical (60°–90°) NE-SW fractures and (2) moderately to steeply-dipping (40°–80°) NW-SE to NNW-SSE fractures (Fig. 6). These fracture types guide most of the network of passages and their salients between the entrance nr. 1 and Malužinský dómik Chamber (Figs. 5A–D and 6).

While the fold-and-thrust structure is unmineralised, the malachite and azurite appear on the NW-SE and NE-SW discontinuities, and blue and green speleothems are associated with the NW-SE fractures. Malachite, azurite, and occasionally black minerals (likely iron oxides) are extensively associated with the NE-SW fault (Figs. 6 and 7E–H). The azurite appears to form an accretion step behind the calcite steps on the slickenside associated with the NE-SW fault (Fig. 7E), indicative of a dextral strike-slip. Other similarly oriented slickensides from other parts of the cave also bear dextral kinematic indicators, but lack the azurite or malachite. On the other hand, the malachite and azurite are also associated with some NW-SE-oriented fractures (Fig. 6). In contrast, the blue and green speleothems are hosted exclusively by the NW-SE fractures (Fig. 6). The speleothems appear most extensively in Sieň modrých šmolkov Hall and Zelená chodba Passage (Figs. 6, 9A and D). Some smaller blue and green speleothems were also observed in the Chodba zeleného súhvezdia Passage and near the entrances nr. 1 and 2 (Figs. 6, 9B and C).

Cave morphology and clastic sediments

The Blue Cave is an inactive phreatic cave with several loops (*sensu* Ford, 1977, 1988, 2000; Ford & Ewers, 1978), in places with steep parallel fractures enlarged into halls and chambers that were later remodelled by collapse. In the direction of the former water flow, the upward leading parts of the loops are mostly controlled by fractures, while the

downward leading parts are controlled by bedding planes of host rock carbonates. Downward inclined oval passages were enlarged from initial bedding-plane anastomoses. Small lateral conduits, featured by a channel-like ceiling and floor covered by fine-grained sediments, sloping along inclined bedding planes, correspond to a morphology and structural control of bedding-plane anastomoses (*sensu* Bretz, 1942; Ewers, 1966; Palmer, 2007 and others). Some of these were formed later than the main cave passages, probably by injected floodwater. Large scallops on the rock wall in the northern part of the cave indicate a former water flow that moved downwards into the bedding-plane conduits. Ceiling solution pockets are developed mostly in the lower part of the loops, mainly in places where they are cut by transverse fractures (Fig. 10D). Conversely, larger ceiling pockets to cupola-like cavities are mostly observed in the upper part of the loops.

The ground plan of the cave shows three partially different parts: (1) a network-like pattern in its south-eastern part composed of main passages controlled mostly by parallel and intersecting fractures developed in massive dolomites; (2) a fold-and-thrust-controlled spacious, elongated chamber-like cavity in its western part (Bociansky banícky dóm Chamber); (3) crossing and less interconnected passages in its northern part controlled mostly by fractures, in some places influenced by bedding planes. Many small lateral passages are represented by dead-end fissures or bedding-plane anastomoses, considered as floodwater injection features (*cf.* Palmer, 1991, 2007).

A degree of connectivity of the whole cave pattern is given by the quantitative parameters = 0.081, = 1.096, and = 0.374 calculated based on the graph analysis applied to the cave pattern according to Howard (1971). A slightly higher degree of connectivity of the labyrinth-like part is given by parameter values = 0.097, = 1.163, and = 0.404. For a large cave network with a very high degree of interconnection and few dead-end passages or exits, these parameters reach the values 0.25, 1.5, and 0.5. For caves with few loops and a dendritic channel pattern, they reach the values 0.1 and 0.33 (Howard, 1971).

The largest cavity in the south-eastern network-like part of the cave is the Malužinský dómik Chamber, which is mainly predisposed by the NW-SE fault and genetically related fractures. A spacious, elongated cavity called the Bociansky banícky dóm Chamber in the western part of the cave is the cave's most voluminous.

Inwardly sloping smooth solution facets (Fig. 10B) – planes of repose *sensu* Lange (1963) developed on both sides of the passage between the Bociansky banícky dóm and Malužinský dómik chambers. They were formed during the sedimentation of fine-grained insoluble rock particles on the floor and inwardly sloping parts of the cave walls. These particles protect the covered bedrock from further dissolution.

Inclined wall half-tube notches, limited in extent, are visible in parts of the cave formed in bedded dolomites and controlled by bedding planes (Fig. 10C, preserved on the right side of the passage). They can probably be classified as paragenetic solution ramps, which form in a phreatic environment at the surface of the sedimentary floor when the dissolution of the wall between a sedimentary fill and the ceiling is preferential (*cf.* Farrant & Smart, 2011). Smaller wall water-table notches originated in standing water (*cf.* Ford, 1988; Lauritzen & Lundberg, 2000 and others) and occur only around small wall niches.

The stalactites in the Sieň modrých šmolkov Hall bear marks of the former flooding of the cave that postdates their growth. The stalagmites are covered by a thin veneer of fine-grained sediments, indicating the level of the floods (Fig. 9D).

The floor of the lower part of the loops is mainly covered by fine-grained sediments deposited from the suspension in slowly flowing to stagnant water (slackwater facies *sensu* Bosch & White, 2004). In several places, granite sand was also exposed in artificial floor trenches. Although granite gravels are preserved on the surface near the cave, they are sporadic in the cave. The northern entrance to the cave was dug through the accumulation of allochthonous gravels, predominantly composed of granitic pebbles, with sporadic pebbles of volcanics and quartz sandstone. The gravels were likely deposited on the original terrace surface and redeposited into the collapsed doline-like depression.

The chambers and halls of the cave were almost completely changed by the breakdown (mostly by block and slab breakdown). The ceiling and the walls of the Malužinský dómik Chamber are featured by a vaulted cross-section with step-like dividing planes of breakdown collapses. Large ceiling breakdown cupolas (*sensu* Slabe, 1995) occur in the northern part of the Bociansky banícky dóm Chamber (Figs. 11A and B). They were formed by the gradual flaking of the slabs of thin carbonate beds as a result of the gravitational disintegration of folded carbonates on the cave roof. The floors of the chambers are covered by debris fields, piles of carbonate blocks, and slabs fallen from the ceiling. A similar character of the ceiling can also be observed near entrance no. 2, but in this case, the breakdown is enhanced by the presence of the pervasive fractures oriented NNW-SSE and E-W. In the northern half of the cave, which is formed in layered dolomites, the breakdown and resulting morphologies are more pronounced.

Interpretation and discussion

Tectonic structure of the Hronic Unit

We believe that the Hronic Unit in the study area comprises two relatively competent tectonic units separated

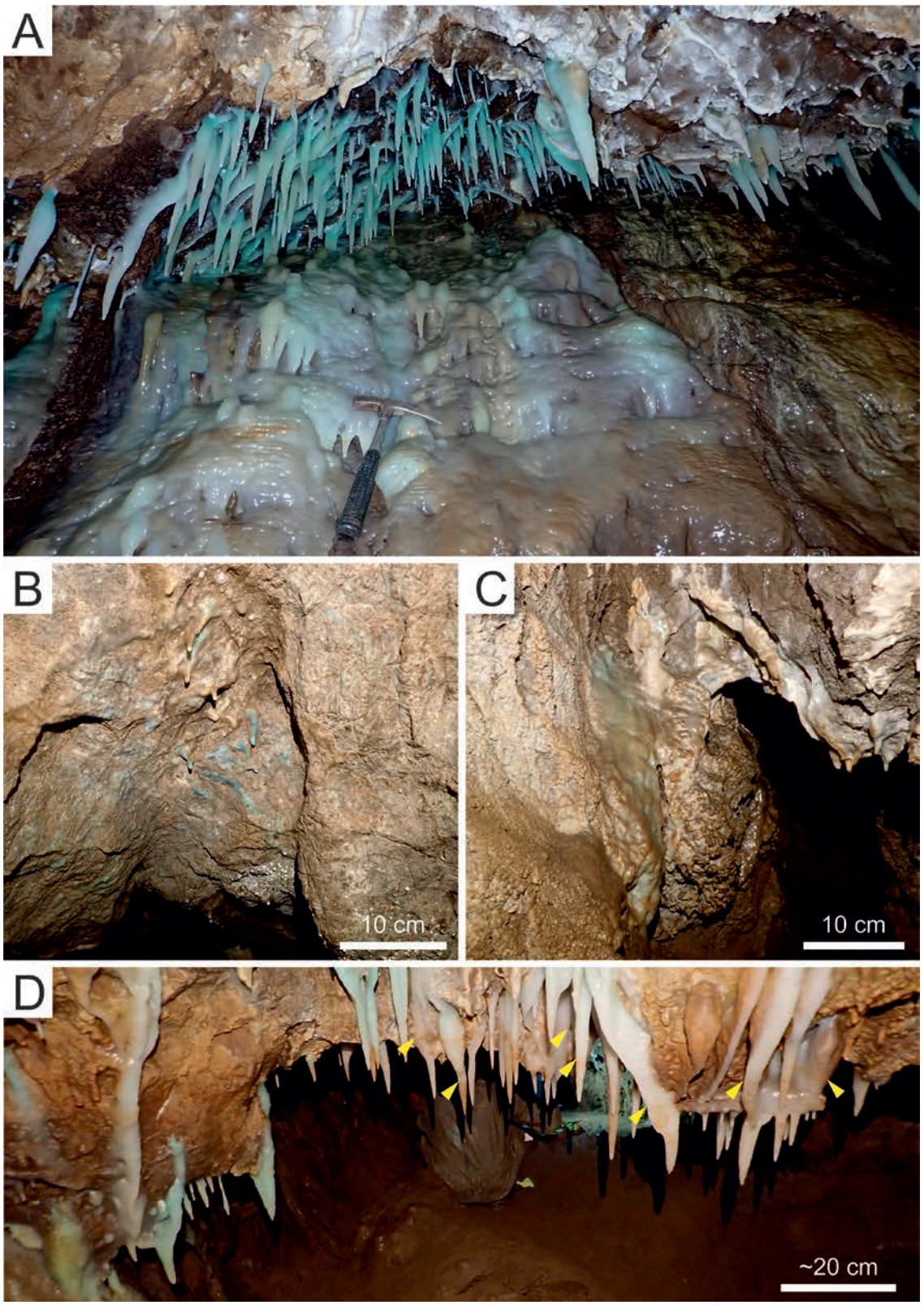

Fig. 9. Coloured speleothems of the Blue Cave. **A** – Blue to green dripstones and flowstones in the Sieň modrých šmolkov Hall. **B** – Blue to green speleothems in the passage leading from the entrance nr. 2. **C** – Greenish flowstones in the passage leading from the entrance nr. 1. **D** – Thin veneer of flood sediments deposited on the stalactites in the Sieň modrých šmolkov Hall. Yellow arrows denote the floodmark level of the past flood events. All photos by J. Littva.

by a structurally imbricated zone. The zone involves tectonic slices typically composed of the Permian to Middle Triassic siliciclastic and carbonate rocks (Fig. 1C). The structurally imbricated zone can occasionally involve the Permian volcanics, but they typically form a thick rigid rock package belonging to a competent tectonic unit below the zone (Fig. 1C). The upper competent unit, belonging to the Svarín nappe is predominantly composed of a thick and rigid sequence of the Mesozoic carbonate rocks (Fig. 1C). The structural imbrication likely developed during the translation of the overriding Svarín nappe between two relatively competent and thick rock packages. The carbonates that host the Blue Cave are part of a tectonic slice involved in this zone (compare Figs. 1C and 2A–C). The Čierny Váh carbonates are further internally deformed, as seen from the fold-and-thrust structure found in the Blue Cave (Figs. 5C and 7B), which shows a top-to-the-west shear sense. This movement sense roughly corresponds with the overall northwestern direction of tectonic transport for the Hronic nappes (Biely, 1963; Biely et al., 1997; Kováč & Filo, 1992; Kováč & Havrila, 1998).

In our opinion, the intensively deformed zone between two nappes should not be recognised as a separate nappe. Hence, the separation of three subordinate Hronic nappes as proposed by some authors (Biely, 1963, 1964, p. 28–29, 1976, p. 60–64; Biely et al., 1997, p. 147–149) is not necessary. Instead, it is more plausible to distinguish two subordinate nappes, with the lower nappe forming local imbrications caused by the translation of the overriding nappe. The nappes differ in the facial character of their Middle to Upper Triassic carbonates, with the upper one containing basinal carbonates, which are absent in the lower nappe. On contrary to previous interpretations, which also divided the Hronic Unit into two tectonic units separated by a deformed zone (Biela, 1960, p. 24–27; Biely, 1960, 1962), we consider the structurally imbricate zone to be a local phenomenon. To the west, the zone of imbricated slices becomes progressively thinner and more complicated, until it eventually pinches out. To the east, the rock succession thickens and becomes stratigraphically more coherent, forming a larger, internally less deformed structure (Pukanec duplex *sensu* Tulis & Novotný, 1998, p. 70–71, Appendix 1).

Some authors suggested that the tectonic imbrication could affect the entire body of the lower nappe (e.g., Badár et al., 1965, p. 69–72; Vozár et al., 1983, p. 83–85; Tulis & Novotný, 1998, p. 70–71, Appendix 1). This idea is supported by the occurrence of the slices of the Lower Triassic siliciclastics and the Middle Triassic carbonates below the Paleozoic rocks of the lower nappe (Olšavský, 2007a, b, 2008, p. 168–173). Given the results of our mapping and the rheological considerations, we still believe the rocks above the Permian volcanics are more intensely deformed than the rest of the lower nappe in the study area. Nonetheless, we cannot exclude the existence of other intensely deformed zones situated between the relatively competent rocks of the lower nappe. For example, further to the east, the Middle Triassic Čierny Váh carbonates of the lower nappe are considerably thicker and therefore more rigid. Here, shales, marlstones, and limestones of the Upper Triassic to Cretaceous age seem to be involved in the deformation zone that separates the lower and upper nappes.

Our map generally corresponds with the map of Tulis & Novotný (1998, Appendix 1) better than with the map of Biely et al. (1992), except for the distinct NW-SE fault that is absent in the former map. Although Biely et al. (1992) might have overemphasised the steep faults over thrust faults, this particular fault, also mapped by Vozár et al. (1983), is also recorded in our map (Fig. 2). The right-lateral movement sense on the fault is obvious from the offset in the basal thrust of the upper nappe by approximately 500 meters Hronic Unit (Figs. 1C and 2A). Interestingly, after restoring the offset, mines in the Olovienka Ravine, Malužinská Cave, and the Blue Cave would be located much closer to each other, perhaps even associated with the same thrust fault.

Geological controls on the speleogenesis

Based on the characteristic features, such as dark colour, bedding thickness, and white veins, we consider the Čierny Váh carbonates that host the Blue Cave to be a dolomitised equivalent of the Anisian carbonate formations. The bedded dolomites could be the equivalent of Gutenstein limestones and dolomites, which are typically distinctly bedded (e.g. Moser et al., 2024). The massive dolomites could represent an equivalent of the younger limestone types, which tend to be thick-bedded or massive, such as Annaberg or Steinalm limestones (e.g. Moser & Piros, 2021; Moser et al., 2024). However, massive dolomites might have arisen as a result of a higher degree of dolomitisation, since the process can obliterate bedding (Fig. 11C in Machel, 2004). Our observations in this regard are inconclusive. On the one hand, the micritic microfacies are absent in the massive dolomites (samples MM-1 and MM-2), which would point to a higher degree of recrystallisation. On the other hand, the lower MgO content and preservation of the original textures in the clasts of breccia in the sample MM-7 contradict the idea of the massive dolomites being more dolomitised.

Although limestones to dolomitic limestones are known to be present in the Čierny Váh carbonates (e.g. Urban, 1959; Srnánek, 1962; Badár et al., 1965), the Blue Cave is hosted mainly in the dolomites with high Mg content (Tab. 1). The Mg content above 20 % was also detected in the dolomites that host the nearby Malužinská Cave (Bella et al., 2014). The breccia from the sample

MM-7, taken from the outcrop above the cave entrance, has the MgO content of 18 %, but this rock type was not identified anywhere in the cave. The location of the caves is even more surprising given the presence of both limestones and dolomitic limestones, with MgO content of 2–2.5 % and 15 % respectively, directly in the study area (Urban, 1959). It seems that the MgO content of the Čierny Váh carbonates did not exert a significant control on the formation of the most spacious caves in the study area. As dolomites are typically less prone to for karstification than the limestones, it seems to be facilitated by other factors. Except for the samples MM-5 and MM-7, the dolomite shows little to no intercrystalline porosity. Thus, other porosity types, such as fracture porosity, played a dominant role in the formation of the Blue Cave.

The bedrock structures that predominantly contributed to the formation of the Blue Cave were the brittle tectonic structures (Fig. 6) that developed after the translation of the Hronic nappes. The bedding controls some of the passages in the northeastern part of the cave, but is irrelevant for the southeastern part of the cave that formed in the massive dolomites (Figs. 5A–D and 6). The same is true for the fold-and-thrust structure, which controls the parts of the cave around the Bociansky banícky dóm Chamber, but its influence in other parts of the cave is minimal (Figs. 5A–D and 6). A prominent steep NE-SW fault that predisposes the Malužinský dómik Chamber, separates the cave into two structurally and lithologically distinctive domains (Figs. 5D and 6). The cave spaces between the entrance nr. 2 and the Bociansky banícky dóm Chamber hosted in bedded dolomite seem to be controlled predominantly by the NNW-SSE and E-W fractures (Fig. 6). Southeast of the fault, between the entrance nr. 1 and the Malužinský dómik Chamber, the massive host rock is permeated by two fracture types: (1) NE-SW and (2) NW-SE to NNW-SSE fractures (Fig. 6). Based on the orthogonal orientation of the fracture sets in both domains one could assume that the fractures had originally the same orientation and were rotated into their current position. However, the orientations of fractures associated with blue and green speleothems are consistent across both domains, contradicting the assumption of rotation.

Due to the Triassic age of the host rock and the general absence of kinematic indicators on the brittle structures, attributing the age to the measured brittle structures was challenging. The formation of the fold-and-thrust structure can be quite confidently correlated to the nappe translation, which occurred during the middle part of the Cretaceous (e.g., Plašienka, 2018; Hók et al., 2022). From the other brittle structures, the age could be constrained only for the dextral NE-SW faults, most prominently the distinctive fault crossing the Malužinský dómik Chamber (Figs. 5D, 6, 7C and D). Faults with this kinematics were active only during the E-W compression from the late Paleocene to the middle Eocene (e.g., Pešková et al., 2009; Vojtko et al., 2010; Sůkalová et al., 2012; Gerátová et al., 2022; Hoppanová, 2024). As we did not observe any cross-cutting relationships in the other fracture types, it is not possible to reliably narrow down the age of their activity. A tenuous upper age bracket can be provided by the estimated post-Middle Pleistocene age of speleothems, which are not tectonically disrupted. Hence, at least the fractures that are closely associated with speleothems could not have been active after the speleothem deposition.

Source of the green and blue colouration of speleothems

Based on our results, the hypothesis proposed by Orvošová et al. (2016) for the source of the copper in the blue and green speleothems warrants a modification. The copper mineralisation is indeed known from the Permian rocks, occurring in the sandstones, but also in the barite-sulphide veins of the volcanics (Stankovič in Vozár et al., 1983, pp. 108 – 112). But the Pb-Zn-Cu mineralisation was also detected throughout the Middle Triassic carbonate bedrock in the area, and the presence of copper was reported near the cave (Kantor, 1957; Hanáček, 1963; Biely, 1964; Ivanov et al., 1965; Kantor, 1975; Kantor & Ďurkovičová, 1977). A mineralised zone in the uppermost interval of the borehole Ma-2, located in extreme proximity to the cave, contains chalcopyrite and malachite, and is therefore the most likely copper source. Hence, it is not necessary to derive the copper in the dripwater from the weathering of the ores in the Permian rocks. Although the copper could have been originally remobilised into the Middle Triassic carbonates from the Permian rocks, more research would be required to test this hypothesis. Furthermore, the mineralisation in the carbonates is not evenly disseminated; rather, it seems to be predisposed by the brittle tectonic structures.

The primary sulphide mineralisation seems to be linked to the shallow-dipping thrust faults, while younger supergene copper oxides occur on the steeper NE-SW and NW-SE fractures. Hence, the Pb-Zn mineralisation at the Olovienka Ravine developed during or after mid-Cretaceous nappe stacking. The rock units in the broader area around the Blue Cave experienced episodes of denudation in the Late Cretaceous to the early Eocene and from the Early Miocene to the Holocene (e.g. Danišík et al., 2011; Kováč et al., 2016; Králiková et al., 2016; Vojtko et al., 2016; Kováč et al., 2017). The primary ore could have therefore experienced multiple episodes of oxidising conditions necessary for the formation of malachite and azurite observed in the Blue Cave. One such episode could be dated to be synchronous with the dextral movement on the NE-SW fault during the late Paleocene to the middle Eocene. In other cases, the malachite and azurite appear to be deposited within the preexisting fractures and could be substantially younger than the fractures hosting them.

Notably, the occurrences of azurite and malachite, as well as the blue and green speleothems, seem to be linked to the specific sets of fractures. While the malachite and azurite occur at the NE-SW and NW-SE fractures, the occurrences of blue and green speleothems are limited to the NW-SE-striking fractures. This indicates that despite the difficulties in pinpointing the age of the fractures, the formation of the malachite and azurite is somehow temporally or spatially linked to these fractures. Uncovering this relationship between the minerals and fractures would require more in-depth research that is beyond the scope of this study. The predisposition of the blue and green speleothems on the NW-SE fractures indicates that these fractures represent a main pathway for vadose water that seeps into the cave and forms the speleothems. The fractures probably encounter the same mineralised zone that was drilled in the borehole Ma-2, as they cross the bedrock from the surface to the cave.

Origin and development of the cave in relation to the evolution of the valley

Despite the association of the sulphide ores with the Blue Cave, the predominant morphological features in the cave are consistent with the formation of the cave by meteoric waters, not by sulphuric acid. Nevertheless, the contribution of the supergene sulphuric acid speleogenesis (*sensu* Webb, 2021), i.e. oxidation of sulphide minerals by meteoric waters, cannot be fully ruled out. In the malachite-bearing dolomite collected from the surface, we observed an open vein with rusty brown iron oxides at its edge, covered by euhedral calcite crystals and malachite (Figs. 4E–G). Thus, the vein could have been dissolutionally enlarged before or during the formation of the iron oxides. In the upper interval of the borehole Ma-2 near the cave, the mineralised zone containing chalcopyrite and other sulphide minerals was observed, as well as the indicators of sulphide weathering (Biely, 1964). Biely (1964) noted malachite incrustations, brown vein fillings (likely an oxidised residue after the sulphide weathering) and the porous dolomites (Fig. 3). The chalopyrite oxidation is also believed to occur currently in the bedrock near the cave, playing a crucial role in the formation of blue and green speleothems (Culková et al., 2025). A finely porous dolomite was also observed in the thin section from the sample MM-5 (Figs. 6 and 8D). The sulphide dissolution could have created the sulphuric acid that created or enhanced the porosity of dolomite. This so-called scattered porosity, as described by De Waele et al. (2024), is insufficient to create a cave by itself. But the porosity could have facilitated the subsequent formation of the Blue Cave by enabling easier penetration of aggressive groundwater into the bedrock and increasing the area of the reactive surface. The elevated amounts of Zn in carbonates, likely associated with the sulphide minerals, near the other sizeable Malužiná Cave, further underscores this possibility.

The morphological evidence indicates that the cave was formed chiefly by the aggressive allochthonous waters and repeated floodwater injections from the surface stream into the carbonate bedrock. The position of the cave immediately downstream from the non-karstic rocks also indicates that the waters of the surface stream played a dominant role in the formation of the cave. Prevailing fine-grained slackwater sediments on the cave floor indicate that the cave was formed by slowly flowing stagnant water in phreatic and epiphreatic conditions (i.e. below and at the level of the groundwater table, respectively). This is further supported by the presence of solution facets (Fig. 10B), which indicate that fine-grained sediments were deposited in the cave during its formation. Morphological forms that would indicate a faster water flow, like smaller scallops, are absent.

The primary phase of the cave evolution probably occurred in a phreatic zone during the formation of a flat rock surface of the upper stream terraces above the cave. The extensive occurrence of phreatic morphological forms in the cave (Fig. 10A) contrasts with the almost complete absence of distinctive epiphreatic and vadose forms (horizontal wall notches, floor channels). This suggests that the most extensive speleogenesis occurred mainly below the level of the surface stream, and in later stages, the cave was only partially remodelled.

After the incision of the valley floor, the cave was remodelled during the formation of middle and lower stream terraces, as the surface water sporadically penetrated into the cave located at the left bank of the surface streambed. Allochthonous water entered the cave through several small swallets and opened fissures that occurred on the inside convex bank of the meandering stream, mostly during floods (bank storage *sensu* Palmer, 1991, 2007). Inflow conduits leading downwards from these inlets were interconnected in the adjacent southeastern part of the cave, creating a network pattern. The limited capacity of the inlets prevented a greater amount of coarse-grained sediments from the surface streambed from being transported into the cave. The solution facets associated with the deposition of the fine-grained sediments (Fig. 10B), as well as thin sediment veneers on stalactites (Fig. 9D), were also formed in this stage. Air traps at the top of the ceiling pockets (Fig. 10E) provide additional evidence of the former flooding of the cave, suggesting that passages were occasionally filled with water under pressure during repeated floods. During the vadose development phase, fine-grained sediments were partially removed from the cave by moderate-flowing water. In elevated areas, the cave bedrock floor could have been slightly lowered.

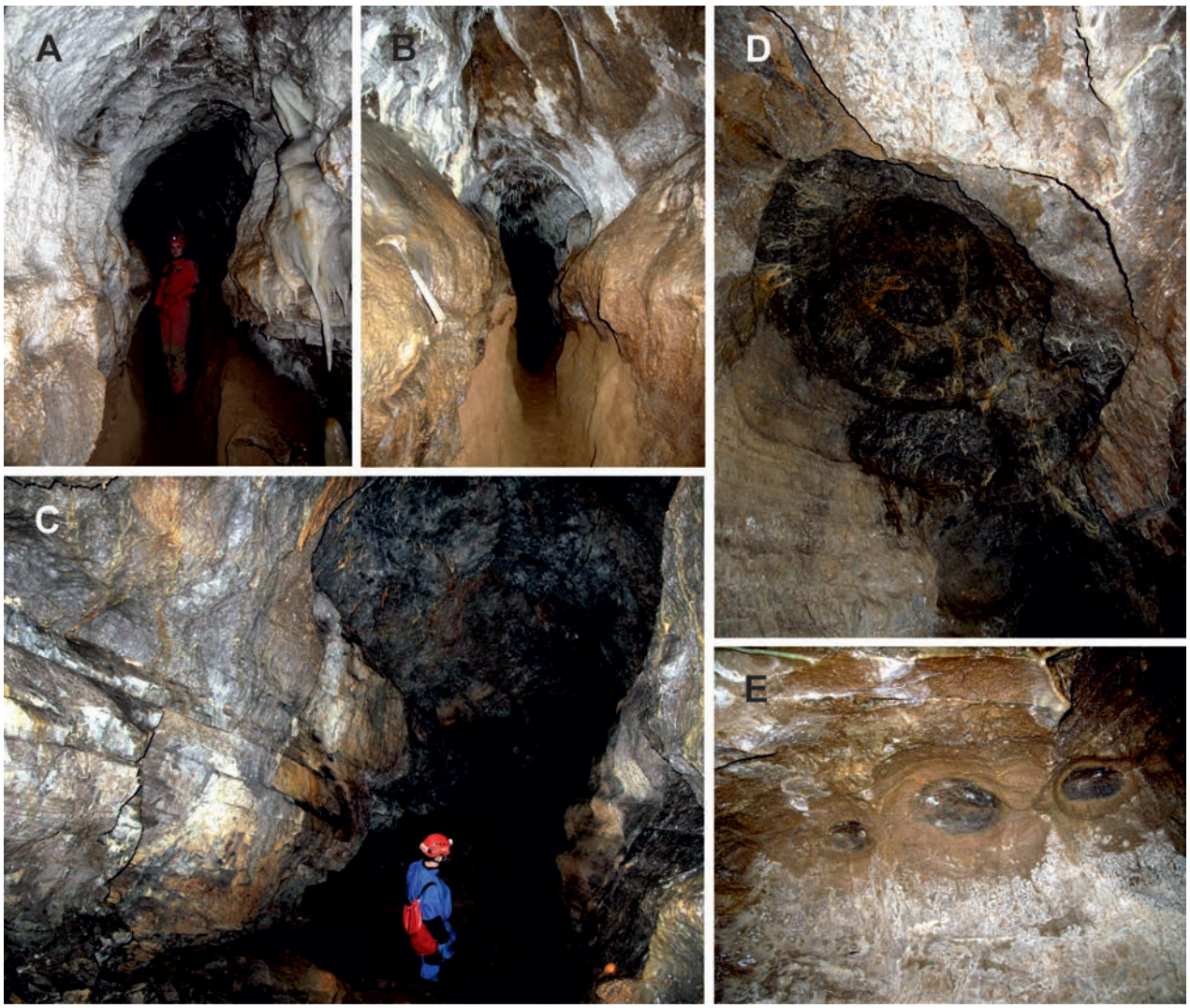

Fig. 10. Solution morphologies in the cave. **A** – Phreatic passage controlled by steep fracture. **B** – Inwardly sloping solution facets (planes of repose) on both sides of phreatic passage controlled by steep fracture. **C** – Multi-phase passage consisting of phreatic tube and lower epiphreatic to vadose incised floor (partly remodelled by breakdown). **D** – Large ceiling pocket. **E** – Air traps at the top of the ceiling pockets. All photos by P. Bella.

In the final stage of cave evolution, phreatic solution morphologies were remodelled by breakdown, mostly in places of increased structural and tectonic disintegration of the bedrock.

The main parts of the cave span relative heights of 20–25 m above the current Boca Stream's surface streambed, which correspond to the relative heights of the upper terraces. In the study area, the upper terraces are the most extensive of the mapped terraces and occur both upstream and downstream from the cave. The distinctive river terrace at almost the same relative height (about 20 m) above the recent streambed occurs on the left side of the Váh River valley between the village of Kráľova Lehota and the town of Liptovský Hrádok (Hromádka, 1931; Kettner & Šťastný, 1931; Vitásek, 1932). Compared with the relative height and estimated age of river terraces further downstream in the Liptovská kotlina Basin (Droppa, 1964, 1970, 1972c; Vitovič & Minár, 2018), and cave levels in the Demänovská dolina and Jánska dolina valleys (e.g. Droppa, 1966, 1972a, b), it can be assumed that the Blue Cave formation initiated during the Middle Pleistocene.

The surface of the upper terraces is perturbed by karst collapse processes. Several collapsed doline-like depressions with numerous granitic pebbles on the bottom, can be observed on the upper terraces (Fig. 2A). They formed due to the higher degree of karstification of the carbonate bedrock below the stream terrace and both cave entrance were excavated in these depressions (Fig. 2A). Comparable, albeit less distinctive depressions with

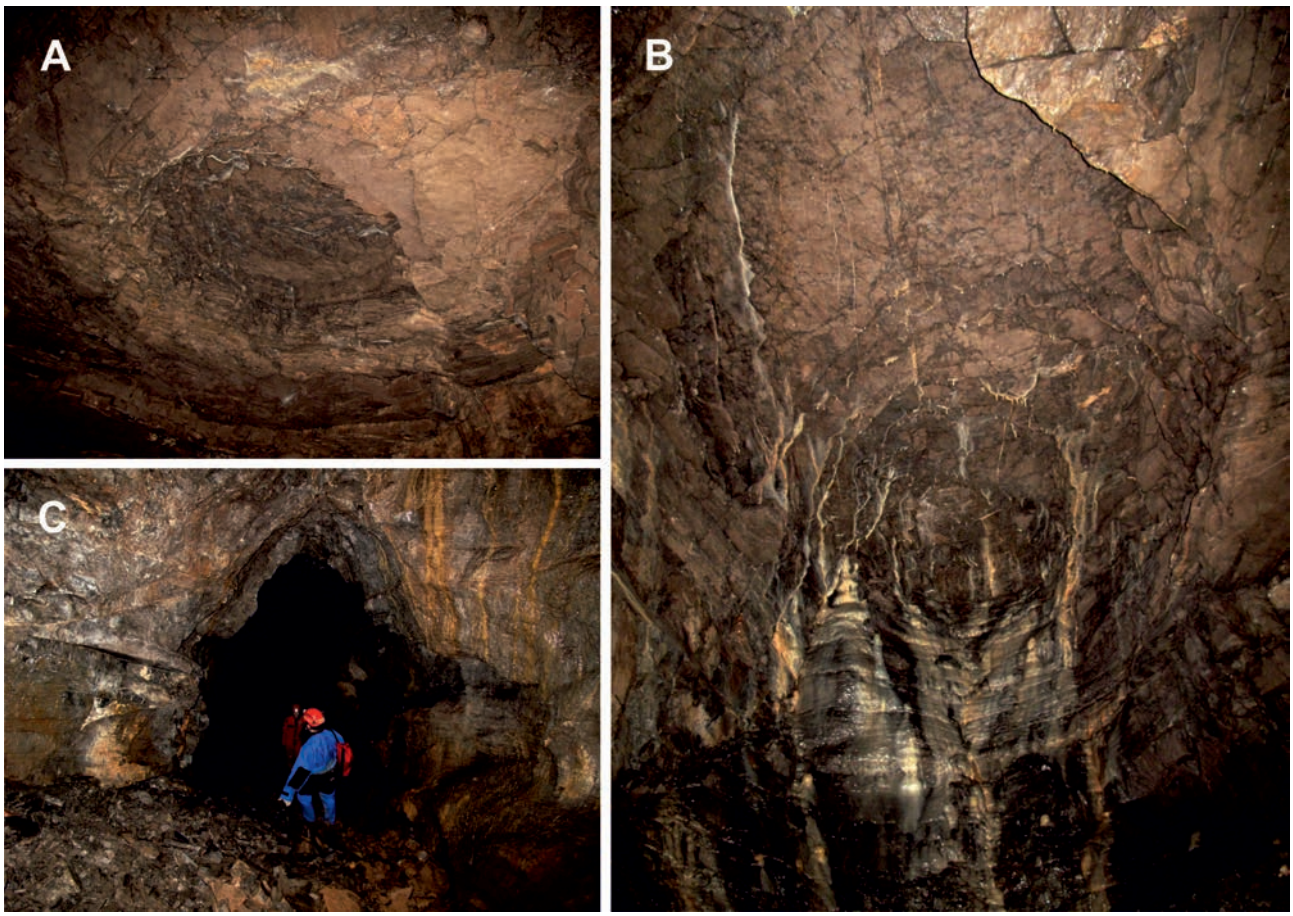

Fig. 11. Breakdown cave morphologies. **A**, **B** – Shallow breakdown cupolas. **C** – Phreatic passage partly remodelled by breakdown, its original floor is covered by debris. All photos by P. Bella.

granitic gravels can be observed on the volcanic bedrock. Assuming the depressions are not anthropogenic, they could be caused by the presence of the karstified Triassic carbonate rocks underthrust below the Permian volcanics.

Utilising the caves in geological research

The observation of several key geological phenomena would not be possible without direct observations of the bedrock in the Blue Cave. For example, the bedded dolomites and geological structures observed in the cave were not observed in the surface mapping. While the malachite was observed in the talus of the surface outcrop, the malachite and azurite in the cave could be observed more clearly and in their original context (compare Figs. 4E–G with Figs. 7E–H). Although important insights were also gleaned from the borehole data, they are much costlier than the observations on the rocky cave walls. Our findings underscore the utility of the caves as a sort of 'natural boreholes' in the geological research (cf. Vlček, 2011; Šebela et al., 2021).

Conclusions

Based on the geological mapping of the Blue Cave's surroundings, the Middle Triassic carbonates that host the cave are strongly perturbed by the mid-Cretaceous stacking of the Hronic nappes. We propose that the Hronic Unit in the study area is separated into two nappes, with the carbonates located atop of the lower nappe perturbed by an array of imbricated thrusts. One such thrust plane hosts the Pb-Zn-Cu mineralisation, which is either coeval with the thrusting or postdates it. Subsequently, the nappe stack was disrupted by the younger generations of steeper brittle structures, with some of them being mineralised by malachite and azurite. The dextral NE-SW faults can be dated to the late Paleocene – middle Eocene, based on the paleostress studies (e.g., Pešková et al., 2009; Vojtko et al., 2010; Sůkalová et al., 2012; Gerátová et al., 2022). The age of the other brittle structures could not be constrained to a reasonably narrow timeframe. As the malachite and azurite form by oxidation of primary ores in the near-surface conditions, their formation should record

denudation events of the Hronic Unit. Such denudation events are possible either from the Late Cretaceous to the early Eocene or from the Early Miocene to the Holocene (Danišík et al., 2011; Kováč et al., 2016, 2017; Králiková et al., 2016; Vojtko et al., 2016).

The high MgO content of the host rock (> 20 %), despite the presence of dolomitic limestones and even limestones in the study area, suggests that the purity of the host rock played a limited role in the cave formation. The cave spaces formed and enlarged along the four types of fracture sets with the following orientations: (1) NE-SW, (2) NNW-SSE to NW-SE, (3) NNE-SSW, and (4) E-W. Although the presence of Pb-Zn sulphide ores can be associated with the unusual cave types formed by the sulphuric acid, there is no evidence that the Blue Cave was created by such a mechanism. Our findings caution against premature attribution of the cave types based purely on the presence of Pb-Zn sulphide ores in carbonate bedrock. Nevertheless, the carbonates in the cave and near the cave contain several clues pointing to the initial enhancement of the bedrock porosity by the sulphide dissolution. The borehole Ma-1 drilled near the cave (Biely, 1964) encountered sulphide minerals and products of their oxidation in its uppermost interval. Moreover, the porous dolomites were also noted in this mineralised zone, their porosity possibly created by the sulphuric acid produced by the sulphide oxidation. Dolomites with fine pores were also observed in the sample MM-5 from the cave. Although this interaction did not directly lead to the formation of the cave, the emergence of the porosity could have been a precursor step for the subsequent formation of the Blue Cave.

Based on the morphological evidence, we propose the Blue Cave was formed predominantly by the aggressive allochthonous waters from the surface stream in three main stages. In Stage I, the phreatic passages developed below the water table during the formation of the stream terrace that presently occurs above the cave. Stage II was marked by the stream downcutting interrupted by the episodic formation of the younger terraces. During this stage, the growth of blue and green speleothems initiated and the cave was periodically flooded, as evidenced by the epiphreatic morphologies and flood sediment veneer covering the lower parts of the stalagmites. Stage III is marked by the collapse and breakdown processes, which significantly remodelled the parts of the cave that are located closest to the surface, namely the entrance parts and the Bociansky banícky dóm Chamber. Based on the relative height of the terrace above the Blue Cave and its comparison with the more extensive river terraces downstream, the estimated age for the terrace is the Middle Pleistocene. Consequently, we estimate a similar age for the initial formation of parts of the Blue Cave, as well as the subsequent initial deposition of some of the blue and green speleothems.

The blue and green colouration of speleothems in the Blue Cave was previously attributed to the copper sourced from the weathering of the Permian rocks neighbouring the cave's Middle Triassic carbonate host rock (Orvošová et al., 2016). However, a discovery of the little-known works that describe the Pb-Zn-Cu mineralisation directly from the carbonate host rock (Kantor, 1957; Hanáček, 1963; Biely, 1964; Ivanov et al., 1965; Kantor, 1977) led us to pursue an alternative hypothesis. Based on the digitised data from these works, in combination with our field data, we propose that the copper is sourced directly from the carbonates that host the cave. The copper most likely originates from the mineralised zone containing chalcopyrite and malachite drilled in the uppermost part of the borehole Ma-2 (Biely, 1964), located approximately 130 m from the cave. The observations from the cave suggest that the zone was intersected by the NE-SW and NW-SE fractures, which host the malachite and azurite. Following the cave formation, the copper was incorporated into blue and green speleothems, albeit these formed only on the NW-SE-striking fractures.

The study of the rock walls in the Blue Cave enabled the observation of geological features that could not be observed on the surface. This work thus underscores the fact that the geological study of the caves can be a useful method in elucidating the local geology. The presented new knowledge about the Blue Cave is also important for its protection as a natural monument (according to the Nature and Landscape Protection Act No. 543/2002 Coll. as amended). The cave occurs in the territory of the Nízke Tatry National Park, but near a frequent road leading through the Čertovica mountain pass. Moreover, a side field roads lead near and above the cave to the adjacent meadow and forest, as well as to several cottages. Several parts of this later discovered cave are located shallowly (at least about 5 m) below the terrain surface. The surface area above the cave does not have a higher level of nature protection than the surrounding part of the national park without caves. The buffer zone of the cave should be considered to prevent the artificial changes of the surface landforms, the deforestation of the surface above the cave, the building of recreational facilities or any other unacceptable human activities in the catchment area of the cave.

Acknowledgements

The geological and geomorphological research presented here was supported by institutional funding from the State Nature Conservancy of the Slovak Republic, the Slovak Caves Administration in Liptovský Mikuláš and the Grant Agency of Slovak Republic (VEGA) under the project no. 1/0323/24. We would like to thank J. Šmoll and G. Majerníčková from the Slovak Speleological Society, and L. Dušeková and P. Staník from the Slovak Caves

Administration for their assistance during the fieldwork. We are also grateful for the comments and remarks from reviewers Peter Šottník and Mário Olšavský, which substantially improved our paper.

References

Badár, J., Novotný, L., Reimont, V. & Švábl, E., 1965: Zpráva ku geologickej mape z lokality Čierny Váh z oblasti Nižná Boca – Liptovská Teplička. Spišská Nová Ves, Geologický prieskum uránového priemyslu. *Manuscript. Bratislava, Archive of St. Geol. Inst. of D. Štúr* (arch. no. 55175), 99 pp.

Bella, P., Littva, J., Pruner, P., Gaál, Ľ., Bosák, P. & Haviarová, D., 2014: Malužinská jaskyňa v severovýchodnej časti Nízkych Tatier: freatická speleogenéza spôsobená vodami vystupujúcimi pozdĺž zlomovej zóny. *Slovenský kras*, 52, 2, 111 – 126.

Biela, A., 1960: Geologické pomery územia na sútoku Bieleho a Čierneho Váhu. Master's Thesis. Katedra geológie a paleontológie, Prírodovedecká fakulta Univerzity Komenského. *Manuscript. Bratislava, Archive of St. Geol. Inst. of D. Štúr* (arch. no. 81079), 53 pp.

Biely, A., 1960: Chočský príkrov na severných svahoch Nízkych Tatier. *Geologické práce, Zprávy*, 20, 127 – 134.

Biely, A., 1962: Niekoľko tektonických a stratigraficko-litologických poznatkov z východnej časti Nízkych Tatier a Tribča. *Geologické práce, Zošit*, 62, 205 – 218.

Biely, A., 1963: Beitrag zur Kenntnis der inneren Baues der Choč-Einheit. *Geologické práce, Zprávy,* 28, 69 – 78.

Biely, A., 1964: Výskum mezozoika v Nízkych Tatrách, list Horná Lehota, ročná správa za rok 1963. *Manuscript. Bratislava, Archive of St. Geol. Inst. of D. Štúr* (archive no. 12924), 35 pp.

Biely, A., 1976: Vysvetlivky k mezozoiku S svahov Nízkych Tatier – východná časť. *Manuscript*. *Bratislava, Archive of St. Geol. Inst. of D. Štúr* (archive no. 38208), 72 pp.

Biely, A., Beňuška, P., Bezák, V., Bujnovský, A., Halouzka, R., Ivanička, J., Kohút, M., Klinec, A., Lukáčik, E., Maglay, J., Miko, O., Pulec, M., Putiš, M. & Vozár, J., 1992: Geologická mapa Nízkych Tatier 1 : 50 000 [map]. *Bratislava, Geologický ústav Dionýza Štúra*.

Biely, A., Bezák, V., Bujnovský, A., Vozárová, A., Klinec, A., Miko, O., Halouzka, R., Vozár, J., Beňuška, P., Hanzel, V., Kubeš, P., Lišč ák, P., Lukáčik, E., Maglay, J., Molák, B., Pulec, M., Putiš, M. & Slavkay, M., 1997: Vysvetlivky ku geologickej mape Nízkych Tatier. *Bratislava, Geologická služba Slovenskej republiky, Vydavateľstvo Dionýza Štúra*, 232 pp.

Bosch, R. F. & White, W. B., 2004: Lithofacies and Transport of Clastic Sediments in Karstic Aquifers. In: Sasowsky, I. D. & Mylroie, J. (eds.): Studies of Cave Sediments. *Boston, MA, Springer US*, 1 – 22. https://doi.org/10.1007/978-1-4419-9118-8_1.

Bretz, J. H., 1942: Vadose and Phreatic Features of Limestone Caverns. *The Journal of Geology*, 50, 6, 675 – 811.

Culková, E., Bellová, R., Littva, J., Bella, P. & Tomčík, P., 2025: Detection of copper in blue-green stalactites using a bare boron doped diamond electrode: Clean and sustainable sensing platform for cave samples analysis. *Microchemical Journal*, 218, 115806. https://doi.org/10.1016/j.microc.2025.115806.

Čechovič, V., 1942: Zpráva o prieskumu barytových ložísk v okolí Malužinej. Handlová, Ústřední ústav geologický. *Manuscript. Bratislava, Archive of St. Geol. Inst. of D. Štúr* (archive no. 8156), 7 pp.

Chovan, M., Slavkay, M. & Michálek, J., 1996: Ore mineralization of the Ďumbierske Tatry Mts. (Western Carpathians, Slovakia). *Geologica Carpathica*, 47, 6, 371 – 382.

CloudCompare, 2023: v2.13.1. Available at: http://www.cloudcompare.org/.

Danišík, M., Kadlec, J., Glotzbach, C., Weisheit, A., Dunkl, I., Kohút, M., Evans, N. J., Orvošová, M. & McDonald, B. J., 2011: Tracing metamorphism, exhumation and topographic evolution in orogenic belts by multiple thermochronology: a case study from the Nízke Tatry Mts., Western Carpathians. *Swiss Journal of Geosciences*, 104, 2, 285 – 298. https://doi.org/10.1007/s00015-011-0060-6.

De Waele, J., D'Angeli, I. M., Audra, P., Plan, L. & Palmer, A. N., 2024: Sulfuric acid caves of the world: A review. *Earth-Science Reviews*, 250, 104693. https://doi.org/10.1016/j.earscirev.2024.104693.

Droppa, A., 1964: Výskum terás Váhu v strednej časti Liptovskej kotliny. *Geografický časopis*, 16, 4, 313 – 325.

Droppa, A., 1966: The correlation of some horizontal caves with river terraces. *Studies in Speleology*, 1, 186 – 192.

Droppa, A., 1970: Výskum riečnych terás v zátopovej oblasti Liptovská Mara. *Vlastivedný zborník Liptov*, 1, 7 – 34.

Droppa, A., 1972a: Geomorfologické pomery Demänovskej doliny. *Slovenský kras*, 10, 9 – 46.

Droppa, A., 1972b: Krasové javy Jánskej doliny na severnej strane Nízkych Tatier. *Československý kras*, 21, 73 – 96.

Droppa, A., 1972c: Výskum riečnych terás v okolí Ružomberka. *Vlastivedný zborník Liptov*, 2, 11 – 25.

Ewers, R. O., 1966: Bedding-Plane Anastomoses and Their Relation to Cavern Passages. *Bulletin of the National Speleological Society*, 28, 3, 133 – 140.

Farrant, A. R. & Smart, P. L., 2011: Role of sediment in speleogenesis; sedimentation and paragenesis. *Geomorphology*, 134, 1, Geomorphology and Natural Hazards in Karst Areas, 79 – 93. https://doi.org/10.1016/j.geomorph.2011.06.006.

Ford, D. C., 1977: Genetic classification of solution cave system. In: Ford, T. D. (ed.): Proceeding of the 7th International Congress of Speleology. Sheffield, 10 – 17 September 1977, *International Union of Speleology British Cave Research Association*, 189 – 192.

Ford, D. C., 1988: Characteristics of Dissolutional Cave Systems in Carbonate Rocks. In: James, N. P. & Choquette, P. W. (eds.): Paleokarst. *New York – Berlin – Heidelberg – London – Paris – Tokyo, Springer*, 25 – 57. https://doi.org/10.1007/978-1-4612-3748-8_2.

Ford, D. C., 2000: Speleogenesis under unconfined settings. In: Klimchouk, A. B., Ford, D. C. & Palmer, A. N. (eds.): Speleogenesis. Evolution of Karst Aquifers. *Huntsville, Alabama, U. S. A., National Speleological Society*, 319 – 324.

Ford, D. C. & Ewers, R. O., 1978: The development of limestone cave systems in the dimensions of length and depth. *Canadian Journal of Earth Sciences*, 15, 11, 1 783 – 1 798. https://doi.org/10.1139/e78-186.

Gerátová, S., Vojtko, R., Lačný, A. & Kriváňová, K., 2022: The structural pattern and tectonic evolution of the Muráň fault revealed by geological data, fault-slip analysis, and paleostress reconstruction (Western Carpathians). *Geologica Carpathica*, 73, 1, 43 – 62. https://doi.org/10.31577/GeolCarp.73.1.3.

Hanáček, J., 1963: Ročná správa o geochemickom výskume karbonatických hornín v okolí Malužinej. *Manuscript. Bratislava, Archive of St. Geol. Inst. of D. Štúr* (archive no. 11358), 15 pp.

Havrila, M., 2011: Hronikum: paleogeografia a stratigrafia (vrchný pelsón – tuval), štrukturalizácia a stavba. *Geologické práce, Správy*, 117, 7 – 103.

Heeb, B., 2020: Paperless Cave Surveying. Available at: https://paperless.bheeb.ch/index.html.

Hók, J., Schuster, R., Pelech, O., Vojtko, R. & Šamajová, L., 2022: Geological significance of Upper Cretaceous sediments in deciphering of the Alpine tectonic evolution at the contact of the Western Carpathians, Eastern Alps and Bohemian Massif. *International Journal of Earth Sciences*, 111, 1 805 – 1 822. https://doi.org/10.1007/s00531-022-02201-5.

Hoppanová, E., 2024: Cu-Sb-As mineralizácia v karbonátových brekciách styku hronika a veporika pri Brezne: štruktúrne pomery a alterácia hostiteľských hornín. Rigorosum Thesis. *Manuscript. Banská Bystrica, Univerzita Mateja Bela v Banskej Bystrici, Fakulta prírodných vied*, 119 pp. Available at: https://opac.crzp.sk/?fn=detailBiblioForm&sid=53EEEDF946F250FB448F2DA3B71B.

Howard, A. D., 1971: Quantitative measures of cave patterns. *Caves and Karst*, 13, 1, 1 – 7.

Hromádka, J., 1931: Povrchové formy Slovenska a jejich výskum. *Časopis učenej spoločnosti P. J. Šafárika*, 5, 3, 484 – 510.

Ilavský, J. & Ilavská, Ž., 1949: Zpráva o prieskume výskytov barytu pri Malužinej. Spišská Nová Ves, Železnorudné bane. *Manuscript. Bratislava, Archive of St. Geol. Inst. of D. Štúr* (archive no. 3397), 4 pp.

Ivanov, M., Hanáček, J. & Biely, A., 1965: Geochemický výskum metasomatických zrudnení v karbonátových horninách centrálnej časti Karpát. *Manuscript. Bratislava, Archive of St. Geol. Inst. of D. Štúr* (archive no. 15687), 201 pp.

Jeremenko, D., 1956: Malužiná – Svidovo – ložiskový list č. 113 – melafýr a porfyrický melafýr. Trenčín, Nerudný prieskum. *Manuscript. Bratislava, Archive of St. Geol. Inst. of D. Štúr* (archive no. 2112), 34 pp.

Kantor, J., 1957: Zpráva o geochemickej prospekcii na olovo v Nízkych Tatrách. *Manuscript. Bratislava, Archive of St. Geol. Inst. of D. Štúr* (archive no. 2555), 11 pp.

Kantor, J., 1975: Izotopy síry na Pb-Zn ložiskách z mezozoických karbonátov Západných Karpát. *Manuscript. Bratislava, Archive of St. Geol. Inst. of D. Štúr* (archive no. 35637), 181 pp.

Kantor, J., 1977: Pb-Zn-Ores of the Westcarpathian Triassic and the Distribution of Their Sulphur Isotopes. In: Klemm, D. D. & Schneider, H.-J. (eds.): Time- and Strata-Bound Ore Deposits. *Berlin – Heidelberg, Springer*, 294 – 304. https://doi.org/10.1007/978-3-642-66806-7_19.

Kantor, J. & Ďurkovičová, J., 1977: Izotopy síry na barytových ložiskách Západných Karpát. *Manuscript. Bratislava, Archive of St. Geol. Inst. of D. Štúr* (archive no. 2555), 237 pp.

Kettner, R. & Šťastný, V., 1931: Geologická mapa severního svahu Nízkých Tater v okolí Liptovského Hrádku [map]. *Praha, Knihovna Statního ústavu geologického Československé republiky; 13, A. Vojenský zeměpisný ústav.*

Kováč, M., Márton, E., Oszczypko, N., Vojtko, R., Hók, J., Králiková, S., Plašienka, D., Klučiar, T., Hudáčková, N. & Oszczypko-Clowes, M., 2017: Neogene palaeogeography and basin evolution of the Western Carpathians, Northern Pannonian domain and adjoining areas. *Global and Planetary Change*, 155, 133 – 154. https://doi.org/10.1016/j.gloplacha.2017.07.004.

Kováč, M., Plašienka, D., Soták, J., Vojtko, R., Oszczypko, N., Less, G., Ćosović, V., Fügenschuh, B. & Králiková, S., 2016: Paleogene palaeogeography and basin evolution of the Western Carpathians, Northern Pannonian domain and adjoining areas. *Global and Planetary Change*, 140, 9 – 27. https://doi.org/10.1016/j.gloplacha.2016.03.007.

Kováč, P. & Filo, I., 1992: Structural interpretation of the Choč nappe outliers of the Chočské vrchy Mts. *Mineralia Slovaca*, 24, 1 – 2, 39 – 44.

Kováč, P. & Havrila, M., 1998: Inner structure of Hronicum. *Slovak Geological Magazine*, 4, 4, 275 – 280.

Králiková, S., Vojtko, R., Hók, J., Fügenschuh, B. & Kováč, M., 2016: Low-temperature constraints on the Alpine thermal evolution of the Western Carpathian basement rock complexes. *Journal of Structural Geology*, 91, 144 – 160. https://doi.org/10.1016/j.jsg.2016.09.006.

Kubáň, T., 1956: Správa o základnom inžiniersko-geologickom výskume pre údolnú priehradu Malužiná na rieke Boca v Liptove. *Manuscript. Bratislava, Archive of St. Geol. Inst. of D. Štúr* (archive no. 3171), 17 pp.

Lange, A., 1963: Planes of repose in caves. *Cave Notes*, 5, 6, 41 – 48.

Lauritzen, S.-E. & Lundberg, J., 2000: Solutional and erosional morphology. In: Klimchouk, A. B., Ford, D. C., Palmer, A. N. & Dreybrodt, W. (eds.): Speleogenesis. Evolution of Karst Aquifers. *Huntsville, Alabama, U.S.A., National Speleological Society*, 408 – 426.

Lexa, J., Bezák, V., Elečko, M., Mello, J., Polák, M., Potfaj, M. & Vozár, J., 2000: Geologická mapa Západných Karpát a priľahlých území [map]. Scale 1 : 500 000. *Bratislava, Ministerstvo životného prostredia Slovenskej republiky, Štátny geologický ústav Dionýza Štúra.*

Lošonská, M., 1984: Plynovod Malužiná. Liptovský Hrádok, Agrostav. *Manuscript. Bratislava, Archive of St. Geol. Inst. of D. Štúr* (archive no. 57054), 13 pp.

Machel, H. G., 2004: Concepts and models of dolomitization: a critical reappraisal. In: Braithwaite, C. J. R., Rizzi, G. & Darke, G. (eds.): The Geometry and Petrogenesis of Dolomite Hydrocarbon Reservoirs. *Geological Society of London*, 0. https://doi.org/10.1144/GSL.SP.2004.235.01.02.

Moser, M. & Piros, O., 2021: Lithostratigraphic definition of the Anisian carbonate-ramp deposit of the Annaberg Formation (Middle Triassic, Northern Calcareous Alps, Austria). *Geologica Carpathica*, 72, 3, 173 – 194. https://doi.org/10.31577/GeolCarp.72.3.1.

Moser, M., Wagreich, M. & Piros, O., 2024: The type-section of the Gutenstein Formation at Gutenstein revisited (Anisian, Northern Calcareous Alps, Lower Austria): Lithostratigraphy, biostratigraphy and regional overview. *Austrian Journal of Earth Sciences*, 117, 1, 113 – 147. https://doi.org/10.17738/ajes.2024.0008.

Mudrák, S. & Budaj, M., 2010: The Therion Book. *Distributed under the GNU General Public License*, 108 pp. Available at: https://github.com/therion/therion/releases/download/v6.3.4/thbook-v6.3.4.pdf.

Olšavský, M., 2007a: Spodný trias na báze bocianskeho čiastkového príkrovu hronika (Nízke Tatry, na JV od Liptovskej Tepličky, Rovienky). *Mineralia Slovaca*, 39, 1, *Geovestník*, 19 – 20.

Olšavský, M., 2007b: Stavba hronika na severovýchodných svahoch Nízkych Tatier. *Mineralia Slovaca*, 39, 4, *Geovestník*, 12.

Olšavský, M., 2008: Faciálna analýza depozičných sekvencií malužinského súvrstvia a jeho geologická stavba na SV svahoch Nízkych Tatier. Doctoral Thesis. *Manuscript. Bratislava, Prírodovedecká fakulta Univerzity Komenského*, 194 pp. Available at: https://www.researchgate.net/publication/321383024_Facialna_analyza_depozicnych_sekvencii_maluzinskeho_suvrstvia_a_jeho_geologicka_stavba_na_SV_svahoch_Nizkych_Tatier.

Orvošová, M., Milovská, S., Mikuš, T., Šmoll, J., Majerníčková, G. & Karošiak, I., 2016: Sintre zafarbené kovovými iónmi v Modrej jaskyni, Nízke Tatry, Slovensko. *Slovenský kras*, 54, 2, 131 – 138.

Palmer, A. N., 1991: Origin and morphology of limestone caves. *Geological Society of America Bulletin*, 103, 1, 1 – 21. https://doi.org/10.1130/0016-7606(1991)103<0001:OAMOLC>2.3.CO;2.

Palmer, A. N., 2007: Cave Geology. *Dayton, Ohio, Cave Books*, 454 pp.

Pešková, I., Vojtko, R., Starek, D. & Sliva, Ľ., 2009: Late Eocene to Quaternary deformation and stress field evolution of the Orava region (Western Carpathians). *Acta Geologica Polonica*, 59, 1, 73 – 91.

Plašienka, D., 2018: Continuity and Episodicity in the Early Alpine Tectonic Evolution of the Western Carpathians: How Large-Scale Processes Are Expressed by the Orogenic Architecture and Rock Record Data. *Tectonics*, 37, 7, 2 029 – 2 079. https://doi.org/10.1029/2017TC004779.

Pristašová, L., 2024: Teplota vzduchu v Malužinskej a Modrej jaskyni v Nízkych Tatrách. *Aragonit*, 29, 2, 61 – 67.

QGIS Development Team, 2024: QGIS Geographic Information System, 3.34. Available at: https://www.qgis.org.

Röller, K. & Trepmann, C. A., 2003: Stereo32, Version 1.0.1.

Slabe, T., 1995: Cave Rocky Relief and its Speleogenetical Significance. *Ljubljana, ZRC SAZU, Založba ZRC*, 128 pp. https://doi.org/10.3986/961618203X.

Srnánek, J., 1962: Inžiniersko-geologická štúdia údolia Čierneho Váhu. Riaditeľstvo vodohospodárskeho rozvoja. *Manuscript. Bratislava, Archive of St. Geol. Inst. of D. Štúr* (archive no. 11118), 36 pp.

Sůkalová, Ľ., Vojtko, R. & Pešková, I., 2012: Cenozoic deformation and stress field evolution of the Kozie chrbty Mountains and the western part of Hornád Depression (Central Western Carpathians). *Acta Geologica Slovaca*, 4, 1, 53 – 64.

Šebela, S., Stemberk, J. & Briestenský, M., 2021: Microdisplacement monitoring in caves at the Southern Alps-Dinarides-Southwestern Pannonian Basin junction. *Bulletin of Engineering Geology and the Environment*, 80, 10, 7 591 – 7 611. https://doi.org/10.1007/s10064-021-02382-4.

Šmoll, J., 2017: The Modrá Cave (The Blue Cave) in the Low Tatra Mts. *Bulletin of the Slovak Speleological Society, Issued for the purpose of the 17th Congress of the IUS, Sydney 2017*, 66 – 68.

Thiele, S. T., Grose, L., Samsu, A., Micklethwaite, S., Vollgger, S. A. & Cruden, A. R., 2017: Rapid, semi-automatic fracture and contact mapping for point clouds, images and geophysical data. *Solid Earth*, 8, 6, 1 241 – 1 253. https://doi.org/10.5194/se-8-1241-2017.

Tulis, J. & Novotný, L., 1998: Zhodnotenie geologických prác na U rudy v mladšom paleozoiku hronika v severnej časti Nízkych Tatier a Kozích chrbtov. *Manuscript. Bratislava, Archive of St. Geol. Inst. of D. Štúr* (archive no. 82752), 144 pp.

Urban, F., 1959: Průzkum kamene v ČSR 1959, Malužiná. Brno, Geologický průzkum. *Manuscript. Bratislava, Archive of St. Geol. Inst. of D. Štúr* (archive no. 8388), 19 pp.

Vitásek, F., 1932: Terasy horního Váhu. A, 4. *Brno, Spisy odboru Československé spoločnosti zeměpisné v Brně*, 23 pp.

Vitovič, L. & Minár, J., 2018: Morphotectonic analysis for improvement of neotectonic subdivision of the Liptovská kotlina Basin (Western Carpathians). *Geografický časopis*, 70, 3, 197 – 216. https://doi.org/10.31577/geogrcas.2018.70.3.11.

Vlček, L., 2011: Geologická stavba severných svahov Ďumbierskych Tatier a jej vplyv na tvorbu krasového fenoménu. Doctoral Thesis. *Manuscript. Bratislava, Univerzita Komenského v Bratislave*, 168 pp.

Vojtko, R., Králiková, S., Jeřábek, P., Schuster, R., Danišík, M., Fügenschuh, B., Minár, J. & Madarás, J., 2016: Geochronological evidence for the Alpine tectonothermal evolution of the Veporic Unit (Western Carpathians, Slovakia). *Tectonophysics*, 666, 48 – 65. https://doi.org/10.1016/j.tecto.2015.10.014.

Vojtko, R., Tokárová, E., Sliva, Ľ., Pešková, I. & Sliva, Ľ., 2010: Reconstruction of Cenozoic paleostress fields and revised tectonic history in the northern part of the Central Western Carpathians (the Spišská Magura and Východné Tatry Mountains). *Geologica Carpathica*, 61, 3, 211 – 225. https://doi.org/10.2478/v10096-010-0012-5.

Vozár, J., 1970: Výskum permských vulkanitov Chočského príkrovu na severných svahoch Nízkych Tatier – západná časť. *Manuscript. Bratislava, Archive of St. Geol. Inst. of D. Štúr*, (archive no. AP4634), 171 pp.

Vozár, J., 1974: Stavba permských vulkanitov chočskej jednotky na severných svahoch Nízkych Tatier. *Západné Karpaty, séria Mineralógia, petrografia, geochémia, metalogenéza, ložiská*, 1, 7 – 49.

Vozár, J., Bujnovský, A., Vaškovský, I., Vozárová, A., Hanzel, V., Šucha, P., Lukáčik, E., Hanáček, J., Stankovič, J., Biely, A., Planderová, E. & Muška, P., 1983: Vysvetlivky na geologickej mape 1 : 25 000, list 36-221 (Malužiná-1). *Manuscript. Bratislava, Archive of St. Geol. Inst. of D. Štúr* (archive no. 57054), 122 pp.

Webb, J. A., 2021: Supergene sulphuric acid speleogenesis and the origin of hypogene caves: evidence from the Northern Pennines, UK. *Earth Surface Processes and Landforms*, 46, 2, 455 – 464. https://doi.org/10.1002/esp.5037.

Zoubek, V., 1952: Zpráva o výzkumu východní časti nízkotatranského jaderného pohoří. *Manuscript. Praha, Ústřední ústav geologický, Bratislava, Archive of St. Geol. Inst. of D. Štúr* (archive no. 3400), 20 pp.

Geologické pomery a vznik Modrej jaskyne s modrými a zelenými sintrovými útvarmi (stredné Slovensko)

Modrá jaskyňa pri obci Malužiná je dosiaľ jedinou jaskyňou na Slovensku, v ktorej bol opísaný výskyt modrej a zelenej sintrovej výzdoby. Jaskyňa sa nachádza na severozápadných svahoch Nízkych Tatier na ľavom brehu toku Boca, v miestach, kde sa doň vlieva prítok Malužiná. Jaskyňa bola vytvorená v strednotriasových karbonátoch hronika. Zastupujú ich prevažne dolomity, v článku neformálne označované ako „čiernovážske karbonáty". Prvotné analýzy jaskynnej výzdoby po jej objavení v roku 2016 ako príčinu zafarbenia sintrovej výzdoby určili prítomnosť medi. Za zdroj medi sa považovali produkty zvetrávania permských vulkanitov malužinského súvrstvia, konkrétne baritovo-sulfidové žilky, ktoré sa vyskytujú vo vulkanitoch. Sporadické zmienky o Pb-Zn-(Cu) mineralizácii prítomnej priamo v čiernovážskych karbonátoch nás však viedli k hľadaniu alternatívneho zdroja medi. Nadväzný rešeršný výskum v archíve Štátneho geologického ústavu Dionýza Štúra smeroval k objaveniu niekoľkých nepublikovaných manuskriptov. Tie sa pomerne rozsiahlo zaoberali zrudnením v okolí Modrej jaskyne a obsahovali pomerne rozsiahle údaje o Pb-Zn-(Cu) zrudnení čiernovážskych karbonátov. Správy o prieskume obsahujú údaje o mineralizácii v okolí baní v úžľabine zvanej Olovienka, prospekčných vrtoch Ma-1 a Ma-2 aj početných chemických a spektrálnych analýzach, ktoré sa realizovali v okolí jaskyne (obr. 1, 2 a 3). Tieto údaje museli nutne viesť k reinterpretácii pôvodných predstáv o zdroji medi.

Údaje z manuskriptov viedli k nutnosti preskúmať jaskyňu z geologického a geomorfologického hľadiska, ako aj nanovo zmapovať okolie jaskyne. Jaskyne vyskytujúce sa v karbonátoch obsahujúcich Pb-Zn zrudnenie môžu byť vytvárané kyselinou sírovou pochádzajúcou z oxidácie sulfidových rúd. Preto sa realizovalo detailné štúdium morfotvarov jaskyne, litológie materskej horniny jaskyne a jej štruktúrno-tektonického porušenia s cieľom objasniť pôvod jaskyne aj pôvod sfarbenia jej výzdoby. Použili sa metódy priameho terénneho výskumu aj nepriameho štúdia z 3D modelu jaskyne zostrojeného pomocou mobilného laserového terestrického skenera. Na geologických mapách z archívnych prác sa v okolí Modrej jaskyne nachádzalo viacero závažných nezhôd. Z nich vyplývali nejasnosti v tektonickej interpretácii hronika, ako aj nekonzistentnosť v distribúcii a rozsahu riečnych terás. Z týchto rozporov vyplynula nutnosť aspoň čiastočne reambulovať geologickú mapu v okolí Modrej jaskyne.

Na základe terénneho mapovania doplneného o digitalizované údaje z manuskriptov v okolí Modrej jaskyne interpretujeme existenciu dvoch príkrovov hronika. „Čiernovážske karbonáty" tvoriace materskú horninu jaskyne budujú vrchnú časť spodného príkrovu, ktorá bola tektonicky imbrikovaná, a niektorí predchádzajúci autori ju považovali za tretí príkrov hronika. Táto deformovaná zóna sa vytvorila medzi dvomi rigidnejšími súbormi hornín – permskými vulkanitmi spodného príkrovu a hrubým telesom strednotriasových karbonátov vrchného príkrovu (obr. 1C, 2 a 4). Podotýkame, že tým nepopierame možnosť existencie troch (prípadne aj viacerých) príkrovov hronika mimo nami študovanej oblasti. Zdá sa, že Pb-Zn-(Cu) zrudnenie sa viaže na plochy prešmykov v imbrikovanej zóne. Príkrovová stavba hronika v oblasti je následne porušená mladšími zlomami, pričom jeden z týchto zlomov mohol narušiť kontinuitu pásu zrudnenia medzi baňami na Olovienke a Modrou jaskyňou (obr. 2A).

Mapovanie riečnych terás v okolí jaskyne bolo sťažené kolapsovými krasovými procesmi a antropogénnou modifikáciou reliéfu, ktoré zastierali pôvodnú morfológiu terás. Napriek tomu bolo možné vyčleniť tri skupiny terás, ktoré sme označili vrchné, stredné a spodné. Modrá jaskyňa bola vytvorená pod povrchom vrchných terás a väčšina jej priestorov sa vyskytuje medzi úrovňami vrchných až stredných terás, s výnimkou niektorých najnižšie položených priestorov. Na základe analógie s terasami Váhu v Liptovskej kotline sa vek vrchných terás (a súčasne vznikajúcej jaskyne) odhaduje na stredný pleistocén.

V jaskyni sú excelentne pozorovateľné geologické pomery jej materskej horniny, ktoré by prostredníctvom čisto povrchových terénnych prác nebolo možné identifikovať (obr. 5, 6 a 7). Severozápadná časť jaskyne je vytvorená vo vrstvovitých dolomitoch, zatiaľ čo v juhozápadnej časti jaskyne sú masívne dolomity a stýkajú sa na sv.-jz. zlome prebiehajúcom Malužinským dómikom. V Bocianskom baníckom dóme možno pozorovať výraznú vrásovo-násunovú štruktúru a v Malužinskom dómiku je viditeľný dextrálny sv.-jz. zlom segmentujú-

ci plocho uklonené prešmyky. Celkovo sme pozorovali štyri súbory strmých krehkých porúch ovplyvňujúcich priebeh jaskynných priestorov: sz.-jv. až ssz.-jjv., v.-z., ssv.-jjz. a sv.-jz. poruchy. Vek aktivity väčšiny porúch nebolo možné vymedziť, no v prípade vrásovo-násunovej štruktúry sa predpokladá aktivita v strednej časti kriedy. Na základe porovnania s paleonapäťovými štúdiami možno zároveň odhadnúť vek dextrálneho zlomu prebiehajúceho Malužinským dómikom na neskorý paleocén až stredný eocén. V jaskyni boli pozorované náteky malachitu a azuritu, ktoré sa vyskytovali na sv.-jz. až sz.-jv. poruchách. Výskyty zafarbených sintrových útvarov sa obmedzovali iba na sz.-jv. poruchy. V jednom prípade sa zdá, že azurit tvorí minerálny akrečný stupeň na dextrálnom zlome v Malužinskom dómiku, čo by umožňovalo presnejšie vekové zaradenie tejto sekundárnej mineralizácie. Vzhľadom na typický spôsob tvorby týchto minerálov v oxidačnej zóne sa však tieto minerály mohli tvoriť vo viacerých etapách, keď v študovanej oblasti dochádzalo k výzdvihu a denudácii horninových súborov. Možný časový diapazón tvorby malachitu a azuritu je teda pomerne široký – krieda až skorý eocén a od skorého miocénu po holocén. Predpokladá sa, že modro až zeleno sfarbené sintre sa začali tvoriť po vzniku jaskyne. Ich maximálny vek je teda stredný pleistocén, mnohé z nich však budú nepochybne aj mladšie.

Na základe morfologického štúdia možno konštatovať, že oxidácia sulfidov a tvorba kyseliny sírovej neboli hlavnými činiteľmi v genéze jaskyne. Napriek tomu existujú určité náznaky, že tieto procesy prispeli k zvýšeniu iniciálnej porozity dolomitov, ktorá neskôr uľahčila jej následnú tvorbu. Ide predovšetkým o blízku prítomnosť mineralizovanej zóny obsahujúcej sulfidové minerály vo vrte Ma-2, ako aj porézne dolomity a o hrdzavohnedé rezíduá v žilkách (azda po oxidácii sulfidov) pozorované vo vrte, na povrchu aj v jaskyni. Jaskyňa bola vytvorená agresívnou povrchovou vodou, ktorá prenikala do skalného masívu v troch hlavných štádiách. Jemnozrnný charakter sedimentov a absencia tvarov indikujúcich rýchle prúdenie vody naznačuje, že jaskyňa sa tvorila rozptýlene vnikajúcou pomaly tečúcou až stagnujúcou vodou. V prvom štádiu sa jaskyňa tvorila vo freatickej zóne (pod hladinou podzemnej vody) počas tvorby vrchných terás, pod ktorými sa nachádza. Svedčí o tom prítomnosť početných freatických foriem sledujúcich vrstvové plochy aj poruchy jaskyne. V druhej fáze, počas epizodického zarezávania doliny a tvorby stredných a spodných riečnych terás, prebiehala remodelácia jaskyne v epifreatickej zóne (t. j. pri hladine podzemnej vody). Jaskyňa bola vystavovaná opakovaným záplavám. Svedčí o tom prítomnosť epifreatickej modelácie skalných stien v niektorých častiach jaskyne. Stopy epizodického zaplavovania nesú na sebe aj zafarbené kvaple. To indikuje, že sa zrejme vytvorili v skorých štádiách druhej fázy vývoja jaskyne. Tretie štádium vývoja jaskyne je spojené s jej remodeláciou rútivými procesmi, ktoré sú najvýraznejšie v jej vstupných častiach, Bocianskom baníckom dóme a Malužinskom dómiku.

Tento článok podčiarkuje význam jaskýň v geológii ako „prirodzených vrtov“, značne uľahčujúcich štúdium geologických pomerov, obzvlášť v horšie odkrytých oblastiach.

Doručené / Recieved: 14. 7. 2025
Prijaté na publikovanie / Accepted: 1. 9. 2025

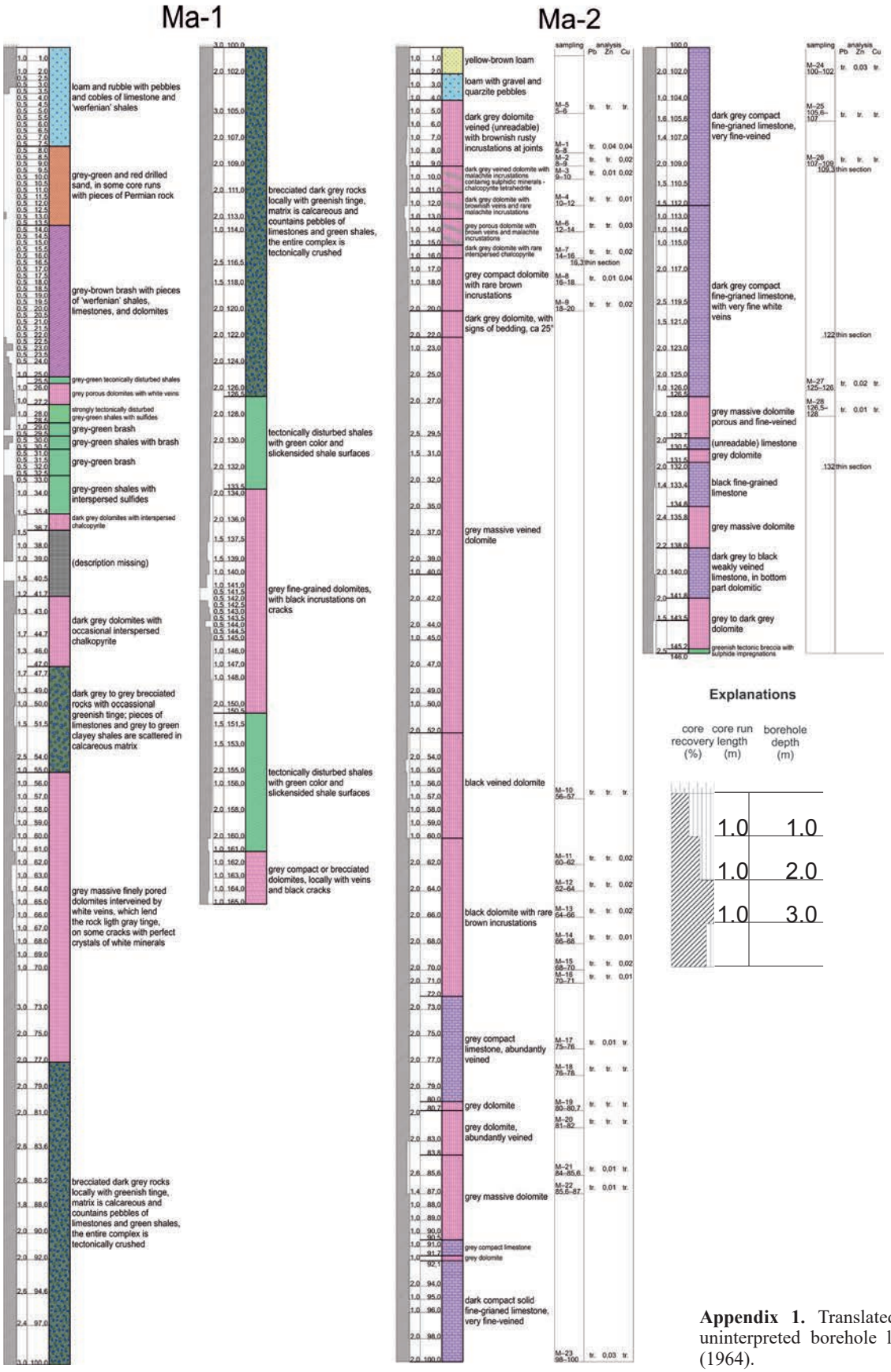

Appendix 1. Translated and coloured uninterpreted borehole logs from Biely (1964).

Appendix 2. A table of the samples with their Pb, Zn, and Cu contents determined by a chemical analysis from Hanáček (1963). The WGS coordinates were determined by georeferencing the author's map. The values are percentual.

Sample id	X	Y	Pb [%]	Zn [%]	Cu [%]	Lithological description
1	48,9842817	19,7641870		0,02		grey to dark grey fine crystalline thin-bedded to bedd dolomites, permeated by an irregular network of fractures
2	48,9842774	19,7641744	0,55	0,06		grey to dark grey fine crystalline thin-bedded to bedd dolomites, permeated by an irregular network of fractures
3	48,9842733	19,7641575	0,55	0,03		grey to dark grey fine crystalline thin-bedded to bedd dolomites, permeated by an irregular network of fractures
4	48,9842682	19,7641412	0,13	0,02		grey to dark grey fine crystalline thin-bedded to bedd dolomites, permeated by an irregular network of fractures
5	48,9842630	19,7641254	0,45	0,61		grey to dark grey fine crystalline thin-bedded to bedd dolomites, permeated by an irregular network of fractures
6	48,9842588	19,7641091	0,05	0,13		grey to dark grey fine crystalline thin-bedded to bedd dolomites, permeated by an irregular network of fractures
7	48,9842558	19,7640924	0,05	0,05		grey to dark grey fine crystalline thin-bedded to bedd dolomites, permeated by an irregular network of fractures
8	48,9842503	19,7640785	0,15	0,24		grey to dark grey fine crystalline thin-bedded to bedd dolomites, permeated by an irregular network of fractures
9	48,9842662	19,7641929	0,21	0,16		grey to dark grey fine crystalline thin-bedded to bedd dolomites, permeated by an irregular network of fractures
11	48,9842584	19,7641730	1,57	1,53	0,04	grey to dark grey fine crystalline thin-bedded to bedd dolomites, permeated by an irregular network of fractures
12	48,9842504	19,7641527	0,27	0,75	0,01	grey to dark grey fine crystalline thin-bedded to bedd dolomites, permeated by an irregular network of fractures
13	48,9818605	19,7694132		0,06		dark grey dolomites
14	48,9814303	19,7709837		0,05		grey limestones
15	48,9814892	19,7711366		0,04		grey dolomites
16	48,9815505	19,7715276		0,04		grey dolomites
17	48,9813546	19,7714617		0,01		grey dolomites
18	48,9811902	19,7713805		0,01		grey dolomites
19	48,9809951	19,7713329		0,01		grey dolomites
20	48,9808454	19,7713113				grey dolomites
21	48,9846194	19,7640968				grey limestones
22	48,9845866	19,7644514				grey limestones with calcite veins
23	48,9845362	19,7649086				grey limestones with calcite veins
25	48,9844229	19,7632567				light grey dolomites
27	48,9844965	19,7632370				light grey dolomites
28	48,9844204	19,7635227		0,03		light grey dolomites
30	48,9842301	19,7627308		0,02	0,03	dark grey dolomites
31	48,9841557	19,7628238		0,05	0,03	grey dolomites
32	48,9837842	19,7613583				dark grey brecciated dolomites
33	48,9835861	19,7610575				grey dolomites
34	48,9837424	19,7615061				grey crystalline dolomites
35	48,9836759	19,7616411				grey crystalline dolomites
36	48,9770855	19,7773092				original description missing

Appendix 2 – continued

Sample id	X	Y	Pb [%]	Zn [%]	Cu [%]	Lithological description
37	48,9767451	19,7768792				original description missing
38	48,9772684	19,7768938			0,05	original description missing
39	48,9775010	19,7766933			0,04	original description missing
40	48,9774078	19,7763300			0,05	original description missing
41	48,9775575	19,7762142			0,02	original description missing
42	48,9781897	19,7730017				original description missing
44	48,9864362	19,7638497				light grey limestones
45	48,9864973	19,7640513	0,2			light grey dolomites
55	48,9748475	19,7387252		0,02		grey limestones with calcite veins – tallus
56	48,9746112	19,7380887		0,01		light grey dolomites – tallus
57	48,9748806	19,7381881		0,02		grey, dark grey massive limestones – rocky outcrop
58	48,9749682	19,7376409		0,26		grey, dark grey massive limestones – rocky outcrop
64	48,9733406	19,7337661				grey massive limestones
65	48,9730303	19,7339559		0,02		dark grey massive limestones
66	48,9728781	19,7333380				dark grey massive limestones
67	48,9721530	19,7262554				dark grey massive limestones
68	48,9718235	19,7254656		0,01		dark grey massive limestones
69	48,9725048	19,7261293		0,01		dark grey limestones
72	48,9709709	19,7204362		0,03		grey bedded limestones
74	48,9710796	19,7213818		0,03		grey massive limestones
75	48,9704967	19,7225164				grey surcose dolomites – tallus
76	48,9707827	19,7229262				grey surcose dolomites – tallus
84	48,9765499	19,7465192				dark grey bedded limestones
89	48,9693474	19,7142686		0,01		grey massive dolomites – outcrop
90	48,9830397	19,7698286				grey massive dolomites – outcrop
91	48,9705224	19,7185005				grey limestones
92	48,9685994	19,7116217				grey dolomitic limestones
114	48,9791450	19,7712074				grey dolomites
115	48,9790837	19,7724781				grey dolomites
116	48,9790363	19,7731426				dark grey dolomites
120	48,9779315	19,7728199				original description missing
121	48,9775792	19,7728553				original description missing
122	48,9770272	19,7728670				original description missing
123	48,9763835	19,7728413				original description missing
124	48,9755806	19,7729462				original description missing
125	48,9780151	19,7734468				original description missing
126	48,9776141	19,7743270				original description missing
132	48,9759709	19,7801822				original description missing

Appendix 3. A table of the samples with their trace element contents determined by a spectral analysis from Hanáček (1963). The WGS coordinates were determined by georeferencing the author's map.

Sample id	X	Y	Ca	Mg	Fe	Si	Al	Mn	Sr	Na	K	Li	Ti	Pb	Zn	Cu	Ag	Bi	Ni	Co	Cr	Ba	V	B	Zr	Cd
1	48,9842817	19,7641870	6	3	2	3	2	1	3	2		1		1	0	1	1				1	1				
3	48,9842733	19,7641575	6	6	5	3	2	4	2	2		1	2	3	3	1	1		2	2	1	1				
6	48,9842588	19,7641091	6	6	4	3	3	4	2	2		1	2	2	3	1	1				1	1				
8	48,9842503	19,7640785	6	6	4	3	2	4	2	2		1	2	3	4	1	1				1	1				
9	48,9842662	19,7641929	6	6	4	3	2	4	2	2		1	2	3	4	1	1				1	1				
11	48,9842584	19,7641730	6	6	3	3	2	4	2	2		1		4	4	1	2				1	1				2
13	48,9818605	19,7694132	6	6	2	3	2	3	2	2		1	2	2	2	1	1				1	1				
14	48,9814303	19,7709837	6	3	2	3	3	2	3	2		1		1	0	1						1				
16	48,9815505	19,7715276	6	6	3	3	3	3	2	2		1	2	2	2	1			1		1	1				
18	48,9811902	19,7713805	6	6	3	3	2	3	2	2		1		0	0	1	1		1		1	1				
21	48,9846194	19,7640968	6	5	3	4	4	2	3	3		1		2	0	2	1				1	2				
22	48,9845866	19,7644514	6	5	3	4	3	2	3	3				1	0	2			1		1	2				
23	48,9845362	19,7649086	6	3	2	3	2	1	3	2		1		1	0	1	1				1	1				
24	48,9846270	19,7625666	5	6	2	3	2	2	2	3		1		2	0	2					1	2				
25	48,9844229	19,7632567	6	6	2	3	3	2	2	2		1		2	0	2			1		1	1				
30	48,9842301	19,7627308	6	6	3	3	3	3	3	2		1		1	2	1	1				1	1				
32	48,9837842	19,7613583	6	6	5	4	3	4	2	2		1		1	0	2	1		1		1	3				
33	48,9835861	19,7610575	6	6	5	4	4	3	2	2	3	2	2	0	0	1	1		1		1	3				
34	48,9837424	19,7615061	6	6	5	4	2	4	3	2	3	2		0	0	1			1		1	2				
35	48,9836759	19,7616411	6	6	5	4	3	3	3	3	3	2		1	0	2	1		1		1	2	2	2		
36	48,9770855	19,7773092	6	6	4	4	3	3	3	3		1		0	0	3	1				1	2				
37	48,9767451	19,7768792	6	6	5	4	4	4	4	3	3	2	2	1	3	0	1				2	3				
38	48,9772684	19,7768938	6	6	5	3	4	4	4	2		1		1	0	0	1	2			1	2				
39	48,9775010	19,7766933	6	6	3	3	4	4	4	2		1		1	0	0	1				1	2				
40	48,9774078	19,7763300	6	6	2	3	2	3	3	2		1		0	0	1			1		1	2				

Appendix 3 – continued

Sample id	X	Y	Ca	Mg	Fe	Si	Al	Mn	Sr	Na	K	Li	Ti	Pb	Zn	Cu	Ag	Bi	Ni	Co	Cr	Ba	V	B	Zr	Cd
41	48,9775575	19,7762142	6	6	4	3	2	3	2	2		1		1	0	2	1				1	1				
42	48,9781897	19,7730017	6	6	4	4	2	4	3	2		1		2	0	2	1		1		1	2				
44	48,9864362	19,7638497	6	3	2	3	3	1	3	2	2	1		0	0	1			1		2	1				
55	48,9748475	19,7387252	6	5	3	4	3	4	3	2		1		2	0	2	1	2	1		1	2	2			
56	48,9746112	19,7380887	6	6	3	4	5	3	2	3		1	2	3	0	2	1		2		1	0	2			
57	48,9748806	19,7381881	6	6	3	3	2	4	3	2		1		3	0	1					1	2				
60	48,9758495	19,7372622	6	5	3	4	5	3		2	3	1	2	1	0	0					1	4				
61	48,9762772	19,7372370	6	5	3	4	3	2	4	3	3	1		2	0	2	1				1	2				
63	48,9744988	19,7330155	6	5	3	3	3	3	4	2		1		2	0	0	1				1	2				
64	48,9733406	19,7337661	6	4	2	3	3	3	4	2		1		2	0	0	1					2				
65	48,9730303	19,7339559	6	5	3	3	3	3	4	3		1		2	3	0	2	2	2		2	2				
66	48,9728781	19,7333380	6	4	2	3	3	3	3	2		1		2	3	1	1				1	2				
67	48,9721530	19,7262554	6	6	3	4	3	3	3	2		1		2	3	2					1	2				
68	48,9718235	19,7254656	6	6	4	4	3	4	3	2		1		1	3	2	1				1	2				
69	48,9725048	19,7261293	6	5	2	4	3	3	4	3		1		1	0	2	1				1	2				
70	48,9740197	19,7213344	6	5	3	4	5	3		3	3	1	2	1	0	0	1	2			1	2				
71	48,9701209	19,7218263	6	4	2	3	3	3	3	2		1		2	3	3					1	2				
72	48,9709709	19,7204362	6	5	2	4	3	3		2		1		1	0	3					1	2				
73	48,9711811	19,7230802	6	5	3	4	3	3	2	2		1		2	3	1		2			1	2				
74	48,9710796	19,7213818	6	6	2	3	3	3	3	2		1		2	3	1	1				1	2				
75	48,9704967	19,7225164	6	6	2	4	3	4	2	2		1		0	0	1					2	2				
76	48,9707827	19,7229262	6	3	3	4	3	3	4	2	3	2		0	3	0					1	2				
77	48,9714196	19,7241371		6	3	4	3	4	3	2		1		0	0	2			2			1	2			
78	48,9713251	19,7205325	6	6	2	4	3	3	3	2		1		1	0	1	1		1		1	2				
80	48,9695588	19,7142018		4	2	3	3	4	4	2		1		2	3	1					1	2				

Appendix 3 – continued

Sample id	X	Y	Ca	Mg	Fe	Si	Al	Mn	Sr	Na	K	Li	Ti	Pb	Zn	Cu	Ag	Bi	Ni	Co	Cr	Ba	V	B	Zr	Cd
81	48,9778625	19,7442604	6	5	3	4	3	4	4	2	3	1		0	0	0		2			1	2				
83	48,9764859	19,7460100	6	4	2	3	2	4	3	2		1		2	0	1					1	2				
84	48,9765499	19,7465192	6	4	2	4	3	4	3	2		1		2	0	2					1	2				
85	48,9775099	19,7477704		6	3	4	3	4	3	2		1		2	0	1					1	2				
86	48,9772344	19,7477348		6	3	4	3	4	3	2		1		2	3	1					1	2				
87	48,9778560	19,7494183		4	2	3	3	4	4	2		1		2	0	1	1				2	2				
89	48,9693474	19,7142686		6	3	4	3	3	3	2		2	2	3	3	1	1				1	2				
90	48,9830397	19,7698286		6	3	3	3	4	3	2		1		2	0	2					1	2				
91	48,9705224	19,7185005	6	5	2	3	3	3	4	2		1		2	0	2					1	2				
92	48,9685994	19,7116217		4	2	3	3	2	4	2		1		1	0	0					1	2				
94	48,9828501	19,7696596	6	5	3	4	4	3	4	2		1		2	3	1	1				1	2				
95	48,9821864	19,7685473	6	6	2	3	3	3	3	2		1	2	1	3	1	1				1	2				
95a	48,9821864	19,7685473	6	6	2	3	3	4	3	2		1		1	0	2			1		1	1	2			
96	48,9797186	19,7601149	6	6	2	3	2	4	3	2		1		2	0	1					1	2				
97	48,9811184	19,7598472	6	5	5	4	3	4	2	2		1	2	1	0	2	1		2		1	1				
98	48,9816359	19,7598312	6	6	4	4	2	4	3	2		1		2	0	2	1		2		2	2				
99	48,9835240	19,7594047	6	6	3	3	3	3	3	2		1		1	0	1			1		1	1				
100	48,9790915	19,7632550	6	6	3	4	3	3	2	3		1		2	0	2	1				1	0				
103	48,9831684	19,7661290	6	6	5	4	3	4	2	2		1		1	0	2	1		1		1	1				
105	48,9835962	19,7664490	6	6	3	3	3	2	2	2		1		0	0	1			2		2	1				
108	48,9819677	19,7681906	6	6	3	3	3	4	2	3		1	2	2	0	0	1		1		1	2				
109	48,9825183	19,7683925	6	5	3	4	3	3	3	2		1		2	3	2	1					1				
110	48,9829824	19,7690261	6	5	3	4	3	2	3	2		1		2	3	1	1				1	1				
111	48,9815768	19,7707909	6	5	2	4	2	3	4	3		1		2	0	2	1				1	2				
112	48,9818031	19,7691618	6	6	3	4	3	4	3	2		1		2	0	2	1		1		1	2		2		

Appendix 3 – continued

Sample id	X	Y	Ca	Mg	Fe	Si	Al	Mn	Sr	Na	K	Li	Ti	Pb	Zn	Cu	Ag	Bi	Ni	Co	Cr	Ba	V	B	Zr	Cd
114	48,9791450	19,7712074	6	5	3	3	3	3	3	2		1		2	3	2	1				1	2				
115	48,9790837	19,7724781	6	6	5	4	4	4	3	2		1		1	0	3		2	1		1	2	2			
116	48,9790363	19,7731426	6	6	5	4	3	4	2	2		2		1	0	3	1		1	2	1	2				
120	48,9779315	19,7728199	6	6	3	4	3	4	2	2		1		1	0	2	1		1		1	1	2			
121	48,9775792	19,7728553	6	6	3	3	3	4		3		1	2	2	0	0	1		1		1	2				
122	48,9770272	19,7728670	6	6	5	4	3	4	2	2		1	2	1	0	2	1		2		1	1				
123	48,9763835	19,7728413	6	6	4	4	3	4	2	2		1		2	0	2			1		1	1	2			
124	48,9755806	19,7729462	6	6	3	4	4	3	2	3		1		1	0	2			1		1	0				
126	48,9776141	19,7743270	6	6	4	3	3	4	2	2		1		1	0	3	1		1		1	1				
127	48,9774122	19,7750863	6	6	5	4	3	4	3	2		1		0	0	2					1	2	2			
129	48,9752718	19,7761723	6	6	5	4	4	4	3	2		2		1	0	2		2	1		1	2				
131	48,9747114	19,7802218	6	5	2	4	3	3	3	2				1	0	1					1	2				
132	48,9759709	19,7801822	6	6	5	4	4	4	3	2		2		1	0	2	1	2	1		1	2				
139	48,9841158	19,7610114	6	6	5	5	5	4		4	5	3	3	1	0	0	1		2	2	2	3	2	2	2	
140	48,9842901	19,7609538	6	6	3	3	3	2	3	2		1		1	0	2			2		1	1				
141	48,9826885	19,7594937	6	6	4	4	4	4	2			1	2	2	3	0			2		2	2				
144	48,9743489	19,7805060	6	6	3	4	3	3	2	2		1	2	2	0	1					1	1	2			

The explanation of the values denoted by numbers:
6: 1 000 000–100 000 ppm
5: 100 000–10 000 ppm
4: 10 000–1 000 ppm
3: 1 000–100 ppm
2: 1 000–10 ppm
1: 100–1 ppm

Mineralia Slovaca, Web ISSN 1338-3523, ISSN 0369-2086, https://doi.org/10.56623/ms.2025.57.1.3
57, 1 (2025), 39 – 58, © Authors 2025. CC BY 4.0

3D Long-Term Monitoring of Recent Tectonic Activity in Demänovská Cave of Liberty

MARIÁN STERCZ[1, 2,*], DANIEL GREGA[1, 2], ĽUBOMÍR PETRO[1], PAVEL BELLA[3, 4], JURAJ LITTVA[3], SILVIA JAJČIŠINOVÁ[1] and MARTIN BEDNARIK[2]

[1]State Geological Institute of Dionýz Štúr, Mlynská dolina 1, 817 04 Bratislava 11, Slovak Republic;
[*]marian.stercz@geology.sk, daniel.grega@geology.sk, lubomir.petro@geology.sk, silvia.jajcisinova@geology.sk,
[2]Faculty of Natural Sciences, Comenius University, Ilkovičova 6, 842 15 Bratislava 4, Slovak Republic;
mbednarik@uniba.sk
[3]Faculty of Education, Catholic University in Ružomberok, Hrabkovská cesta 1, 031 04 Ružomberok,
Slovak Republic; pavel.bella@ku.sk
[4]State Nature Conservancy of the Slovak Republic, Slovak Cave Administration, Hodžova 11,
Liptovský Mikuláš, Slovak Republic; pavel.bella@ssj.sk; juraj.littva@ssj.sk

Abstract: The topic of the article is the analysis of recorded data and the presentation of results from almost 24 years of monitoring tectonic movements along a neotectonic fault within the extensive underground space of the Demänovská Cave of Liberty. Displacements and rotations at the fault were measured using a mechanical-optical 3D extensometer TM-71. The measurement results subjected to statistical analysis showed a trend in two components of the spatial motion vector – vertical (Z) and horizontal (Y), which is paralel to the strike of the fault. Recent activity along the fault reflects the action of the contemporary stress field and also seismic activity within the Western Carpathians. The study also examines the relationship between the movements recorded by TM-71 and seismic events in the wider vicinity of the cave. Although long-term measurements show a significant trend of movement along the fault, its magnitude is minimal. From the perspective of cave safety, the detected neotectonic activity does not pose any risk.

Key words: Demänovská Cave of Liberty, Jalovec Fault, recent tectonics, monitoring, 3D extensometer

Graphical abstract

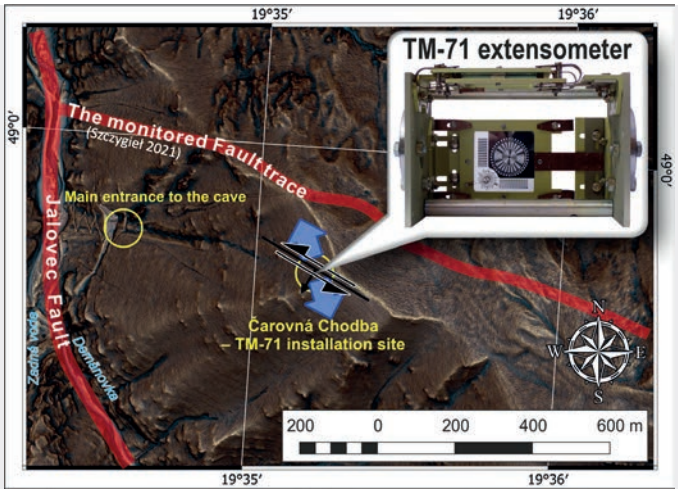

Highlights

- We present results of 3D long-term monitoring of fault activity inside Demänovská Cave of Liberty.
- Trend analyses have been used for data set processing.
- Almost 24 years results have proven permanent but very slow movements along tectonic line.
- Displacements are not continuous but occur in sudden leaps and may be associated with seismic events.

Introduction

Demänovská Cave of Liberty, located in the Demänovská dolina Valley (Nízke Tatry Mts), is a part of the larger Demänová Cave System. It is the longest underground system in Slovakia, and is listed as a National Nature Monument. Its underground spaces are controlled by several tectonic fractures of multiple directions and orientations. The cave was selected in 2001 for 3D monitoring of slow movements along one of the faults due to the occurrence of multiple instances of damage to dripstones (already pointed out by Pokorný, 1952), as well as the neotectonic nature of the faults in the area (Maglay et al., 1999). The start of monitoring is linked to an international project COST-625 *3-D Monitoring of Active Tectonic Structures* solved during the period 2000–2006 (Piccardi, 2006). The site was later included in the national project *Partial Monitoring System – Geological Factors* financed from the budget of the Ministry of the

Environment of the Slovak Republic. Monitoring results are presented in the form of annual reports and are available on the State Geological Institute of Dionýz Štúr (SGIDŠ) website (Ondrus, 2025).

A special 3D extensometer of the TM-71 type with high accuracy (Košťák, 1969, 1991) was chosen to detect displacements on the selected fault. Devices of this type are widely used in Slovakia at a total of 36 locations to monitor not only neotectonic activity on selected faults (e.g. Petro et al., 2004a, b, 2011a; Briestenský et al., 2007, 2011, 2018; Stercz et al., 2025), but also block slope failures (e.g. Petro et al., 1999, 2011b; Wagner et al., 2000; Ondrejka et al., 2014) and historical objects (e.g. Vlčko & Petro, 2002; Petro et al., 2012; Jánová et al., 2021).

The article presents the results of long-term 3D recording of microdisplacements along one of the fault zones in the Demänovská Cave of Liberty, conjugate to the Jalovec Fault, which traverses the axis of the Demänová Valley. The recorded data are subjected to trend analysis, individual phases of neotectonic activity are characterised, and the results are compared with the seismic activity in the broader region.

Location and geology of the study area

The Demänovská Cave of Liberty is situated in the Demänová Valley on the northern slope of the Nízke Tatry Mountains. The valley, approximately 10 km in length

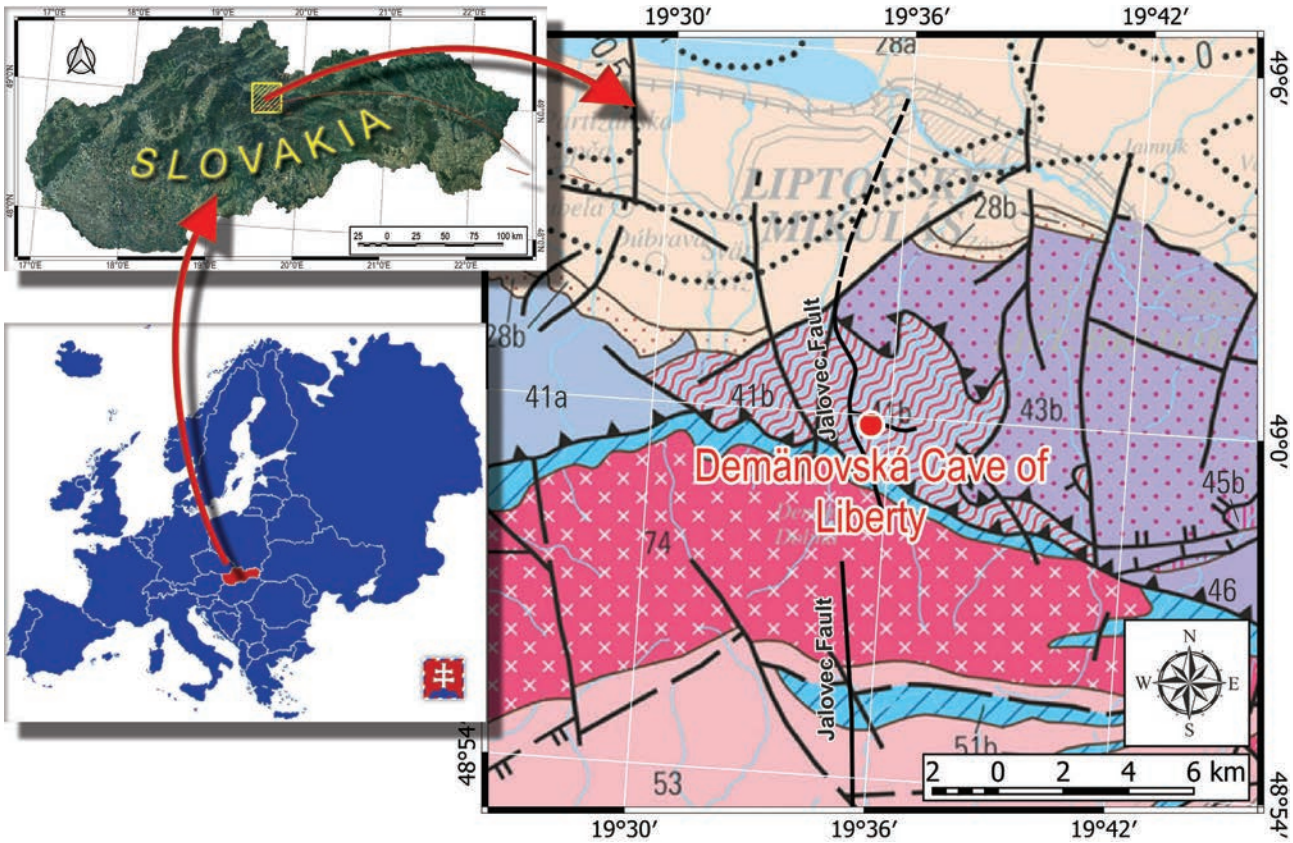

Fig. 1. Excerpt from the Tectonic Map of Slovakia showing the area around the Demänovská Cave of Liberty (Bezák et al., 2004). Neo-Alpine tectonic structures of the Inner and Outer Western Carpathians include sedimentary basins filled with Paleogene and Upper Cretaceous sediments: 28 – Intra-Carpathian extensional basins in the back-arc setting (Middle Eocene–Lower Miocene): a) deep-water sediments of the outer shelf, slope, and oceanic plateaus; b) shallow-marine shelf sediments. Paleo-Alpine tectonic units of the Inner Western Carpathians comprise the following: Fatricum – 41: a) Mesozoic formations with deep-water sediments (Jurassic–Lower Cretaceous); b) Mesozoic formations with shallow-marine sediments (Jurassic–Lower Cretaceous); c) clastic Permian sediments. Hronicum – 43: nappes formed from Triassic intraplatform basins (Biely Váh-type development): b) from the Biely Váh-type basin; 45: nappes formed from Triassic carbonate platform (Čierny Váh-type development): b) from the Čierny Váh-type carbonate platform; 46: clastic and volcanic sequences of the Carboniferous–Lower Triassic. Tatricum – 51: cover formations (Upper Paleozoic–Middle Cretaceous): a) Mesozoic formations with deep-water sediments (Jurassic–Lower Cretaceous); b) Mesozoic formations with shallow-marine sediments (Jurassic–Lower Cretaceous); c) Upper Paleozoic clastic sediments. Hercynian tectonic units in the crystalline basement (Proterozoic?–Paleozoic) – 53: upper lithotectonic unit (originally high-grade metamorphic paragneisses, amphibolites, migmatites, and orthogneisses – mainly Paleo-Hercynian granitoids). Meso-Hercynian collisional granitoids – 74: suite of I-type granitoids (crust-mantle granitoids dominated by granodiorites and tonalites, Devonian–Lower Carboniferous).

and pear-shaped in outline, is bordered by the following elevations: Demänovská Poludnica (1 304.3 m), Magura (1 376.4 m), Krakova hoľa (1 750.6 m), Krúpova hoľa (1 927.2 m), Chopok (2 023.3 m), Poľana (1 873.0 m), Siná (1 559.6 m) and Opálenisko (1 143.3 m). Its morphological character is primarily conditioned by the geological structure and tectonic framework of the area.

The Nízke Tatry Mountains are composed of three tectonic units – Tatricum, Fatricum, and Hronicum (Biely et al., 1997). The Ďumbier segment of this range, where the Demänová Valley belongs, is situated within the Tatra–Fatra zone of the Inner Western Carpathians' core mountains.

The valley was formed by the Demänovka Stream and its tributaries. Its upper (southern) parts on the Tatricum crystalline basement display fluvial and glacial landforms, while the lower (northern) section is featured by fluviokarst landforms, monoclinal morphostructures and sharply arched carbonate ridges and cliffs (Droppa, 1972). The Demänovská Cave of Liberty is the most significant section of the multi-level Demänová Cave system, with a currently known total length exceeding 51 km (Slovak Speleological Society, 2025). It was formed by sinking allochthonous waters of the Demänovka and Zadná voda streams in the Triassic limestones of the Fatricum (Krížna Nappe), which overlies the Tatricum crystalline basement and its sedimentary cover from the north (Fig. 1).

The faults and joints controlled the valley's position and directed watercourses, significantly influencing the shaping of the surface relief of the Demänová Valley. These faults thus guided the origin and development of the Demänovská Cave System and other karst features (Droppa, 1972).

The cave passages and chambers, formed mostly in the Middle Triassic Gutenstein Formation of the Fatricum, are aligned along two fracture systems oriented NW–SE and NE–SW (Droppa, 1957, 1972). The principal fault system traversing the axis of the Demänová Valley is the Jalovec Fault (Hók et al., 2000), which trends N–S (to the north) and NNW–SSE (to the south of the site) in the vicinity

Fig. 2. Damaged speleothem decorations in the underground passages of the Demänovská Cave of Liberty. The TM-71 extensometer is visible in the bottom right photograph (Čarovná chodba Passage – photo by M. Stercz).

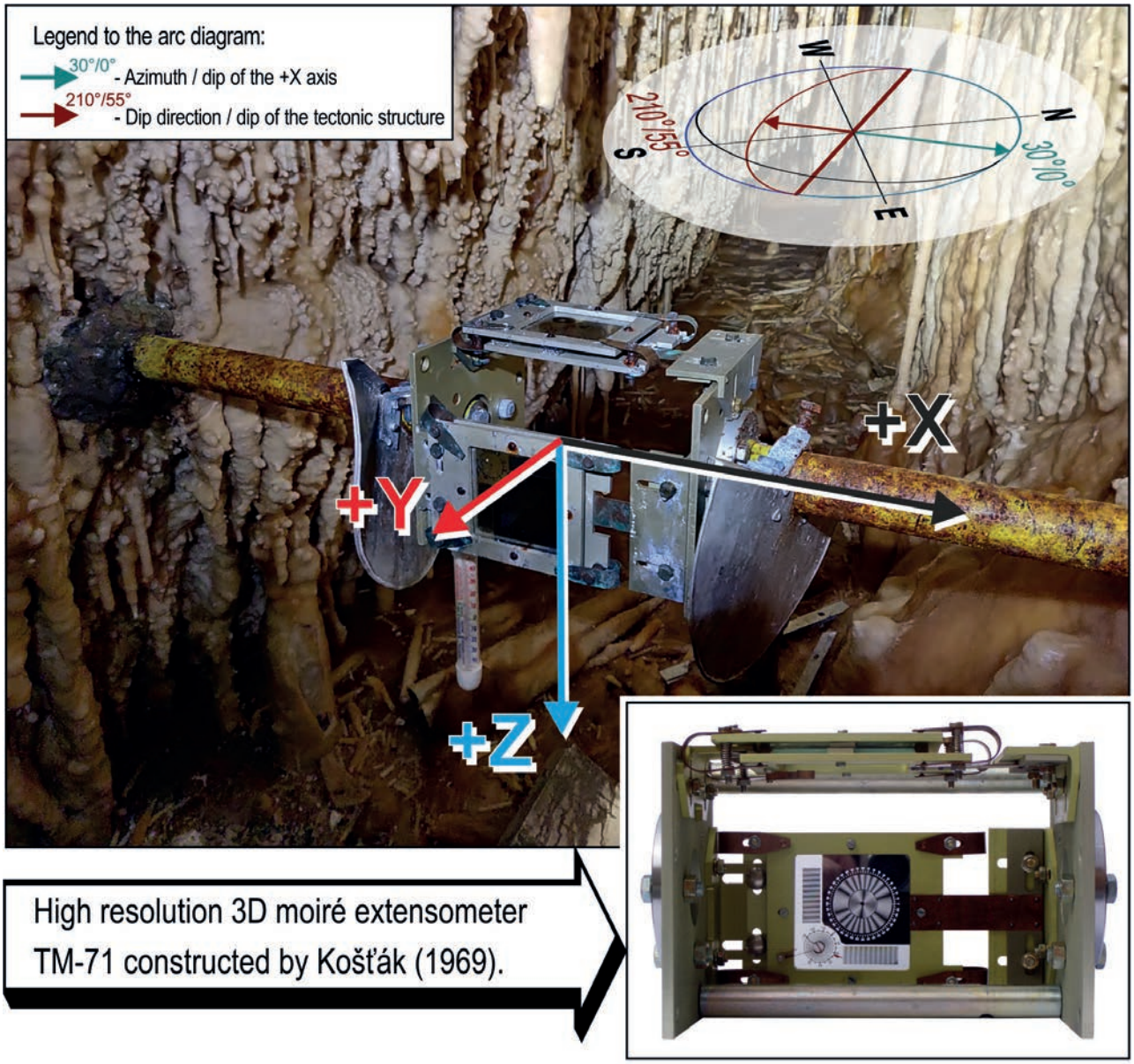

Fig. 3. Installation of the TM-71 mechanical-optical extensometer in the Čarovná chodba Passage of the Demänovská Cave of Liberty (photo by Ľ. Petro).

of the monitored site. The monitored fault direction is WNW–ESE and is conjugate to the aforementioned fault system.

The TM-71 extensometer was installed in the so-called Čarovná chodba Passage, which developed through corrosive widening of this fault under phreatic conditions, with minimal evidence of fluvial modification (Bella et al., 2014; Bella, 2016).

The aim of installing the TM-71 device in the Demänovská Cave of Liberty was to determine whether the tectonic processes that contributed to the cave's formation are still active today. In the Čarovná chodba Passage – the site of the instrument's installation – macroscopic evidences of neotectonic movements were observed, including fractures and cracks in speleothems (Petro et al., 2004b; Briestenský et al., 2010), as well as numerous broken stalactites and stalagmites of varying size and age (Fig. 2). The TM-71 extensometer was intended to confirm and quantify the magnitude of these movements, and to define their attributes – direction, rate, and character.

The Čarovná chodba Passage, where the instrument was installed at the end of August 2001 (Fig. 3), was formed, as previously mentioned, by the activity of groundwater in a structurally weakened zone aligned in a WNW–ESE direction (with a general fault dip orientation of 210°/55°). The X-axis of the device points NE and represents the

installation orientation. The monitored fault dips towards the SW at an angle of 55°, and to some extent reflects the inclination of the terrain surface.

Data readings at this site are not recorded automatically but are instead taken manually, with the assistance of staff from the Slovak Caves Administration (SCA). Since the installation of the device, a total of 81 measurements have been taken to date, at intervals of approximately three to four months (3–4 readings per year).

Methodology of Data Acquisition and Processing

Based on the data measured so far, the movement along the monitored fault is not particularly significant. Over a period of 24 years, its magnitude has ranged from hundredths to tenths of a millimetre. If the instrument had been installed on the surface rather than underground – where it would be exposed to more pronounced climatic factors – it probably would not have been possible to evaluate the data reliably, as the distortion caused by external factors would greatly exceed the measured manifestations of neotectonic movements. In this case, however, the climatic conditions within the cave are highly stable, and therefore the measured data – regardless of their small magnitude – can be considered valid.

At small magnitudes of recorded microdisplacements, the sensitivity of the instrument is critical to the usability of the data. The minimum detectable displacement – i.e. the lower detection threshold – is determined by the physical principle of measurement and the characteristics of the applied moiré grating (Rowberry et al., 2016). For the instrument currently in use, the standard uncertainty of Type B associated with its construction can be estimated in accordance with the principles outlined in the Guide to the Expression of Uncertainty in Measurement (GUM) (BIPM et al., 2008), using the following general expression:

$$u_B = \frac{Z_{max}}{\sqrt{3}}$$

where Z_{max} denotes the maximum possible deviation due to the instrument's resolution or design limitations – in this case, equal to the smallest division of the instrument's scale, i.e. its resolution (1 moiré fringe = 0.05 mm).

$$u_B = 0.029\ mm$$

This value refers to the length of the displacement vector in the measured plane, expressed in polar coordinates. When converted to Cartesian coordinates, the instrument's minimum resolution becomes a function of the angle (sine or cosine) between the projection of the spatial displacement vector in the analysed plane and the respective axis of the coordinate system. As a result, the minimum resolution when using the manual fringe-counting method may vary within the interval $< 0; 0.029 >$ mm.

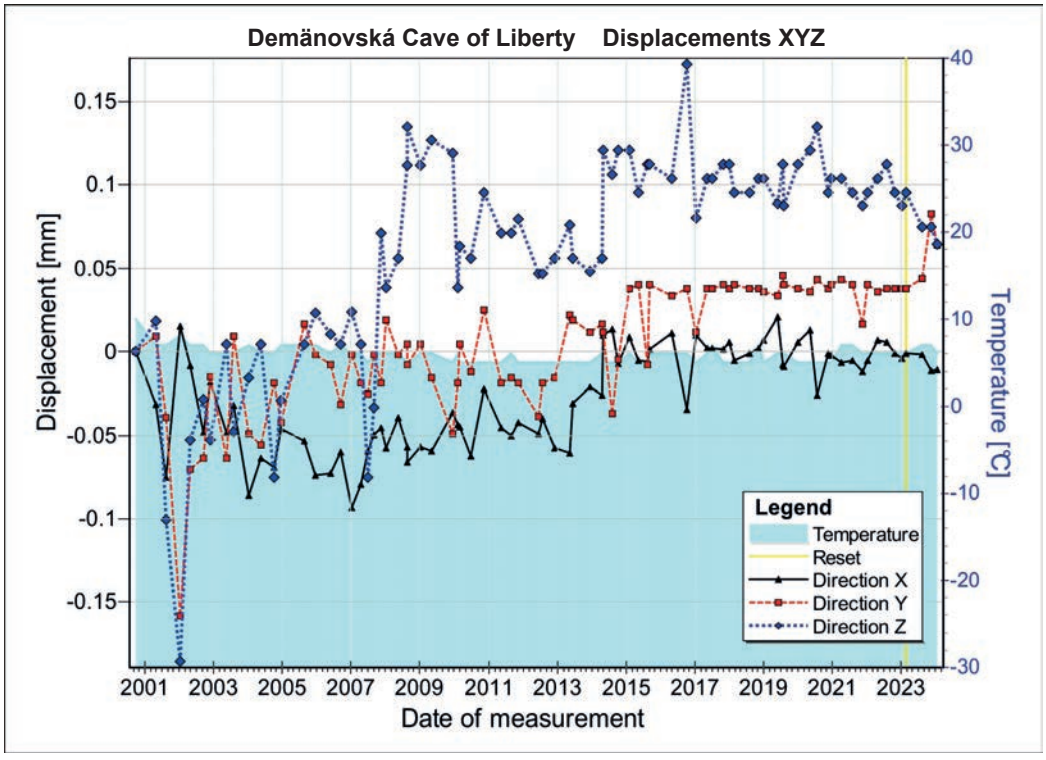

Fig. 4. Representation of measured displacement data in a 2D graph – graphical output from the MSDilat software.

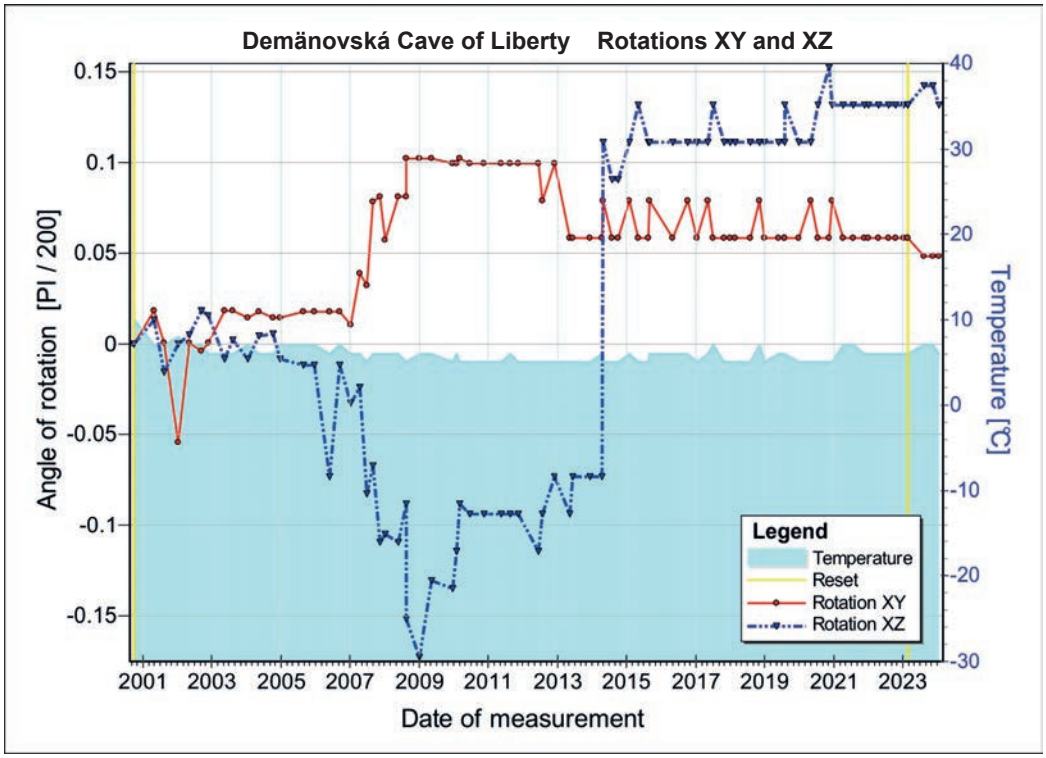

Fig. 5. Representation of measured rotation data in a 2D graph – graphical output from the MSDilat software.

In Table 1, the values marked with an asterisk (*) represent data points that are either at the threshold of the instrument's detection capability or fall below the detection limit, indicating minimal or undetectable movement.

The measured data were converted into units of length (for microdisplacements) and angular degrees (for rotations) using the MSDilat software (Stercz, 2021). Figs. 4 and 5 show 2D graphs of displacement and rotation. The displacement graph displays the decomposed spatial vector of movement into X, Y, and Z directional components over time. Rotations represent the tilting of monitored rock blocks relative to each other within the XY plane (horizontal) and the XZ plane (vertical, perpendicular to axis Y).

Table 1 presents the data recorded during the entire monitoring period. For simplicity and clarity, values in each direction were aggregated by calendar year – producing so-called interval time series, thereby partially removing seasonal variations. The index indicates the identified yearly measurements used in graphical representations in the three fundamental orthogonal planes.

The process of calculating the geographic parameters of motion and interpreting the data in the horizontal plane is illustrated in Fig. 6. The angle α for each partial motion vector represents the angle between the horizontal projection of the vector and the X-axis direction in the TM-71 coordinate system (the formula is shown in the figure). The resulting azimuth δ is calculated as the sum of α and β, where β is the horizontal deviation of the instrument's axis from geographic north. At the Demänovská Cave of Liberty site, the resulting direction of horizontal movement in the instrument coordinate system over the entire monitoring period is α = 99.5°. Since the +X axis is offset by β = 30° from geographic north, **the calculated geographic azimuth of horizontal movement is δ = 129.5°.** This indicates that in the horizontal plane, the mobile block shifts in the NW–SE direction, with the total movement over the entire monitoring period amounting to only about 0.065 mm (rounded to three decimal places).

In the following two figures (Figs. 7 and 8), the procedure for calculating the movement direction in the vertical plane – i.e. the values of angles λX and λY for the vertical, mutually perpendicular planes XZ and YZ – is illustrated schematically (Fig. 7 – XZ plane; Fig. 8 – YZ plane). These values represent the dip magnitude (i.e. the deviation of the resultant movement vector from the horizontal plane) as viewed from the XZ or YZ plane, respectively. The calculation principle, along with the mathematical formulae, is shown in the figures. The actual resultant dip is a combination of dips in both vertical planes and can be calculated using the following formula:

$$\lambda = arctan \frac{\Delta Z}{\sqrt{\Delta X + \Delta Y}} * 180/\pi$$

The resultant dip of the motion vector at the Demänovská Cave of Liberty over the entire monitoring period is, after rounding, λ = 45°.

Tab. 1

Measured and calculated data for individual years of monitoring

Measurements			Displacements			Rotations	
INDEX	**Year of**	**Number of**	**X**	**Y**	**Z**	**XY**	**XZ**
1	2001	1	0.000	0.000	0.000	0.000	0.000
2	2002	3	0.015	–0.158	–0.186	–0.051	0.011
3	2003	3	–0.018	–0.015	–0.053	0.003	0.027
4	2004	3	–0.086	–0.049	–0.016	0.017	0.003
5	2005	3	–0.046	–0.042	–0.029	0.017	0.003
6	2006	2	–0.074	–0.002	0.023	0.021	0.000
7	2007	3	–0.094*	–0.002	0.024	0.013	–0.021
8	2008	5	–0.058	0.019	0.039	0.060	–0.093
9	2009	4	–0.057*	0.005*	0.112	0.106	–0.161
10	2010	2	–0.036	–0.049	0.119*	0.103	–0.123
11	2011	4	–0.022	0.025	0.096*	0.103	–0.082
12	2012	3	–0.042	–0.019	0.079*	0.103	–0.082
13	2013	3	–0.057*	–0.015*	0.056*	0.103	–0.062
14	2014	3	–0.021	0.011	0.048	0.062	–0.062
15	2015	5	0.009	0.038	0.121	0.082	0.123
16	2016	3	0.001*	0.040*	0.112*	0.082	0.123
17	2017	3	0.010*	0.011*	0.080*	0.062	0.123
18	2018	4	0.005*	0.038*	0.112*	0.062	0.123
19	2019	4	0.007*	0.036*	0.104*	0.062	0.123
20	2020	4	0.005*	0.038*	0.112*	0.062	0.123
21	2021	4	–0.002*	0.040*	0.104*	0.082	0.144
22	2022	4	–0.005*	0.040*	0.096*	0.062	0.144
23	2023	4	–0.004*	0.038*	0.087*	0.062	0.144
24	2024	4	–0.011*	0.064*	0.065*	0.051	0.144

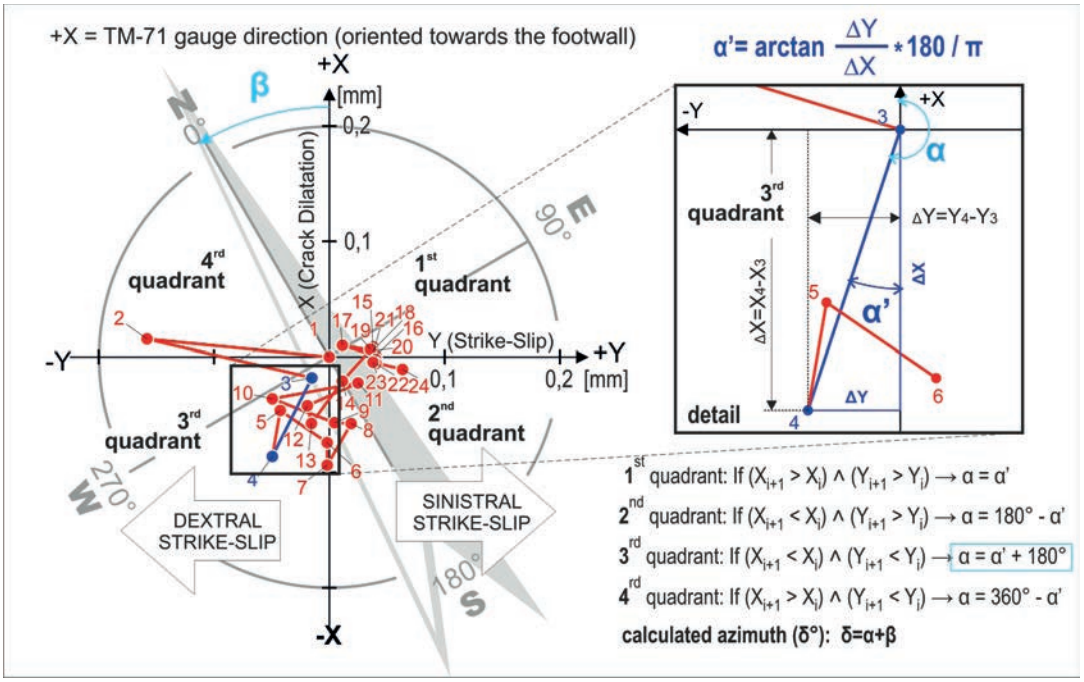

Fig. 6. Schematic representation of movement direction calculation in the horizontal XY plane (adapted from Briestenský et al., 2018).

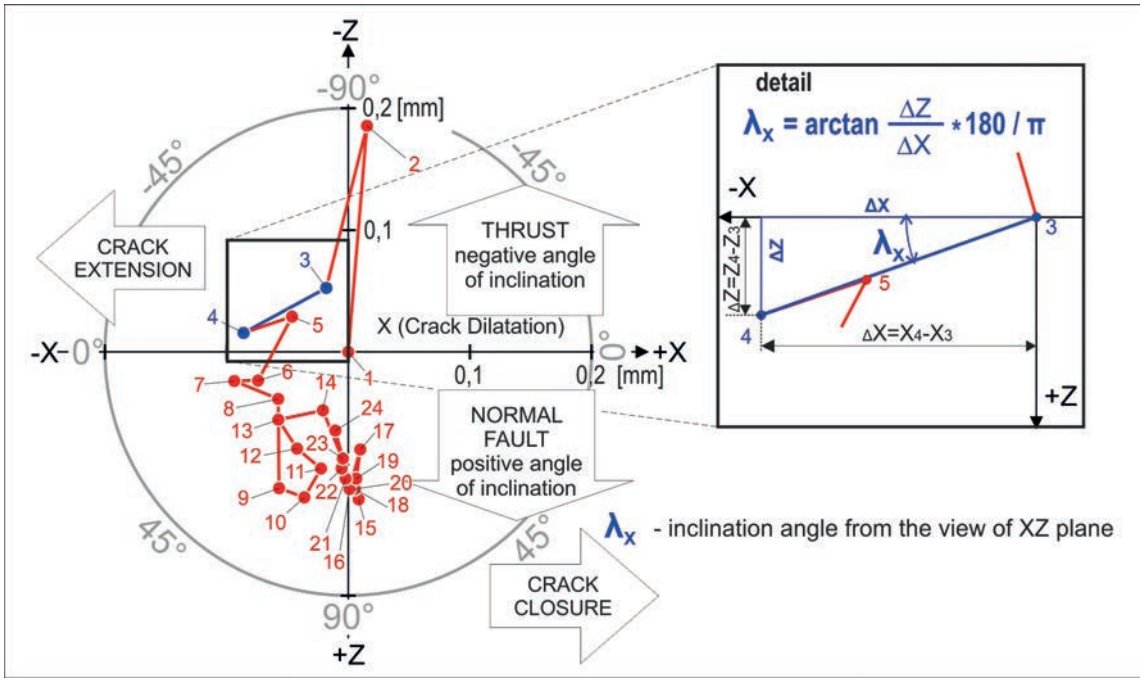

Fig. 7. Schematic representation of dip λX calculation (movement direction in the vertical XZ plane; adapted from Briestenský et al., 2018).

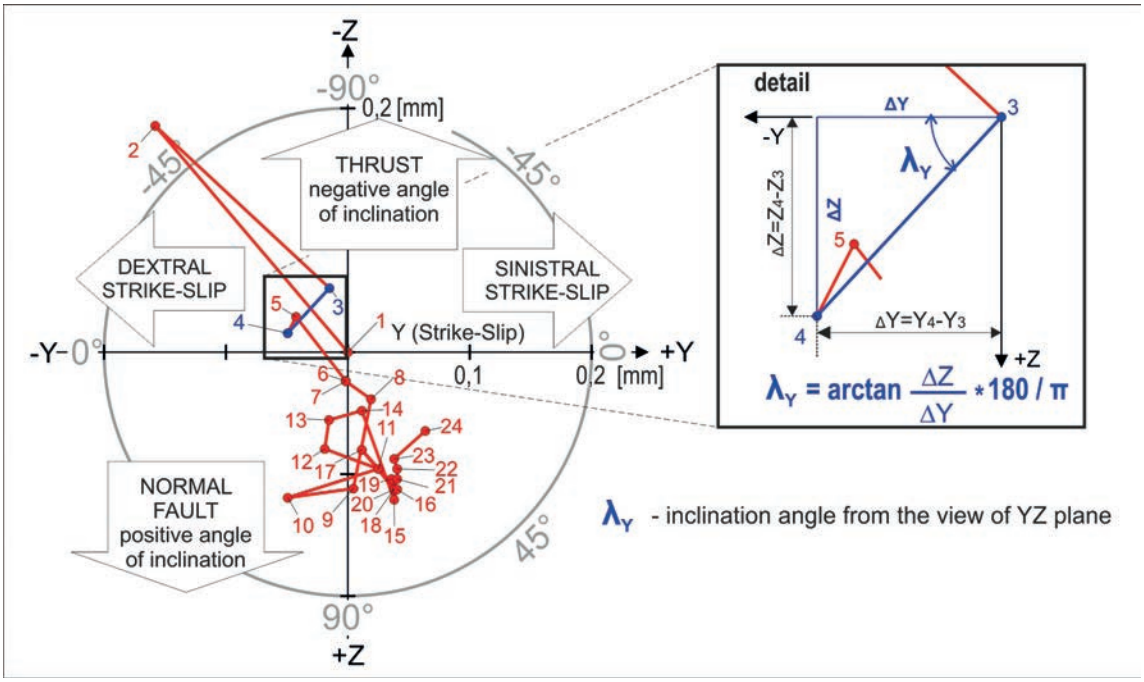

Fig. 8. Diagram of the calculation of dip angle λY (direction of movement in the vertical YZ plane; adapted from Briestenský et al., 2018).

The magnitude of the motion vector is representing the total displacement over the monitored period (from August 2001 to December 2024).

It represents the vector sum of the measured movements in the horizontal and vertical planes. It can be calculated according to the formula:

$$|XYZ| = \sqrt{|XY|^2 + |Z|^2}$$

where |XY| is the magnitude of the movement in the horizontal plane, calculated using the formula:

$$|XY| = \sqrt{|X|^2 + |Y|^2}$$

The magnitude of the total motion vector is 0.092 mm. When decomposed into individual components |X|, |Y|, and |Z|, it can be stated that the Y and Z components contribute almost equally to the total magnitude of the movement vector – each accounting for more than 45 % – while the X component contributes only marginally, less than 8 %. In summary, the detected movement along the tectonic structure may be described as a minor sinistral (left-lateral) displacement with a slight subsidence of the SW block, accompanied by a tendency for the fault to open. Calculated values of all the components are given in Table 2.

Tab. 2

Calculated values of the components of the total motion vector

Component of motion vector	|X|	|Y|	|Z|	|XY|	|XYZ|
Magnitude of movement [mm]	0.011	0.064	0.065	0.065	0.092

The representation of the individual measured motion vectors on a spherical surface in the form of a tectonogram is shown in Fig. 9. The diagram also includes the installation parameters of the instrument (in turquoise color) – azimuth of the X-axis: 30°, and its dip: 0°. Similarly, structural data of the monitored fault are displayed – dip direction and dip (210° / 55°), along with the resultant direction of movement derived from the data – the horizontal projection of the spatial vector and its inclination from the horizontal plane (129° / 45°).

Unlike a standard tectonogram, where data are plotted using stereographic projection only on the lower hemisphere (as dip angle ranges from 0° to 90°), data in this diagram may be plotted on both hemispheres since the dip of the movement vector can be positive (downward) or negative (upward), ranging from –90° to +90°. Measurements plotted on the lower hemisphere are shown in red, those on the upper hemisphere in green.

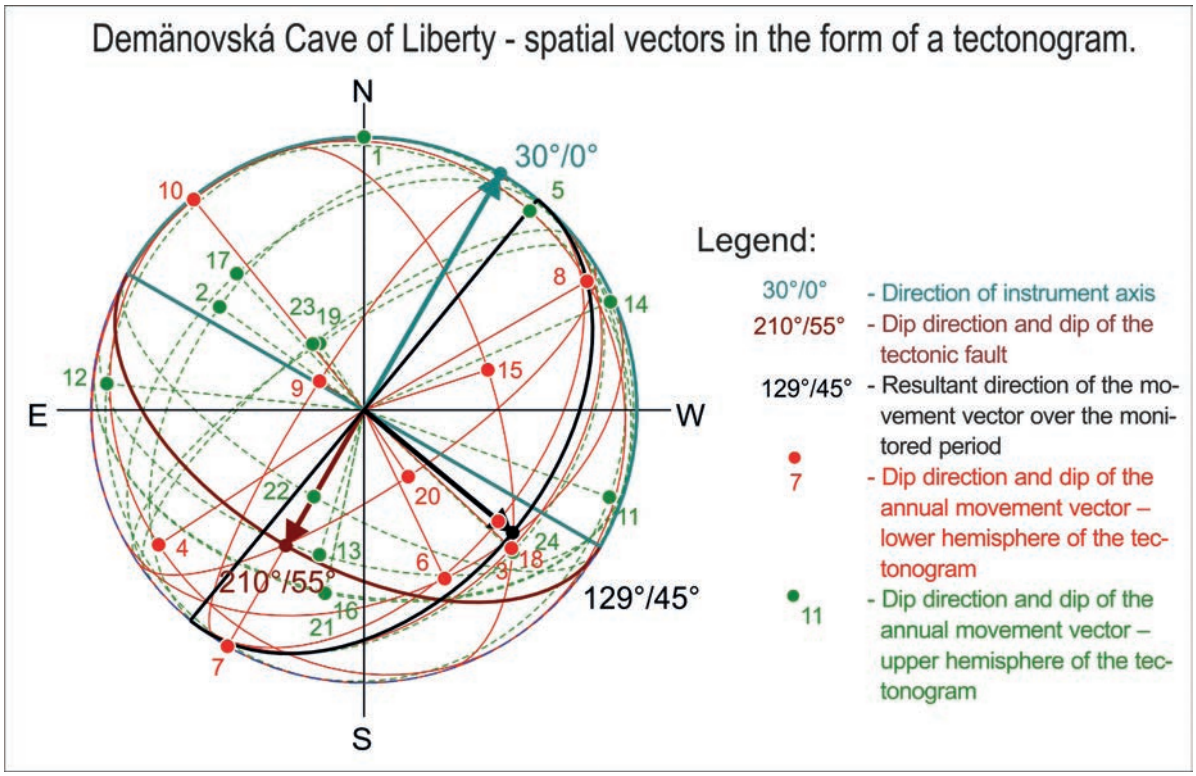

Fig. 9. Display of spatial vectors of aggregated annual measurements in the form of a tectonogram.

Aggregated values for each calendar year are plotted, with the adjacent number corresponding to the index used to identify the measurement in Table 1. An examination of the diagram shows that the measured data exhibit a slight predominance of movements with steep inclinations (points located closer to the centre of the diagram) and a prevailing NW–SE orientation. The number of upward-directed measurements is comparable to those directed downward, indicating that no significantly dominant movement occurs in either direction within the vertical plane.

In order to evaluate microdisplacements relative to the fault being monitored, the instrument installation parameters and the structural attributes of the fault must be carefully recorded. Although the TM-71 can measure movements in any general direction, it is recommended to install it following standard principles to simplify calculations. Typically, the device is mounted so that the X-axis, if possible, is horizontal and aligned with the direction of opening or closing of the fault (i.e. along the dip azimuth), and the Y-axis is perpendicular to the dip direction and always horizontal. Installation data are recorded and considered during evaluation in the processing software. In the case of the Demänovská Cave of Liberty site, the instrument was installed in accordance with standard practice, with the X-axis aligned with the

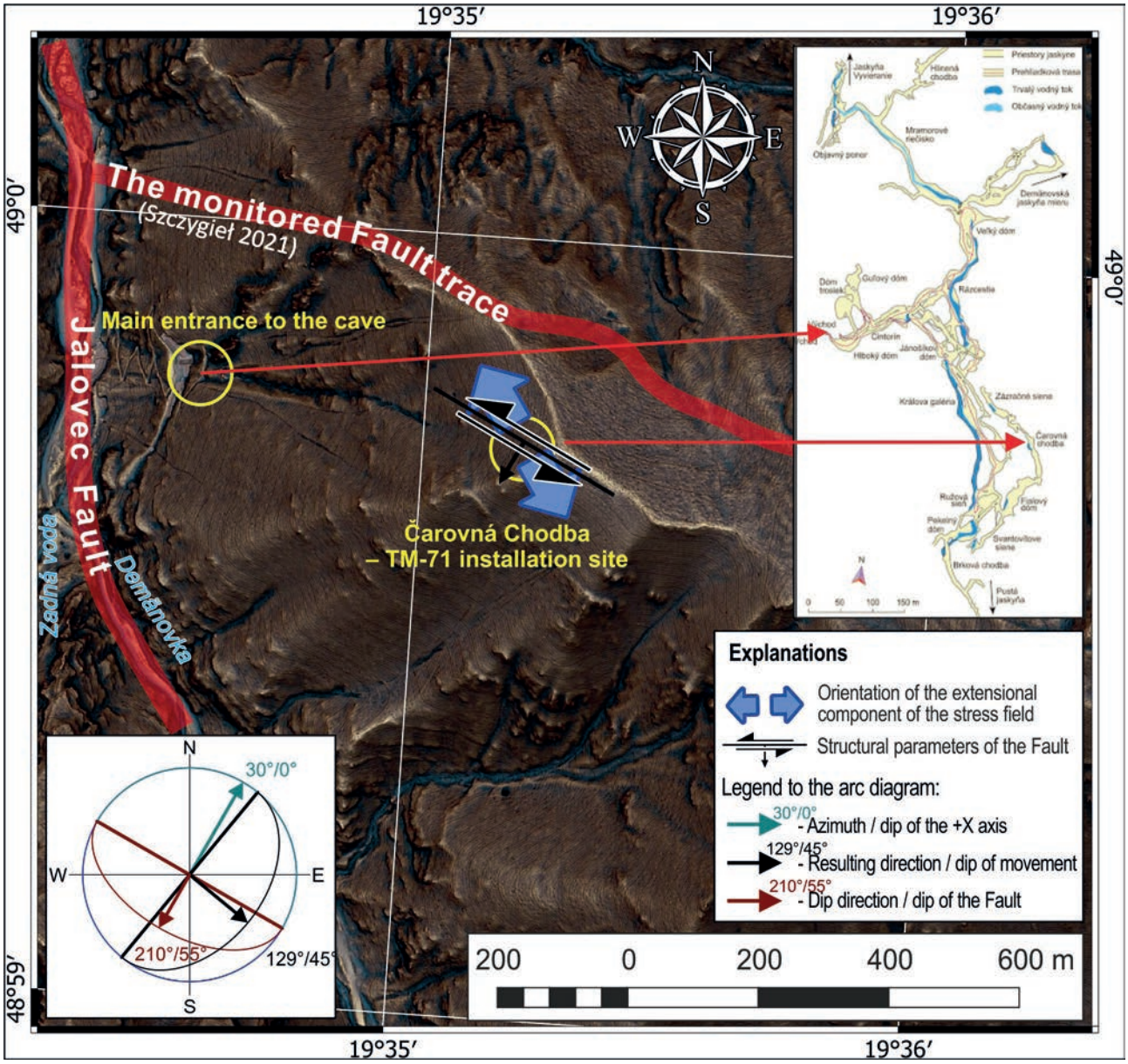

Fig. 10. Surface projection of the TM-71 instrument installation site, showing its orientation.

dip direction of the monitored fracture. Both X and Y axes lie in the horizontal plane, +Z points downward, and the +X direction points toward the assumed stable block of the monitored fault line. The surface projection of the TM-71 instrument installation site is shown in Fig. 10, illustrating its orientation, the orientation of the fault, and the resulting direction of the movement vector. By entering the measured data into the structural geological software GS2PS (Sasvári & Baharev, 2014), the orientation of the extensional component of the stress field was calculated and is illustrated in the figure.

Assuming that the source of the monitored activity in the rock mass is a regionally persistent (monotonic) recent neotectonic process (RNP) over the duration of the monitoring, this should manifest as a continuous and long-term consistent movement along the fault, characterised by a distinct trend component in the time series. To verify this assumption, trend analysis is appropriate.

Trend Analysis of the Measured Data

When the measured data from the TM-71 are arranged chronologically, they form a time series for each component of the motion vector. The aim of analysing these datasets is not only to determine whether any movements are occurring along the tectonic line, but also to identify whether such movements exhibit a definable long-term trend potentially associated with neotectonic processes. In this case, the statistical analysis of microdisplacement trend curves was employed to confirm or refute the hypothesis of a long-term trend in the measured movements, which could indicate the nature of the stress regime within the rock mass over an extended time frame.

For the trend analysis, the non-parametric Mann-Kendall (MK) trend test (Mann, 1945) was applied in combination with Sen's method for calculating the slope of the regression line (Sen, 1968). The trend analysis was applied to the primary data, aggregated into time series

Tab. 3

Results of trend analysis of the measured values at the Demänová site

Demänová – statistical trend analysis of TM-71 microdisplacement and rotation curves					
Tested time series	**Microdisplacement**			**Rotation curves in XY a XZ planes [π/200]**	
	X	**Y**	**Z**	**XY**	**XZ**
MK-test statistics	**Mann-Kendall test (MK-test)**				
n	24	24	24	24	24
α	0.05	0.05	0.05	0.05	0.05
S	78	177	124	69	121
Var(S)	1	1	1	1	1
σ	40.291	40.112	40.183	39.594	39.804
Zs	1.960	1.960	1.960	1.960	1.960
p	0.05599	0.00001	0.00221	0.08590	0.00257
Trend	**NO**	**YES**	**YES**	**NO**	**YES**
SM statistics	**Sen's method**				
α	–	0.05	0.05	–	0.05
N	–	276	276	–	276
k	–	78.619	78.757	–	78.014
β	–	0.0035	0.0058	–	0.007
β-lower	–	0.002	0.003	–	0.003
β-upper	–	0.006	0.009	–	0.011
Δd[mm] | Δφ[π/200]	–	0.084	0.140	–	0.169
Δd | Δφ – lower	–	0.056	0.067	–	0.072
Δd | Δφ – upper	–	0.132	0.209	–	0.252

n – number of observations; α – significance level; S – Mann-Kendall test statistic; Var(S) – variance of the S statistic; σ_s – standard deviation of S; Z_s – standardised test statistic (positive values indicate an increasing trend, negative values a decreasing trend); p – p-value (statistical significance of the trend); k – rank index used for calculating the confidence interval of the slope; β – Sen's slope (estimated median slope of all pairwise data combinations); Δd [mm] / Δφ [π/200] – estimated displacement per unit time in the horizontal (Δd) and angular (Δφ) component

with an interval length of one year (Tab. 1). The results for the individual time series are summarised in Table 3. The following findings emerged from this statistical analysis:

- A statistically significant trend at the 95 % confidence interval was demonstrated in the examined primary datasets of displacements in the Y and Z directions.
- For the data representing movement along the X axis, no statistically significant trend was confirmed.
- In the datasets of measured movements in Y and Z directions, the trend is positive (the statistical value of the MK test $S > 0$); the implications of the direction of the curves in relation to their geographic orientation are described further in the subchapter *Characteristics of the Curves*.
- Based on the p-value, which expresses the probability of rejecting the null hypothesis (the null hypothesis H_0 assumes no trend exists in the tested dataset), the reliability of trend detection is highest in the Y direction – that is, for horizontal displacement perpendicular to the direction of the instrument's installation (p-value << significance level $\alpha = 5$ %).

In the datasets of measured rotations, the presence of a trend is less reliable. The curve representing rotation in the XY plane does not show a trend, and the measured data appear random and independent. For the XZ curve, the presence of a trend is demonstrated based on the p-value, although the level of reliability is somewhat lower than that of the Y curve. As with the other curves, the trend in this case is also positive.

If a statistically significant trend is confirmed, its magnitude can be determined using the Sen coefficient – the slope of the trend line β (Tab. 3). Sen's method (Sen, 1968) assumes a linear trend within time series data, which is generally expected in long-term observations of fault movements. In reality, however, the release of stress in rock masses rarely occurs smoothly in the short term. It typically manifests as short episodes of temporary changes in measured parameters, which may be associated with other indicators of tectonic activity, such as seismic events.

Although tectonic activity in the Demänovská Cave of Liberty can be considered relatively stable over the monitored period, certain time intervals can still be identified that display a similar character in monitored indicators (see interpretation below). This reflects how accumulated stress in the rock environment is released over time. For example the data clearly show that activity of displacements along the monitored fault was most pronounced up to the end of 2015. From the beginning of 2016, however, this activity significantly decreased and remained subdued until the end of 2024. It should be noted, that the same period of tectonic inactivity was observed also at other monitored sites (Hochmuth et al., 2020).

Characteristics of Measured Components

The data outputs from the TM-71 instrument installed in the Demänovská Cave of Liberty are in the form of time series. The X, Y, and Z components represent the spatial characteristics of the 3D vector of relative movement between blocks along the fault, while XY and XZ denote their mutual rotation in two orthogonal planes.

X-Component of the Movement Vector

The X-component corresponds to horizontal movement in the dip direction of the tectonic fault. Based on the geometry of the instrument's installation, this component indicates the opening or closing of the gap between the measured blocks. According to the trend analysis, the X-component data did not exhibit a statistically significant trend. The curve initially shows a downward trend (fault opening) until the end of 2007, followed by an upward trend until mid-2015 (fault closing). In the years following, the curve stagnates or shows a slight decrease.

The curve is relatively irregular – though this term is used cautiously due to the very low magnitude of changes between readings. The measured values fluctuate around the mean with an average amplitude of 0.02 mm, which is near the detection limit of the instrument. The highest annual displacement in the X direction was recorded in 2004, at only 0.068 mm. The net change over the entire monitoring period is 0.01 mm, with a total range of 0.115 mm.

In such cases, the statistically adjusted average value is more meaningful than individual measurements. Nonetheless, individual readings may be relevant in connection with seismic events, where sudden displacements on the fault may be indicative of specific earthquakes (see: Measurement Interpretation).

Y-Component of the Movement Vector

This component reflects horizontal movement along the fault, where positive values (+Y) indicate sinistral (left-lateral) displacement, and negative values indicate dextral. Based on the MK test, the Y curve demonstrates a statistically significant positive (increasing) trend, with an average annual increment slope $\beta = 0.0035$ mm. However, immediately after installation in August 2001, the trend was negative ($\beta = -0.18$ mm), and it shifted sharply to an increasing trend only at the end of 2002, which persisted until the end of the monitored period. As with the X-component, this curve is characterised by sudden shifts alternating with longer stable periods. The data fluctuate around the mean with a slightly higher amplitude of up to 0.04 mm. The overall range over the full

period is slightly greater (0.24 mm), with the maximum annual displacement reaching 0.158 mm. The net change over the entire period is 0.064 mm.

Z-Component of the Movement Vector

Movement along the Z-axis reflects the vertical component of displacement. If the X-axis points toward the stable block (i.e. the presumed immobile side of the fault) and the +Z axis points downward (as is the case here), positive Z values indicate subsidence of the moving block, while negative values represent uplift or reverse faulting. Like the Y-component, the MK test confirms a statistically significant increasing trend. The full range of measured values spans from –0.186 mm to +0.173 mm.

During the first year of measurement, the Z-component had a similar pattern to the Y-component. An initial downward trend transitioned sharply to an upward trend, which persisted in subsequent years. From April 2015, a gradual stagnation or slight decline was observed. The final value of the Z-component over the full monitoring period is positive at 0.065 mm.

Measurements of rotations

As previously mentioned, the TM-71 instrument can detect rotations – mutual angular displacements between measured blocks in the horizontal (XY) and vertical (XZ) planes. These values are sensitive to stress changes in the rock mass along the fault and may also reflect short-term geodynamic pulses or seismic events.

Although trend analysis confirmed a statistically significant trend in XZ-plane rotations over the entire monitoring period, this indicator has limited spatial relevance since rotational displacement between blocks is not expected to increase indefinitely in one direction. More crucial are short-term changes in trends, which indicate shifts in the mechanics of force and stress distribution within the rock mass. At the Demänovská Cave of Liberty site, several such moments can be identified in the rotation curves. At the end of 2007, a change in trend occurred in both rotation curves, lasting for approximately two years. Afterwards, XY-plane rotations stagnated for four to five years, while XZ-plane rotations showed an increasing trend. In spring 2015, a sudden change in the XZ rotation by 0.2° was recorded, representing a significant shift. No further major changes were observed in the rotation data: the XY rotation curve remained stable, and the XZ curve showed only a slight increase. Total rotation in the horizontal plane did not exceed 0.1°, while in the vertical plane (dip direction of the fault), the range was approximately 0.3° (from –0.15° to +0.15°).

Seismic Events

Despite the lack of historical records of major seismic events in the area, it is assumed that extensive damage to

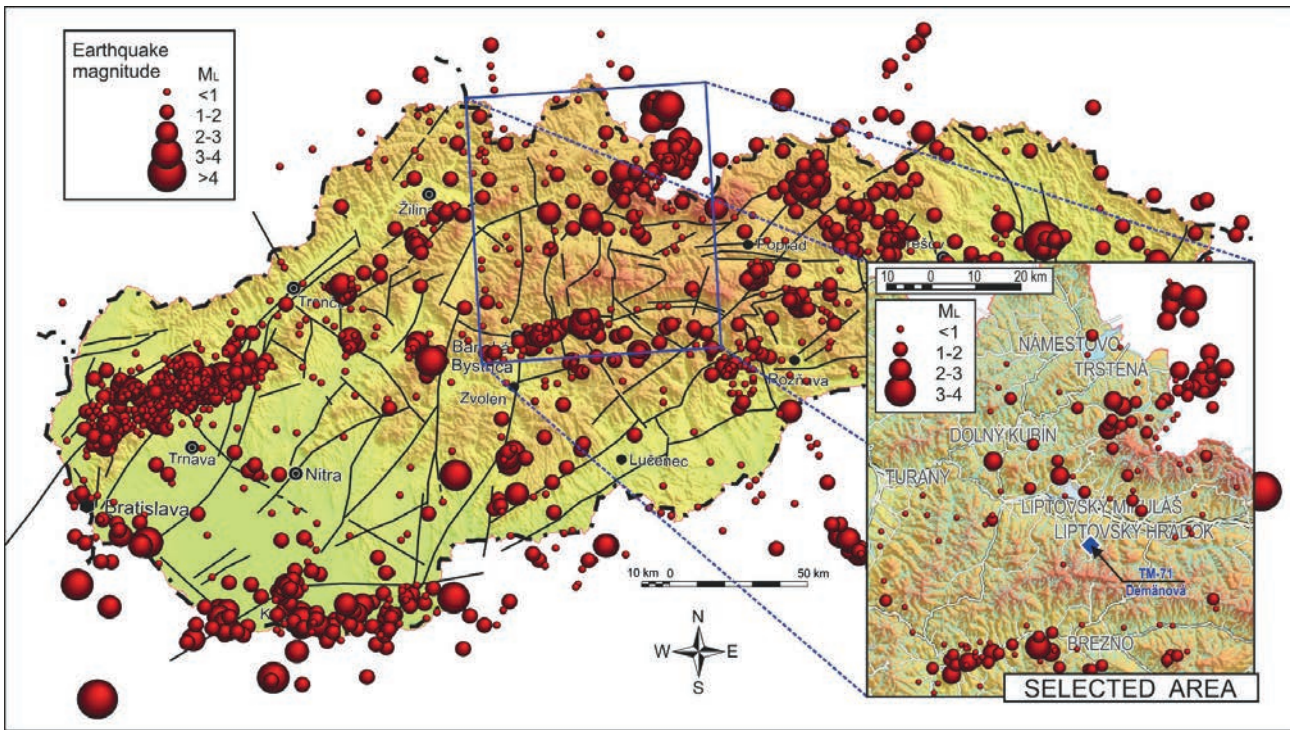

Fig. 11. Observed earthquakes in the territory of Slovakia within the period 2000–2023 with selected ones in the Demänová region (processed using the data from https://dionysos.geology.sk/cmsgf).

Tab. 4

List of seismic events with M_L > 1.5 and epicentral areas in the broader vicinity of Demänová

Date and time of earthquake	Magnitude [M_L]	Epicentre coordinates [X_WGS84 / Y_WGS84]	Epicentral region	Monitoring stage
14 Dec 2002 – 00:27	2.4	49.160 / 19.270	Banská Bystrica and surroundings	A
10 Jan 2004 – 07:43	2.2	48.770 / 19.310	Banská Bystrica and surroundings	B
12 Jun 2004 – 09:59	2.2	48.720 / 19.190	Polish-Slovak border area	B
30 Nov 2004 – 17:18	4.4	49.350 / 19.910	Polish-Slovak border area	B
01 Dec 2004 – 23:25	2.6	49.480 / 19.850	Polish-Slovak border area	B
02 Dec 2004 – 18:25	3.2	49.520 / 19.800	Polish-Slovak border area	B
09 Dec 2004 – 01:09	2.9	49.500 / 19.790	Polish-Slovak border area	B
11 Dec 2004 – 17:25	2.3	49.380 / 19.970	Polish-Slovak border area	B
13 Dec 2004 – 03:29	2.5	49.410 / 19.920	Polish-Slovak border area	B
13 Dec 2004 – 00:05	2.3	49.470 / 19.780	Polish-Slovak border area	B
23 Jan 2005 – 23:33	2.5	49.530 / 19.800	Polish-Slovak border area	B
29 Jan 2005 – 17:16	3.0	49.520 / 19.860	Polish-Slovak border area	B
07 Feb 2005 – 06:08	1.8	49.380 / 19.920	Polish-Slovak border area	B
01 May 2005 – 16:17	1.7	49.200 / 19.930	Polish-Slovak border area	B
02 Jun 2005 – 07:43	2.7	49.370 / 19.830	Polish-Slovak border area	B
07 Jun 2005 – 11:00	2.0	48.780 / 19.490	Brezno and surroundings	B
24 Aug 2005 – 15:46	1.7	49.380 / 19.900	Polish-Slovak border area	B
10 May 2008 – 17:33	1.5	49.310 / 19.790	Orava	C
27 May 2015 – 14:39	1.9	49.110 / 19.560	Liptovský Mikuláš and surroundings	E
03 Nov 2015 – 13:02	3.2	48.790 / 19.450	Brezno and surroundings	E
15 Apr 2017 – 04:12	1.6	48.760 / 19.190	Banská Bystrica and surroundings	E
14 Nov 2018 – 23:16	2.1	49.290 / 19.660	Orava	E
13 Apr 2019 – 04:04	1.6	48.780 / 19.850	Brezno and surroundings	E
15 Sep 2019 – 00:44	2.1	49.300 / 19.630	Orava	E
31 Aug 2020 – 07:50	1.6	48.750 / 19.610	Brezno and surroundings	E
22 Mar 2021 – 17:29	2.1	49.140 / 19.480	Liptovský Mikuláš and surroundings	E
29 Jul 2021 – 07:58	1.9	48.760 / 19.650	Brezno and surroundings	E
13 Oct 2021 – 01:02	1.8	48.810 / 19.450	Brezno and surroundings	E
06 Apr 2022 – 17:04	2.1	48.748 / 19.238	Banská Bystrica and surroundings	E
09 Oct 2023 – 18:23	4.9	49.058 / 21.717	Veľká Domaša	E

speleothems (Fig. 2) was caused by strong earthquakes. Based on the dating of these disruptions and fractures, along with mathematical modelling and other scientific methods, the probable source of the seismic activity was identified as the Sub-Tatra Fault, located approximately 17.5 km from the cave (Szczygieł et al., 2021).

To explore potential links between block displacements and seismic activity at the Demänovská Cave of Liberty, measured TM-71 data were compared with records of seismic events detected by the National Seismic Network of the Earth Science Institute of the Slovak Academy of Sciences (ESI SAS) in Bratislava. During the TM-71 monitoring period, over 1 600 earthquakes of various magnitudes and epicentral locations were recorded across Slovakia and surrounding areas (https://dionysos.geology.sk/cmsgf/). However, none of these events had epicentres located directly in the vicinity of Demänová or along the aforementioned Sub-Tatra Fault (Fig. 11).

To investigate further, approximately 150 seismic events were selected – mostly minor earthquakes with epicentres in the broader vicinity of the monitored site. Several more distant but stronger events were also considered. The local magnitudes (M_L) of these selected earthquakes ranged from nearly undetectable to a maximum of 4.9 (Veľká Domaša – Ďapalovce, October 9, 2023). Table 4 lists selected seismic events with M_L > 1.5, including

their assignment to specific stages of recorded neotectonic activity, showing a similar pattern on the monitored fault.

Synthesis and Interpretation of TM-71 Measurements

The Demänová Valley area, based on available data during the monitoring period, appeared to be seismically quiet, classifying it as an aseismic zone.

As previously mentioned, throughout the entire period of monitoring duration at this site using the TM-71, no earthquake has been recorded with a calculated epicentral area located in the immediate vicinity of the monitored site.

Nonetheless, a certain correlation can be observed between some seismic events with broader epicentral regions and variations in the measured data. Such changes may include, for example, abrupt jumps in one or more curves simultaneously, or reversals in long-term trends, for which no alternative explanation is acceptable. These moments – the instances of change – along with recorded seismic events, form the basis for interpreting the temporal characteristics of neotectonic activity at the measured fault.

Based on the synthesis of all data, the entire monitoring period has been subdivided into shorter temporal segments characterised by consistent or similar expressions across all monitored indicators during each phase. Within the Demänovská Cave of Liberty site, phases A–E were delineated for interpretative purposes (see Fig. 12).

The first interpreted period (A) is temporally bounded by an earthquake in the Orava Basin region (M_L = 2.4) recorded on December 14, 2002. Approximately at this time, a sudden change in trend orientation was observed on the Y- and Z-curves, and a peak at –0.05 degrees was registered on the XY rotation curve. This event may not necessarily relate to tectonic activity; however, it is noteworthy that in the subsequent years, only minimal changes occurred on this curve. The X-component displays a declining trend, which continues – albeit with a slightly altered slope – throughout the subsequent period (B). In contrast, the Y and Z curves show a reversal to a mildly increasing trend at the beginning of phase B, diverging from the development seen in the X-component. Rotations in the horizontal (XY) plane exhibit a slight increasing trend, while those in the vertical (XZ) plane show a subtle decrease.

The entire period until May 2008 can be considered relatively stable, with no significant changes. Seismically, numerous moderate to weak earthquakes were recorded during this phase (Tab. 4), predominantly with epicentres north of the site, some near the Polish-Slovak border. Notably, the earthquake on November 30, 2004 (M_L = 4.4) did not visibly affect the recorded data.

During this period, the activity along the fault can be characterised as a sinistral subsidence of the mobile block accompanied by fault opening, with horizontal block rotation resulting in the crack opening towards the southeast, and vertical rotation contributing to the upward opening of the crack (Fig. 13).

Phase C, by contrast, can be described as a period of increased instability based on the observed data. It began with a moderate earthquake (M_L = 1.5) on May 10, 2008, centred near Orava. From May 2008 to July 2009, significant changes occurred on all curves. The most pronounced ones were in the rotation curves – XY rotations exhibited a rapid increase, rising sixfold in this short interval, while XZ rotations declined sharply, with a decrease of nearly 0.15 degrees. These values suggest modifications in the stress state along the tectonic line. The Z-curve initially decreased, then sharply increased by nearly +0.2 mm, indicating a vertical mutual displacement of the blocks relative to each other by 0.2 mm – a potentially macroscopically observable phenomenon, particularly on stalactite formations.

The X-curve during this phase shows a sharp rise initially (possibly associated with an earthquake, similar to other curves), followed by a relatively steady upward trend that persisted until 2015 without responding to seismic events. This indicates a gradual closing of the crack at approximately 0.01 mm per year – which is a minor value. **The activity during this period can thus be interpreted as a displacement of the moving block (or relative mutual displacement of the blocks to each other) along the fault line with simultaneous closing of the crack, without substantial lateral movement, but coupled with a right-lateral (clockwise) rotation in the horizontal plane and a left-lateral (counterclockwise) rotation vertically.**

Subsequent Period D (July 2009 – April 2015) showed no changes in the prevailing trends of the X and Y curves. The X-component showed a slightly increasing trend, indicating crack closing, while the Y-component remained stable – apart from a sudden sinistral shift of approximately 0.05 mm at the end of the phase. Almost all curves (with the exception of XY rotation) exhibited distinct stepwise displacements in the positive direction at the end of this phase. The Z-component reversed orientation at the beginning of the period, indicating uplift of the block (reverse faulting), and returned to its original value through a sharp shift at the end of the phase.

The most pronounced effects were recorded in the rotation curves. At the beginning of the period, the XZ rotation trend reversed sharply and continued to increase significantly throughout. A sudden increase of nearly 0.2° in the positive direction occurred at the end of the period. The horizontal (XY) rotation curve stagnated at first, but between 2013 and 2014, there was a slight left-lateral

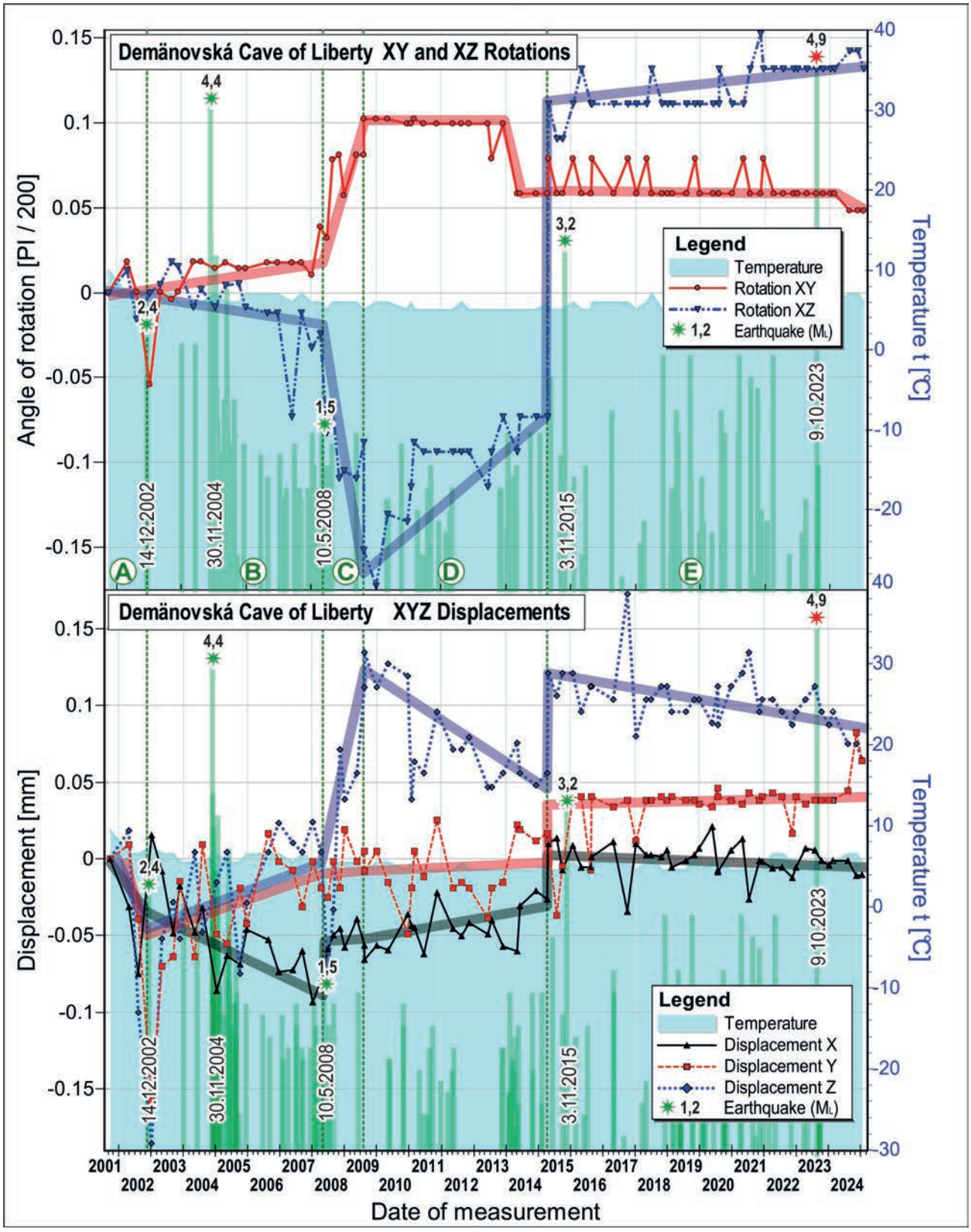

Fig. 12. Displacement records (X, Y, Z) and rotations (XY – horizontal, XZ – vertical) of tectonic blocks detected by the TM-71 extensometer installed inside the Demänovská Cave of Liberty

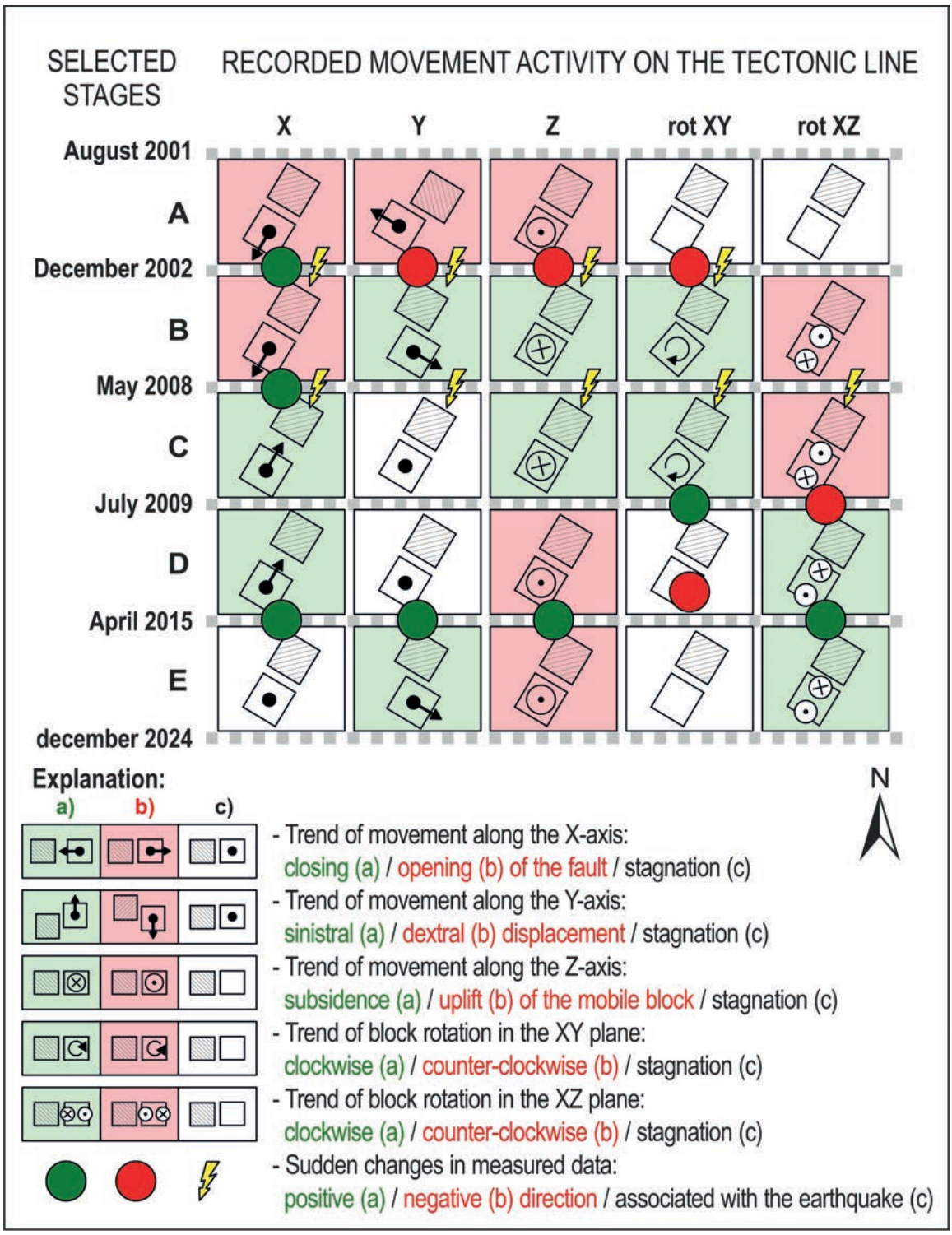

Fig. 13. Overview of neotectonic activity during the individual interpreted phases.

rotation of approximately 0.05°, followed by continued stagnation until the end of the observation period. **The overall movement in this phase can be characterised as uplift of the mobile block accompanied by crack closing, with no significant lateral movement, and vertical rotation toward the crack (closing of the upper part of the crack, opening of the lower part).**

Final Period E (April 2015 – December 2024) was markedly more stable. This entire interval may be characterised as stable, without significant changes. Most curves show stagnation or only slight decreasing (Z) or increasing (Y and XZ) trends. Early in this period (3 November 2015), a stronger earthquake was recorded near Brezno, which may correlate with a change in the Y-curve – namely, a sinistral shift of about 0.05 mm, after which the curve remained notably stable until the present.

A strong earthquake (M_L = 4.9) recorded near Veľká Domaša (Ďapalovce) on October 9, 2023 did not produce any observable response in the data (Fig. 12). **The movements observed in this period are characterised by uplift, sinistral shift, and vertical rotation toward the crack (closing of the upper side, opening of the lower side).**

Summary of Results

Based on the measured data, neotectonic activity along fault structures in the Demänovská Cave of Liberty is not particularly intense, but it is nonetheless present and, under the given conditions, measurable. It is important to emphasise that the displacements are very small – close to the detection threshold of the extensometer – and that the data would likely be unreliable in less stable climatic conditions. Therefore, it is concluded that the threat to human safety in this location from neotectonic activity is considered minimal.

From the perspective of the nature of monitored movements along the tectonic line, it can be concluded that displacements are generally not continuous but more often occur in sudden jumps and may sometimes be associated with seismic events. Moreover, the direction of movement does not necessarily correspond to the long-term trend and may exhibit oscillations around a mean value (i.e., periodic shifts in movement direction). During the monitoring period, several changes were observed that served as the basis for dividing the data into temporal segments A–E, within which the character of the recorded data related to neotectonic activity remains consistent (Fig.12). The periods showing the most pronounced manifestations of neotectonic activity in the character of the recorded curves at the Demänovská Cave of Liberty site are Phase C and the short interval between Phases D and E. Interestingly, neither of these episodes appears to be associated with any seismic event.

Szczygieł et al. (2021) interpreted numerous broken and fallen dripstones and flowstones in the Čarovná chodba Passage as the result of oscillation accompanying fault reactivation. The healed speleothems observed in the fractured deformation of older speleothems, especially columns and flowstones, are undoubtedly associated with ancient seismotectonic activity (Sala et al., 2022).

Acknowledgements

The authors would like to express their thanks to EC and the Ministry of Environment of the Slovak Republic for funding several scientifically contributing geological and tectonic projects, including the project entitled *Monitoring System of the Environment of the Slovak Republic – Partial Monitoring System – Geological Factors*.

References

Bada, G., 1999: Cenozoic stress field evolution in the Pannonian Basin and surronding orogens. Academisch proefschrift. *Vrije Universiteit Amsterdam*, 1 – 187.

Bella, P., Haviarová, D., Kováč, Ľ., Lalkovič, M., Sabol, M., Soják, M., Struhár, V., Višňovská, Z. & Zelenka, J., 2014: Jaskyne Demänovskej doliny. *Liptovský Mikuláš, ŠOP SR, SSJ,* 200 pp.

Bella, P., 2016: Multi-levelled cave system and associated morphological segments in the contact middle-mountain karst: the case study from the Demänová Caves, the Nízke Tatry Mts. *Geomorphica Slovaca et Bohemica*, 16, 1, 13 p.

Bezák, V., Broska, I., Ivanička, J., Reichwalder, P., Vozár, J., Polák, M., Havrila, M., Mello, J., Biely, A., Plašienka, D., Konečný, V., Lexa, J., Kaličiak, M., Žec, B., Vass, D., Elečko, M., Janočko, J., Pereszlényi, M., Marko, F., Maglay, J. & Pristaš, J., 2004: Tectonic Map of Slovak Republic 1 : 50 000. *Bratislava, Ministry of Environment of the Slovak Republic – State Geological Institute of Dionýz* Štúr.

Biely, A., Bezák, V., Bujnovský, A., Vozárová, A., Klinec, A., Miko, O., Halouzka, R., Vozár, J., Beňuška, P., Hanzel, V., Kubeš, P., Liščák, P., Lukáčik, E., Maglay, J., Molák, B., Pulec, M., Putiš, M. & Slavkay, M., 1997: Explanation to the geological map of the Nízke Tatry Mountains 1 : 50 000. *Bratislava, GS SR, Dionýz Štúr Publisher.*

BIPM, IEC, IFCC, ISO, IUPAC, IUPAP, OIML, 2008: Evaluation of measurement data – Guide to the expression of uncertainty in measurement (GUM 1995 with minor corrections). JCGM 100. *Joint Committee for Guides in Metrology*, 120 p.

Briestenský, M., Stemberk, J. & Petro, Ľ., 2007: Displacements registered around March 13, 2006 Vrbové earthquake, M=3.2 (Western Carpathians). *Geologica Carpathica*, 58, 487–493.

Briestenský, M., Košťák, B., Stemberk, J., Petro, L., Vozár, J. & Fojtíková, L., 2010: Active tectonic fault microdisplacement analyses: a comparison of results from surface and underground monitoring in western Slovakia. *Acta Geodynamica et Geomaterialia*, 7, 4 (160), 387–397.

Briestenský, M., Košťák, B., Stemberk, J. & Vozár, J., 2011: Long-term slope deformation monitoring in the high

mountains of the Western Carpathians. *Acta Geodynamica et Geomaterialia*, 8, 4 (164), 403–412.

Briestenský, M., Hochmuth, Z., Littva, J., Hók, J., Dobrovič, R., Stemberk, J., Petro, Ľ. & Bella, P., 2018: Present-day stress orientation and tectonic pulses registered in the caves of the Slovenský kras Mts. (South-Eastern Slovakia). *Acta Geodynamica et Geomaterialia*, 15, 2, 93–103. https://doi.org/ 10.13168/AGG.2018.0007.

Slovak speleological society, 2025: The list of the longest caves in Slovakia as of March 10, 2025. *Bulletin of the Slovak Speleological Society*, 56, 1, 110.

Droppa, A., 1957: Demänovské Caves, Karst Landforms of the Demänová Valley. *Bratislava, Slovak Academy of Sciences*, 289 pp. (in Slovak with Russian and German Summary).

Droppa, A., 1972: Geomorfologické pomery Demänovskej doliny. *Slovenský kras*, 10, 9–46.

Hochmuth, Z., Briestenský, M., Zacharov, M., Stemberk, J., Petro, Ľ., Littva, J., Bella, P., Gaál, Ľ., Hraško, Ľ. & Stankovič, J., 2020: Monitoring mikropohybov v jaskyniach Slovenského a Ochtinského krasu [Microdisplacements monitoring in the caves of Slovak and Ochtiná karsts]. *Slovenský kras*, 58, 2, 169–180.

Hók, J., Bielik, M., Kováč, P. & Šujan, M., 2000: Neotectonic character of Slovakia (in Slovak with English summary). *Mineralia Slovaca*, 32, 459–470.

Jánová, V., Liščák, P. (eds.), Kopecký, M., Bednarik, M., Šimeková, J., Ondrášik, M., Pauditš, P., Tupý, P., Petro, Ľ., Ondrejka, P., Greif, V. & Ondrus, P., 2021: Zosuvy na Slovensku. *Banská Bystrica, Slovenská agentúra životného prostredia*, 166–169.

Košťák, B., 1969: A new device for in-situ movement detection and measurement. Experimental Mechanics. *SESA (American Society for Experimental Stress Analysis) Journal*, 9, 374–379.

Maglay, J., Halouzka, R., Baňacký, V., Pristaš, J. & Janočko, J., 1999: Neotektonická mapa Slovenska. *Bratislava, Ministerstvo životného prostredia SR, GS SR.*

Mann, H. B, 1945: Nonparametric tests against trend. Econometrica. *Econometrica*, 13, 245–259.

Ondrejka, P., Wagner, P., Petro, Ľ., Žilka, A., Balík, D., Iglárová, Ľ. & Fraštia, M., 2014: Main results of the slope deformations monitoring. *Slovak Geological Magazine*, 14, 89–114.

Ondrus, P. (ed.), 2025: Čiastkový monitorovací systém [online]. *Bratislava, Štátny geologický ústav Dionýza Štúra.* Available online: https://dionysos.geology.sk/cmsgf/.

Petro, Ľ., Košťák, B., Polaščinová, E. & Spišák, Z., 1999. Block movements monitoring in the Slanské vrchy Mts. (Eastern Slovakia). *Mineralia Slovaca*, 31, 549–554 (in Slovak with English summary).

Petro, Ľ., Vlčko, J., Ondrášik, R. & Polaščinová, E., 2004a: Recent tectonics and slope failures in the Western Carpathians. *Engineering Geology*, 74, 103–112.

Petro, Ľ., Bella, P., Polaščinová, E., Hók, J. & Stercz, M., 2004b: Monitoring of tectonic movements in the Demänovská Cave of Liberty. *Aragonit*, 9, 26–29 (in Slovak with English Summary).

Petro, Ľ., Košťák, B., Stemberk, J. & Vlčko, J., 2011a: Geodynamic reactions to recent tectonic events observed on selected sites monitored in Slovakia. *Acta Geodynamica et Geomaterialia*, 8, 4 (164), 453–467.

Petro, Ľ., Bóna, J., Kováčik, M., Fussgänger, E., Antonická, B. & Imrich, P., 2011b: The Cave under the Spišská hill: Preliminary results of the block movements. *Mineralia Slovaca*, 43, 121–128.

Petro, Ľ., Brček, M., Vlčko, J., Šimková, I., Balík, D. & Žilka, A., 2012: Stability of selected historical objects in Slovakia: Monitoring results. *Mineralia Slovaca*, 44, 403–422 (in Slovak with English summary).

Piccardi, L. (ed.), 2006: 625 – 3-D Monitoring of Active Tectonic Structure. *Brussels, COST.* Available online: https://www.cost.eu/actions/625/.

Pokorný, M., 1952: Vznik a vývoj starších prostor jeskyň Demänovských. *Časopis Moravského musea v Brně*, 37, 13–51 (in Czech with English summary).

Rowberry, M. D., Kriegner, D., Holy, V., Frontera, C., Llull, M., Olejnik, K. & Marti, X., 2016: The instrumental resolution of a moiré extensometer in light of its recent automatisation. *Measurement*, 90, 237–243. https://doi.org/10.1016/j.measurement.2016.05.048.

Sala, P., Bella, P., Szczygieł, J., Wróblewski, W. & Gradziński, M., 2022: Healed speleothems: A possible indicator of seismotectonic activity in karst areas. *Sedimentary Geology*, 430, 106105. https://doi.org/10.1016/j.sedgeo.2022.106105.

Sasvári, Á. & Baharev, A., 2014: SG2PS (Structural Geology to Post Script Converter) – A graphical solution for brittle structural data evaluation and paleostress calculation. *Computers & Geosciences*, 66, 81–93.

Sen, P. K., 1968: Estimates of the Regression Coefficient Based on Kendall's Tau. *Journal of the American Statistical Association*, 63, 324, 1379–1389.

Stercz, M., 2021: MSDilat V3.1 – application for computer processing of the TM-71 3D measurements. *Prepared by M. Stercz in Delphi language for MS Windows platform.*

Stercz, M., Grega, D., Petro, Ľ., Hók, J., Németh, Z., Stemberk, J. & Bednarik, M., 2025: 3D Long-Term Monitoring of Recent Tectonic Activity in the Branisko Tunnel (Eastern Slovakia). *Geologica Carpathica*, 76, 1, 55–67. https://doi.org/10.31577/GeolCarp.2025.04.

Szczygieł, J., Gradziński, M., Bella, P., Hercman, H., Littva, J., Mendecki, M., Sala, P. & Wroblewski, W., 2021: Quaternary faulting in the Western Carpathians: Insights into paleoseismology from cave deformations and damaged speleothems (Demänová Cave System, Low Tatra Mts). *Tectonophysics*, 820, 229111. https://doi.org/10.1016/j.tecto. 2021.229111.

Vlcko, J. & Petro, L., 2002. Monitoring of subgrade movements beneath historic structures. In: Van Roy, J. L. & Jermy, C. A. (Eds.): *Proc. of 9th Inter. Congress IAEG*, *Durban, South Africa*, 1432–1437.

Wagner, P., Iglárová, Ľ. & Petro, Ľ., 2000: Methodology and some results of slope movement monitoring in Slovakia. *Mineralia Slovaca*, 32, 359–367.

Dlhodobé 3D monitorovanie recentnej tektonickej aktivity v Demänovskej jaskyni Slobody

Práca sa zaoberá analýzou údajov takmer 24-ročného monitorovania tektonických pohybov pozdĺž neotektonickej poruchy v Demänovskej jaskyni Slobody. Posuny a rotácie na poruche boli merané pomocou mechanicko-optického 3D extenzometra TM-71. Výsledky meraní podrobené štatistickej analýze ukázali trend v dvoch zložkách priestorového vektora pohybu – vo vertikálnej (Z) a v horizontálnej (Y), ktorá je kolmá na smer sklonu zlomu. Nedávna aktivita pozdĺž zlomu odráža pôsobenie recentného napäťového poľa a seizmickú aktivitu v rámci Západných Karpát. Štúdia skúma aj vzťah medzi pohybmi zaznamenanými TM-71 a seizmickými udalosťami v širšom okolí jaskyne.

Na základe nameraných údajov je neotektonická aktivita pozdĺž zlomových štruktúr v Demänovskej jaskyni Slobody nízka, ale za daných podmienok merateľná. Posuny sú veľmi malé, blízko detekčnej hranice extenzometra. V menej stabilných klimatických podmienkach by údaje pravdepodobne neboli spoľahlivé. Zistená neotektonická aktivita nepredstavuje žiadne riziko z hľadiska bezpečnosti jaskynných priestorov.

Z hľadiska povahy monitorovaných pohybov pozdĺž tektonickej línie možno konštatovať, že posuny vo všeobecnosti nie sú kontinuálne, ale častejšie sa vyskytujú v náhlych skokoch a niekedy môžu súvisieť so seizmickými udalosťami. Navyše, smer pohybu nemusí nevyhnutne zodpovedať dlhodobému trendu a môže vykazovať oscilácie okolo strednej hodnoty (t. j. periodické posuny v smere pohybu).

Počas monitorovacieho obdobia bolo pozorovaných niekoľko zmien, ktoré slúžili ako základ na rozdelenie údajov do časových segmentov A – E. V rámci nich charakter zaznamenaných údajov týkajúcich sa neotektonickej aktivity zostáva konzistentný (obr. 12). Obdobia s najvýraznejšími prejavmi neotektonickej aktivity v charakteristike zaznamenaných kriviek v Demänovskej jaskyni Slobody sú fáza C a krátky interval medzi fázami D a E. Nezdá sa, že by niektorá z týchto epizód bola spojená so seizmickou udalosťou.

Doručené / Recieved: 18. 6. 2025
Prijaté na publikovanie / Accepted: 1. 9. 2025

Mineralia Slovaca, Web ISSN 1338-3523, ISSN 0369-2086, https://doi.org/10.56623/ms.2025.57.1.4
57, 1 (2025), 59 – 80, © Authors 2025. CC BY 4.0

Santonian-Campanian marly and biodetritic facies in the Púchov Formation in the Orava sector of the Pieniny Klippen Belt (Slovakia)

ONDREJ PELECH[1], ŠTEFAN JÓZSA[2] and MÁRIO OLŠAVSKÝ[3]

[1]State Geological Institute of Dionýz Štúr, Mlynská dolina 1, SK-81704, Bratislava 1, Slovak Republic; ondrej.pelech@geology.sk
[2]Comenius University, Faculty of Natural Sciences, Department of Geology and Paleontology, Ilkovičova 6, SK-84215, Bratislava, Slovak Republic
[3]State Geological Institute of Dionýz Štúr, Zelená 5, SK-97404, Banská Bystrica, Slovak Republic

Abstract: The Pieniny Klippen Belt is characterized by the block-in-matrix fabric with Jurassic to Lower Cretaceous rigid klippen embedded in less competent Upper Cretaceous flysch and marlstone matrix. The studied area is located in the Orava sector of the Pieniny Klippen Belt. Based on results of recent geological mapping and biostratigraphic analysis, the paper distinguishes a new formal lithostratigraphic unit – the Kňažia Member/Beds composed dominantly of white marly limestone, with lenses of biodetritic limestone, calcarenite to conglomerate of the Bradlo-type limestone. The new member occurs at several localities along the studied Orava sector of the Pieniny Klippen Belt, with the largest volumes north of Dolný Kubín (Opálené Hill) and Podbiel (Lučivný vrch Hill). Both lithostratigraphic units contain relatively abundant planktonic foraminifera co-occurring in the middle Campanian Contusotruncana plummerae Zone. The interbedding biodetritic limestones correlated with the Bradlo-type limestone are rich in *Pseudosiderolites* spp. and contain Santonian–Campanian rudists. The Kňažia Member represents the lower part of the pelagic basinal sediments within the Upper Cretaceous Púchov Formation. The occasional bodies of allodapic calcarenites of the Bradlo-type limestone represent channel fills composed of shallow water carbonate detritus.

Key words: Upper Cretaceous, geological mapping, foraminifera, microfacies, Kňažia Member, Bradlo-type limestone

Graphical abstract

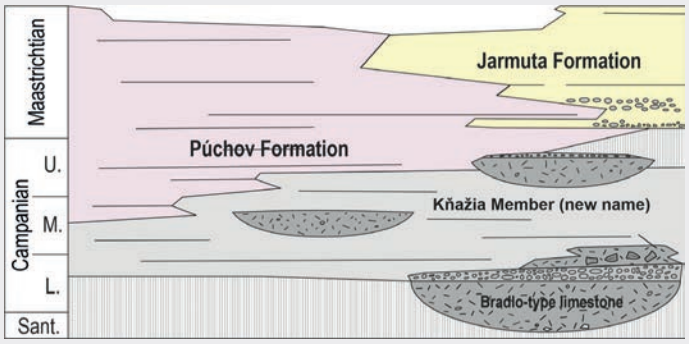

Highlights

- Occurrence of upper Santonian-Campanian white marly limestone and biodetritic limestone within the Púchov Formation is documented in the Orava sector of the Pieniny Klippen Belt
- The white marly limestones – wackestones (planktonic foraminiferal biomicrites) are herein defined as the Kňažia Member (new name)
- The grey packstones to grainstones (calcarenites to microconglomerates or breccia) formerly known as the "Lučivný vrch facies" are correlated with the Bradlo Limestone

Introduction

The Pieniny Klippen Belt (PKB) is a long and narrow lithotectonic unit forming boundary of Cenozoic accretionary wedge of the Carpathian Flysch Belt in the North and Internal Western Carpathian orogenic zones formed by the Tatric, Fatric and Hronic units in the South (Andrusov, 1938; Birkenmajer, 1986; Mišík, 1997; Lexa et al., 2000; Bezák et al., 2008, 2009; Plašienka, 2018a, b). The geological structure of the PKB is characterized by the block-in-matrix fabric, represented by rigid Jurassic or Lower Cretaceous limestone klippen tens of meters to kilometre large, surrounded by less competent Cretaceous flysch and marlstones (often referred to as "klippen cover"). The Jurassic to Cretaceous klippen are divided based on the lithofacial character into several contrasting successions, namely the shallow water Czorzstyn succession and the deep-water Kysuca-Pieniny succession (Andrusov, 1938, 1959).

The studied area is located in the Orava sector of the PKB (Fig. 1A). From the northern side the PKB rocks are bounded by the Magura Group of Nappes and from the south by the rocks of the Central Carpathian Paleogene Basin. The studied area is largely composed of Upper Cretaceous "klippen cover", mostly consisting of the Turonian Snežnica Formation and Coniacian–Santonian Sromowce Formation reaching thickness 100–500 m. Both formations are represented by grey quartz-carbonate flysch with interbedded conglomerate bodies. The conglomerates locally acquire thickness up to 100 m (e.g., Marschalko & Samuel, 1978; Marschalko, 1986). Due to similar lithology and deformation in the PKB mélange, it is usually not possible to distinguish between the Snežnica and Sromowce formations without biostratigraphic knowledge, therefore they are treated together in this paper.

The "klippen cover" formations contain scattered limestone klippen belonging mainly to the Kysuca and Orava/Podbiel successions. The oldest rocks are represented by Lower Jurassic quartz sandstones of "Gresten Beds" recently named as Dutkov vrch Formation (Plašienka et al., 2021). Their continuity to the younger parts of the sedimentary sequence is unclear. The only larger klippe with continual sedimentary succession from Lower Jurassic to Cretaceous is the Červená skala Hill near Podbiel village (Fig. 1C; Haško, 1978; Borza et al., 1993). The basal part of the sedimentary sequence is composed of the Sinemurian–Pliensbachian spotted marlstone and limestone of the Allgäu Formation and Kozinec Beds, Toarcian (lower) red nodular limestone; and grey, red and green radiolarites of the Czajakowa Formation of Oxfordian–Kimmeridgian age. The middle part is represented by the Czorsztyn Formation – (upper) red nodular limestones of the Kimmeridgian–Tithonian age and the Tithonian–Barremian grey and white calpionellid and nannoconid limestones of the Pieniny Formation. The upper portion of the Pieniny Fm. gradually passes into the Aptian–Albian grey shales and siltstones of the Koňhora or Kapuśnica Formation, which is followed by the Maastrichtian flysch, an analogy of the Jarmuta Formation.

Unlike the aforementioned klippe which is the typical representative of the Orava/Podbiel succession; the prevailing klippen are composed of the Kysuca succession that differs by the presence of grey shales and spotted limestones of Posidonia (Harcygrund) and Supraposidonia (Podzamcze) formations of Aalenian–Callovian age (e.g., Andrusov, 1931a, b; Gross et al., 1993).

The Czorsztyn succession is preserved only locally, especially on the northern margin of the PKB. It is represented mainly by the Upper Cretaceous pink pelagic marlstones and limestones of the Púchov Formation with small klippen of red nodular limestones of Upper Jurassic Czorsztyn Formation.

Separate type of sequence is represented by the Upper Cretaceous Pavláškova skala Formation developed in sandstone and variegated facies, often associated with Jarmuta and Proč fms. (Andrusov, 1938; Bezák et al., 2009; Teťák et al., 2025), which can be correlated with Šariš succession (e.g., Plašienka et al., 2012; Plašienka et al., 2021, however with certain differences compared to the cited works). It should be noted that both formations have nearly identical lithology and differ only in age, as the Jarmuta Fm. is Maastrichtian while the Proč Fm. is Paleocene–early Eocene. Therefore, both formations are not separated in this work.

The main aim of this paper is to describe in more detail the peculiar lithofacies of the Púchov Fm. present in the studied area, especially in the area between Dolný Kubín town and Oravský Podzámok – Široká settlement and in the area of the Lučivný vrch Hill (841 m a.s.l.) north of Podbiel village. The particularly important sections are summarized in the Tab. 1 and Fig. 1.

Overview of previous research

The Late Cretaceous lithofacies of the PKB are usually divided into the siliciclastic sandy turbidites and conglomerates (Snežnica and Sromowce fms.) and variegated pelagic marlstones (Púchov Fm.), probably representing the paleotopographic heights without coarser siliciclastic input, usually unaffected by mass wasting processes (Marschalko, 1986).

The term Púchov Beds or Púchov Marlstone was originally introduced in the PKB in the Middle Váh Valley area for red and grey marlstones of Late Cretaceous age (Stur, 1860, p. 115). It is a typical representant of the "couches rouges" facies, also known as Cretaceous Oceanic Red Beds (CORB, Hu et al., 2006). Today, however, the pink marlstones do not crop out in the Púchov town; and in the wider area (Vieska, Dohňany and Ihrište), several types of Cretaceous red marlstones with different stratigraphic age were defined (Kantorová & Andrusov, 1958; Andrusov, 1959; Andrusov & Scheibner, 1960; Salaj, 1990; Mello et al., 2011). Moreover, several other names for the Cretaceous red and variegated marlstones were defined in the PKB (Albian Chmielowa Beds, Turonian Kysuca Beds, Cenomanian Lalinok Beds, Campanian–Maastrichtian Gbeľany Beds; Cenomanian–Campanian Jaworki Fm. etc., see Birkenmajer, 1977; Haško & Polák, 1978, 1979; Gross et al., 1993; Potfaj, 1993; Stráník et al., 1995; Bezák et al., 2009; Plašienka et al., 2012, 2021). Some of aforementioned terms overlap, or are used for the same rocks of the same age but in different tectonic units and are likely to require revision in the future.

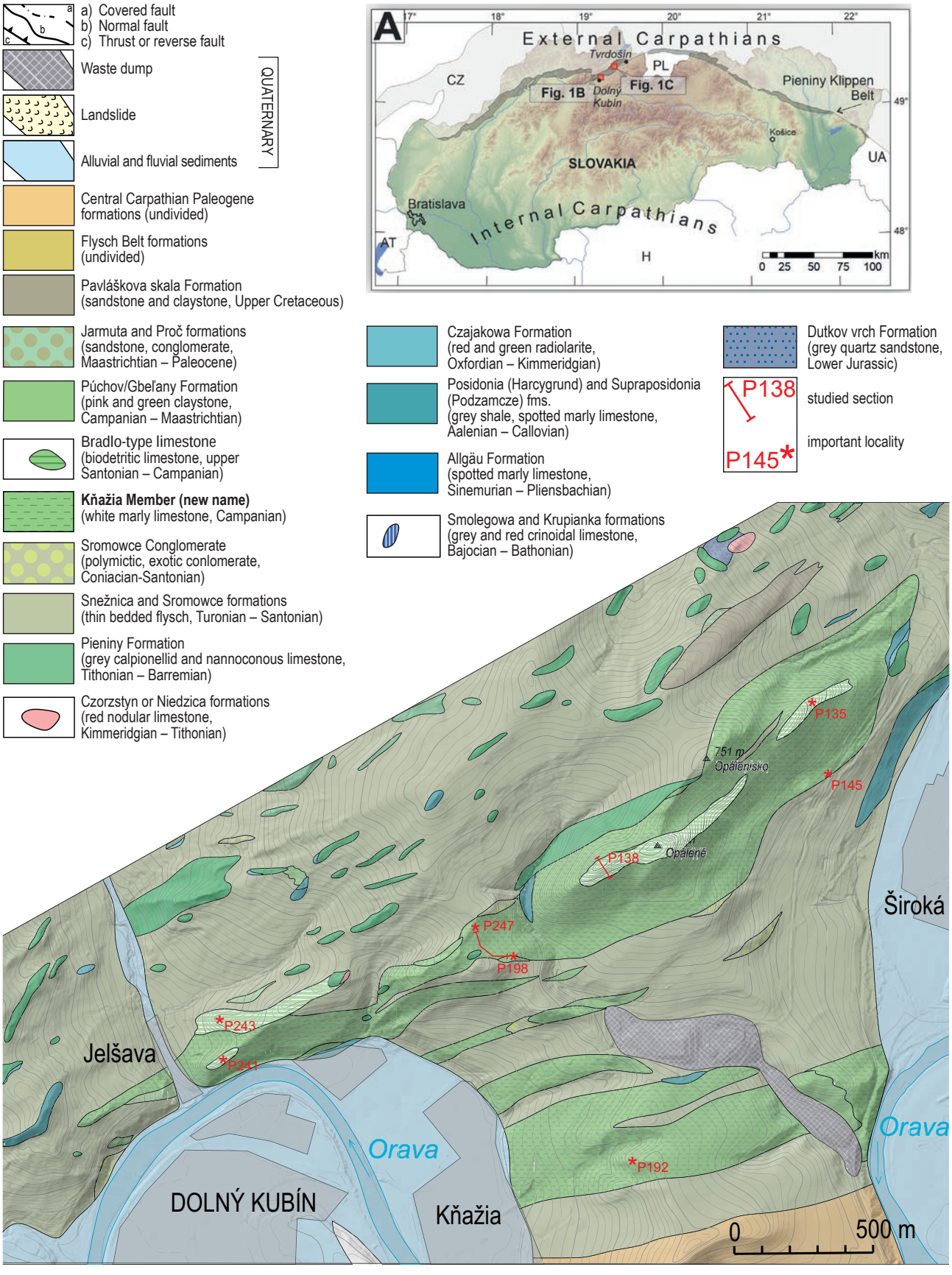
a) Covered fault
b) Normal fault
c) Thrust or reverse fault
QUATERNARY
Waste dump
Landslide
Alluvial and fluvial sediments
Central Carpathian Paleogene formations (undivided)
Flysch Belt formations (undivided)
Pavláškova skala Formation (sandstone and claystone, Upper Cretaceous)
Jarmuta and Proč formations (sandstone, conglomerate, Maastrichtian – Paleocene)
Púchov/Gbeľany Formation (pink and green claystone, Campanian – Maastrichtian)
Bradlo-type limestone (biodetritic limestone, upper Santonian – Campanian)
Kňažia Member (new name) (white marly limestone, Campanian)
Sromowce Conglomerate (polymictic, exotic conlomerate, Coniacian-Santonian)
Snežnica and Sromowce formations (thin bedded flysch, Turonian – Santonian)
Pieniny Formation (grey calpionellid and nannoconous limestone, Tithonian – Barremian)
Czorzstyn or Niedzica formations (red nodular limestone, Kimmeridgian – Tithonian)
A
External Carpathians
Tvrdošín
PL
CZ
Fig. 1B
Dolný Kubín
Fig. 1C
Pieniny Klippen Belt
Košice
SLOVAKIA
UA
Bratislava
Internal Carpathians
AT
H
km
0 25 50 75 100
17° 18° 19° 20° 21° 22°
49°
48°
Czajakowa Formation (red and green radiolarite, Oxfordian – Kimmeridgian)
Posidonia (Harcygrund) and Supraposidonia (Podzamcze) fms. (grey shale, spotted marly limestone, Aalenian – Callovian)
Allgäu Formation (spotted marly limestone, Sinemurian – Pliensbachian)
Smolegowa and Krupianka formations (grey and red crinoidal limestone, Bajocian – Bathonian)
Dutkov vrch Formation (grey quartz sandstone, Lower Jurassic)
P138
studied section
P145*
important locality
P135
751 m
Opálenisko
P145
Opálené
P138
P247
P198
Široká
P243
Jelšava
P241
Orava
P192
Orava
DOLNÝ KUBÍN
Kňažia
0
500 m

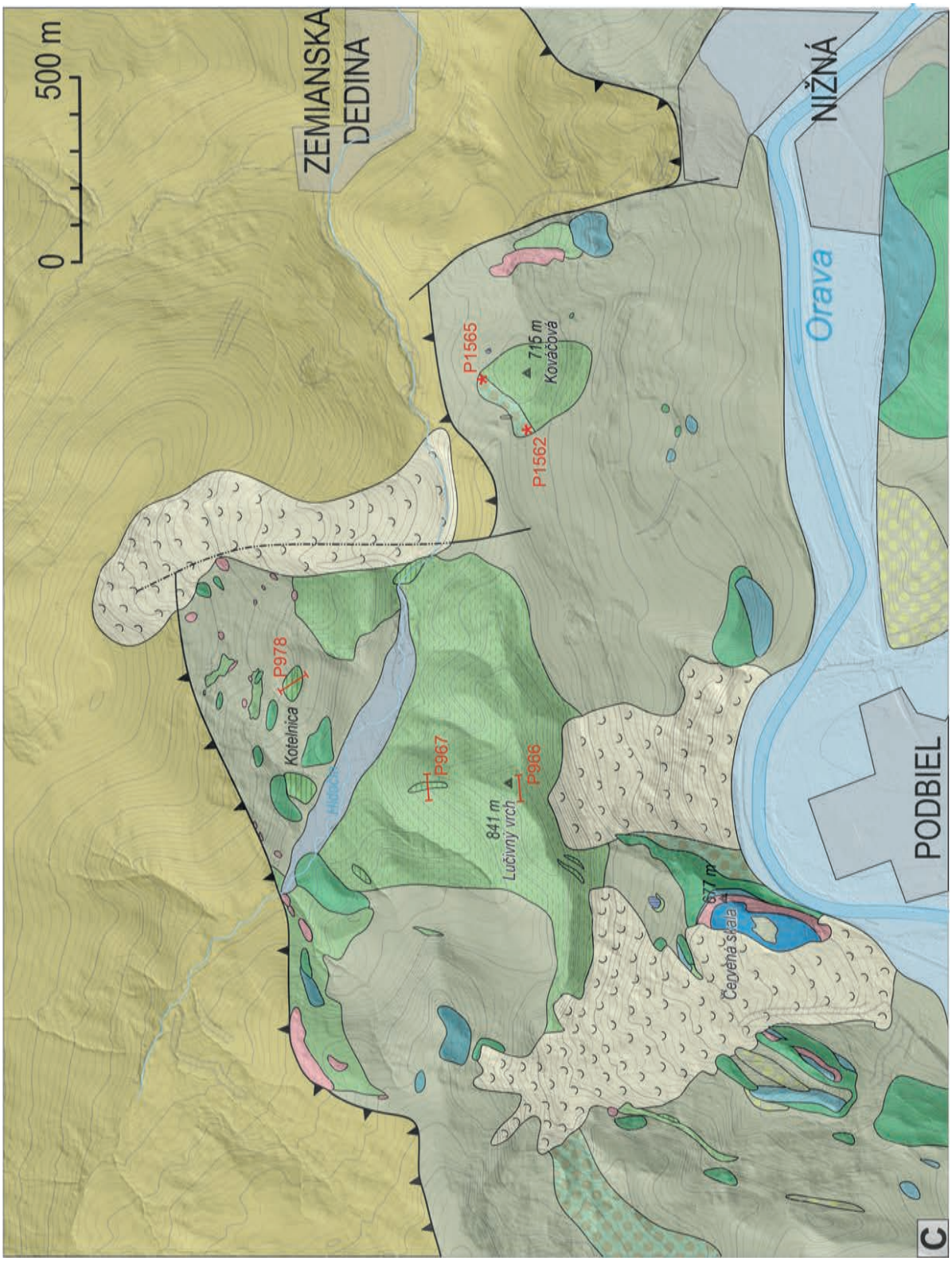

Fig. 1. A – Location of studied area. B – Geological map of the Opálené Hill surroundings, north of the Dolný Kubín town. C – Geological map of the Lučivný vrch Hill surroundings, north of the Podbiel village. Geological maps based on Andrusov (1931a, b) and Teťák et al. (2024, 2025).

Tab. 1

Description and location of main localities and important sections with studied samples or description in the text

Number	Description	Locality	WGS X (N) [°]	WGS Y (E) [°]
P135	Outcrops of marly limestone and calcarenite in the ridge (Kňažia Mb.)	NE ridge of Opálenisko Hill	49.250263	19.332689
P138	Outcrop of calcarenite between the white marly limestones (Kňažia Mb.)	W Ridge of Opálené Hill	49.246311	19.325987
P145	Debris in the slope under power lines (Kňažia Mb.)	W of Široká (Oravský Podzámok)	49.248277	19.334142
P192	Debris of white marly limestone (Kňažia Mb.)	Ridge N of Kňažia	49.2362447	19.3256996
P198	Outcrop white marly limestone (Kňažia Mb.)	Road cut NW of Kňažia	49.2424821	19.3194897
P241	Outcrop of calcarenite between the white marly limestones (Kňažia Mb.)	Ridge E of Jelšava	49.239117	19.3057518
P243	Outcrop of calcarenite between the white marly limestones (Kňažia Mb.)	Ridge E of Jelšava	49.240412	19.305832
P247	Outcrop white marly limestone (Kňažia Mb.)	Road cut NW of Kňažia	49.2434883	19.3176626
P529	Outcrop of pink marlsotne (Púchov Fm.)	Ridge N of Horná Lehota	49.2811111	19.4070028
P564	Outcrop of white marly limestone (Kňažia Mb.)	Riedky diel ridge NW of Malý Bysterec	49.216861	19.258994
P579	Outcrop of calcarenite and white marly limestone (Kňažia Mb.)	Slope above cemetery near Beňova Lehota	49.2334951	19.2603735
P785	Outcrop of calcarenite within the white marly limestones (Kňažia Mb.)	N of Červená skala	49.3170011	19.4822077
P789	Outcrop of calcarenite (Bradlo-type limestone) with intraclasts of red Púchov-type marlstone	Lučivný vrch Hill	49.3172842	19.477742
P792	Debris of calcarenites and white marly limestones (Kňažia Mb.)	Lučivný vrch Hill	49.3174840	19.4762231
P819	Outcrop of calcarenite (Bradlo-type limestone)	Vyšné skalky, N of Podbiel	49.3144436	19.4725977
P966	Forest road cut with white marly limestone and calcarenite interbeds (Kňažia Mb.)	Lučivný vrch Hill	49.3186335	19.4855090
P967	Calcarenite body between the marly limestones (Kňažia Mb.)	Ridge N of Lučivný vrch Hill	49.3209594	19.4858471
P978	Calcarenite with rudists (Bradlo-type limestone) and exotic conglomerate	N slope of Hldočín	49.3247027	19.4897558
P1067	Calcarenite (Bradlo-type limestone) with exotic conglomerate	Cut of Oravica river	49.3597029	19.6341564
P1087	Debris of white marly limestone (Kňažia Mb.)	W of Trstená collective farm	49.3525679	19.6065869
P1101	Debris of white marly limestone (Kňažia Mb.)	Cut of Zábiedovčík brook, SE of Tvrdošín	49.3476157	19.5898878
P1373	Debris red Púchov-type marlstones, white marly limestone (Kňažia Mb.), calcarenite and conglomerates	Repiská, elevation point 730 m a.s.l.	49.2390682	19.2740471
P1562	Outcrop of calcareous sandstones, Jarmuta Fm.	Road cut S of Kováčová Hill	49.3183562	19.5006571
P1565	Debris of carbonate conglomerate to breccia, with Pieniny Fm. radiolarian limestone clasts, Jarmuta Fm.	NW slope of Kováčová Hill	49.3195973	19.5024442
P1653	Outcorp of Bradlo-type limestone calcarenite with exotic conglomerate	E of elevation point 675 m a. s. l. (Dolný Kubín-Veľký Bysterec)	49.2342132	19.2799016

The studied rock complexes of the Upper Cretaceous variegated marls with thin sandstone interbeds were originally imaged on the pre-World War II 1:25 000 geological map of the studied region as "*upper Senonian of the Klippen belt (Púchov Beds)*" [Czech: "*svrchní senon útesového pásma (púchovské vrstvy)*]" (Andrusov, 1931a, b, 1938). The Santonian–Campanian biodetritic limestone with shallow water rudist macrofauna accompanying the exotic conglomerates was documented in the area West of Zemianska Dedina (Kühn & Andrusov, 1942; Andrusov, 1959). Later an inconspicuous map showed bodies of "*organodetritic limestones of the Gbeľany Beds*" in the area of the Opálené Hill north of the Dolný Kubín town and documented Late Cretaceous resedimentation (Marschalko et al., 1979). A brief description of "*a facies of variegated Púchov marlstones with interbeds of turbiditic sandstones, organodetritic sandstones and olistolith bodies of the Gbeľany Beds*" was provided, however their occurrence was not localized neither in the text of the monograph nor in the attached map (Haško in Gross et al., 1993). Another brief description was provided from the road cut near Jelšava (Dolný Kubín; Jablonský & Halásová, 1994), where tectonic imbrication of 4 thrust sheets in the studied section interpreted as tectonic mélange was documented. Finally, benthic foraminiferal microfauna of biodetritic sandstones in the Homôľka Hill (in fact the Opálené Hill) and the Lučivný vrch Hill (north of Podbiel) areas were studied, and the term "*Lučivný vrch facies*" (Slovak: "*vývoj Lučivného vrchu*") was proposed (Salaj & Köhler, 2001).

The age of the Púchov Fm. in the studied region is determined by the nanoplankton and foraminiferal microfauna as Campanian–Maastrichtian (Salaj in Gross et al., 1980; Gross et al., 1993; Jablonský & Halásová, 1994), however, identical pink marlstone interbeds within the Snežnica and Sromowce fms. are of Cenomanian and Turonian age (Matějka & Hanzlíková, 1962; Potfaj et al., 1981; Gross et al., 1984).

Methods

The geological mapping of the region was carried out in terms of a standard methodology, and according to the Directive of the Ministry of the Environment of Slovak Republic No. 4/1996-3.1. for the compilation of basic geological maps and explanatory notes at scale 1:25 000 and regional geological maps at scale 1:50 000. The present work is based on the results of LiDAR assisted detailed geological mapping at scale 1:10 000 (e.g., Liščák et al., 2022). The accuracy of the GNSS equipment used for location of the documentation points was within 5 m. The presented biostratigraphic results are based on the microfacies analysis of the 24 thin sections by standard methods (e.g., Flügel, 2010). The taxonomy and biostratigraphy of planktonic foraminifera is based on Robaszynski et al. (1984), Caron (1995), Premoli Silva & Verga (2004), Falzoni & Petrizzo (2011) and Coccioni & Premoli Silva (2015).

The formal definition of new lithostratigraphic unit follows the recommendations of the International Stratigraphic Guide (Michalík et al., 2007; Salvador, 2013).

Results

The geological mapping in the Orava sector of the PKB revealed new knowledge about the less known lithofacies of the Upper Cretaceous Púchov Fm. Especially, the correct assignment of the white marly limestones – newly designated Kňažia Member/Beds (new name), posed an initial problem. White to grey limestones were initially considered as possible variety of the Jurassic Kozinec Limestone. However, doubts were cast due to the absence of other Jurassic facies that commonly accompany the Kozinec Limestone, as well due the presence of calcarenites, quartz-carbonate sandstones, and the frequent association with the variegated marlstones of the Púchov Fm. The problem was definitively solved by a microfacies study, which confirmed the presence of Late Cretaceous planktonic foraminifera.

Púchov Formation

The typical Púchov Fm. consists of pink to brick-red, rarely green or grey, marlstone to clayey limestone or clayey shale. The weathered surface of the marlstone to limestone may contain weathered planktonic foraminifera observable under a magnifying glass. Weathered marlstones sometimes form red eluvial clay which, in cases of poor exposure, represents the only indication of their presence. Deformed marlstone is often penetrated by slickensides, and numerous calcite accretionary steps which are relatively resistant to weathering and are preserved in the debris as well. The formation may also contain interbeds of medium-bedded (5–30 cm thick beds) quartz-carbonate sandstones. The red Púchov marlstones are rich in planktonic foraminifera (e.g., sample P529, Tab. 2). The lower part of the formation in the studied area, is often interbedded with white marly limestones, which are defined in this paper as the Kňažia Member (new name) and the associated white biodetritic limestones are correlated with the Bradlo-type limestones. The Púchov Fm. is first metres to 100 metres thick and forms separate bodies or thinner interbeds in the "klippen cover" flysch (Snežnica and Sromowce fms.). The red Púchov-type marlstone interbeds in the Snežnica and Sromowce fms. can be of a dual character. More often, they are in a normal stratigraphic contact. However, in some cases the alternation is clearly result of thrusting and imbrication.

The uppermost part of the Púchov Fm. locally includes grey and variegated marlstones, breccia with olistoliths of the Záskalie Breccia, that represents the youngest, syn-orogenic deposits of the formation.

According to the results of geological mapping, the tectonic position of the studied Púchov Fm., including the newly defined Kňažia Mb. with the Bradlo-type limestone, is associated with the rocks of deep-water Orava/Podbiel and Kysuca successions.

Kňažia Member (new name)

Lithology: Prevailing portion of the lithostratigraphic unit is formed by thin- to thick-bedded white to pale grey, fine- to medium-grained pelagic limestone (calcilutite; Figs. 2A–B, F and 3) to marlstone. The microfauna consists predominantly of planktonic foraminifera. It can also be characterized as a white indurated variety of the Púchov Marlstone. The marly limestones locally contain interbeds of variably thick (up to 4 m) thin- to medium-bedded biodetritic limestones – calcarenites. The calcarenites are distinguished as a separate Bradlo-type limestone, which is described below. The white marly limestones also contain up to first meters thick interbeds of pink and green Púchov-type marlstone and up to 1 m thick quartz-carbonate sandstone beds.

Microfacies are represented by micritic limestones (wackestone to packstone) with abundant cross sections of planktonic foraminifera with globular chambers and representatives of the family Globotruncanidae, described hereinafter (Figs. 6A–B, 8 and 9). Locally fragments of thin-shelled bivalves and echinoderm fragments are present. Rare spotted texture is a result of bioturbation.

White marly limestone with planktonic foraminifera may macroscopically resemble the Lower Cretaceous Pieniny Limestone, especially due to white colour on weathered surfaces. The Kňažia Mb., however, differs by aleuritic texture (Figs. 2A and 3F) and lower degree of lithification (disintegration even after a light hammer strike) and typical splitting into elongated or spindle sharp-edged chips (Fig. 2B, D and G). Also, the Jurassic Kozinec Limestone can be confused with the Kňažia Mb., due to grey colour and similar aleuritic texture.

Name: The name Kňažia Member/Beds (Slovak: "*vrstvy Kňažej, člen Kňažej*") is derived from the name of the Kňažia settlement, today part of Dolný Kubín town, where stratotype is located.

Rank: Member within the Púchov Fm.; and contains bodies of the Bradlo-type limestone (Figs. 1 and 7).

Type section: Lithostratigraphic unit occurs in different parts of the studied Orava sector of the PKB. The proposed stratotype is located at the forest road cut north of Kňažia between points P198 and P247 (N 49.242911°, E 19.317906°; Tab. 1, Fig. 1). Well accessible localities with white marly limestone is present in the unpaved road East of the Kňažia settlement (locality P192) and in the slope West of Široká (OFZ factory, locality P145).

Other exposures in this area are in the ridge east of the Jelšava settlement (locality P240). The auxiliary section is at the forest road cut at the Lučivný vrch Hill (840 m a.s.l.) north of the Podbiel village (localities P963 – P967). It should be noted, that the road cut between Jelšava and Kňažia exposes tectonically strongly imbricated section with higher abundance of sandstones and pink marlstones, representing otherwise infrequent lithological types. Smaller occurrences are in the wider area of the Trstená town, west of the cooperative farm (P1087) and at the locality Vrch lazov (locality P1101) and in the cut of the Oravica river (P1051 and P1055). The lithostratigraphic unit is documented also from the locality Riedky diel (P564) NW of the Dolný Kubín – Malý Bysterec municipality, in the Repiská Hill (P1373) and the area W of the Beňova Lehota village (P579).

Thickness and boundaries: The thickness is irregular, 50–150 m in the area of the Opálené Hill, 50–200 m in the area of the Lučivný vrch Hill, and approx. 65 m east of Trstená. Larger thickness is obviously a result of the tectonic repetition of the sedimentary sequence or folding.

The lithostratigraphic unit represents lower part of the Púchov Fm. It is mostly surrounded by the Upper Cretaceous "klippen cover" flysch of the Snežnica and Sromowce fms. The poor outcrop conditions do not allow adequate documentation of the nature of the contact. It may be a stratigraphic contact, where the Kňažia Mb. overlaps a slightly older flysch, as well as at least partly tectonic contact. It should be noted, that in a map scale and from the sedimentological point, the Kňažia Mb. represents antagonistic facies to the sandstone flysch of the Snežnica and Sromowce fms. and is younger.

The member is locally in a tectonic contact with older rocks of the Posidonia (Harcygrund) and Pieniny formations. It may be overlapped by the calcareous sandstone and conglomerate of the Jarmuta Fm.

Age: The white marly limestone is of the middle Campanian age based on a presence of planktonic foraminiferal assemblage with *Contusotruncana plummerae*, *Globotruncana arca*, *G. bulloides*, *G. lapparenti*, *G. linneiana*, *G. ventricosa*, *G. hilli*, *Globotruncanita elevata*, *G. insignis* and *G. stuartiformis* (see Tab. 2).

Depositional environment: Studied white marly limestone was deposited in a basinal pelagic environment without any significant coarse siliciclastic sediment input. Pelagic sediments are locally cut by channels and aprons of coarser-grained shallow water calciclastic detritus.

Fig. 2. A – Detail on fresh surface of white marly limestone (Opálené Hill, P138); B – Exposure of the stratotype of white marly limestone in the unpaved road N of Kňažia (between points P198 and P247); C – Cut below the power line with the debris of white marly limestone (P145); D – Detail on the calcarenite with intraclasts of white marly limestone (P145); E – calcarenite with angular intraclasts of white marly pelagic Kňažia Mb. limestone; F – Outcrop of the grey marly limestones W of Beňova Lehota (P579); G – Calcarenite with angular fragments of grey limestone (P579).

Fig. 3. The Kňažia Member. A – Detail on white marly limestone with characteristic medium-grained texture, Lučivný vrch Hill (P956); B – Debris of white marly limestone in the forest road cut NW of Lučivný vrch Hill (P963); C – Grey calcarenites W of Lučivný vrch Hill (P788); D – Exposure of the white limestone at the Lučivný vrch Hill (P966); E – Exposure of Kňažia Mb. in the cut of Oravica river (P1055); F – Detail on white marly limestone on the previous locality (P1055); G – Debris of white to grey marly limestone, cut of Zábiedovčík brook (P1101).

Bradlo-type limestone

Lithology: Grey thin- to thick-bedded biodetritic (allodapic) limestone or medium- to coarse-grained calcarenite to calcirudite (microbreccia). Usually massive, locally laminated or cross-bedded (Figs. 4 A–D). The carbonate grains are predominantly of the psammite fraction, rarely with rounded or angular clasts of the psephite fraction (carbonate conglomerates). Intraclasts of white limestone with planktonic foraminifera (Kňažia Mb.) up to 4 cm in diameter are frequent (Figs. 2D–E). Grey calcarenites are relatively resistant to erosion, therefore often form ridges and are better exposed than the finer-grained Kňažia Mb.

Carbonate as well as polymictic, rarely also exotic conglomerate bodies or interbeds may be present. The interbeds of the exotic conglomerates with clasts of granites and rhyolites 2–30 cm in diameter were observed at several localities near Kňažia, Hldočín Valley and cut of the Oravica river (P247; P978, P1067; P1653; Figs. 4F and 5F).

Rarely *Thalassinoides* burrows (Fig. 5C) and rudists are observed at the Hldočín Valley west of the Zemianska Dedina settlement (locality P978; Figs. 5D–E). At this locality also otherwise uncommon coalified plant detritus was present in the calcarenites. The rudist fauna from this locality was described by Kühn & Andrusov (1942) and Andrusov (1959).

According to microfacies study, the limestone represents packstone to grainstone (biomicrite to biomicrosparite) with minor or almost no siliciclastic admixture. It contains small-sized planktonic foraminifera with globular chambers, larger representatives of the family *Globotruncanidae* and large benthic foraminifera belonging mostly to the genus *Preasiderolites*. In addition, the calcarenite commonly contained fragments of echinoderms, inoceramus shells, rudists, bryozoans and coralline algae. Frequent clasts of dolomites, micritic limestones with *Calpionella alpina* or radiolarians and silicified clasts are present. Additionally, also sandstone and mafic volcanic clasts were scarcely observed.

Clastic monocrystalline quartz is present only locally. Usually only small, angular to poorly-rounded grains with a diameter below about 0.2–0.25 mm and undulatory extinguishing are present.

Name: Term Bradlo-type limestone (Slovak: *vápence bradlianskeho typu*; originally defined as Široké bradlo Limestone Member – part of the Bradlo Formation of the Brezová Group; Samuel et al., 1980; now redefined as the Bradlo Formation by Potfaj et al., 2014; Teťák et al., 2015) is proposed, due to identical lithological content and stratigraphic age. The studied limestone was formerly described as "*organodetritic limestone of Gbeľany Formation*" (Marschalko et al., 1979; Gross et al., 1993). It should be noted, that Salaj & Köhler (2001) referred to the biodetritic limestones as the so-called "*Lučivný vrch facies*" (Slovak: "*vývoj Lučivného vrchu*") based on the occurrence at the Lučivný vrch Hill north of the Podbiel village. However, we do not recommend using this name anymore, because of the possibility of confusion with the Maiolica facies Lučivná Formation (see Polák & Bujnovský, 1979).

Rank: Informal lithostratigraphic unit within the Púchov Formation. According to present knowledge, the lithostratigraphic unit usually occurs together with and within the newly defined Kňažia Mb. (Figs. 1 and 7).

Type section: The type section within the studied sector of the PKB is located in the ridge of the Opálené Hill (locality P138, between the Široká and Jelšava settlements). The auxiliary section is located in the northern and southern slopes of the Lučivný vrch Hill (localities P963 – P967, north of Podbiel). Particular attention should be paid to the occurrence of the biodetritic limestones with rudist and exotic conglomerates in the Hldočín Valley (location P978, west of the Zemianska Dedina settlement).

Thickness and boundaries: Biodetritic limestones form 5–30 m thick lenticular bodies within the white marly limestones of the Kňažia Mb. The Bradlo-type limestone occurs in the lower, middle, and upper parts of the Kňažia Mb. In the area of the Hldočín Valley (locality P978) the biodetritic limestones with rudists and exotic conglomerates are up to 50 m thick and cut into the flysch of the Snežnica and Sromowce fms. Similar situation is in the area north of Dolný Kubín (P1653). The occurrence in the Hldočín Valley represents the base of the Bradlo-type limestone.

Age: Middle-upper Campanian, based on planktonic foraminifera (this study, see Biostratigraphy chapter below), and larger benthic foraminifera *Praesiderolites douvillei*, *Praesiderolites dordoniensis*, *Pseudosiderolites vidali*, with accompanying assemblage of other larger foraminifera *Orbitoides* sp., *Lepidorbitoides* sp., *Goupillaudina* sp. *Helicorbitoides* sp. and *Dicyclina* sp. (Salaj & Köhler, 2001). The upper Santonian–Campanian age was determined according the rudist macrofauna from the calcarenite body in Hldočín valley (Kühn & Andrusov, 1942). Despite the samples from this locality are devoid of planktonic foraminifera and age indicative larger benthic foraminifera; an older age of this body can be assumed, also based on the fact that its position can be interpreted as a channel cut into the uppermost part of the Snežnica and Sromowce fms.

Depositional environment: Studied calciclastic limestone is interpreted as allodapic slope aprons and channel fill composed of shallow water carbonate debris within the white marly limestones of the Kňažia Mb. or cut into the older Snežnica and Sromowce fms. The presence of white marly limestone intraclasts within the biodetritic

Fig. 4. Bradlo-type limestone. A – Detail on fresh surface of grey calcarenite, Opálené Hill (P138); B – Laminated calcarenite, Opálené Hill, W of Široká; C – Weathering of thick bedded calcarenites, Opálené Hill (P138); D – Cross-bedded calcarenites, N of Lučivný vrch Hill (P967); E – Fresh surface of coarse grained calcarenite to breccia N of Lučivný vrch Hill; F – Admixture of exotic conglomerates with rhyolite clasts, cut of Oravica river (P1067

Fig. 5. Calcarenites in the Hldočín section. A – Detail on calcarenite with cross-section of inoceramus shell; B – Calcarenite with coalified plant detritus (P978); C – *Thalassinoides* burrows (P978); D – Calcarenite with rudists (P978); E – Biodetritic limestone with fragmented shell detritus; F – Exposure of contact of rudist-bearing calcarenites above the exotic conglomerate bed (P978).

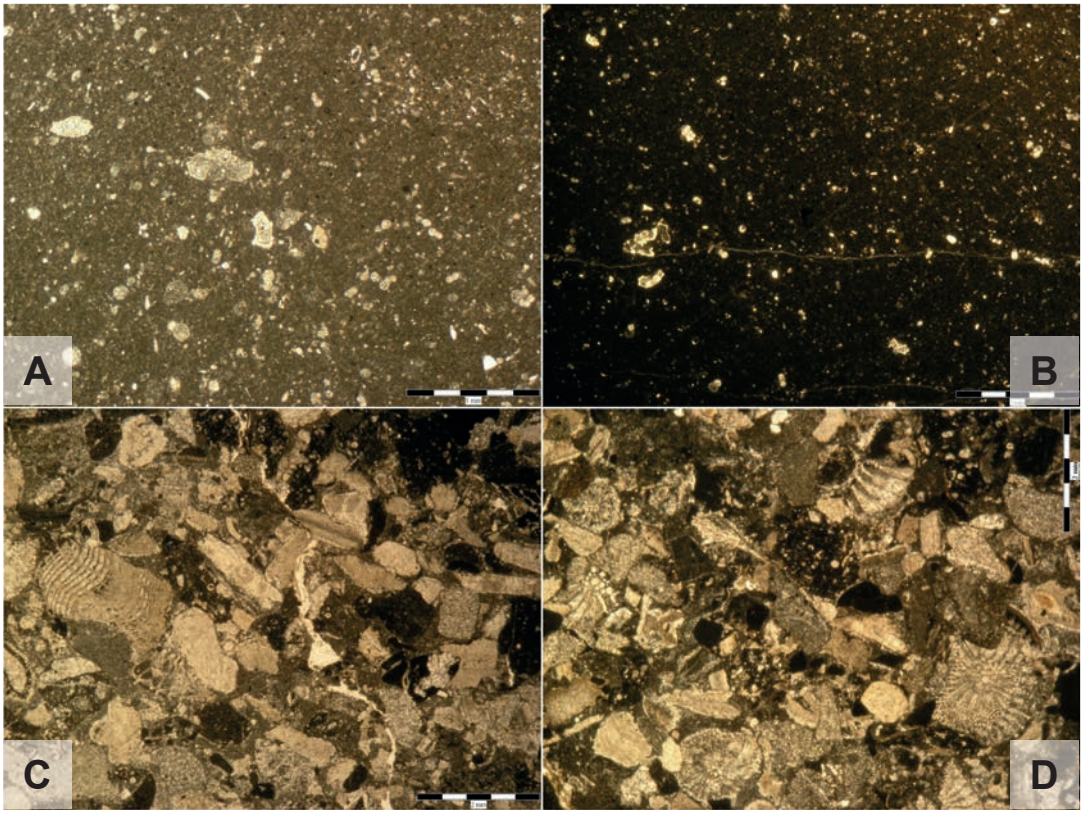

Fig. 6. Microfacies of the studied rocks. A–B – Kňažia Member; A – Wackstone with planktonic foraminifera (P135); B – Wackstone with planktonic foraminifera (P138H); C–D – Bradlo-type limestone: C – Grainstone with dominant rudist fragments and other biodetritus (P138C); D – Grainstone with fragments of larger benthic foraminifera (*Praesiderolites* spp.) (P138E).

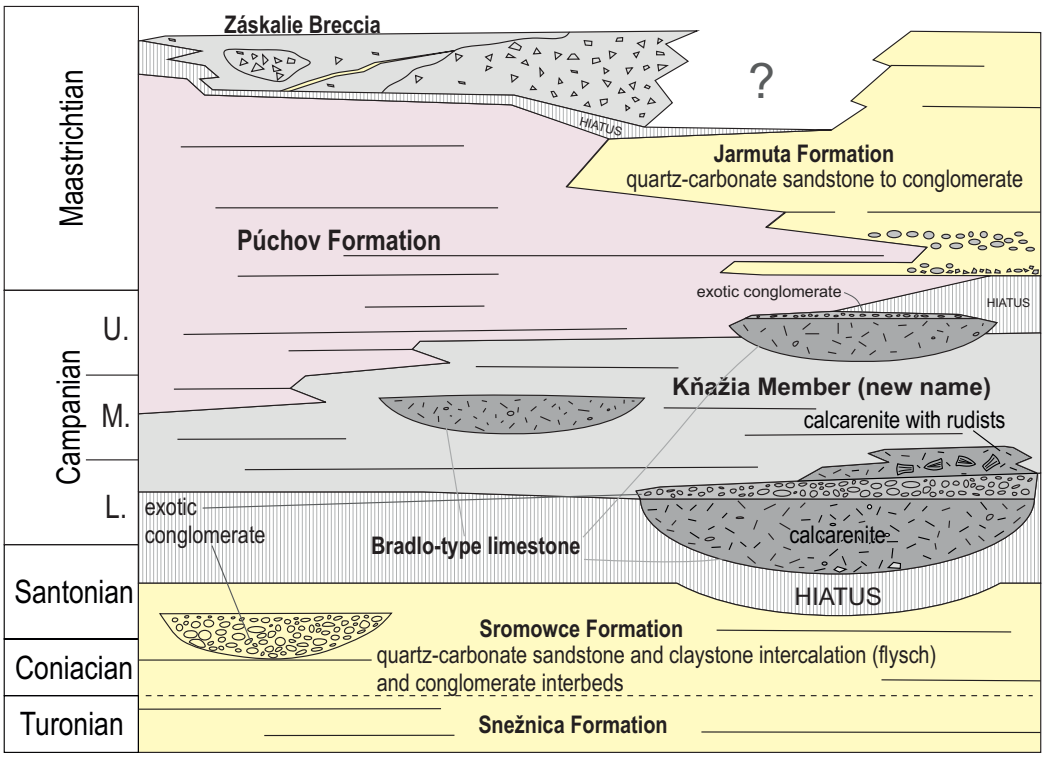

Fig. 7. Proposed sedimentary scheme of the Púchov Formation and its relationship with the Kňažia Member and the Bradlo-type limestone.

limestone points to erosion and redeposition of unconsolidated surrounding slope and basinal deposits.

Biostratigraphy

The marly limestones of the Kňažia Mb. are rich in planktonic foraminifera, while planktonic foraminifera from calcarenites with *Praesiderolites* spp. and beds of distal calciturbidites are mostly accessory. The microfacies of the Kňažia Mb. is represented by wackestones-packstones (planktonic foraminiferal biomicrites; Tab. 2) Microfacies of the Bradlo Mb. is represented by (fine-grained biodetritic-larger benthic foraminiferal biomicrites/biomicrosparites with lithoclasts). The most abundant in the samples are smaller planktonic foraminifera with globular chambers of *Muricohedbergella* spp. and scarce *Rugoglobigerina* spp. (trochospiral morphotypes). Planispiral morphotypes represented by *Laeviella* cf. *bollii* (Pessagno) are scarce (Fig. 8D–E). Relatively common are smaller biserial types of *Heterohelix* spp. (Fig. 8B). The globotruncanids are occasional to abundant, represented by diverse assemblage including *Globotruncana arca* (Cushman), *Globotruncana bulloides* Vogler, *Globotruncana falsostuarti* Sigal, *Globotruncana hilli* Pessagno, *Globotruncana lapparenti* Brotzen, *Globotruncana linneiana* (d'Orbigny), *Globotruncana orientalis* El Naggar, *Globotruncana ventricosa* (White) (Fig. 9), rare *Contusotruncana plummerae* (Gandolfi) (Fig. 9L), occasional *Globotruncanita elevata* (Brotzen), *Globotruncanita insignis* (Gandolfi) and *Globotruncanita stuartiformis* (Dalbiez) (Fig. 8).

The composition of the planktonic foraminiferal assemblage from the marly limestones and fine-grained varieties of biodetritic limestones points to the middle Campanian age. The FO *G. ventricosa* is traditionally determined between the FO of *G. elevata* and FO *Rd. calcarata* by various authors (Robaszinski et al., 1984; Premoli Silva & Verga, 2004; Petrizzo et al., 2011). The value of *G. ventricosa* as a global biostratigraphic marker species is however questioned (Falzoni et al., 2011; Coccioni & Premoli Silva, 2015). Cushman (1927) defined the co-occurrence of *C. plummerae* and *G. elevata* and absence of *Rd. calcarata* as the *C. plummerae* Zone. Axial sections of *C. plummerae* are rare in the sample material however the presence of *G. insignis* might refine the age determination. The FO of *G. insignis* is determined between the FO of *C. plummerae* and the FO of *Rd. calcarata* (Robaszinski et al., 1984; Premoli Silva & Verga, 2004; Falzoni & Petrizzo, 2011).

In the Bradlo-type biodetritic limestone frequent *Praesiderolites* spp. are present. Salaj & Köhler (2001) determined two species *P. douvillei* and *P. dordoniensis*. Range of the species *P. douvillei* is known from the middle-upper Campanian (Velić, 2007; Vicedo & Robles Salcedo, 2022).

Discussion

Despite relatively common occurrence of the Upper Cretaceous Púchov Fm. and its equivalents in the PKB and adjacent tectonic units, it has not been subject of detailed sedimentological and biostratigraphical research. Most of the knowledge is limited to basic mapping works, biostratigraphic and only general stratigraphic knowledge (e.g., Kantorová & Andrusov, 1958; Salaj & Began, 1963; Birkenmajer, 1977; Mello et al., 2011). Given that equivalents of the Púchov Fm. occur in several lithotectonic units and have many local names (Krováriky Fm., Kysuca Beds, Lalinok Fm., Gbeľany Fm. etc.), it may be more appropriate to redefine the Púchov Fm. as a lithostratigraphic unit at the group rank in the future.

While the lithological composition and position of the Kňažia Mb. (new name) can be considered more or less unique, the Santonian–Campanian biodetritic limestones are correlated with the Bradlo Formation (Samuel et al., 1980; Potfaj et al., 2014; Teťák et al., 2015) and denoted here as the Bradlo-type limestone. It should be noted that the biodetritic limestones with the exotic conglomerate interbeds and rudists documented at the Hldočín Valley west of the Zemianska Dedina settlement, are partly equivalent of the Hradisko Formation (Kysela et al., 1982) or Bezdedov Limestone of the Ihrište Formation (Salaj, 1990). However, a correlation of these formations requires a further detailed study and is beyond the scope of this paper.

One of the remaining open questions is the nature of the contact of the Kňažia Mb. with the flysch of the Snežnica and Sromowce fms. There are several places where the Kňažia Mb. is interbedded within the Snežnica and Sromowce fms. (e.g., NE of the Kňažia settlement; E and W of the Jelšava settlement). Considering the Coniacian–Santonian age of the Snežnica and Sromowce fms., the expected interfingering is not possible. A similar problem is posed by the position of the klippen of calcarenites of the Bradlo-type limestone in the Hldočín Valley (P978), or N of Dolný Kubín (P1653), situated within the Snežnica and Sromowce fms. At Hldočín locality, upper Santonian–Campanian age is documented (Kühn & Andrusov, 1942). However, one cannot agree with the interpretation that the rudists are in a growth position. The rudists are clearly redeposited (Fig. 5F). Based on the structural position and documented age, the Hldočín Valley exposure is interpreted as the base of the Bradlo-type limestone.

The geological mapping of the studied lithostratigraphic units suggests affiliation with the Orava/Podbiel or Kysuca succession. However, we do not see the complete stratigraphic sequences in the tectonic mélange of the Orava sector of PKB, and therefore tectonic classification to the Pieniny Unit is considered tentative.

Tab. 2

Planktonic foraminifera and *Praesiderolites* spp. occurrence in the studied samples

Locality	**Tvr.**	**Luč.v.**		**Podb.**	**H.L.**	**Kňažia - Široká**												**Luč.v.W**		**J-K.**
Microfacies	**W**	**W**	**R (M)**	**G (M)**	**W**	**W**	**W**	**W**	**P**	**P**	**R**	**R**	**R**	**R**	**R**	**W**	**P**	**G**	**R (M)**	**R (G)**
Species/samples	OP1011OM	OP966aOM	OP967OM	OP819OM	OP529OM	OP149OM	OP138H	OP138AO	OP138A	OP138bOM	OP138cOM	OP138dOM	OP138eOM	OP138fOM	OP138gOM	OP135OM	OP145OM	OP792OM	OP789OM	OP240OM
Heterohelix spp.	+	+	+	+	+	+	+	+	+							+	+	+	+	+
Muricohedbergella spp.	+	+	+	+	+	+	+	+	+		+				+	+	+	+	+	+
Rugoglobigerina spp.		+							+							+				+
Laeviella cf.*bollii*		+			+															
Contusotruncana plummerae				+	?													+		+
Globotruncana arca	+	+	+	+	+	+	+	+	+	+	+				+	+	+	+	+	+
Globotruncana bulloides	+	+		+	+	+	+		+	?						+				+
Globotruncana lapparenti	+	+	+	+	+	+	+	+	+							+	+			
Globotruncana linneiana	+	+		+	+	+	+		+							+		+		
Globotruncana hilli	+				+				+									+		+
Globotruncana orientalis		+							+											
Globotruncana ventricosa	+	+		+	+	+	+	+	+							+			+	+
Globotruncanita elevata		+				+	?		+							+	+			
Globotruncanita falsostuarti			+	?	+	+			+											+
Globotruncanita insignis		+	+						?							+				
Praesiderolites spp.			+						+	+	+	+	+	+	+		+		+	+

W – Wackestones (planktonic foraminiferal biomicrites). P – Packestones (fine-grained crinoidal-biodetritic biomicrites with admixture of planktonic foraminifera). G – Grainstones (M – microbreccia). R – Rudstones. Localities: Tvr. – Tvrdošín, Luč.v. – Lučivný vrch Hill, Podb. – Podbiel, H.L. – Horná Lehota, Luč.v.W. – Lučivný vrch, western side. J-K. – Jelšava-Kňažia.

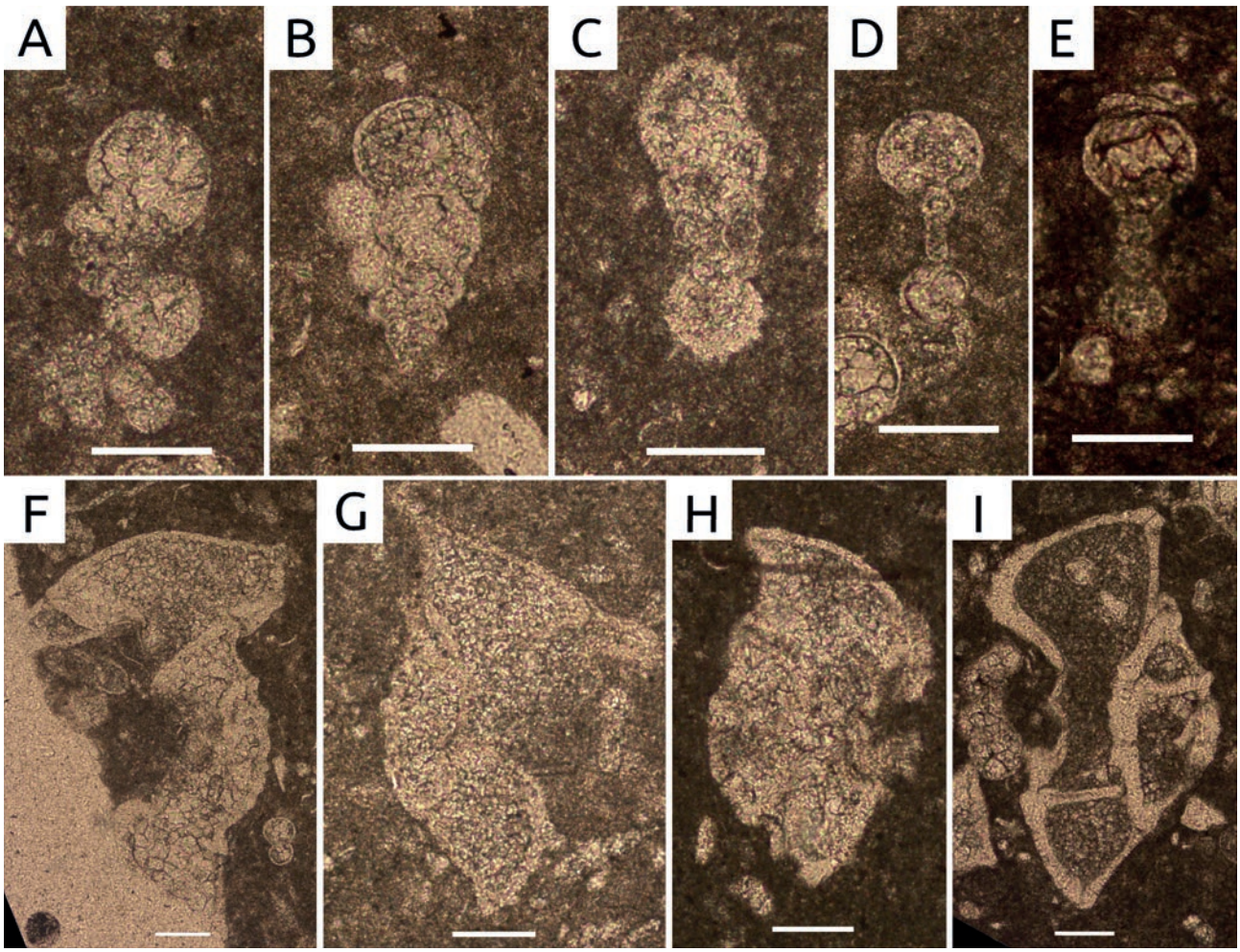

Fig. 8. A – *Muricohedbergella* cf. *monmouthensis* (Olsson), P966a; B – *Heterohelix* sp. P966a; C – *Rugoglobigerina* sp., P135; D–E – *Laeviella* cf. *bollii* (Pessagno), D – P966, E – P529; F–G – *Globotruncanita elevata* (Brotzen), F – P966a; G – P135; H – *Globotruncanita insignis* (Gandolfi), P135; I – *Globotruncanita stuartiformis* (Dalbiez), P149. Scale bar 100 μm.

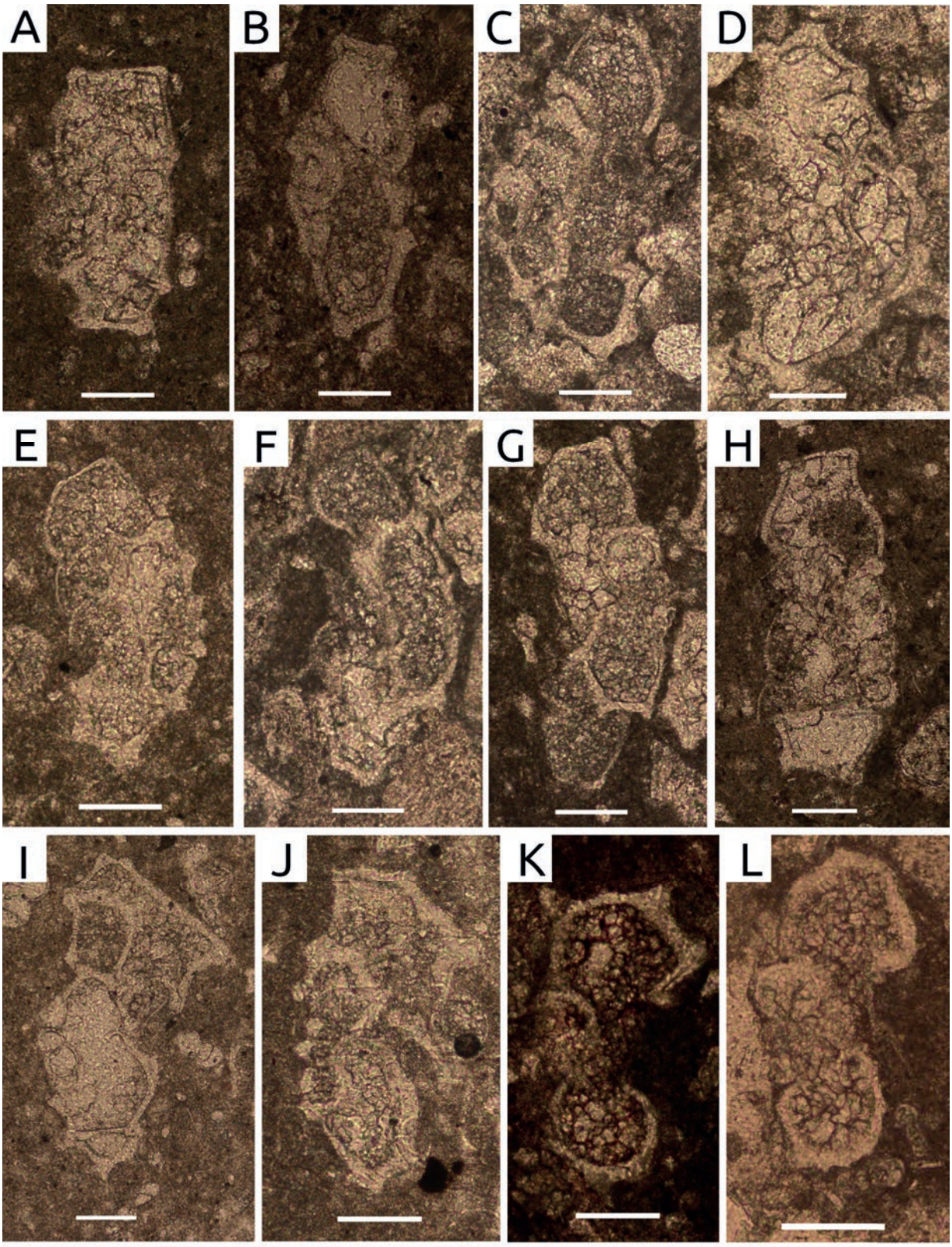

Fig. 9. A – *Globotruncana linneiana* (d'Orbigny), P1101; B – *Globotruncana lapparenti* Brotzen, P138a. C–D – *Globotruncana arca* (Cushman); C – P138a; D – P792; E–F – *Globotruncana orientalis* El Naggar; E – P966a; F – P138a; G–H – *Globotruncana bulloides* Vogler; G – P149; H – P1101; I–J – *Globotruncana ventricosa* (White); I – P1101; J – P138h; K – *Globotruncana hilli* Pessagno, P529; L – *Contusotruncana plummerae* (Gandolfi), P819.

Conclusions

The results of geological mapping, microfacies and biostratigraphic study in the area of Orava sector of the Pieniny Klippen Belt allow to distinguish new lithostratigraphic unit named the Kňažia Mb. of the Púchov Fm. The Kňažia Mb. is represented by white or grey marly limestone with planktonic foraminifera of middle Campanian age. Thickness varies between 50–200 m. The marly limestone locally contains interbeds of grey calcarenite or biodetritic limestone and conglomerate correlated with the Bradlo-type limestone. The calcarenites are also cut into the underlying Snežnica and Sromowce fms. The Bradlo-type limestone contains apart of planktonic and benthic foraminifera also rudist macrofauna which points to upper Santonian–Campanian age. The overall thickness of the member does not exceed 50 m. The studied lithostratigraphic units are tentatively assigned in the Orava/Podbiel resp. Kysuca succession of the Pieniny Unit.

Acknowledgements

The study was financially supported by the Ministry of Environment of Slovak Republic project no. 02 20 *Geological map of the Oravská Magura Mts.* at scale 1:50,000. Š. Józsa wishes to thank the projects APVV-22-0523 and VEGA 2/0106/23 for financial support. The authors thank reviewers Prof. RNDr. Roman Aubrecht, Dr., and RNDr. Miroslav Bubík, CSc., for their constructive comments and Prof. RNDr. Dušan Plašienka, DrSc., for oversight as handling editor.

References

Andrusov, D., 1931a: Geologická mapa útesového pásma v údolí Oravy 1 : 25 000. Díl východní. In: Matějka, A. & Andrusov, D. (eds.): Guide des excursions dans les Carpathes occidentales. *Praha, Státní geologický ústav Československé republiky*, 397 pp.

Andrusov, D., 1931b: Geologická mapa útesového pásma v údolí Oravy 1 : 25 000. Díl západní. In: Matějka, A. & Andrusov, D. (eds.): Guide des excursions dans les Carpathes occidentales. *Praha, Státní geologický ústav Československé republiky*, 397 pp.

Andrusov, D., 1938: Geologický výzkum vnitřního bradlového pásma v Západních Karpatech, část III.: Tektonika. *Rozpr. St. geol. Úst. Čs. republiky*, IX, 1 – 136 (in Czech, French summary).

Andrusov, D., 1959: Geológia Československých Karpát, Zv. II. *Bratislava, Veda, Vydavateľstvo Slovenskej akadémie vied*, 375 pp. (in Slovak).

Andrusov, D. & Scheibner, E., 1960: Prehľad súčasného stavu poznatkov o geológii bradlového pásma medzi Vlárou a Tvrdošínom. *Geologický sborník*, 11, 2, 239–279 (in Slovak, English summary).

Bezák, V. (ed.), Elečko, M., Fordinál, K., Ivanička, J., Kaličiak, M., Konečný, V., Kováčik, M. (Košice), Maglay, J., Mello, J., Nagy, A., Polák, M., Potfaj, M., Biely, A., Bóna, J., Broska, I., Buček, S., Filo, I., Gazdačko, Ľ., Grecula, P., Gross, P., Havrila, M., Hók, J., Hraško, Ľ., Jacko, S. Jr., Jacko, S. Sr., Janočko, J., Kobulský, J., Kohút, M., Kováčik, M. (Bratislava), Lexa, J., Madarás, J., Németh, Z., Olšavský, M., Plašienka, D., Pristaš, J., Rakús, M., Salaj, J., Siman, P., Šimon, L., Teťák, F., Vass, D., Vozár, J., Vozárová, A. & Žec, B., 2008: Prehľadná geologická mapa Slovenskej republiky 1 : 200 000. *Bratislava, Ministerstvo životného prostredia SR, Štátny geologický ústav Dionýza Štúra.*

Bezák, V. (ed.), Elečko, M., Fordinál, K., Ivanička, J., Kaličiak, M., Konečný, V., Maglay, J., Mello, J., Nagy, A., Polák, M., Potfaj, M., Šimon, L., Biely, A., Broska, I., Buček, S., Filo, I., Grecula, P., Hraško, Ľ., Jacko, S., Kobulský, J., Kohút, M., Kováčik, M., Lexa, J., Olšavský, M., Plašienka, D., Pristaš, J., Teťák, F., Vass, D. & Vozárová, A., 2009: Vysvetlivky k Prehľadnej geologickej mape Slovenskej republiky 1 : 200 000. *Bratislava, Štátny geologický ústav Dionýza Štúra*, 534 pp. (in Slovak, English summary).

Birkenmajer, K., 1977: Jurassic and Cretaceous lithostratigraphic units of the Pieniny Klippen Belt, Carpathians, Poland. *Studia geologica Polonica*, 45, 1–158.

Birkenmajer, K., 1986: Stages of structural evolution of the Pieniny Klippen Belt, Carpathians. *Studia geologica Polonica*, 88, 7–32.

Borza, V., Ondrejíčková, A. & Halásová, E., 1993: Litostratigrafia strednej jury – spodnej kriedy Podbielskeho bradla (Orava). *Manuscript. Bratislava, Archive of St. Geol. Inst. of D. Štúr* (arch. no. 78633), 34 pp. (in Slovak).

Caron, M., 1985: Cretaceous planktic foraminifera. In: Bolli, H. M., Saunders, J. B. & Perch-Nielsen, K. (eds.): Plankton Stratigraphy, Volume 1: Planktic Foraminifera, Calcareous Nannofossils and Calpionellids. *Cambridge, Cambridge University Press*, 17–86.

Cushman, J. A., 1927: An outline for the re-classification of the foraminifera: Contributions from the Cushman Laboratory for Foraminiferal Research, 3. *Sharon*, 105 pp.

Coccioni, R. & Premoli-Silva, I., 2015: Revised Upper Albian-Maastrichtian planktonic foraminiferal biostratigraphy and magnetostratigraphy of the classical Tethyan Gubbio section (Italy). *Newsletter Stratigraphy*, 48, 1, 47–90. https://doi.org/10.1127/nos/2015/0055.

Falzoni, F. & Petrizzo, M. R., 2011: Taxonomic overview and evolutionary history of *Globotruncanita insignis* (Gandolfi, 1955). *Journal of foraminiferal research*, 41, 4, 371–383. https://doi.org/10.2113/gsjfr.41.4.371.

Flügel, E., 2010: Microfacies of Carbonate Rocks Analysis, Interpretation and Application. *Berlin, Springer*, 984 pp. https://doi.org/10.1007/978-3-642-03796-2.

Gross, P., Haško, J., Dovina, V., Halouzka, R. & Szalaiová, V., 1980: Vysvetlivky k listu Dolný Kubín 1 : 25 000. Čiastková záverečná správa za rok 1979. *Manuscript. Bratislava, Archive of St. Geol. Inst. of D. Štúr* (arch. no. 45327).

Gross, P., Haško, J. & Halouzka, R., 1984: Vysvetlivky ku geologickej mape 1 : 25 000, list 26 413 (Trstená 3). Čiastková

záverečná správa. Manuscript. *Bratislava, Archive of St. Geol. Inst. of D. Štúr* (arch. no. 57740), 86 pp. (in Slovak).

Gross, P., Köhler, E., Mello, J., Haško, J., Halouzka, R., Nagy, A., Kováč, P., Filo, I., Havrila, M., Maglay, J., Salaj, J., Franko, O., Zakovič, M., Pospíšil, L., Bystrická, H., Samuel, O. & Snopková, P., 1993: Geológia južnej a východnej Oravy. *Bratislava, Geologický ústav Dionýza Štúra*, 319 pp. (in Slovak, English summary).

Haško, J., 1978: Oravská séria – nová séria bradlového pásma Západných Karpát. *Geologické práce, Správy*, 70, 115–121 (in Slovak).

Haško, J. & Polák, M., 1978: Geologická mapa Kysuckých vrchov a Krivánskej Malej Fatry v mierke 1 : 50 000. *Bratislava, Geologický ústav Dionýza Štúra*.

Haško, J. & Polák, M., 1979: Vysvetlivky ku geologickej mape Kysuckých vrchov a Krivánskej Malej Fatry 1 : 50 000. *Bratislava, Geologický Ústav Dionýza Štúra*, 145 pp. (in Slovak).

Hu, X., Jansa, L., Wang, Ch., Sarti, M., Bak, K., Wagreich, M., Michalík, J. & Soták, J., 2006: Upper Cretaceous oceanic red beds (CORBs) in the Tethys: occurrences, lithofacies, age, and environments. *Cretaceous Research*, 26, 3 – 20. https://doi.org/10.1016/j.cretres.2004.11.011.

Jablonský, J. & Halásová, E., 1994: Resedimentation as a reflection of Laramian processes in the Pieniny Klippen Belt near Jelšava, Orava region, Western Carpathians. In: Michalík, J. & Reháková, D. (eds.): Abstract Book in the IGCP 362 Project Annual Meeting, Smolenice 1994, Konferencie, Sympóziá, Semináre. *Bratislava, Geologický ústav Dionýza Štúra*, 93–94.

Kantorová, V. & Andrusov, D., 1958: Mikrobiostratigrafický výskum strednej a vrchnej kriedy Považia a Oravy. *Geologický sborník*, 9, 2, 165–177 (in Slovak, French summary).

Kühn, O. & Andrusov, D., 1942: Stratigraphie und Palaogeographie der Rudisten. III. Rudistenfauna und Kreideentwicklung in den Westkarpathen. *Neues Jahrbuch Mineralogie Geologie Paläontologie Beitrag*, 86, 450–480 (in German).

Kysela, J., Marschalko, R. & Samuel, O., 1982: Litostratigrafická klasifikácia vrchnokriedových sedimentov manínskej jednotky. *Geologické práce, Správy*, 78, 134–167 (in Slovak, English summary).

Lexa, J., Bezák, V., Elečko, M., Mello, J., Polák, M., Potfaj, M. & Vozár, J. (eds.), 2000: Geological map of Western Carpathians and adjacent areas 1:500,000. Ministry of the Environment of Slovak Republic. *Bratislava, Geological Survey of Slovak Republic*.

Liščák, P., Pauditš, P., Bystrická, G., Teťák, F., Maglay, J., Dananaj, I., Ondrus, P., Mašlár, E., Mašlárová, I., Olšavský, M., Pelech, O., Vitovič, L., Leitmannová, K., Fraštia, M. & Papčo, J., 2022: Využitie DMR 5.0 z leteckého laserového skenovania pri riešení geologických úloh ŠGÚDŠ. *Geodetický a kartografický obzor*, 68, 110, 8, 149–159 (in Slovak, English summary).

Marschalko, R., 1986: Vývoj a geotektonický význam kriedového flyšu bradlového pásma. Bratislava, Veda, vydavateľstvo SAV, 137 pp. (in Slovak, English summary).

Marschalko, R. & Samuel, O., 1978: Poznámky k tektonickej príslušnosti flyšu v okolí Sedliackej Dubovej (bradlové pásmo). *Geologické práce, Správy*, 71, 111–122 (in Slovak, English summary).

Marschalko, R., Haško, J. & Samuel, O., 1979: Záskalské brekcie a proces vzniku olistostrómov (Bradlové pásmo na Dolnej Orave). *Geologické práce, Správy*, 73, 75–88 (in Slovak, English summary).

Matějka, A. & Hanzlíková, E., 1962: O paleogénu od obce Kňažia na Oravě. Zprávy o geologických výzkumech v roce 1961. *Praha, Ústřední ústav geologický*, 194–196 (in Czech).

Mello, J., Potfaj, M., Teťák, F., Havrila, M., Rakús, M., Buček, S., Filo, I., Nagy, A., Salaj, J., Maglay, J., Pristaš, J. & Fordinál, K., 2011: Vysvetlivky ku geologickej mape Stredného Považia 1 : 50 000. *Bratislava, Štátny geologický ústav Dionýza Štúra*, 378 pp. (in Slovak).

Michalík, J., Vass, D., Hudáčková, N., Kováčová, M., Lintnerová, O., Reháková, D., Soták, J., Schlögl, J., Aubrecht, R., Vozárová, A., Sliva, Ľ., Lexa, J., Konečný, V., Túnyi, I. & Potfaj, M., 2007: Stratigrafická príručka: slovenská stratigrafická terminológia, stratigrafická klasifikácia a postupy. *Bratislava, Veda, vydavateľstvo SAV*, 166 pp. (in Slovak).

Mišík, M., 1997: The Slovak part of the Pieniny Klippen Belt after the pioneering works of D. Andrusov. *Geologica Carpathica*, 48, 4, 209–220.

Petrizzo, M. R., Falzoni, F. & Premoli Silva, I., 2011: Identification of the base of the lower-to-middle Campanian Globotruncana ventricosa Zone: comments on reliability and global correlations. *Cretaceous Research*, 32, 387–405. https://doi.org/10.1016/j.cretres.2011.01.010.

Plašienka, D., 2018a: The Carpathian Klippen Belt and types of its klippen – An attempt at a genetic classification. *Mineralia Slovaca*, 50, 1, 1–24.

Plašienka, D., 2018b: Continuity and episodicity in the early Alpine tectonic evolution of the Western Carpathians: How large-scale processes are expressed by the orogenic architecture and rock record data. *Tectonics*, 37. https://doi.org/10.1029/2017TC004779.

Plašienka, D., Soták, J., Jamrichová, M., Halásová, E., Pivko, D., Józsa, Š., Madzin, J. & Mikuš, V., 2012: Structure and evolution of the Pieniny Klippen Belt demonstrated along a section between Jarabina and Litmanová villages in Eastern Slovakia. *Mineralia Slovaca*, 44, 1, 17–38.

Plašienka, D., Aubrecht, R., Bezák, V., Bielik, M., Broska, I., Bučová, J., Fekete, K., Gaži, P., Gedl, P., Golej, M., Halásová, E., Hók, J., Hrdlička, M., Jamrich, M., Józsa, Š., Klanica, R., Konečný, P., Kubiš, M., Madarás, J., Majcin, D., Marko, F., Molčan Matejová, M., Potočný, T., Schlögl, J., Soták, J., Suan, G., Šamajová, L., Šimonová, V., Teťák, F. & Vozár, J., 2021: Structure, composition and tectonic evolution of the Pieniny Klippen Belt – Central Western Carpathian contiguous zone (Kysuce and Orava regions, NW Slovakia). *Bratislava, Comenius University*, 148 pp.

Polák, M. & Bujnovský, A., 1979: The Lučivná formation (New designation of a formal lithostratigraphical unit of the lower Cretaceous of envelope groups in the West Carpathians). *Geologické práce, Správy*, 73, 61–70.

Potfaj, M., 1993: Postavenie bielokarpatskej jednotky v rámci flyšového pásma. *Geologické práce, Správy*, 98, 55–78 (in Slovak, English summary).

Potfaj, M., Haško, J., Gašpariková, V., Snopková, P. & Samuel, O., 1981: Vysvetlivky ku geologickej mape 1 : 25 000, list 26-411 (Trstená). Čiastková záverečná správa za rok 1977 – 1981. *Manuscript. Bratislava, Archive of St. Geol. Inst. of D. Štúr* (arch. no. 50488), 47 pp. (in Slovak).

Potfaj, M., Teťák, F. (eds.), Havrila, M., Filo, I., Pešková, I., Olšavský, M. & Vlačiky, M., 2014: Geological map of the Biele Karpaty Mts. (southern part) and the Myjavská pahorkatina Upland 1:50,000. *Bratislava, Štátny geologický ústav Dionýza Štúra.*

Premoli Silva, I. & Verga, D., 2004: Practical Manual of Cretaceous Planktonic Foraminifera. In: Verga, D. & Rettori, R. (eds.): International School on Planktonic Foraminifera, Universities of Perugia & Milano. *Perugia, Tipografia Pontefelcino*, 283 pp.

Robaszynski, F., Caron, M., Gonzales Donoso, J. M. & Wonders, A. A. H. (eds.), 1984: Atlas of Late Cretaceous Globotruncanids. *Revue de micropaléontologie*, 26, 3–4, 305 pp.

Salaj, J., 1990: Geologická stavba bradlovej a pribradlovej zóny stredného Považia a litologická klasifikácia kriedových sedimentov novovymedzených sekvencií. *Mineralia Slovaca*, 22, 2, 155–174 (in Slovak, English summary).

Salaj, J. & Began, A., 1963: Faciálne vývoje a mikrobiostratigrafia vrchnej kriedy bradlového pásma. *Geologické práce, Zprávy*, 30, 113 – 120 (in Slovak, German summary).

Salaj, J. & Köhler, E., 2001: Kampánsky rod *Praesiderolites* zo Západných Karpát. *Mineralia Slovaca*, 33, 351–360 (in Slovak, English summary).

Salvador, A. (ed.), 2013: International Stratigraphic Guide. *Boulder, Geological Society of America*, 214 pp. https://doi.org/10.1130/9780813774022.

Samuel, O., Salaj, J. & Began, A., 1980: Litostratigrafická charakteristika vrchnokriedových a paleogénnych sedimentov Myjavskej pahorkatiny. *Západné Karpaty, séria Geológia*, 6, 81 – 111 (in Slovak, English summary).

Stráník, Z., Bubík, M., Krejčí, O., Marschalko, R., Švábenická, L. & Vůjta, M., 1995: New litostratigraphy of the Hluk Development of the Bílé Karpaty unit. *Geologické práce, Správy*, 100, 57–69.

Stur, D., 1860: Bericht über die geologische Uebersichts--Aufnahme des Wassergebietes der Waag und Neutra. *Jb. K.-Kön. geol. Reichsanst.*, XI, 1, 17–151 (in German).

Teťák, F. & Potfaj, M. (eds.), Havrila, M., Filo, I., Pešková, I., Boorová, D., Žecová, K., Laurinc, D., Olšavský, M., Siráňová, Z., Buček, S., Kucharič, Ľ., Gluch, A., Šoltés, S., Pažická, A., Iglárová, Ľ., Liščák, P., Malík, P., Fordinál, K., Vlačiky, M. & Köhler, E., 2015: Vysvetlivky ku geologickej mape Bielych Karpát (južná časť) a Myjavskej pahorkatiny v mierke 1 : 50 000. *Bratislava, Štátny geologický ústav Dionýza Štúra*, 306 pp. (in Slovak).

Teťák, F., Pelech, O., Laurinc, D., Olšavský, M., Fekete, K., Vitovič, L., Maglay, J., Madzin, J., Demko, R. & Žecová, K., 2024: Geologická mapa Oravskej Magury v mierke 1 : 25 000 (západná časť). Čiastková záverečná správa geologickej úlohy. *Manuscript. Bratislava, Archive of St. Geol. Inst. of D. Štúr*, 153 pp. (in Slovak).

Teťák, F., Pelech, O., Laurinc, D., Olšavský, M., Fekete, K., Vitovič, L., Maglay, J., Demko, R. & Korábová, K., 2025: Geologická mapa Oravskej Magury v mierke 1 : 25 000 (východná časť). Čiastková záverečná správa geologickej úlohy. *Manuscript. Bratislava, Archive of St. Geol. Inst. of D. Štúr*, 150 pp. (in Slovak).

Velić, I., 2007: Stratigraphy and Palaeobiogeography of Mesozoic Benthic Foraminifera of the Karst Dinarides (SE Europe). *Geologia Croatica*, 60, 1, 1–113.

Vicedo, V. & Robles-Salcedo, R., 2022: Late Cretaceous larger rotaliid foraminifera from the westernmost Tethys. *Cretaceous Research*, 133, 105137, 1–31. https://doi.org/10.1016/j.cretres.2022.105137.

Santónsko-kampánske jemnozrnné a biodetritické fácie v púchovskom súvrství zdokumentované v oravskom úseku pieninského bradlového pásma

Táto práca predstavuje nové poznatky o púchovskom súvrství oravského úseku bradlového pásma. Termín púchovský slieň v bradlovom pásme na Strednom Považí zaviedol Stur (1860, s. 115) pôvodne na označenie červených a sivých slieňov vrchnokriedového veku. Pestré, najčastejšie červené sliene majú názvy definované pomerne nevhodne, len na základe svojho veku, geografického výskytu alebo príslušnosti k rôznym tektonickým jednotkám [v čorštynskej sukcesii chmielowské sliene (alb) a púchovské sliene s. s., resp. súvrstvie Jaworiek (cenoman – mástricht); kysucké (turón), lalinocké (cenoman) a gbelianske vrstvy, resp. súvrstvie (santón – mástricht) v kysuckej sukcesii atď.]. Súvrstvie tvoria ružové až tehlovo červené, zriedkavo aj zelené alebo sivé slieňovce až ílovité vápence alebo vápnité bridlice. Navetraná sutina slieňovcov až vápencov môže obsahovať vyvetrané globotrunkány pozorovateľné pod lupou. Zvetrané slieňovce niekedy tvoria červené eluviálne hliny. Pri geologickom mapovaní bolo možné od červených slieňovcov odlíšiť biele jemnozrnné až prachovité vápence s globotrunkánami a telesami kalkarenitov. Osobitosť týchto hornín, čiastočne odčleňovaných od púchovských vrstiev,

bola známa už skôr (Marschalko et al., 1979; Gross et al., 1993). Salaj a Köhler (2001) ich označovali ako tzv. vývoj Lučivného vrchu. Tento názov však ďalej neodporúčame používať pre možnosť zámeny s lučivnianskym súvrstvím.

Dominantnú časť novodefinovanej litostratigrafickej jednotky označenej ako **kňažiansky člen** alebo člen Kňažej (nový termín), resp. vrstvy Kňažej, tvoria tenkodoskovité až lavicovité biele až svetlosivé prachovité vápence s globotrunkánami. Litostratigrafická jednotka je súčasťou púchovského súvrstvia. Niekedy môžu byť podobné pieninskému súvrstviu, odlišujú sa však prachovitým vzhľadom, slabšou litifikáciou (rozpad aj po ľahšom údere kladiva) a ostrohranným až čriepkovitým rozpadom. Mikrofaciálne predstavujú kalové vápence (*wackstone* až *packstone*) s hojnými prierezmi planktonických dvojkýlových foraminifer. Miestami obsahujú prevrstvenia rôzne hrubých (2 – 4 m) doskovitých biodetritických vápencov – kalkarenitov. Vrstvy Kňažej sú pomenované podľa miestnej časti Dolného Kubína – Kňažia. Stratotyp sa nachádza v počve a záreze lesnej cesty severne od Kňažej medzi bodmi P198 a P247 (obr. 1, tab. 1). Druhým podobným výskytom je oblasť Lučivného vrchu (841 m n. m.) severne od Podbiela. Celkovo dosahujú hrúbku okolo 50 – 200 m. Vek globotrunkánových vápencov vrstiev Kňažej je na základe výskytu planktonických a bentických foraminifer stredný kampán.

Vápence bradlianskeho typu (alebo pôvodne vápence Širokého bradla redefinované v práci Teťák et al., 2015) predstavujú sivé kalkarenity, biodetritické vápence, brekcie a zlepence. Väčšinou sú masívne, miestami laminované alebo šikmo zvrstvené. Často obsahujú intraklasty bielych globotrunkánových vápencov vrstiev Kňažej. Tvoria výplne kanálov alebo vejáre plytkovodného detritu zarezané v rôznych častiach vrstiev Kňažej, resp. môžu erodovať najvyššiu časť podložného snežnicko-sromowského súvrstvia. Zriedkavo obsahujú aj medzivrstvy exotických zlepencov a vzácne v nich boli pozorované aj telesá s fragmentmi rudistových rifov. Termín zaužívaný v brezovskej skupine (Samuel et al., 1980; Potfaj et al., 2014) bol použitý kvôli zhodnému litologickému charakteru a zhodnej stratigrafickej pozícii uvedených kalkarenitov. Kalkarenity, resp. biodetritické vápence tvoria šošovkovité telesá hrubé 5 – 50 m. Hierarchicky sú súčasťou púchovského súvrstvia.

Stratotyp v rámci skúmaného úseku bradlového pásma sa nachádza v hrebeni Opáleného (lokalita P138 z. od Širokej, resp. Oravského Podzámku). Ďalšie profily sú v oblasti zárezu lesnej cesty v masíve Lučivného vrchu (lokality P963 – P967 severne od Podbiela). Osobitý význam má výskyt s asociáciou biodetritických vápencov s rudistami a exotikami v doline Hldočín (lokalita P978 z. od Zemianskej Dediny). Vek vápencov bradlianskeho typu bol doložený na základe mikrofauny planktonických a bentických foraminifer a makrofauny rudistov ako vrchný santón – vrchný kampán (Salaj a Köhler, 2001; Kühn a Andrusov, 1942).

Doručené / Recieved: 6. 6. 2025
Prijaté na publikovanie / Accepted: 1. 9. 2025

Mineralia Slovaca, Web ISSN 1338-3523, ISSN 0369-2086, https://doi.org/10.56623/ms.2025.57.1.5
57, 1 (2025), 81 – 96, © Authors 2025. CC BY 4.0

Alternative interpretation of the Bystrica Unit in Klanečnica KLK-1 borehole (Magura Nappe)

FRANTIŠEK TEŤÁK[1], KATARÍNA KORÁBOVÁ[1] and DUŠAN LAURINC[1]

[1]State Geological Institute of Dionýz Štúr, Mlynská dolina 1, 817 04 Bratislava, Slovak Republic;
frantisek.tetak@geology.sk

Abstract: In 1986, the KLK-1 (Klanečnica) borehole was drilled northwest of Moravské Lieskové as part of a regional oil and gas exploration programme. The well reached a total depth of 662 m and was intended to verify the occurrence and potential accumulation of hydrocarbons within the Drietoma anticline, a geophysically indicated structural high in the St. Hrozenkov–Drietoma area. The drilled succession was originally assigned to the Svodnice Fm. of the Biele Karpaty Unit down to 75 m, and to the Zlín Fm. of the Rača Unit below this depth. However, a re-examination of the preserved core material suggests that the presence of glauconitic sandstones and an inferred middle to late? Eocene age do not support the previous correlation with the Rača Unit. The lower interval of the borehole, below approximately 90 m, is here reinterpreted as belonging to the Bystrica Mb. of the Bystrica Unit. The borehole cores reinterpretation is supported by the abundant occurrence of larger foraminifera, lithologically variable quartz-glauconitic sandstones, and thick beds of dark grey silty claystones to marlstones, all characteristics also of the Bystrica Mb. Furthermore, the western extent of the Bystrica Unit does not appear to terminate at the Nezdenice Faults, as previously supposed, but continues westwards beneath the Biele Karpaty Unit, albeit to a limited subsurface extent.

Key words: Bystrica Mb., Vsetín Mb., Magura Nappe, Flysch Belt, structural high, hydrocarbon exploration

Graphical abstract

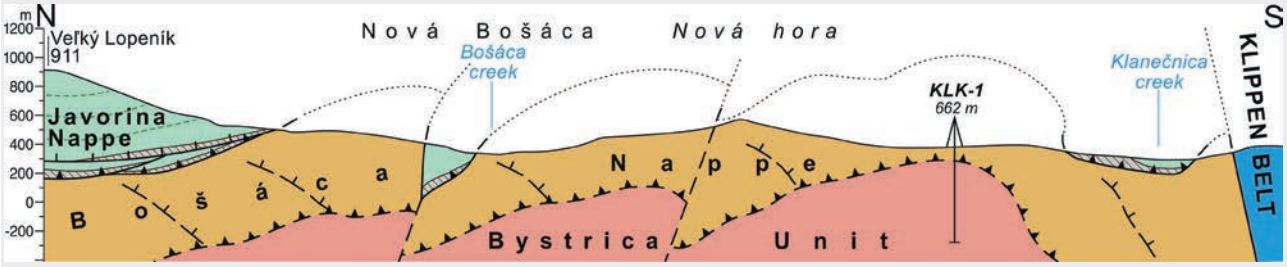

Highlights

- KLK-1 borehole – depth 662 m – drilled in 1986 as part of hydrocarbon exploration – may represent one of the few known occurrences of the Bystrica Unit west of the Nezdenice Faults
- 0–90 m: Svodnice Fm. (Biele Karpaty Unit – Paleocene to early Eocene quartz-carbonate sandstones)
- 90–662 m: previously assigned to the Zlín Fm. (Vsetín Mb. of Rača Unit), is here reinterpreted as the Bystrica Mb. (Bystrica Unit), all in Magura Nappe (quartzy glauconitic sandstones with abundant redeposited larger foraminifera, and thick beds of dark grey silty claystones to marls; nannoplankton: middle Eocene – NP17, Bartonian)

Introduction

Drilling in the western part of the Flysch Belt commenced before and continued during the First World War, targeting structures considered prospective for oil accumulation. Deep wells were drilled in the Kysuce region, including Korňa T1 and Svrčinovec SVR-1. During the interwar period, additional wells were completed – T2 (Predmier) and S-1 (Staškov) (Plička et al., 1958).

At the turn of the 1950s and 1960s, the B-2 well (665 m; Oravská Polhora; Porubský et al., 1963) continued the verification of potential hydrocarbon accumulations. In the 1980s, drilling depths increased to 1200 m: in addition to shallow mapping wells such as KLK-1 (Klanečnica, 662 m), several deep structural boreholes were realised mainly in eastern Slovakia, including Zboj-1 (5002 m; Ďurkovič et al., 1982), Smilno-1 (5700 m; Leško et al., 1987), FPJ-1 Oravská Polhora (2417 m; Potfaj et al., 1989), and Zborov-1 (5500 m; Wunder et al., 1990).

This period coincided with deep structural drilling in the Czech Flysch Belt, e.g. Jablůnka-1 (6506 m; Pesl et al., 1982) and Gottwaldov-2 (4790 m). Although Lubina-1 (3236 m; Leško et al., 1982) was located south of the Flysch Belt, it penetrated Magura Nappe flysch successions at interval 2706–3236 m. Some boreholes also served multidisciplinary purposes: FPJ-1 (Oravská

Polhora) was also aimed at the exploration of a I-Br water reservoir (Franko & Potfaj, 1983), and SVR-1 evaluated the potential for Carboniferous coal seams beneath the Flysch Belt (Plička et al., 1958).

Leško (1980) proposed drilling a 6500 m borehole to investigate the basement of the Flysch Belt and potential hydrocarbon accumulations in the St. Hrozenkov–Drietoma area. Significant seismic reflectors beneath the flysch sequences, between 4000–6500 m depth, were targeted. Gravimetric and seismic data (Tomek, 1976) suggested low-density bodies beneath the Bystrica Unit in the Zárieče–Kolárovice area represented Oligocene–Miocene molasse deposits folded beneath the flysch and Inner Carpathian units.

The Drietoma area was selected for its presumed basement uplift, the "Drietoma Structure", interpreted from seismic and gravimetric data (Leško, 1980). Reflectors at ~3500 m were attributed to the base of the Biele Karpaty Unit, at ~6000 m to the base of the Magura Nappe, and at ~7000 m to the crystalline basement, possibly overlain by a Paleozoic–Mesozoic to Miocene(?) sedimentary cover.

Similar conclusions were reached by Němec (1978, 1980), who termed the structure in front of the Pieniny Klippen Belt the "Hrozenkov Elevation" based on seismic profiles 109R/76, 124R/76, and 124A–C/77. Potfaj (1986a, b) later summarised geophysical data from Drietoma–Klanečnica, highlighting the ambiguity in interpreting such elevation. Although the projected deep borehole (Leško, 1980) was planned for 1981, it had been never drilled.

Another borehole within the Drietoma elevation was initially proposed by Kysela (1984 in Potfaj & Bodiš, 1987) in the Drietoma Valley, but the location was later changed to the right-bank valley of a Klanečnica tributary opposite the settlement of Plevovec, but was ultimately relocated and drilled in the valley of its left-bank tributary northwest of Moravské Lieskové village, approximately 40 m from the stream, on the right bank at an elevation of 345 m (approx. 48.86236° N; 17.76045° E; Potfaj et al., 1986; Dvořáková et al., 1989).

Drilling of the KLK-1 borehole took place from August to November 1986, reaching 662 m instead of the

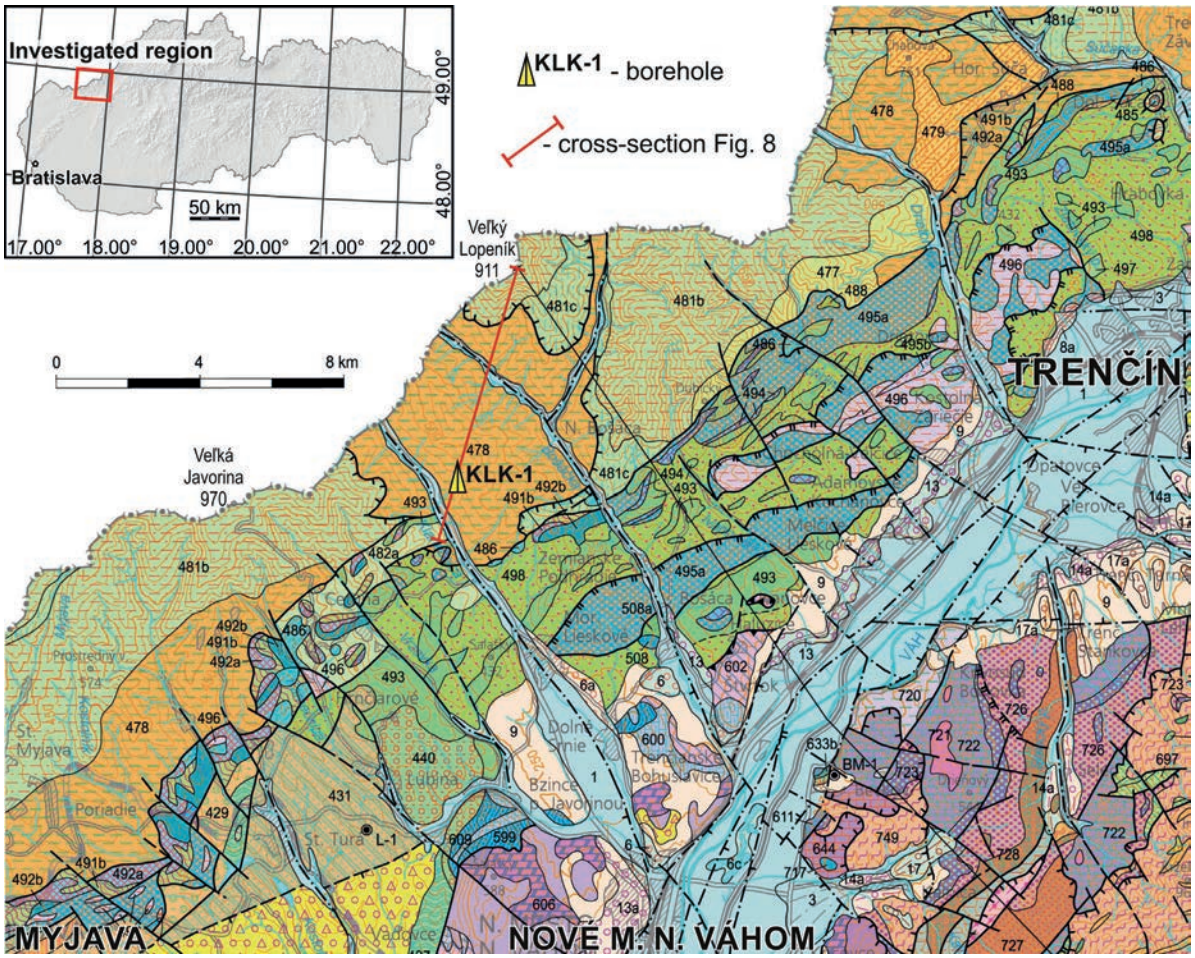

Fig. 1. Geological map displaying the location of the Klanečnica KLK-1 borehole (geological map of Elečko et al., 2008).
(Biele Karpaty Unit: 477 – Drietomica Beds, 478 – Svodnice Fm., 481b – Javorina Beds, 481c – Ondrášovec Beds, 482-513 – Pieniny Klippen Belt)

planned 650 m. Project documentation and detailed well evaluation are not preserved in the Geofond archive; only brief characterisations exist (Potfaj et al., 1986; Potfaj & Bodiš, 1987).

The borehole was part of hydrocarbon exploration in the Flysch Belt, targeting the verification of an anticlinal structure in the Nová hora area. Objectives included assessing basal sequences of the Biele Karpaty Unit and, where possible, the tectonic footwall, alongside petrogeochemical analyses (organic content, maturation) and reservoir properties (Potfaj et al., 1986).

Lithostratigraphic interpretation by Potfaj et al. (1986) assigned the uppermost 75 m of the borehole to the Svodnice Fm. of the Biele Karpaty Unit (Paleocene to early Eocene) and below a breccia interval interpreted as a thrust zone of the Biele Karpaty Unit; from approximately 75 m depth the underlying succession was assigned to the Zlín Fm. of the Rača Unit. Methane emissions were observed within the tectonic breccia at 75 m. At depths of 118, 134, 216, 318, and 505 m, methane-rich Na–Cl–HCO_3–I–Br waters were encountered, with maximum flow rates of 0.1 to 3.5 $l \cdot s^{-1}$ and temperatures up to 16 °C.

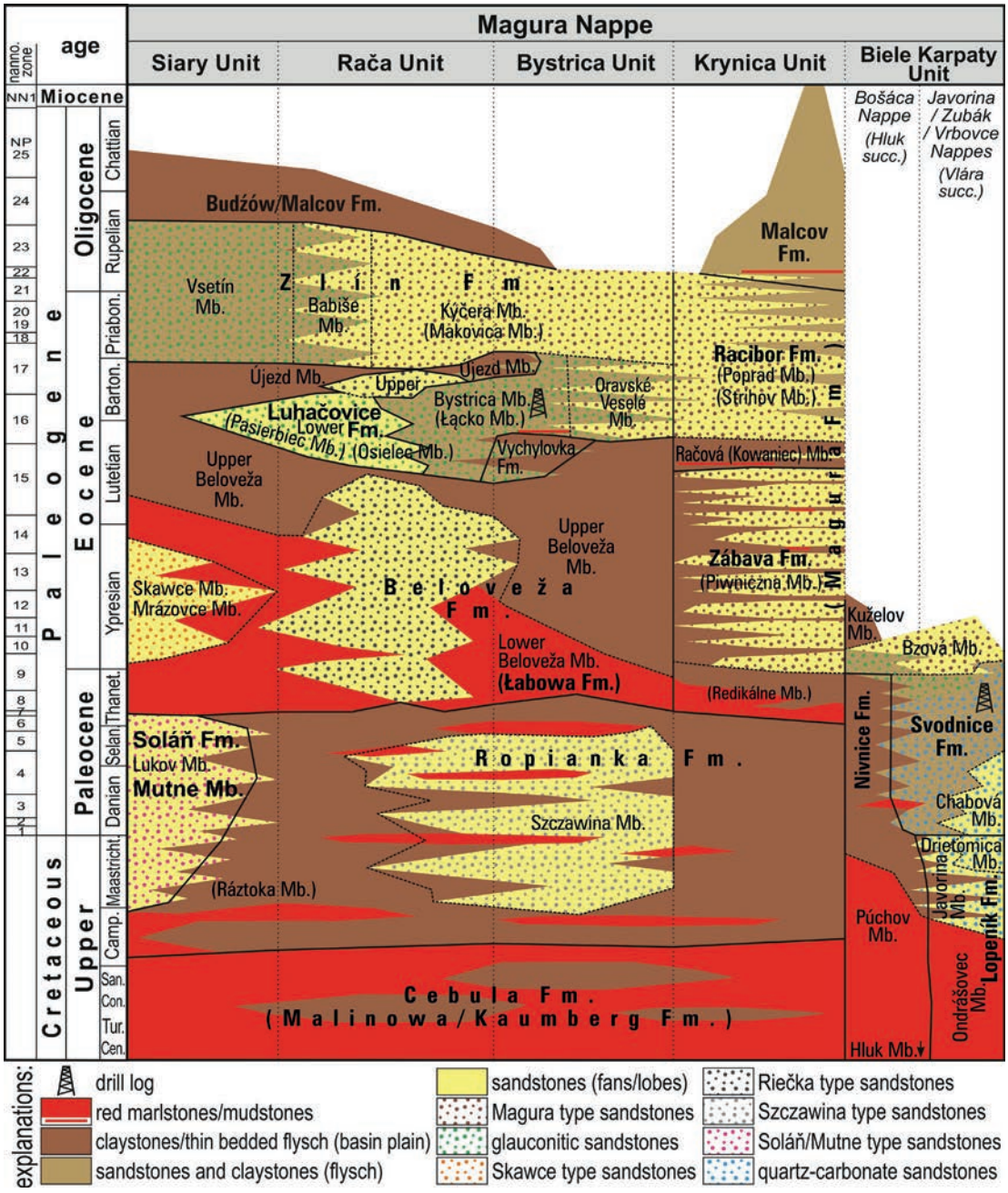

Fig. 2. Lithostratigraphic scheme of the Slovak western part of the Magura Nappe (Hók et al., 2019).

Iodine concentrations reached approximately 27 mg·l^{-1}. These waters are hosted in fracture-controlled reservoirs within sandstones and sandy claystones (Potfaj & Bodiš, 1987). Rock physical properties of the KLK-1 were studied by Dvořáková et al. (1989).

Simplified KLK-1 borehole profile (detailed description: Potfaj et al., 1986, p. 49; Potfaj & Bodiš, 1987)**:**

0–7.3 m: Quaternary alluvium: brown sandy-clayey gravels and clays with sandstone pebbles.

7.3–75.6 m: Svodnice Fm., Biele Karpaty Unit: alternating sandstones and claystones. The sandstones are predominantly fine-grained to silty, less commonly medium- to coarse-grained, with Ta, Tb, and Tc Bouma intervals. They are grey, laminated, contain muscovite, and show abundant plant detritus on lamination surfaces. Basal bed surfaces commonly exhibit bioglyphs. Bed thickness ranges from 1 to 250 cm. Claystones are grey, calcareous, occasionally dark grey, often with silty admixture. Dark grey claystones dominate within the deeper parts. The sandstone-to-claystone ratio is approximately 0.6, increasing to 0.8 at greater depths. Both sandstone proportion and bed thickness gradually increase with depth. At interval 25–25.5 m, a light grey marlstone to limestone occurs (so-called "treskúň" or "ruin marble"; Fig. 3; Marko et al., 2003). The succession is tectonically disturbed, with zones of slaty cleavage.

72.2–75.6 m: Tectonic breccia composed of fine-grained laminated sandstones within a slaty clay matrix.

75.6–80.5 m: Light grey calcareous muscovitic fine-grained sandstones, 5–20 cm thick, interbedded with grey to dark grey calcareous claystones, 5–10 cm thick. Sandstone-to-claystone ratio ~0.7.

80.5–84.3 m: Tectonic breccia of strongly shaly grey calcareous claystones containing fragments of fine-grained laminated muscovitic sandstones and siltstones, with two beds of 15–20 cm thick fine-grained sandstones.

75.6–662 m: Zlín Fm., Rača Unit: alternating sandstones and claystones. The dominant lithology is dark grey to brown silty calcareous claystones, 1–4 m thick. In the upper parts of cycles, thin 1–3 cm layers of bluish-green non-calcareous claystones occur. Rare pyrite streaks and nests are present in the brown claystones; contacts with grey-green claystones are usually bioturbated. The sandstones are represented by three types: a) greenish-grey glauconitic, fine-grained, with muscovite-rich laminae; b) light grey arkosic, displaying well-developed grading from coarse to fine-grained, some of which contain larger foraminifera, with bed thicknesses from a few cm up to 5.5 m; c) grey, poorly sorted, medium- to coarse-grained wacke sandstones up to 2 m thick. The sandstone-to-claystone ratio is ~0.3, locally higher in sandstone-dominated zones. Beds dip up to 40°, locally up to 75°. The succession is folded, with several overturned sequences; cores are cross-cut by calcite veins, and open fractures are present throughout the borehole.

Methods

Revision of KLK-1 was carried out as part of the geological mapping and research of the Biele Karpaty Mts. region during 2016–2020 (Pešková et al., 2021; Teťák et al., 2024) studying 48 core samples (Tab. 1). Samples were macroscopically examined and photographed. Two grey calcareous claystone samples from depths of 386.8 m and 482.2 m were analyzed for nannoplankton assemblages, while two quartzy glauconitic sandstone samples from depths of 197.0 m and 568.5 m were studied petrographically. Modal analysis of 500 grains per thin section was performed using an Eltinor 4 point-counting system.

Results

Based on the inspection of preserved core samples, we note a striking similarity in the macroscopic appearance of the glauconitic sandstones with the sandstones of the Bystrica Mb. (Tab. 1). We conclude that neither the presence of glauconitic sandstones nor a middle to late? Eocene age justify assignment to the Zlín Fm. (Vsetín Mb.) of the Rača Unit. In the upper part of the borehole, down to approximately 90 m, we agree with the assignment to the Svodnice Fm. of the Biele Karpaty Unit, consistent with the sequence observed in the vicinity of the borehole (Potfaj et al., 1986; Pešková et al., 2021).

Below the ~90 m, the borehole is reinterpreted as the Bystrica Mb. of the Bystrica Unit, characterized in core samples by abundant occurrence of larger not determined redeposited foraminifera in quartzy glauconitic sandstones and thick beds of dark grey claystones. In certain cases, the Svodnice Fm. of the Hluk succession of the Biele Karpaty Unit with glauconitic sandstones could be considered (cf. Teťák, 2016); however, its Paleocene to early Eocene age is older than the middle Eocene age determined for the sediments. The glauconitic sandstones from the borehole cores differ macroscopically indistinctly from those of the Vsetín Mb.

Nannoplankton analysis (Korábová in Pešková et al., 2020; Teťák et al., 2024) confirms a middle Eocene (NP17, Bartonian) age for samples at 386.8 m and 482.2 m. The assemblage, although low-diversity (Tab. 2), includes characteristic species typical of the middle Eocene: *Cyclicargolithus floridanus* (Roth & Hay) Bukry, *Reticulofe-*

Tab. 1

Macroscopic description of KLK-1 Klanečnica borehole core samples (explanations of abbreviations: cgs./mgs./fgs. – coarse-/medium-/fine-grained sandstone, Qks – quartz-carbonate sandstone, tectonics – tectonically fractured and calcite-healed).

Depth [m]	Lithology	Stratigraphy	Figure
17.4	fgs. Qks plant detritus, convolute and wavy laminated	Svodnice sst.	
25.2	limestone brownish-grey bioturbated	limestone	Fig. 3
25.8	fgs. Qks plant detritus, pyrite, laminated, + siltstone laminated, plant detritus	Svodnice sst.	
31.4	mgs.-(fgs.) Qks, plant detritus, massive, muscovite, tectonics	Svodnice sst.	
37.7	fgs. quartzy, dark green to glassy, laminated, a lot of glauconite	glauc. sst.	
48.6	fgs. Qks, plant detritus, laminated, (muscovite), tectonics	Svodnice sst.	
65.2	fgs. Qks, plant detritus, massive?, tectonics	Svodnice sst.	
77.2	fgs. Qks, plant detritus, cross bedded, muscovite, tectonics	Svodnice sst.	Fig. 4A
89.0	silty claystone hard grey calcareous, plant detritus, fissured (filled by fgs. Qks.), tectonics	Svodnice sst.	
92.8	fgs. quartzy greenish-grey, a lot of glauconite, muscovite, plant detritus, laminated	glauc. sst.	
108.6	silty claystone hard calcareous grey, fissured, plant detritus, tectonics (rusty a calcite veins)	claystone	
124.6	silty claystone brownish-grey calcareous, plant detritus, tectonics	claystone	
129.6	marlstone light grey, pyrite fills bioturbation), fissured, tectonics	claystone	
133.4	mgs. poorly sorted (?slump) massive, larger foraminifera, less glauconite, plant detritus, muscovite, tectonics	glauc. sst.	
142.6	silty claystone to siltstone light, plant detritus, tectonics	claystone	
144.8	siltstone light grey, plant detritus, muscovite, ?glauconite	claystone	
153.3	fgs. laminated, plant detritus, muscovite, medium glauconite, tectonics	glauc. sst.	
156.3	siltstone brownish-grey calcareous, plant detritus, muscovite, medium glauconite	glauc. sst.	
163.5	fgs. Qks laminated, muscovite, plant detritus, (?no glauconite)	Svodnice sst.?	
169.8	claystone light, soft, calcareous	claystone	
197.0	mgs. to fgs. Qks grey massive, a lot of glauconite, larger foraminifera, muscovite, plant detritus	glauc. sst.	Fig. 4B, 6
208.6	fgs. quartzy, a lot of glauconite, laminated, plant detritus, muscovite	glauc. sst.	Fig. 4C
211.7	siltstone dark brownish-grey, bioturbation (filled by fgs.), plant detritus, muscovite, (?glauconite), laminated	claystone	
212.4	silty claystone brownish-grey, plant detritus, muscovite, tectonics	claystone	
263.7	claystone dark grey, muscovite	claystone	
266.5	fgs. grey quartzy, a lot of glauconite, laminated, plant detritus, muscovite	glauc. sst.	
271.5	mgs. quartzy, medium glauconite, massive	glauc. sst.	Fig. 4D
279.3	fgs. quartzy, a lot of glauconite, tectonics, fissured	glauc. sst.	
285.5	claystone-siltstone claystone dark brownish-grey, bioturbated, plant detritus, (?glauconite)	claystone	
313.2	claystone-silty claystone dark brownish-grey calcareous, bioturb., plant detritus, (?glauconite)	claystone	
317.8	fgs. quartzy, a lot of glauconite, larger foraminifera, laminated, plant detritus	glauc. sst.	Fig. 4E
342.0	silty claystone grey, plant detritus	claystone	
383.5	fgs. quartzy, a lot of glauconite, laminated, tectonics	glauc. sst.	Fig. 4F
386.8	claystone grey calcareous plant detritus, muscovite	claystone	Fig. 5
425.0	mgs. to fgs. quartzy massive, a lot of glauconite	glauc. sst.	Fig. 4G

Tab. 1 – continued

Depth [m]	Lithology	Stratigraphy	Figure
436.5	fgs. quartzy, a lot of glauconite, larger foraminifera, massive	glauc. sst.	
441.2	claystone dark grey, plant detritus, tectonics	claystone	
469.5	fgs. quartzy, a lot of glauconite, massive, tectonics	glauc. sst.	Fig. 4H
482.8	claystone dark grey calcareous	claystone	Fig. 5
531.5	fgs. quartzy, a lot of glauconite, muscovite, plant detritus, laminated	glauc. sst.	
561.4	silty claystone dark grey, plant detritus, bioturbation (filled by glauconite fgs.)	glauc. sst.	
568.5	cgs. grey quartzy, larger foraminifera, massive, a lot of glauconite, (tectonics)	glauc. sst.	Fig. 4I, 6
580.5	silty claystone dark grey, plant detritus, bioturbation (filled by glauconite fgs.)	glauc. sst.	
608.5	mgs. to fgs. quartzy, a lot of glauconite, larger foraminifera	glauc. sst.	Fig. 4J
619.5	silty claystone dark grey, plant detritus, muscovite	claystone	
635.0	siltstone-(fgs.) laminated, plant detritus, a lot of glauconite, muscovite, tectonics	glauc. sst.	
660.0	silty claystone dark grey, plant detritus, muscovite, (laminated), tectonics	claystone	
661.0	fgs. quartzy, a lot of glauconite, (laminated), (plant detritus)	glauc. sst.	

nestra bisecta (Hay, Mohler & Wade) Roth, *R. hillae* Bukry & Percival, *R. lockeri* Müller. The samples contained *Helicosphaera compacta* Bramlette & Wilcoxon, *Coccolithus pelagicus pelagicus* (Wallich) Schiller, *Reticulofenestra* cf. *dictyoda* (Deflandre) Stradner, *Sphenolithus anarrhopus* Bukry & Bramlette, *S. moriformis* (Brönnimann & Stradner) Bramlette & Wilcoxon, *Coccolithus formosus* (Kamptner) Wise, and *Zygrhablithus bijugatus bijugatus* (Deflandre) Deflandre, as well. Potfaj et al. (1986) reports the similar assemblage from the depths 121 m, 184 m, 374 m and 552 m.

Tab. 2

Nannoplankton species determined in claystone samples from KLK-1 borehole.

386.8 m	482.2 m	Depth / Nannoplankton species
●	●	*Coccolithus formosus* (Kamptner) Wise
●		*Coccolithus pelagicus pelagicus* (Wallich) Schiller
	●	*Coccolithus* sp.
●	●	*Cyclicargolithus floridanus* (Roth & Hay) Bukry
●		*Discoaster deflandrei* Bramlette & Riedel
●	●	*Helicosphaera compacta* Bramlette & Wilcoxon
●		*Chiasmolithus grandis* (Bramlette & Riedel) Radomski
●		*Chiasmolithus* sp.
	●	*Pontosphaera multipora* (Kamptner) Roth
●	●	*Reticulofenestra bisecta* (Hay, Mohler & Wade) Roth
●		*Reticulofenestra* cf. *dictyoda* (Deflandre) Stradner
●	●	*Reticulofenestra hillae* Bukry & Percival
●		*Reticulofenestra lockeri* Müller
●		*Sphenolithus anarrhopus* Bukry & Bramlette
●		*Sphenolithus moriformis* (Brönnimann & Stradner) Bramlette & Wilcoxon
	●	*Zygrhablithus bijugatus bijugatus* (Deflandre) Deflandre
Middle Eocene NP17 Bartonian	Middle Eocene	Age

Petrographically analyzed sandstone samples from depths of 197.0 m and 568.5 m are medium- to coarse-grained, from moderately to well-sorted, and from slightly to very well-rounded, unidirectional, calcareous glauconitic sublitharenites to subarkoses (Tab. 3). Glauconite occurs both as intergranular cement and as oval grains. No chloritization was observed. Fossil organic fragments are variously represented by larger and small foraminifera, filaments, and, for example, red algae. Lithic fragments include carbonates (micro- to sparitic), felsite fragments, and less commonly sandstones, phyllites to gneisses, and granites are present. Calcite cement (sparite) binds the sandstones.

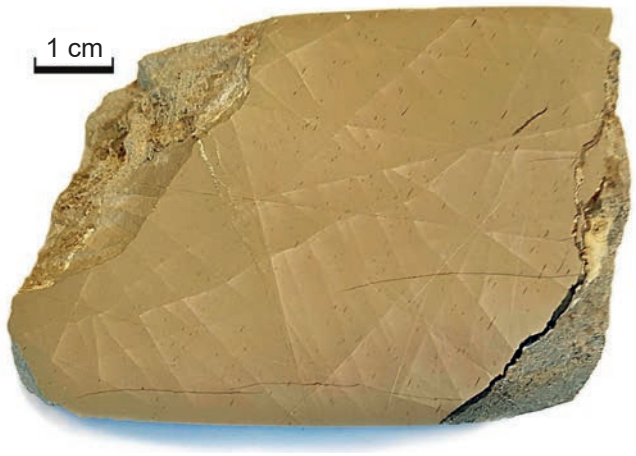

Fig. 3. Light brownish-grey marlstone to limestone (so-called "treskúň" or "ruin marble") from the 25–25.5 m interval.

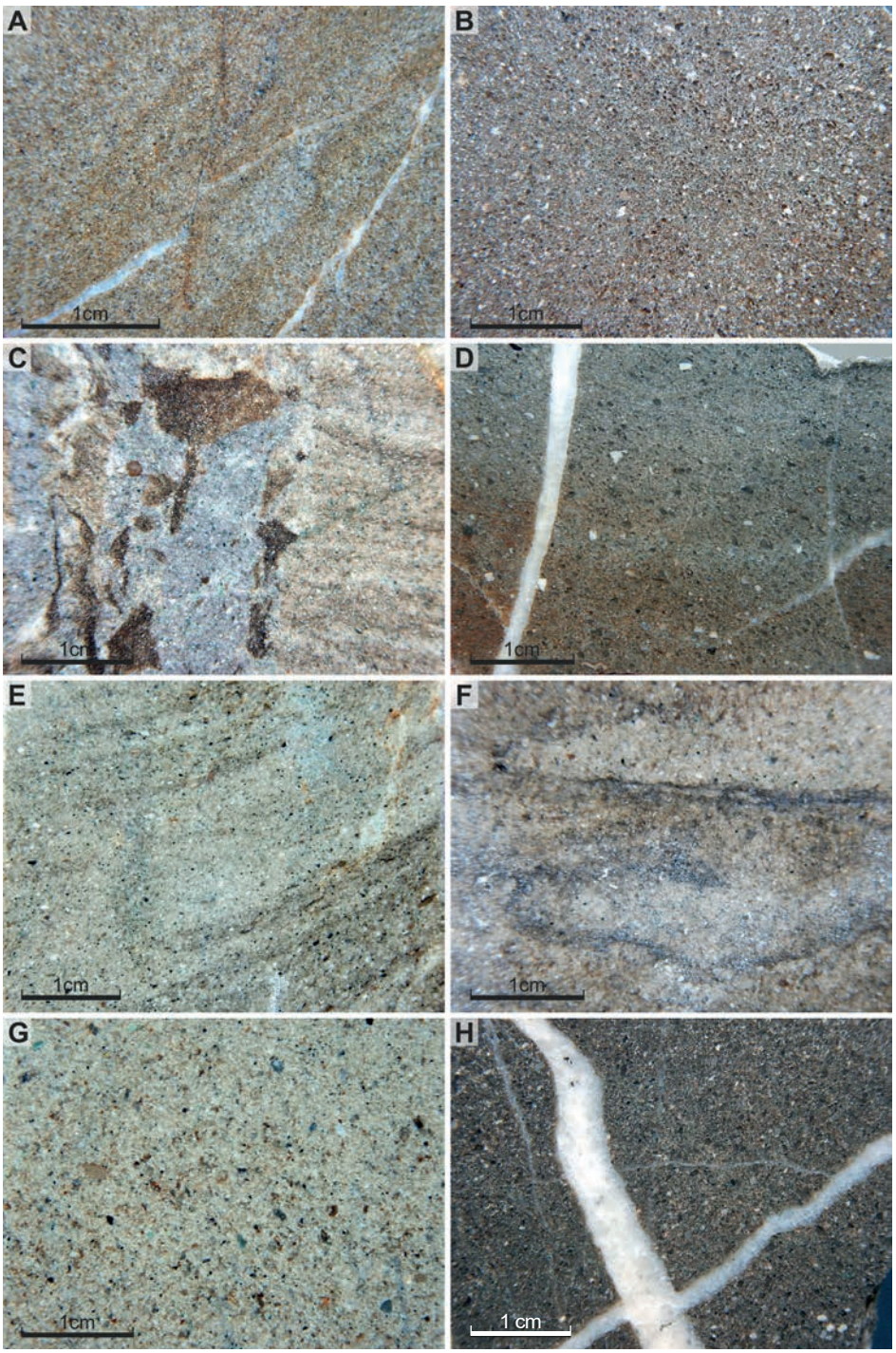

Fig. 4. Polished slabs from sandstone samples of the Klanečnica KLK-1 borehole: (A) laminated fine-grained quartz-carbonate sandstone with muscovite and plant detritus, tectonically fractured – depth 77.2 m (Svodnice Fm.); (B) grey, massive, medium- to fine-grained quartz–carbonate sandstone with muscovite, abundant glauconite, larger foraminifera, and plant detritus – depth 197.0 m (Bystrica Mb.); (C) laminated fine-grained quartzy sandstone with muscovite, abundant glauconite, and plant detritus – depth 208.6 m (Bystrica Mb.); (D) medium-grained quartzy sandstone, medium glauconitic, massive – depth 271.5 m (Bystrica Mb.); (E) laminated fine-grained quartzy sandstone with abundant glauconite and plant detritus – depth 317.8 m (Bystrica Mb.); (F) laminated fine-grained quartzy sandstone with abundant glauconite, tectonically fractured – depth 383.5 m (Bystrica Mb.); (G) massive medium- to fine-grained quartzy sandstone with abundant glauconite – depth 425.0 m (Bystrica Mb.); (H) massive fine-grained quartzy sandstone with abundant glauconite, tectonically fractured – depth 469.5 m (Bystrica Mb.); (I) massive coarse-grained grey quartzy sandstone with larger foraminifera and abundant glauconite – depth 568.5 m (Bystrica Mb.); (J) medium- to fine-grained quartzy sandstone with abundant glauconite – depth 608.5 m (Bystrica Mb.).

Tab. 3

Modal composition of glauconitic sandstone samples of the KLK-1 borehole at depths of 197.0 m and 568.5 m. (Legend: Qm – monocrystalline quartz, Qp – polycrystalline quartz, Silicite – chert, Plg – plagioclase, Kfs – potassium feldspar, Ls – sedimentary rock fragments, Lc – carbonate rock fragments, Lm – metamorphic rock fragments, Lv – volcanic rock fragments, Ms – muscovite, Bt – biotite, Acc – accessory heavy minerals, Fos – fossils, Gl – glauconite, Mx – matrix, Cm – cement).

Depth	Qm	Qp	Silicit	Plg	Kfs	Ls	Lc	Lm	Lv	Ms	Bt	A	Fos	Gl	Mx	Cm
197.0 m	44.04	12.42	0.5	0.33	1.66	0.99	7.45	0.33	0.33	4.64	0	0.83	5.79	9.11	0	11.9
568.5 m	38.1	32.38	1.9	1.9	6.86	0.95	0.95	0.38	2.86	1.52	0.76	1.33	1.14	0.57	0	8.38

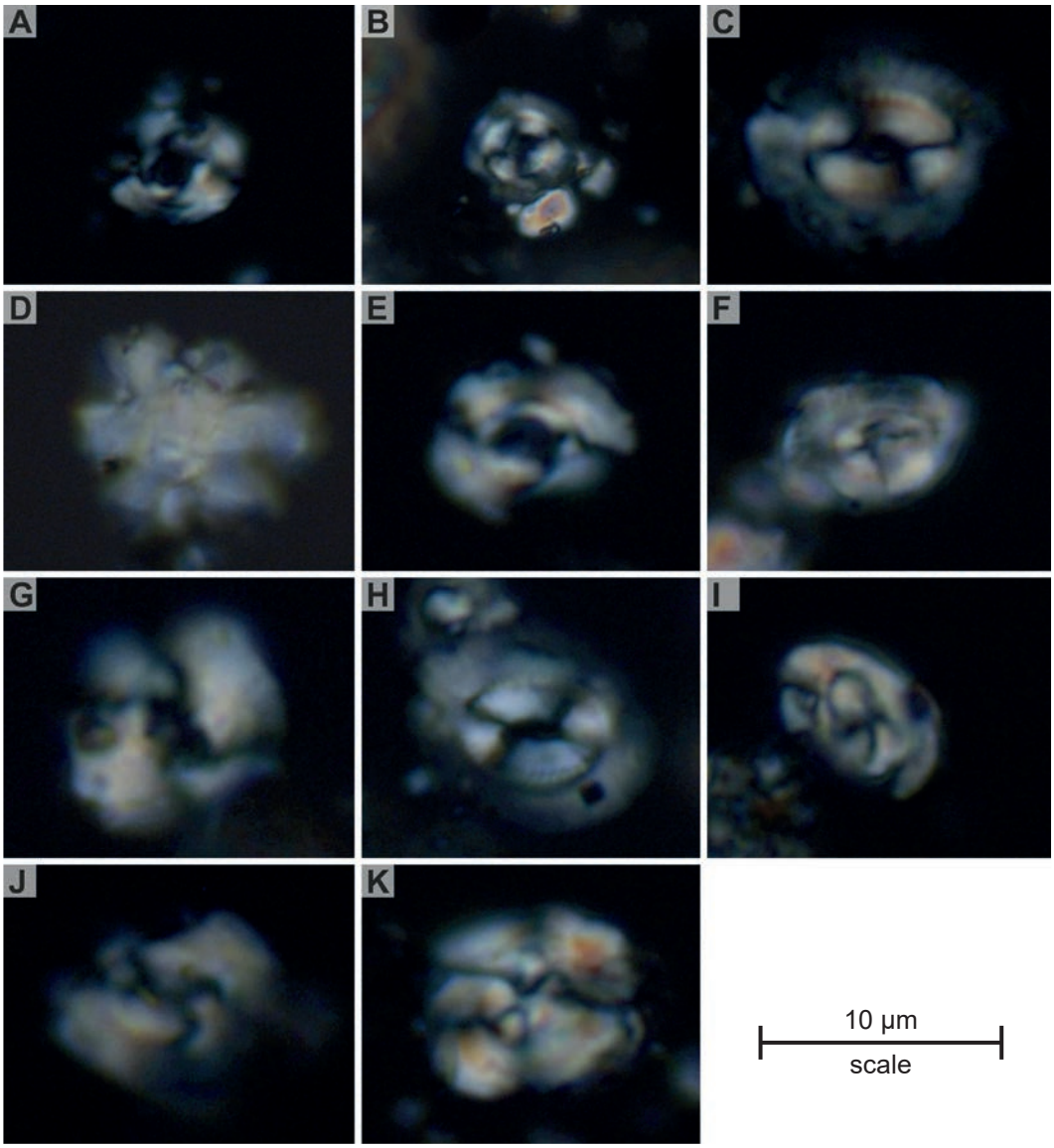

Fig. 5. Representative nannoplankton species from claystone samples of the Klanečnica KLK-1 borehole, observed under crossed nicols, Bystrica Mb. of Zlín Fm. Scale bar = 10 µm: (A) *Cyclicargolithus floridanus* (Roth & Hay) Bukry, depth 482.2 m; (B) *Coccolithus formosus* (Kamptner) Wise, depth 386.8 m; (C) *Coccolithus pelagicus pelagicus* (Wallich) Schiller, depth 386.8 m; (D) *Discoaster deflandrei* Bramlette & Riedel, depth 386.8 m; (E) *Cyclicargolithus floridanus* (Roth & Hay) Bukry, depth 386.8 m; (F) *Helicosphaera compacta* Bramlette & Wilcoxon, depth 386.8 m; (G) *Cyclicargolithus floridanus* (Roth & Hay) Bukry, depth 386.8 m; (H) *Coccolithus pelagicus pelagicus* (Wallich) Schiller, depth 386.8 m; (I) *Helicosphaera compacta* Bramlette & Wilcoxon, depth 482.2 m; (J) *Reticulofenestra* cf. *lockeri* Müller, depth 386.8 m; (K) *Reticulofenestra bisecta* (Hay, Mohler & Wade) Roth, depth 482.2 m.

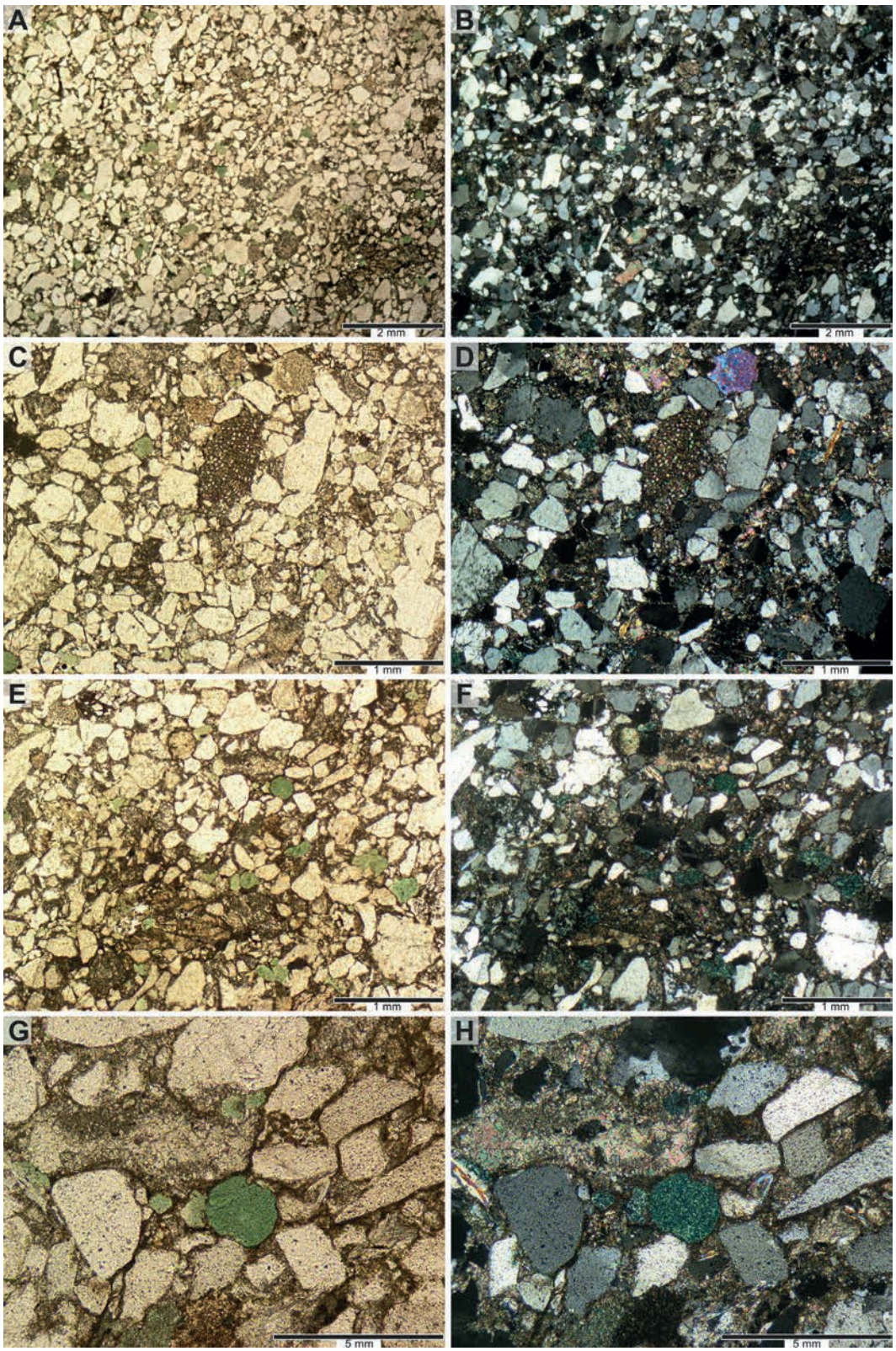
A
2 mm
B
2 mm
C
1 mm
D
1 mm
E
1 mm
F
1 mm
G
5 mm
H
5 mm

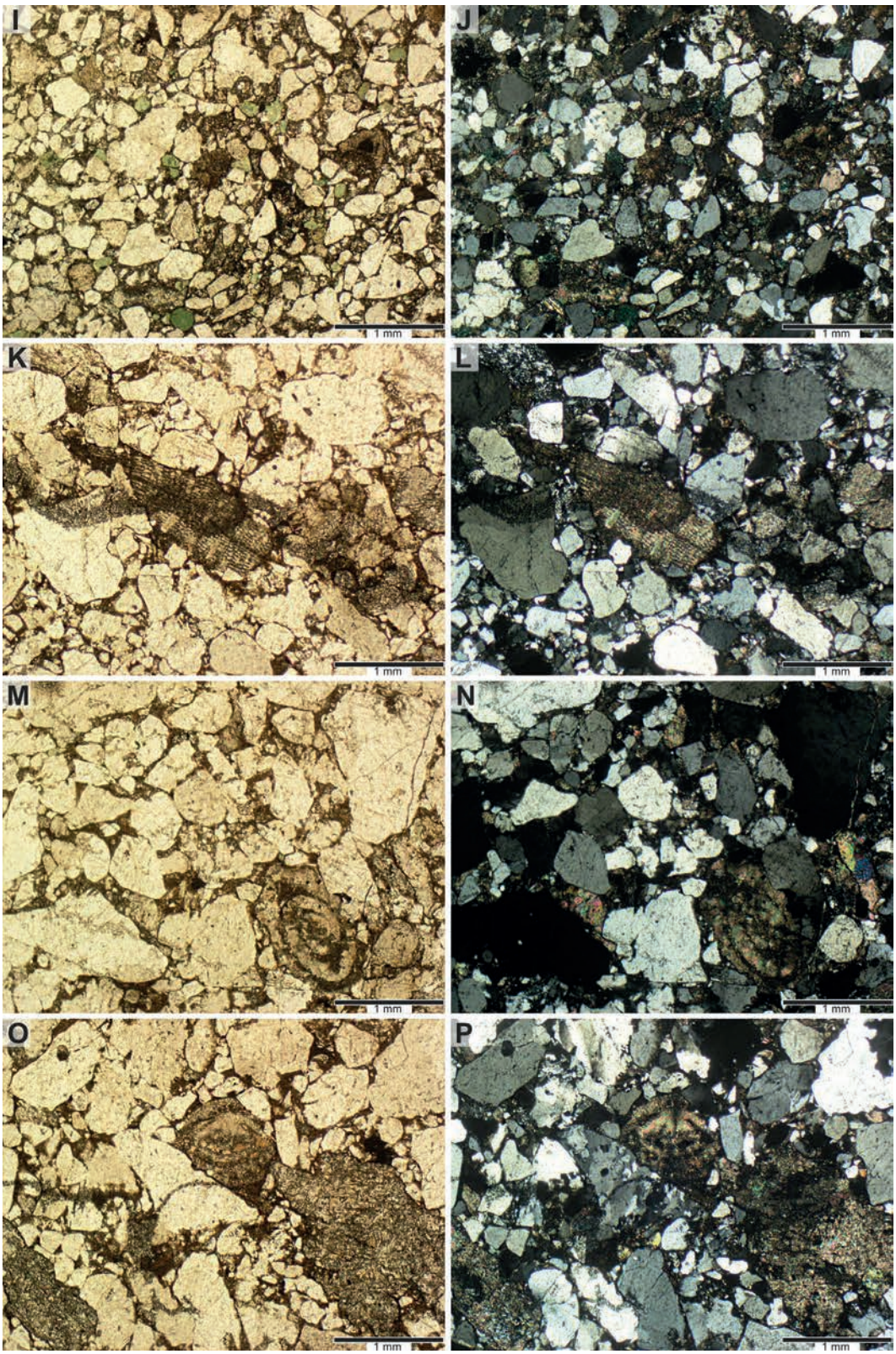

Fig. 6. Quartzy glauconitic sandstones of the Bystrica Mb. from samples of the Klanečnica KLK-1 borehole (IIN and XN pairs): (A–J) grey, massive, medium- to fine-grained quartz-carbonate sandstone with muscovite, abundant glauconite, larger foraminifera, and plant detritus – depth 197.0 m; (K–P) massive, coarse-grained, grey, quartzy sandstone with abundant glauconite and larger foraminifera – depth 568.5 m.

Discussion

Pesl (1968), who introduced the Vsetín Mb., points out that the Vsetín Mb. is very similar to the Bystrica Mb., with the most important diagnostic feature distinguishing the Bystrica Mb. from the Vsetín Mb. being "the presence of hard bluish-grey, whitish, and yellowish-weathering marlstones to limestones and marls with shell-like prismatic disintegration – the so-called Lącko marls". Potfaj et al. (1986) document claystones to marls with thicknesses up to 300 cm in the interval 84.3–141 m in their borehole description.

Another distinguishing feature may be the lithological variability of the sandstones. Even a macroscopic inspection of the sandstone samples from the borehole suggests an affinity to the Bystrica Mb. It is notably lithologically and texturally diverse, with abundant shells of larger foraminifera. Teťák et al. (2016) emphasize the lithological diversity of glauconitic sandstones of the Bystrica Mb. from the Orava region, explaining it by the spatially and temporally varied character of the source area and transport. They distinguish five main types of sandstones, including slump and debris flow bodies observed also in the KLK-1 borehole.

The increased occurrence of larger foraminifera in the glauconitic sandstones of the Bystrica Mb. has been mentioned in several studies (Köhler & Salaj, 1999; Buček & Teťák, 2020). Köhler & Salaj (1999), based on apparently redeposited material from the Bystrica Mb. at the Škaredá locality west of Bytča, assign the described assemblage with *Orbitoclypeus douvillei douvillei* (Schlumberger), *O. varians angoumensis* Less, and *Asterocyclina stellata adourensis* Less to the early Lutetian. Buček & Teťák (2020) studied larger foraminifera in more detail from the Javorníky and Orava localities. Older species, from the Ypresian to Bartonian, were redeposited into the sediments. The age of the sediments can be represented by the youngest species of the Lutetian SBZ 13–16 to the younger Bartonian SBZ 18. The occurrence of larger foraminifera in the Vsetín Mb. is reported but not so typical.

Potfaj et al. (1986) reported the age of sediments from the deeper part of the borehole, based on nannoplankton assemblages, as at least late middle Eocene, possibly even late Eocene. This age does not exclude correlation with either the Vsetín or Bystrica members. The described assemblage includes: *Coccolithus pelagicus* (Wallich) Schiller, *C.* cf. *eopelagicus* (Bramlette & Riedel) Kamptner, *Reticulofenestra umbilica* (Levin) Martini & Ritzkowski, *R.* cf. *coenura* (Reinhardt) Roth, *Chiasmolithus grandis* (Bramlette & Riedel) Radomski, *Ch. expansus* (Bramlette & Sullivan) Gartner, *Ch.* cf. *gigas* (Bramlette & Sullivan) Radomski, *Nannotetrina fulgens* (Stradner) Achuthan & Stradner, *N.* cf. *pappii* (Stradner) Perch-Nielsen, *Discoaster saipanensis* Bramlette & Riedel, *D. tani nodifer* Bramlette & Riedel, *D. barbadiensis* Tan, and *Cyclicargolithus floridanus* (Roth & Hay) Bukry. At present, this assemblage can be considered of middle Eocene age (NP15). Based on the youngest species, *Reticulofenestra umbilica* (NP16–NP22), the sediments can be assigned at most to the upper part of the middle Eocene. However, this would not exclude the Vsetín Mb.

Potfaj et al. (1986) interpret the lower boundary of the Biele Karpaty Unit at the base of the tectonic breccia zone at a depth of 72.2 to 75.6 m. Furthermore, the sandstone samples from depths of 77.2 and 89.0 m are clearly quartz–carbonate sandstones, more characteristic of the Biele Karpaty Unit. Another zone of tectonic breccias occurs at a depth of 80.5–84.3 m. The nearest sandstone core sample from 92.8 m already belongs to glauconitic sandstones. Therefore, we estimate the tectonic interface slightly lower than previously assumed, at approximately 90 m.

The sandstone sample from 163.5 m, based on macroscopic examination, can be classified as quartz-carbonate sandstones typical for the Svodnice Fm. Potfaj et al. (1986) document occasional sandstones without glauconite, or sandstones containing carbonate fragments, as well. Such sandstones were observed in the same stratigraphic position in co-occurrence with glauconite sandstones, in smaller quantities, at several places on the surface in the southernmost part of the Bystrica Unit in the Púchovská dolina Valley (Teťák, 2024), which may indicate that the borehole intersected the southernmost tectonic slices of the Bystrica Unit.

The Bystrica Mb. crops out as well in the southernmost tectonic slice of the Rača Unit in Javorníky Mts., up to a thickness of 450 m (Mello et al., 2005). At the time of drilling the KLK-1 borehole, this position was not known.

Since the Vsetín Mb. occurs in the northern (external) part of the Rača Unit, it is unlikely that the Biele Karpaty Unit would rest on the external part of the Rača Unit without the central part of unit with the Babiše Mb. and the southern part with the Kýčera Mb., as well as the Bystrica Unit with the Bystrica Mb., being preserved at the surface.

At the surface, the Bystrica Unit essentially ends at the Nezdenice Faults, which are among the most prominent neotectonically active transverse faults of the Flysch Belt. This was already pointed out by Potfaj & Bodiš (1987). The Bystrica Unit crops out southwest of the Nezdenice Faults only in minor occurrences near the Vlčnov municipality. The continuation of the Bystrica Unit in the subsurface of the Vienna Basin and the Rhenodanubian region has not been proven (Stráník et al., 2021). The Klanečnica borehole was one of the arguments for terminating the Bystrica Unit at the Nezdenice Faults in the subsurface.

It can therefore be assumed that the Bystrica Unit may continue subsurface to a limited extent further west,

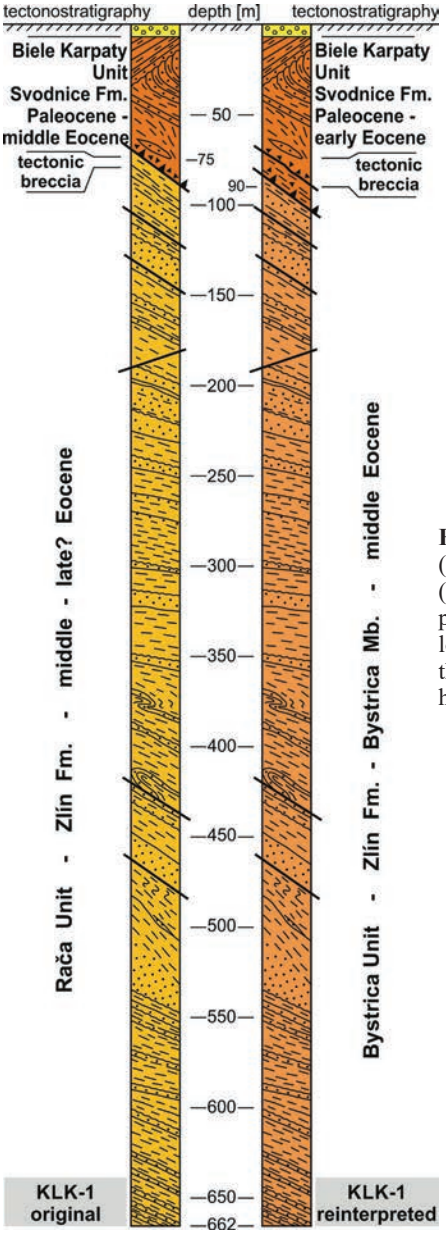

Fig. 7. Original (Potfaj et al., 1986) (left) and reinterpreted (right) lithological profile of the KLK-1 borehole.

where the outer margin of the Biele Karpaty Unit crops out; the sediments of its upper middle Eocene and younger parts have not been preserved, and it is likely that folding had already begun in this part of the Magura Basin in connection with the Rhenodanubian Zone (Teťák et al., 2019).

A detailed technical report with a thorough evaluation of the KLK-1 core is not available in the Geofond archive, nor is the drilling project, which later studies refer to (Kysela, 1984 in Potfaj & Bodiš, 1987). Only preliminary brief information from Potfaj et al. (1986), Potfaj & Bodiš (1987), and Dvořáková et al. (1989), as well as a few preserved core samples, can be used. Based on these data, we assign the deeper part of the borehole to the Bystrica Mb. of the Bystrica Unit and estimate the boundary between the Biele Karpaty and Bystrica units at approximately 90 m depth.

In the near-surface part of the Magura Nappe, we agree with the conclusion of Potfaj (1993): "… *we could look for the Bystrica Unit in the rear part of the Rača Unit in a 'scar' position (i.e., forming only a narrow, steeply inclined zone at the southern boundary of the Rača Unit)*." However, according to our conclusions, the Bystrica Unit may have locally significant volumes at greater depths underlying the Biele Karpaty Unit.

Conclusions

The KLK-1 borehole, drilled northwest of Moravské Lieskové village in 1986 as part of hydrocarbon exploration of the Drietoma Structure, reached a total depth of 662 m. The upper 90 m of the succession confirmed the presence of the Svodnice Fm. (Biele Karpaty Unit). The succession below the tectonic breccia at approximately 90 m, previously assigned to the Zlín Fm. (Rača Unit), is here reinterpreted as the Bystrica Mb. (Bystrica Unit). This interval is characterised by quartz-rich glauconitic sandstones with abundant redeposited larger foraminifera, and thick beds of dark grey silty claystones to marls.

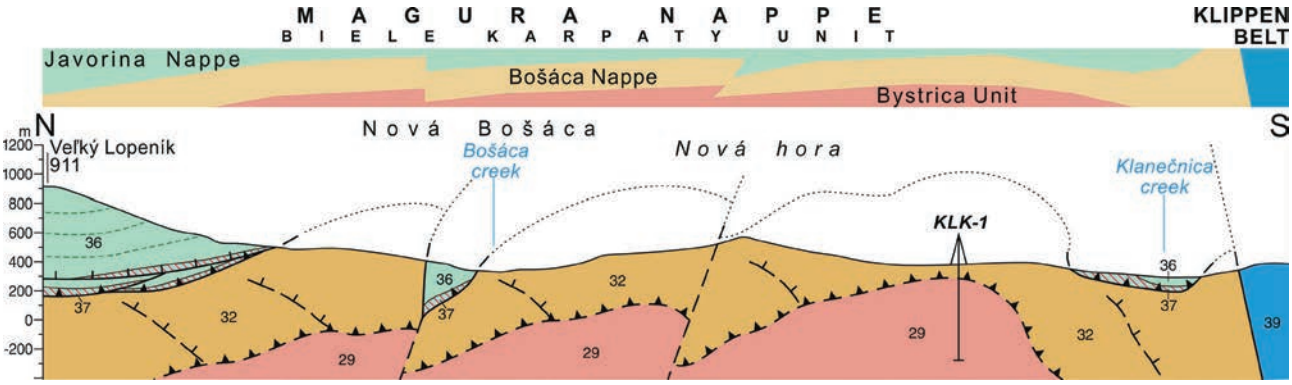

Fig. 8. The geological cross-section with the Bystrica Unit interpreted in the complex structural elevation beneath the Bošáca Nappe in the KLK-1 borehole (based on Pešková et al., 2021). A few minor backthrusts dislocate the structure. (Bystrica Unit: 29 – Bystrica Mb.; Biele Karpaty Unit: 32 – Svodnice Fm., 36 – Javorina Mb., 37 – Ondrášovec Mb.; 39 – Klippen Belt in general).

Examination of preserved core material, together with analyses of selected samples (nannoplankton and sandstone petrography), indicates that the occurrence of glauconitic sandstones and a middle to possibly late Eocene age alone are insufficient to justify assignment of these sediments to the Vsetín Mb. (Rača Unit) or to the Bystrica Mb. (Bystrica Unit).

The KLK-1 borehole may represent one of the few known occurrences of the Bystrica Unit west of the Nezdenice Faults. The unit continues beneath the Biele Karpaty Unit, indicating that its western extent is not terminated by the faults.

Acknowledgements:
The author thanks the Ministry of the Environment of the Slovak Republic for funding large-scale regional geological projects, thereby supporting the advancement of geological knowledge, and is also grateful to the reviewers Ján Soták and Michal Potfaj for their constructive comments, which helped to improve the manuscript.

References

Bučeк, S. & Teťák, F., 2020: Veľké bentické dierkavce z eocénnych glaukonitových pieskovcov magurského príkrovu (Orava a Javorníky). *Geologické práce, Správy*, 135, 3 – 15.

Dvořáková, V., Červenka, J. & Mitevová, J., 1989: Fyzikální vlastnosti hornin vrtu KLK-1 Klanečnica. *Manuscript. Bratislava, Archive of State Geological Institute of Dionýz Štúr* (arch. no. 72082), 55 pp.

Ďurkovič, T., Koráb, T., Rudinec, R., Gašpariková, V., Snopková, P., Köhler, E. & Zakovič, M., 1982: Hlboký štruktúrny vrt Zboj-1. *Regionálna geológia Západných Karpát*, 16, 76 pp.

Elečko, M. (ed.), Maglay, J, Pristaš, J., Fordinál, K., Nagy, A., Konečný, V., Šimon, L., Potfaj, M., Gross, P., Salaj, J., Polák, M., Mello, J., Havrila, M., Ivanička, J., Bučeк, S., Olšavský, M., Kohút, M., Kováčik, M., Bezák, V., Vozárová, A., Hók, J., Broska, I. & Madarás, J., 2008: Prehľadná geologická mapa SR 1 : 200 000, list 35 – Trnava. *Bratislava, MŽP SR, Štátny geologický ústav Dionýza Štúra.*

Franko, O. & Potfaj, M., 1983: Geologický projekt výskumného vrtu FPJ-1 Oravská Polhora na geotermálne jódo-brómové vody, čiastková záverečná správa. *Manuscript. Bratislava, Archive of State Geological Institute of Dionýz Štúr* (arch. no. 68353), 40 pp.

Hók, J., Pelech, O., Teťák, F., Németh, Z. & Nagy, A., 2019: Outline of the geology of Slovakia (W. Carpathians). *Mineralia Slovaca*, 51, 31 – 60.

Köhler, E. & Salaj, J., 1999: Ortophragminae (veľké foraminifery) v magurskej jednotke Nízkych Javorníkov (Západné Slovensko). *Zem. Plyn Nafta*, 44, 73 – 81.

Kysela, J., 1984: Geologický projekt mapovacieho vrtu KLK-1 (650 m). *Manuscript. Bratislava, Archive of State Geological Institute of Dionýz Štúr*.

Leško, B., 1980: Výskum hlbokých štruktúr Západných Karpát s ohľadom na výskyt živíc, roky 1971 – 1980. Záverečná správa. *Manuscript. Bratislava, Archive of State Geological Institute of Dionýz Štúr* (arch. no. 48879), 149 pp.

Leško, B., Samuel, O., Snopková, P., Ďurkovič, T., Smetana, J., Wünder, D., Širáňová, V., Rudinec, R., Losík, L., Píchová, E., Korkoška, F., Filková, V., Janků, J. & Hradil, F., 1987: Oporný vrt Smilno-1 (5 700 m). *Regionálna geológia Západných Karpát*, 22, 133 pp.

Marko, F., Pivko, D. & Hurai, V., 2003: Ruin marble: a record of fracture-controlled fluid flow and precipitation. *Geological Quarterly*, 47, 3, 241 – 252.

Němec, F., 1978: Průzkum na ropu a zemní plyn v předneogénních formacích Slovenska. *Geologický průzkum*, 20, 4, 97 – 101.

Němec, F., 1980: Předpokládané pokračovaní jv. svahů Českého masivu v přibradlové oblasti a jejich nafto- a plynomatěčnosti. *Hodonín, Moravské naftové doly*.

Pesl, V., 1968: Litofacie paleogénu v magurské jednotce vnějších flyšových Karpat na území ČSSR a PLR. *Sborník geologických vied – Západné Karpaty*, 9, 71 – 118.

Pesl, V., Hanzlíková, E. & Peslová, H., 1982: Stratigraphie tektonischer Einheiten der äusserren Karpaten in der Bohrung Jablůnka-1 bei Vsetín (Mähren). *Věst. Ústř. Úst. geol*., 57, 1, 1 – 15.

Pešková, I., Teťák, F. (eds.), Pelech, O., Sentpetery, M., Olšavský, M., Kováčik, M., Boorová, D., Laurinc, D., Demko, R., Maglay, J., Vlačiky, M., Žecová, K., Zeman, I., Gluch, A., Dananaj, I., Marcin, D. & Kúšik, D., 2020: Geologická mapa regiónu Biele Karpaty (severná časť) v mierke 1 : 50 000. Záverečná správa. *Manuscript. Bratislava, Archive of State Geological Institute of Dionýz Štúr* (arch. no. 100010).

Pešková, I., Teťák, F. (eds.), Pelech, O., Sentpetery, M., Olšavský, M., Kováčik, M., Maglay, J. & Vlačiky, M., 2021: Geologická mapa Bielych Karpát (severná časť) v mierke 1 : 50 000. *Bratislava. MŽP SR – Štátny geologický ústav Dionýza Štúra.*

Pličка, M., Liškutínová, D. & Švejdová, K., 1958: Systematický výskum a vyhodnotenie výskytu živíc v ČSR, záverečná správa k problému. Vyhodnotenie výskytu živíc v magurskom flyši a vo vnútornej flyšovej skupine. *Manuscript. Bratislava, Archive of State Geological Institute of Dionýz Štúr*, 224 pp.

Porubský, A., Chmelík, F. & Leško, B., 1963: Predbežné zistenie tektonických pomerov a chemizmu vôd v hlbších častiach antiklinálneho pásma Kohútovej doliny – Oravská Polhora, predbežný HGP, účel: zistenie geologickej štruktúry okolia Oravskej Polhory a možnosti zaistenia jódobromových vôd pre potreby MZ o väčšej výdatnosti. *Manuscript. Bratislava, Archive of State Geological Institute of Dionýz Štúr* (arch. no. 11669), 36 pp.

Potfaj, M., 1986a: Zhodnotenie geologických a geofyzikálnych údajov z oblasti Drietoma – Klanečnica. Záverečná správa. *Manuscript. Bratislava, Archive of State Geological Institute of Dionýz Štúr* (arch. no. 63985), 33 pp.

Potfaj, M., 1986b: Zhodnotenie geologických a geofyzikálnych údajov z oblasti Drietoma – Klanečnica. Dizertačná práca. *Manuscript. Bratislava, Archive of State Geological Institute of Dionýz Štúr*, 37 pp.

Potfaj, M., 1993: Postavenie bielokarpatskej jednotky v rámci flyšového pásma. *Geologické práce, Správy*, 98, 55 – 78.

Potfaj, M., Began, A., Nižňanský, G., Bodiš, D., Boorová, D., Čechová, A., Dovina, V., Fejdiová, O., Kováčik, M., Priechodská, Z., Samuel, O. & Šucha, P., 1986: Vysvetlivky ku geologickej mape M 1 : 25 000, listy Strání 35-122 a 35-123. Čiastková záverečná správa. *Manuscript. Bratislava, Archive of State Geological Institute of Dionýz Štúr* (arch. no. 62843), 97 pp.

Potfaj, M. & Bodiš, D., 1987: Nálezová správa o výskyte slanej I-Br vody vo vrte Klanečnica (KLK-1) – (Moravské Lieskové). *Manuscript. Bratislava, Archive of State Geological Institute of Dionýz Štúr* (arch. no. 64887), 14 pp.

Potfaj, M., Ďurkovič, T., Jurkovičová, H., Raková, J., Samuel, O., Snopková, P., Siráňová, Z., Sůrová, E. & Širáňová, V., 1989: Komplexné geologické vyhodnotenie štruktúrno-hydrogeologického vrtu FPJ-1 Oravská Polhora. Čiastková záverečná správa. *Manuscript. Bratislava, Archive of State Geological Institute of Dionýz Štúr* (arch. no. 68353), 38 pp.

Stráník, Z., Bubík, M., Gilíková, H. & Tomanová Petrová, P. (eds.), 2021: Geologie Vnějších Západních Karpat a jihovýchodního okraje Západoevropské platformy v České republice. *Praha, Czech geological survey*, 320 pp.

Teťák, F., 2016: Bielokarpatská jednotka, geologická stavba a vývoj západne od Veľkej Javoriny. *Námestovo, Štúdio F*, 32 pp.

Teťák, F., 2024: Revízia geologickej mapy západného úseku flyšového pásma Západných Karpát s diskusiou k vybraným geologickým problémom. Revision of the geological map of the western part of the Flysch Belt of the Western Carpathians with a discussion of selected geological problems. *Geologické práce, Správy*, 140, 75 – 106. https://doi.org/10.56623/gps.140.3.

Teťák, F. (ed.), Kováčik, M., Pešková, I., Nagy, A., Buček, S., Maglay, J. & Vlačiky, M., 2016: Geologická mapa regiónu Biela Orava v mierke 1 : 50 000. *Bratislava, MŽP SR – Štátny geologický ústav Dionýza Štúra*.

Teťák, F., Pivko, D. & Kováčik, M., 2019: Depositional systems and paleogeography of Upper Cretaceous-Paleogene deep-sea flysch deposits of the Magura Basin (Western Carpathians). *Palaeogeography, Palaeoclimatology, Palaeoecology*, Elsevier, 533, 1 – 21.

Teťák, F., Pešková, I. (eds.), Pelech, O., Sentpetery, M., Olšavský, M., Kováčik, M., Boorová, D., Laurinc, D., Demko, R., Maglay, J., Vlačiky, M., Korábová, K., Zeman, I., Gluch, A., Dananaj, I., Marcin, D. & Kúšik, D., 2024: Vysvetlivky ku geologickej mape Bielych Karpát (severná časť) v mierke 1 : 50 000. *Bratislava, Štátny geologický ústav Dionýza Štúra*, 246 pp.

Tomek, Č., 1976: Jednotné zpracování a interpretace tíhových podkladů Vídeňské pánve a přilehlého pásma vnitřních a flyšových Karpat. *Brno, Geofyzika*.

Wunder, D., Ďurkovič, T., Siráňová, Z., Fejdiová, O., Gašpariková, V., Korábová, K., Píchová, E., Červenka, J., Kožel, J., Snopková, P., Rudinec, R. & Smetana, J., 1990: Prognózne overenie zdrojov prírodných uhľovodíkov v zborovskom antiklinóriu. Geologické zhodnotenie vrtu Zborov-1, čiastková záverečná správa. *Manuscript. Bratislava, Archive of State Geological Institute of Dionýz Štúr* (arch. no. 75500), 20 pp.

Alternatívna interpretácia bystrickej jednotky vo vrte KLK-1 Klanečnica (magurský príkrov)

Hlboký vrt na preskúmanie podložia flyšového pásma a potenciálnych akumulácií uhľovodíkov v oblasti Starého Hrozenkova a Drietomy, ktorý navrhoval Leško (1980), mal dosahovať až 6 500 m. Oblasť Drietomy bola vybraná kvôli jej predpokladanej elevácii podložia, „drietomskej štruktúre“ alebo „hrozenkovskej elevácii“. Gravimetrické a seizmické údaje (Tomek, 1976; Němec, 1978, 1980) v tejto oblasti naznačovali prítomnosť telies s nízkou hustotou pod flyšovými a vnútrokarpatskými jednotkami. Potfaj (1986a, b) neskôr zhrnul geofyzikálne údaje a zdôraznil nejednoznačnosť pri interpretácii takejto elevácie. Hlboký vrt, plánovaný na rok 1981 (Leško, 1980), sa neuskutočnil.

Vrt KLK-1 bol realizovaný v roku 1986 (cca 48,862 36°; 17,760 45°) a dosiahol hĺbku 662 m. Projektová dokumentácia a podrobné vyhodnotenie vrtu sa v archíve geofondu nezachovali. Existujú len stručné charakteristiky (Potfaj et al., 1986; Potfaj a Bodiš, 1987). Potfaj et al. (1986) interpretovali najvrchnejších 75 m vrtu ako svodnické súvrstvie bielokarpatskej jednotky (paleocén až starší eocén) a pod intervalom brekcií považovaným za násunovú plochu bielokarpatskej jednotky bolo interpretované zlínske súvrstvie račianskej jednotky. V tektonickej brekcii v hĺbke 75 m boli zaznamenané emisie metánu, v hĺbke 118 m, 134 m, 216 m, 318 m a 505 m zas prílev Na–Cl–HCO_3–I–Br vody bohatej na metán s maximálnym prietokom 0,1 až 3,5 $l \cdot s^{-1}$ a teplotou do 16 °C. Koncentrácia jódu dosiahla približne 27 $mg \cdot l^{-1}$ (Potfaj a Bodiš, 1987).

Na základe makroskopickej prehliadky zachovaných vzoriek jadier sme zaznamenali výraznú podobnosť vo vzhľade glaukonitových pieskovcov z vrtu s pieskovcami bystrických vrstiev (tab. 1). Dospeli sme k záveru, že ani prítomnosť glaukonitových pieskovcov, ani vek stredný až neskorý eocén nedokazujú zaradenie k vsetínskym vrstvám zlínskeho súvrstvia račianskej jednotky. V hornej časti vrtu, približne do hĺbky 90 m, súhlasíme so zaradením k svodnickému súvrstviu bielokarpatskej jednotky. Je to v súlade s horninami pozorovanými v blízkosti vrtu (Potfaj et al., 1986; Pešková et al., 2021).

Pod hĺbkou asi 90 m vrt reinterpretujeme ako bystrické vrstvy bystrickej jednotky. Naznačuje to hojný výskyt väčších foraminifer a hrubé vrstvy tmavosivých ílovcov vo vzorkách jadra v kremitých glaukonitových pieskovcoch. Podľa litofaciálnej podobnosti by sa dalo uvažovať aj o svodnickom súvrství hluckého vývoja bielokarpatskej jednotky s glaukonitovými pieskovcami (Teťák, 2016). Jeho paleocénny až ranoeocénny vek je však starší ako strednoeocénny vek stanovený v prípade sedimentov z vrtu. Podobne, keďže sa vsetínske vrstvy vyskytujú len v severnej (externej) časti račianskej jednotky, je málo pravdepodobné, že by bielokarpatská jednotka ležala priamo na vonkajšej časti račianskej jednotky bez prítomnosti internejších častí magurského príkrovu, ktoré vystupujú na povrchu.

Glaukonitové pieskovce z vrtu sa od pieskovcov vsetínskych vrstiev makroskopicky líšia len nevýrazne. Rozlišovacím znakom môže byť litologická a textúrna variabilita pieskovcov spolu s hojnými schránkami väčších foraminifer. Teťák et al. (2016) zdôrazňujú z Oravy litologickú pestrosť glaukonitových pieskovcov bystrických vrstiev a vysvetľujú ju priestorovo a časovo rozmanitým charakterom zdrojovej oblasti a transportu. Rozlišujú päť hlavných typov pieskovcov vrátane sklzov a úlomkotokov, ktoré boli pozorované aj vo vrte KLK-1.

Analýza nanoplanktónu (Korábová in Pešková et al., 2020; Teťák et al., 2024) potvrdzuje vek vzoriek z hĺbky 386,8 m a 482,2 m stredný eocén (NP 17, bartón). Potfaj et al. (1986) uvádzajú podobné spoločenstvo z hĺbky 121 m, 184 m, 374 m a 552 m.

Preskúmanie zachovaného horninového materiálu naznačuje, že samotný výskyt glaukonitických pieskovcov a stredný až možno neskorý eocénny vek nie sú dostatočné na zaradenie týchto sedimentov k vsetínskym vrstvám (račianska jednotka), ale ani k bystrickým vrstvám (bystrickej jednotky). Vrt KLK-1 môže predstavovať jeden z mála známych výskytov bystrickej jednotky západne od nezdenických zlomov. Bystrická jednotka pokračuje pod bielokarpatskou jednotkou, čo naznačuje, že jej západný rozsah sa týmito zlomami nekončí.

Doručené / Recieved: 8. 10. 2025
Prijaté na publikovanie / Accepted: 28. 10. 2025

Inštrukcie autorom

www.geology.sk/mineralia položka ***Inštrukcie autorom***

1. Manuskripty sa do redakcie zasielajú e-mailom (editovateľné súbory formátu .doc, .docx alebo .odt a verzia v PDF formáte) na adresu vedeckého redaktora alebo mineralia.slovaca@geology.sk.
2. **Súčasne s manuskriptom je potrebné redakcii poslať autorské vyhlásenie o originalite textu a obrázkov. Kópie obrázkov z iných publikácií musia byť legalizované získaním práva na publikovanie. Vyhlásenie musí obsahovať meno autora (autorov), akademický titul** a tr**valé bydlisko.** Články sú uverejnené pod licenciou *Creative Commons Attribution (CC BY)*. Autori článkov majú možnosť požiadať aj o iný typ licencie *Creative Commons*.
3. Rozsah manuskriptu na publikovanie je štandardne do 40 rukopisných strán (font Times New Roman, veľkosť písmen 12 bodov, riadkovanie 1,5) vrátane literatúry, obrázkov, popisov obrázkov a tabuliek. V prípade veľkého odborného prínosu sú v ojedinelých prípadoch povolené aj dlhšie články. Rozsiahlejšie doplňujúce materiály v prípade potreby je možné publikovať ako prílohu online.
4. Články sú publikované v angličtine, výnimočne aj v slovenčine. Články písané v angličtine musia obsahovať slovenské resumé. Články v slovenčine musia obsahovať anglický preklad názvu, abstraktu, kľúčových slov, resumé a popisov k obrázkom a tabuľkám.

Text

Úprava textu aj zoznamu literatúry musí korešpondovať so súčasnou úpravou článkov v časopise. Predkladaný manuskript musí spĺňať tieto požiadavky:

1. Text manuskriptu musí mať priebežne číslované riadky.
2. Na začiatku manuskriptu je uvedený názov, ktorý by mal byť stručný a informatívny.
3. Meno a priezvisko autora alebo autorov musí byť uvedené spolu s názvom pracoviska a adresou (mesto, krajina). Korešpondujúci autor musí byť riadne označený a musí byť uvedená jeho e-mailová adresa. Ak je k dispozícii aj ORCID autorov, treba ho uvádzať.
4. V úvode v časti Highlights a v závere príspevku musí autor jasne deklarovať, čím konkrétnym je jeho príspevok prínosný pre rozvoj geovied.
5. Abstrakt stručne sumarizuje článok. Môže mať najviac 200 slov a nemá obsahovať citácie. Počet kľúčových slov je maximálne 6.
6. Text má takéto členenie: úvod, charakteristika (stav) skúmaného problému vrátane prehľadu dôležitých starších výskumov, použitá metodika, nové zistenia (výsledky), ich interpretácia, diskusia, záver, poďakovanie, zoznam literatúry a resumé v slovenskom, resp. anglickom jazyku (pri článku v slovenčine). Východiskové údaje musia byť zreteľne odlíšené od interpretácií. V texte musia byť odvolávky na všetky použité obrázky a tabuľky.
7. V texte je možné použiť maximálne 3 hierarchické úrovne podnadpisov.
8. V texte sa uprednostňuje citácia v zátvorke, napr. (Dubčák, 1987; Hrubý et al., 1988), pred formou napr. podľa Dubčáka (1987).
9. Manuskript odporúčame zasielať s obrázkami vloženými v texte alebo na konci manuskriptu.
10. V texte treba prednostne používať platné jednotky SI, napr. s (sekunda, nie sec), m (meter), kg (kilogram). V oprávnených prípadoch možno použiť aj iné miery zaužívané v odbornej literatúre a v zátvorke uviesť ich ekvivalent v jednotkách SI, napr. 3 kbar (300 MPa, resp. 0,3 GPa), 30 kt, resp. 30 000 t (3,107 kg), 800 K (527 °C), 4,26 Å (4,26 . 10^{-10} m).
11. V texte sa môžu používať len názvy minerálov oficiálne schválené Komisiou pre nové minerály a nomenklatúra schválená Medzinárodnou mineralogickou asociáciou (CNMNC IMA). Ich zoznam (inovovaný každé dva mesiace) je prístupný na stránke https://cnmnc.units.it/ (*IMA-CNMNC List of Mineral Names*). Rovnako sa môžu používať len odporúčané skratky minerálov (*Updated list of IMA-CNMNC mineral symbols*). Pokiaľ autori disponujú chemickou analýzou minerálu, treba napísať jeho celý platný názov, napr. fluórapatit (nie apatit), monazit-(Ce) (nie monazit). Neúplné názvy minerálov (napr. apatit, monazit) možno použiť pri petrografickom opise hornín alebo názve metódy (napr. monazitové datovanie). Použitie názvov izomorfných sérií minerálov zaužívaných v geologickej literatúre (napr. biotit, zinnwaldit, olivín) alebo skupinových názvov minerálov (napr. granáty, turmalíny, amfiboly, spinely) je akceptované. V prípade nejasností sa autori môžu písomne obrátiť na redakčnú radu.

Obrázky, ilustrácie a tabuľky

1. Ilustrácie a tabuľky vysokej kvality bývajú publikované buď **na šírku stĺpca** (81 mm)**, alebo strany (170 mm)**. Optimálna veľkosť písma a čísiel v publikovaných obrázkoch je 2 mm. Články v angličtine majú všetky texty v angličtine. Články v slovenčine musia mať popisy v obrázkoch a tabuľkách v slovenčine, záhlavie tabuliek a texty pod obrázkami a tabuľkami sú v slovenčine a angličtine. **Maximálny rozmer ilustrácie a tabuľky vytlačený v časopise je 170 x 230 mm**. Väčšie (skladané) ilustrácie sú publikované len v ojedinelých prípadoch.
2. Ilustrácie vrátane fotografií musia obsahovať **grafickú mierku** v centimetrovej či metrovej škále, prípadne sa rozmer zobrazených objektov vyjadrí v popise obrázka. Mapy a profily musia mať aj **azimutálnu orientáciu** a jednotné vysvetlivky, ktoré sa uvedú pri prvom obrázku. Zoskupené obrázky, napr. fotografie a diagramy, sa uvádzajú ako jeden obrázok s jednotlivými časťami označenými písmenami (a, b, c atď.).
3. **Ilustrácie, mapy a fotografie je nutné uložiť vo formátoch JPG, PNG alebo TIF v rozlíšení minimálne 600 dpi, vektorovú grafiku vo formátoch EPS, PDF, AI alebo COR.**

Redakcia si vyhradzuje právo vrátiť autorovi grafické prílohy na opravu po jazykovej úprave, resp. požiadať o ich nahradenie za prílohy v požadovanej kvalite.

Literatúra

Zoznam použitej literatúry musí obsahovať iba publikované alebo akceptované práce. Pri jednom autorovi sú práce v zozname zoradené abecedne podľa priezviska autora každého diela. Pri dvoch autoroch sa práce uvádzajú abecedne najprv podľa priezviska prvého autora, potom podľa priezviska spoluautora a potom chronologicky. Pri viac ako dvoch autoroch sa práce zoradia abecedne iba podľa priezviska prvého autora, potom chronologicky. Ak má publikácia DOI, vždy sa uvádza za číslom citovaných strán vo forme https://doi.org/číslo.

Spôsob uvádzania literatúry v zozname literatúry:

Knižná publikácia: Gazda, L. & Čech, M., 1988: Paleozoikum medzevského príkrovu. Bratislava, Alfa, 155 s.

Časopis: Hók, J. & Olšavský, M., 2023: Vernaricum – regional distribution, lithostratigraphy, tectonics and paleogeography. Mineralia Slovaca, 55, 1, 3 – 12. https://doi.org/10.56623/ms.2023.55.1.1.

Zborník: Návesný, D., 1987: Vysokodraselné ryolity. In: Romanov, V. (ed.): Stratiformné ložiská gemerika. Špec. publ. Košice, Slovenská geologická spoločnosť, 203 – 215.

Manuskript: Tulis, J. & Novotný, L., 1998: Zhodnotenie geologických prác na U rudy v mladšom paleozoiku hronika v severnej časti Nízkych Tatier a Kozích chrbtov. Manuskript. Bratislava, archív Štátny geologický ústav Dionýza Štúra (arch. č. 82752), 144 s.

Instructions to authors

www.geology.sk/mineralia item ***Instructions to authors***

1. The manuscripts must be sent to Editorial Office by e-mail (editable files in .doc, .docx or .odt format, plus complete preview version in PDF format) to the Scientific Editor or mineralia.slovaca@geology.sk.
2. **Simultaneously with the manuscript the Editorial Office must receive the author´s proclamation that no part of the manuscript was already published and figures and tables are original as well. Copied illustrations from other publications must contain a copyright.** The articles are published under a Creative Commons Attribution (CC BY) license. Authors have the option to apply for other types of Creative Commons licenses.
3. The extent of the manuscript for publishing is limited to 40 manuscript pages (12 points Times New Roman font, line spacing 1.5) including figures, tables, explanations and references. In the case of contribution with a high scientific value, the longer manuscripts for publishing are exceptionally permitted. More extensive supplementary material can be published as an online annex if required.
4. Articles are published in English (preferably) or Slovak languages. The title, abstract, key words, graphical abstract, highlights, shortened text (summary), as well as description to figures and tables in Slovak articles are published also in English. Articles published in English contain Slovak resumé.

Text

The format of the text and the reference list must correspond to the current format of the papers in the journal. The submitted manuscript must meet the following requirements:

1. The text of the manuscript must have continuously numbered lines.
2. The title at the beginning of the manuscript should be brief and informative.
3. The name and surname of the author(s) must be given together with affiliation(s) to the institutions and the address (city, country). The corresponding author must be properly marked and his/her e-mail address must be given. If the ORCID of the authors is also available, it should be provided.
4. The Highlights section in the beginning of the manuscript and in the conclusions at the end of the paper, must clearly declare main results and importance for the Earth sciences.
5. Abstract briefly summarizing the manuscript is limited to 200 words, no references are allowed. The maximum number of key words is 6.
6. The text must be structured as follows: the introduction, characterization (state) of investigated problem, applied methodology, obtained new findings (results), interpretation, discussion, conclusion, acknowledgements and references. The obtained data must be distinctly separated from interpretations. All applied figures and tables must be referred in the text.
7. A maximum of 3 hierarchical levels of headings may be used in the text.
8. In the case of references in the text the parentheses are preferred, e.g. (Dubčák, 1987; Hrubý et al., 1988). The form "according to Dubčák (1987)" should be used only exceptionally.
9. We recommend submitting the manuscript with figures inserted in the text or at the end of the manuscript.
10. Valid SI units ought to be used in the text, preferably, e.g. s (second, not sec), m (metre), kg (kilogram). Where justified, other units used in the literature may be used and their equivalent in SI units may be given in brackets, e.g. 3 kbar (300 MPa or 0.3 GPa), 30 kt or 30 000 t (3.10^7 kg), 800 K (527 °C), 4.26 Å (4.26 . 10^{-10} m).
11. Only mineral names officially approved by the Commission for New Minerals and nomenclature approved by the International Mineralogical Association (CNMNC IMA) may be used in the text. A list of these (updated every two months) is available at https://cnmnc.units.it/ (IMA-CNMNC List of Mineral Names). Also, only recommended mineral abbreviations may be used (Updated list of IMA-CNMNC mineral symbols). If the authors have a chemical analysis of the mineral, its full valid name should be written, e.g. fluorapatite (not apatite), monazite-(Ce) (not monazite). Incomplete mineral names (e.g. apatite, monazite) may be used in the petrographic description of the rocks or the name of the method (e.g. monazite dating). The use of isomorphic mineral series names established in the geological literature (e.g. biotite, zinnwaldite, olivine) or mineral group names (e.g. garnets, tourmalines, amphiboles, spinels) is accepted. It is recommended to contact the Editorial Board in unclear cases.

Figures and tables

1. The high-quality figures and tables can be published either in **maximum width of column (81 mm) or page (170 mm)**. The optimum size of letters and numbers in the printed figure is 2 mm. Manuscripts published in Slovak contain the Slovak descriptions in figures and tables, the tables headings and descriptions beneath figures and tables are in Slovak and English. English manuscripts contain all texts in English. **Maximum dimension of figures and tables in the journal is 170 x 230 mm. Larger (folded)** illustrations are published only exceptionally.
2. Illustrations including photographs must contain graphic (metric) scale, eventually the dimensions of visualized objects have to be stated in the describing text to figure. Maps and profiles must contain also the azimuth orientation; their unified explanations are stated at the first figure. Grouped figures, e.g. photographs and diagrams, are compiled as one figure with separate parts designated by letters (a, b, c, etc.).
3. **Illustrations, maps and photographs must be saved in JPG, PNG or TIFF formats with a resolution of at least 600 dpi, vector graphics in EPS, PDF, AI or COR formats**.

The editors reserve the right to return illustrations to the author for correction after language editing, or to request their replacement with illustrations of the required quality.

References

The list of references used must include only published or accepted works. Single-authored works are listed alphabetically by the surname of the author of each work. For two authors, the works are listed alphabetically first by the surname of the first author, then by the surname of the co-author, and then chronologically. For more than two authors, the works are listed alphabetically only by the surname of the first author, then chronologically. If a publication has a DOI, it is always listed after the citation page number in the form https://doi.org/number.

References examples:

Book: Gazda, L. & Čech, M., 1988: Paleozoikum medzevského príkrovu [Paleozoic of the Medzev nappe]. Bratislava, Alfa, 155 pp.

Journal: Hók, J. & Olšavský, M., 2023: Vernaricum – regional distribution, lithostratigraphy, tectonics and paleogeography. Mineralia Slovaca, 55, 1, 3 – 12. https://doi.org/10.56623/ms.2023.55.1.1.

Proceedings contribution: Návesný, D., 1987: Vysokodraselné ryolity. In: Romanov, V. (ed.): Stratiformné ložiská gemerika [High-potassium rhyolites. In: Romanov, V. (ed.): Stratiform deposits of Gemericum]. Spec. publ. Košice, Slov. geol. soc., 203 – 215.

Manuscript: Tulis, J. & Novotný, L., 1998: Zhodnotenie geologických prác na U rudy v mladšom paleozoiku hronika v severnej časti Nízkych Tatier a Kozích chrbtov. [Assessment of geological works on U ore in the Late Paleozoic of Hronicum in the northern part of the Nízke Tatry and Kozie chrbty Mts.] Manuscript. Bratislava, Archive of State Geological Institute of Dionýz Štúr (arch. no. 82752), 144 pp. (in Slovak).

Ďalšie informácie / Further information: mineralia.slovaca@geology.sk; ondrej.pelech@geology.sk

OBSAH/CONTENT

Indexed / Abstracted / Accessed by SCOPUS, WEB OF SCIENCE and EBSCO
Indexované / abstraktované / sprístupňované databázami SCOPUS, WEB OF SCIENCE a EBSCO

www.geology.sk/mineralia